

Pathogenic mechanism of porcine viral disease

Edited by

Mengmeng Zhao, Lingxue Yu and Weili Kong

Coordinated by

Xuelian Zhang

Published in

Frontiers in Veterinary Science



FRONTIERS EBOOK COPYRIGHT STATEMENT

The copyright in the text of individual articles in this ebook is the property of their respective authors or their respective institutions or funders. The copyright in graphics and images within each article may be subject to copyright of other parties. In both cases this is subject to a license granted to Frontiers.

The compilation of articles constituting this ebook is the property of Frontiers.

Each article within this ebook, and the ebook itself, are published under the most recent version of the Creative Commons CC-BY licence. The version current at the date of publication of this ebook is CC-BY 4.0. If the CC-BY licence is updated, the licence granted by Frontiers is automatically updated to the new version.

When exercising any right under the CC-BY licence, Frontiers must be attributed as the original publisher of the article or ebook, as applicable.

Authors have the responsibility of ensuring that any graphics or other materials which are the property of others may be included in the CC-BY licence, but this should be checked before relying on the CC-BY licence to reproduce those materials. Any copyright notices relating to those materials must be complied with.

Copyright and source acknowledgement notices may not be removed and must be displayed in any copy, derivative work or partial copy which includes the elements in question.

All copyright, and all rights therein, are protected by national and international copyright laws. The above represents a summary only. For further information please read Frontiers' Conditions for Website Use and Copyright Statement, and the applicable CC-BY licence.

ISSN 1664-8714
ISBN 978-2-8325-5488-3
DOI 10.3389/978-2-8325-5488-3

About Frontiers

Frontiers is more than just an open access publisher of scholarly articles: it is a pioneering approach to the world of academia, radically improving the way scholarly research is managed. The grand vision of Frontiers is a world where all people have an equal opportunity to seek, share and generate knowledge. Frontiers provides immediate and permanent online open access to all its publications, but this alone is not enough to realize our grand goals.

Frontiers journal series

The Frontiers journal series is a multi-tier and interdisciplinary set of open-access, online journals, promising a paradigm shift from the current review, selection and dissemination processes in academic publishing. All Frontiers journals are driven by researchers for researchers; therefore, they constitute a service to the scholarly community. At the same time, the *Frontiers journal series* operates on a revolutionary invention, the tiered publishing system, initially addressing specific communities of scholars, and gradually climbing up to broader public understanding, thus serving the interests of the lay society, too.

Dedication to quality

Each Frontiers article is a landmark of the highest quality, thanks to genuinely collaborative interactions between authors and review editors, who include some of the world's best academicians. Research must be certified by peers before entering a stream of knowledge that may eventually reach the public - and shape society; therefore, Frontiers only applies the most rigorous and unbiased reviews. Frontiers revolutionizes research publishing by freely delivering the most outstanding research, evaluated with no bias from both the academic and social point of view. By applying the most advanced information technologies, Frontiers is catapulting scholarly publishing into a new generation.

What are Frontiers Research Topics?

Frontiers Research Topics are very popular trademarks of the *Frontiers journals series*: they are collections of at least ten articles, all centered on a particular subject. With their unique mix of varied contributions from Original Research to Review Articles, Frontiers Research Topics unify the most influential researchers, the latest key findings and historical advances in a hot research area.

Find out more on how to host your own Frontiers Research Topic or contribute to one as an author by contacting the Frontiers editorial office: frontiersin.org/about/contact

Pathogenic mechanism of porcine viral disease

Topic editors

Mengmeng Zhao — Foshan University, China

Lingxue Yu — Shanghai Veterinary Research Institute, Chinese Academy of Agricultural Sciences, China

Weili Kong — Gladstone Institutes, United States

Topic coordinator

Xuelian Zhang — Foshan University, China

Citation

Zhao, M., Yu, L., Kong, W., Zhang, X., eds. (2024). *Pathogenic mechanism of porcine viral disease*. Lausanne: Frontiers Media SA. doi: 10.3389/978-2-8325-5488-3

Table of contents

- 04 **Editorial: Pathogenic mechanism of porcine viral disease**
Mengmeng Zhao, Xuelian Zhang, Lingxue Yu and Weili Kong
- 06 **Genetic background influences pig responses to porcine reproductive and respiratory syndrome virus**
Yangli Pei, Chenghong Lin, Hua Li and Zheng Feng
- 16 **Host cellular factors involved in pseudorabies virus attachment and entry: a mini review**
Lei Tan, Kaixin Wang, Ping Bai, Shuo Zhang, Mengting Zuo, Xianghua Shu, Aibing Wang and Jun Yao
- 23 **Genome stability assessment of PRRS vaccine strain with new ARTIC-style sequencing protocol**
Szilvia Jakab, Ádám Bálint, Karolina Cseri, Krisztina Bali, Eszter Kaszab, Marianna Domán, Máté Halas, Krisztina Szarka and Krisztián Bányai
- 31 **First detection and molecular characterization of porcine reproductive and respiratory syndrome virus in Namibia, Africa**
Umberto Molini, Lauren M. Coetzee, Maria Y. Hemberger, Bernard Chiwome, Siegfried Khaiseb, William G. Dundon and Giovanni Franzo
- 38 **RNA recombination: non-negligible factor for preventing emergence or reemergence of Senecavirus A**
Yan Li, Tianyu Liu, Youming Zhang, Xiaoxiao Duan and Fuxiao Liu
- 44 **Nucleotide metabolism-related host proteins RNA polymerase II subunit and uridine phosphorylase 1 interacting with porcine epidemic diarrhea virus N proteins affect viral replication**
Yifan Xu, Heyou Yi, Qiyuan Kuang, Xiaoyu Zheng, Dan Xu, Lang Gong, Liangyu Yang and Bin Xiang
- 55 **Comparative transcriptomics analysis on Senecavirus A-infected and non-infected cells**
Yan Li, Huanhuan Chu, Yujia Jiang, Ziwei Li, Jie Wang and Fuxiao Liu
- 67 **Reverse genetics construction and pathogenicity of a novel recombinant NADC30-like PRRSV isolated in China**
Jinyao Guo, Chenxi Li, Huipeng Lu, Bin Wang, Linjie Zhang, Jingjing Ding, Xue Jiao, Qingyu Li, Shanyuan Zhu, Anping Wang and Yanhua Li
- 81 **Exploratory application of a cannulation model in recently weaned pigs to monitor longitudinal changes in the enteric microbiome across varied porcine reproductive and respiratory syndrome virus (PRRSV) infection statuses**
Tanja Opriessnig, Patrick Halbur, Jenna Bayne, Gaurav Rawal, Hao Tong, Kathy Mou, Ganwu Li, Danyang Zhang, Jianqiang Zhang and Adrian Muwonge
- 95 **Development of a TaqMan-based multiplex real-time PCR for simultaneous detection of porcine epidemic diarrhea virus, *Brachyspira hyodysenteriae*, and *Lawsonia intracellularis***
Jing Ren, Fujun Li, Xue Yu, Yang Li, Meng Li, Yujie Sha and Xiaowen Li



OPEN ACCESS

EDITED AND REVIEWED BY
Michael Kogut,
Agricultural Research Service, United States
Department of Agriculture, United States

*CORRESPONDENCE
Lingxue Yu
✉ yulingxue@shvri.ac.cn

RECEIVED 29 August 2024
ACCEPTED 03 September 2024
PUBLISHED 17 September 2024

CITATION
Zhao M, Zhang X, Yu L and Kong W (2024)
Editorial: Pathogenic mechanism of porcine
viral disease. *Front. Vet. Sci.* 11:1488296.
doi: 10.3389/fvets.2024.1488296

COPYRIGHT
© 2024 Zhao, Zhang, Yu and Kong. This is an
open-access article distributed under the
terms of the [Creative Commons Attribution
License \(CC BY\)](#). The use, distribution or
reproduction in other forums is permitted,
provided the original author(s) and the
copyright owner(s) are credited and that the
original publication in this journal is cited, in
accordance with accepted academic practice.
No use, distribution or reproduction is
permitted which does not comply with these
terms.

Editorial: Pathogenic mechanism of porcine viral disease

Mengmeng Zhao¹, Xuelian Zhang¹, Lingxue Yu^{2*} and Weili Kong³

¹Guangdong Provincial Key Laboratory of Animal Molecular Design and Precise Breeding, College of Animal Science and Technology, Foshan University, Foshan, China, ²Shanghai Veterinary Research Institute, Chinese Academy of Agricultural Sciences, Shanghai, China, ³University of California, San Francisco, San Francisco, CA, United States

KEYWORDS

swine viral diseases, PRRSV, pathogenic mechanism, PRV, PEDV

Editorial on the Research Topic

Pathogenic mechanism of porcine viral disease

1 Introduction

Porcine viral disease is the most serious disease in the pig industry. Bacterial diseases have been widely controlled because of the use of antibiotics. Although some drugs or vaccines have been used in viral diseases, many of them are not effective and the treatment cost is high (1). And many of them stay in the laboratory exploration stage, and it is difficult to conduct large-scale experiments in clinical productions. Exploring the pathogenesis of animal viral diseases is helpful to the pathogenesis research of viral diseases, the rational use of drugs and vaccines, and the development of new vaccines. Nowadays, new viral diseases are constantly emerging in swine diseases, including the recombination and variation of old viral diseases, and the emergence and cross-species transmission of new viruses. Taking China as an example, in recent years, a new variant PRRSV NADC-34 strain appeared in 2014 (2), and the African classical swine fever virus appeared in 2018 (3). The old virus has not been eliminated, and new viruses have appeared, which makes the disease prevention and control of pigs increasingly complicated.

There are many reasons behind it, including the variation of natural climate and the unreasonable abuse of vaccines. Many factors lead to more and more animal diseases.

2 Organization of the Research Topic

The theme of this Research Topic mainly discusses the *Pathogenic mechanism of porcine viral disease*. This Research Topic has received 30 manuscripts, 10 manuscripts (two reviews, one opinion, one brief report, and six original articles) were accepted, 20 papers were rejected, the acceptance rate was 33.3%, and two Manuscript Summaries were also received. This Research Topic covers porcine reproductive and respiratory syndrome virus (PRRSV), pseudorabies virus (PRV), and Senecavirus A virus and porcine epidemic diarrhea virus (PEDV). These manuscripts were from nine laboratories in China, Hungary, Britain, and Namibia.

Ren et al. constructed a multiplex qRT-PCR method, which can distinguish PEDV, *B. hyodysenteriae*, and *L. intracellularis*. These three diseases are often shown as mixed infection in clinic diseases. Guo et al. successfully constructed a new infectious clone against the current epidemic PRRSV strain, and successfully saved the virus, laying a foundation for studying the characteristics of the new strain. Senecavirus A (SVA) does great harm to pig industry. Li, Chu et al. made a transcriptome analysis of cells infected by Senecavirus A and found 565 upregulated and 63 downregulated ones, which laid a foundation for revealing the infection mechanism of this virus. Opriessnig et al. developed a weaned piglet intubation model, and all vaccinated pigs showed strong immune responses and maintained protection against PRRSV attack. Xu et al. identified the protein that interacts with the N protein of PEDV through interactive genomics, such as the second-largest subunit of RNA polymerase II (RPB2) and uridine phosphorylase 1 (UPP1), both of which are involved in nucleotide metabolism. Overexpression of RPB2 was observed to significantly promote viral replication, while overexpression of UPP1 was found to inhibit viral replication significantly. The study of the interaction between PEDV N and host proteins provides a theoretical foundation for further exploration of the pathogenic mechanisms and strategies for the prevention and control of PEDV. Li, Liu et al. specifically explored the role and mechanism of RNA recombination in Senecavirus A, suggesting that attention should be paid attention. Jakab et al. demonstrated the development of a tiling amplicon sequencing protocol for the analysis of genome sequence stability in the context of the modified live PRRSV vaccine strain, Porcilis MLV. The results indicated that ARTIC-style protocols can be employed in the evaluation of genomic stability in PRRS MLV strains. Molini et al. detected PRRSV in Africa for the first time, which is type I and may be introduced from Europe. Tan et al. identified the proteins that interacted with the host during the adsorption and invasion of PRV infection, which laid the foundation for further research. Pei et al. summarized that differences in genetic background lead to different biological shapes, including resistance to PRRSV, internal immunological mechanism, mechanism of entering cells, differences in symptoms and lesions after infection, differences in viral load, and differences in non-coding RNA.

References

1. Vu HLX, McVey DS. Recent progress on gene-deleted live-attenuated African swine fever virus vaccines. *NPJ Vaccines*. (2024) 9:60.
2. Tian K. NADC30-like porcine reproductive and respiratory syndrome in China. *Open Virol J*. (2017) 11:59–65.
3. Ge S, Li J, Fan X, Liu F, Li L, Wang Q, et al. Molecular characterization of African Swine Fever Virus, China, 2018. *Emerg Infect Dis*. (2018) 24:2131–3. doi: 10.3201/eid2411.181274

3 Conclusion

This Research Topic reveals the interaction and replication mechanism of different viruses from many aspects, which is helpful to further reveal the replication mechanism of these viruses and provide theoretical reference for controlling these diseases in the future.

Author contributions

MZ: Writing – original draft. XZ: Writing – review & editing. LY: Writing – review & editing. WK: Writing – review & editing.

Funding

The author(s) declare financial support was received for the research, authorship, and/or publication of this article. This research was funded by the Characteristic Innovation Project of Guangdong Provincial Department of Education (2023KTSCX128) and National Natural Science Foundation of China (31902279).

Conflict of interest

The authors declare that the research was conducted in the absence of any commercial or financial relationships that could be construed as a potential conflict of interest.

Publisher's note

All claims expressed in this article are solely those of the authors and do not necessarily represent those of their affiliated organizations, or those of the publisher, the editors and the reviewers. Any product that may be evaluated in this article, or claim that may be made by its manufacturer, is not guaranteed or endorsed by the publisher.



OPEN ACCESS

EDITED BY

Lingxue Yu,
Chinese Academy of Agricultural Sciences,
China

REVIEWED BY

Pu Sun,
Chinese Academy of Agricultural Sciences,
China
Qingkui Jiang,
Rutgers University, Newark, United States

*CORRESPONDENCE

Zheng Feng
✉ greatz@126.com

RECEIVED 06 September 2023

ACCEPTED 09 October 2023

PUBLISHED 20 October 2023

CITATION

Pei Y, Lin C, Li H and Feng Z (2023) Genetic background influences pig responses to porcine reproductive and respiratory syndrome virus.
Front. Vet. Sci. 10:1289570.
doi: 10.3389/fvets.2023.1289570

COPYRIGHT

© 2023 Pei, Lin, Li and Feng. This is an open-access article distributed under the terms of the [Creative Commons Attribution License \(CC BY\)](https://creativecommons.org/licenses/by/4.0/). The use, distribution or reproduction in other forums is permitted, provided the original author(s) and the copyright owner(s) are credited and that the original publication in this journal is cited, in accordance with accepted academic practice. No use, distribution or reproduction is permitted which does not comply with these terms.

Genetic background influences pig responses to porcine reproductive and respiratory syndrome virus

Yangli Pei, Chenghong Lin, Hua Li and Zheng Feng*

Guangdong Provincial Key Laboratory of Animal Molecular Design and Precise Breeding, Key Laboratory of Animal Molecular Design and Precise Breeding of Guangdong Higher Education Institutes, School of Life Science and Engineering, Foshan University, Foshan, China

Porcine reproductive and respiratory syndrome virus (PRRSV) is a highly infectious and economically significant virus that causes respiratory and reproductive diseases in pigs. It results in reduced productivity and increased mortality in pigs, causing substantial economic losses in the industry. Understanding the factors affecting pig responses to PRRSV is crucial to develop effective control strategies. Genetic background has emerged as a significant determinant of susceptibility and resistance to PRRSV in pigs. This review provides an overview of the basic infection process of PRRSV in pigs, associated symptoms, underlying immune mechanisms, and roles of noncoding RNA and alternative splicing in PRRSV infection. Moreover, it emphasized breed-specific variations in these aspects that may have implications for individual treatment options.

KEYWORDS

porcine reproductive and respiratory syndrome, pig breeds, genetic backgrounds, PRRSV, PRRSV receptors, innate immunity, acquired immunity

1. Introduction

Porcine reproductive and respiratory syndrome (PRRS) is a highly destructive disease that was first identified in the United States in 1987, and later spread to Europe in 1990 (1, 2). It poses a considerable economic risk to the swine industry (3–5). The estimated economic impact of PRRS on the entire herd of four Chinese farms experiencing outbreaks is ¥1424.37 per sow (4). The PRRS virus (PRRSV) is the pathogen responsible for causing PRRS, characterized by its positive-stranded RNA nature and enveloped structure (6). It belongs to the order Nidovirales and the family Arteriviridae (6). PRRSVs are classified into PRRSV-1 and -2 genotypes that occur in Europe and North America, respectively (7). PRRSV-1 and -2 share approximately 60% nucleotide identity (1, 8); however, it is believed that they underwent separate evolutionary paths, originating from a distant common ancestor (9). PRRSV-2 primarily targets cells of the monocyte/macrophage lineage, particularly porcine alveolar macrophages (PAMs) (10).

The Prevention and control of PRRS poses a significant challenge. Current strategies include vaccination, herd management, biosecurity, and antiviral treatment (11). However, the effectiveness of these measures varies depending on specific circumstances and implementation strategies. Vaccination shows promising results in reducing the incidence and severity of PRRS; however, it does not offer a complete solution (12). Effective herd management (including monitoring and controlling pig movement) can help reduce the disease spread. Furthermore, biosecurity measures, such as disinfection and cleaning of facilities may help to prevent disease

transmission (11). Although antiviral treatment can reduce disease severity, although it is not a permanent cure and may not be cost-effective in all situations (13). Therefore, further research is necessary to identify and develop more effective methods to prevent and control PRRS.

The genetic background of pigs is a significant factor determining their response to PRRSV. Various pig breeds and lines exhibit different levels of resistance to PRRSV infection (14, 15). Meishan and Tongcheng (TC) breeds, known for their elevated resistance to PRRSV, are less susceptible to infection when compared to other breeds, such as the Large White (LW) (16–18). Moreover, specific pig tissues such as the lungs and lymph nodes may exhibit varying susceptibilities to PRRSV, which may be influenced by genetic factors (19). Enhanced knowledge of the genetic factors contributing to the differences in PRRSV resistance among pig breeds potentially improves pig health and welfare, ultimately reducing the economic losses associated with PRRSV infection.

Overall, controlling PRRS remains a challenge, owing to the complex host-pathogen interactions despite extensive research efforts. Further research is required to develop effective countermeasures against the virus. This review focuses on the influence of genetic factors on pig responses to PRRSV, including differences among pig breeds and lines. Furthermore, we investigated PRRSV infection mechanisms and factors affecting the host response, such as the innate and adaptive immune systems. Additionally, alternative splicing events and noncoding RNAs involved in PRRSV infection and replication were explored. The potential implications of this research were to develop effective control strategies and breeding programs that utilize genetic information to improve pig health and productivity. This extensive knowledge will potentially enhance pig well-being, increase productivity, and promote worldwide sustainability of pig farming.

2. Varied receptor responses in different pig breeds upon PRRSV invasion

2.1. Mechanisms of host cell entry

The PRRSV genome is approximately 15 kbp in size and has a specific organization. The replicase genes are situated at the 5'-end of the genome, whereas the genes encoding structural proteins are found at the 3'-end (20, 21). The viral genome consists of more than 10 open reading frames (ORFs). Over 66% of the viral genome is made up of ORF1a and ORF1b, which encode nonstructural proteins that serve crucial functions including protease and replicase activities. These proteins also modulate host genes that are vital for the replication of the virus. Conversely, ORFs 2–7 encode the structural proteins required for virus formation (21).

PRRSV processes of eight structural proteins, which include a small non-glycosylated protein and a group of glycosylated proteins: Glycoprotein (GP) 2ab, GP3, GP4, GP5, GP5a, matrix (M), and nucleocapsid (N) (21, 22). The primary structural proteins encoded by ORFs 5, 6, and 7 are GP5, M, and N, respectively. While GP5 typically forms a heterodimer with M, there have been reports of GP5 homodimers (23). Among the surface glycoproteins, GP2, GP3, and GP4, derived from ORFs 2, 3, and 4, respectively, act as minor

components. Additionally, two very small non-glycosylated proteins, designated as 2b or E and 5a, are translated from ORF2b and ORF5a, respectively (24, 25). The smooth exterior of the PRRSV virion is primarily attributed to the presence of short peptide sequences in the ectodomains of M and GP5. However, the larger ectodomains of GP2, GP3, and GP4 can also give rise to a few protrusions on the virus surface (21).

Macrophages are the primary target cells for PRRSV infection (10, 26–28), playing a crucial role in immune modulation and contributing to the respiratory distress observed in pigs affected by the porcine respiratory disease complex. The following section provides an overview of the recognition of the virus by recipient cells (Table 1) and the mechanisms involved.

CD163 serves as a crucial receptor for PRRSV and plays a critical role in determining cell susceptibility to the virus (29). It is a scavenger receptor glycoprotein predominantly found in mature macrophages and monocytes. The extracellular portion of CD163 comprises nine scavenger receptor cysteine-rich domains (SRCR) and two motifs rich in proline-serine-threonine (PST), which are repeated multiple times (56). The heterotrimeric GP2, GP3, and GP4 proteins of PRRSV bind to CD163, with GP2 and GP4 forming multiple interactions with different receptors (30, 56). Pigs with a *CD163* gene knockout (KO) are non-permissive to PRRSV-2 infection (31), and their macrophages show resistance to PRRSV-1 and -2 (32). Recent studies show that CD163 SRCR5-deficient pigs are resistant to specific PRRSV-2 strains (33, 34). Genetically engineered pigs with a modified CD163 SRCR5 domain display normal growth under standard conditions (34, 35). This suggests that gene editing techniques targeting CD163 can potentially control and eradicate PRRS outbreaks.

CD163 participates in viral apoptotic mimicry, a strategy employed by certain viruses to infect host cells (57). This mechanism involves viruses disguising themselves as apoptotic debris and engaging receptors on the surface of phagocytes that recognize phosphatidylserine (PtdSer), a marker of apoptosis (58). These interactions activate signaling cascades and lead to actin rearrangements to facilitate endocytic engulfment, and subsequent degradation of viral particles (59). Viruses adopt distinct mechanisms of apoptotic mimicry, giving rise to the concepts of classical and nonclassical apoptotic mimicry (60). PRRSV capitalizes on viral apoptotic mimicry to induce macropinocytosis through the involvement of T cell immunoglobulin and mucin domain proteins TIM-1 and -4 (57). During PRRSV infection, CD163 plays a vital role in facilitating TIM-induced macropinocytosis (61). Consequently, PRRSV adopts an alternative route of infection via macrophage activity involving CD163.

Mammalian cells contain heparin sulfate (HS) as a glycosaminoglycan on their surface and in their extracellular matrix (62). Heparin sulfate plays an important role in adhesion during PRRSV infection by interacting with M and GP5-M proteins during PRRSV infection (37). Although not essential for PRRSV invasion of porcine alveolar macrophages (PAMs), HS enables PRRSV to adhere to non-susceptible cell lines without completing the subsequent infection steps (38). PRRSV-1 and -2 exhibit different sensitivities to HS (37). The treatment of PAMs with heparinase (which degrades HS) reduces PRRSV infection (37). Moreover, PRRSV infection can activate NF- κ B and cathepsin L, resulting in heparinase upregulation and processing, reduction in HS surface expression, and promotion of viral replication and release (63).

TABLE 1 Major receptors and function during PRRSV infection.

Receptor	Function	References
CD163	CD163 interacts with PRRSV glycoproteins GP4 and GP2a to form a multiprotein complex. The presence of CD163 SRCR5 is essential for PRRSV infection, with its absence in pigs conferring resistance against different PRRSV strains. Furthermore, CD163 plays a vital role in TIM-induced macropinocytosis during PRRSV infection	(29–36)
Heparin sulfate (HS)	HS interacts with the M and GP5-M proteins of PRRSV, enabling efficient attachment of the virus to cells. However, it is not a prerequisite for PRRSV invasion of macrophages	(37, 38)
Sialoadhesin (Sn)	The N-terminal immunoglobulin domain of porcine Sn is critical factor that promotes PRRSV attachment to porcine alveolar macrophages (PAMs). Although it does not contribute to viral uncoating, Sn facilitates PRRSV internalization in expressing cells	(39–44)
Vimentin	Vimentin directly interacts with PRRSV nucleocapsid protein, and the application of antivimentin antibodies effectively block PRRSV	(45–48)
CD151	CD151 functions as an RNA-binding protein, and directly interacts with the 3'-UTR RNA of PRRSV. CD151 overexpression enhances PRRSV infection in non-susceptible cells, whereas blocking CD151 with antibodies inhibits PRRSV infection in susceptible cells	(49, 50)
Non-muscle myosin heavy chain 9 (MYH9)	Interaction of MYH9 with PRRSV GP5 protein is indispensable to facilitate PRRSV internalization and intercellular spread	(51–53)
Heat shock protein member 8 (HSPA8)	The PB domain of HSPA8 interacts with PRRSV GP4, and the ATPase activity of HSPA8 is crucial for PRRSV infection through clathrin-mediated endocytosis (CME). Furthermore, HSPA8 co-localizes with PRRSV on the cell surface, and plays a pivotal role in facilitating viral fusion and entry	(54, 55)

Sialoadhesin (Sn), also referred to as CD169 or SIGLIC-1, acts as a co-receptor for PRRSV invasion. The N-terminal immunoglobulin domain of porcine Sn is necessary and sufficient (39, 40). Cells expressing Sn facilitate PRRSV internalization, but do not promote viral uncoating (40). The collaboration between Sn and other receptors, such as CD163, sensitizes cells to PRRSV infection, promoting effective attachment, internalization, and disassembly of viral particles (41, 42). The absence of Sn in genetically-edited pigs does not disrupt PRRSV attachment/internalization or have any effect on disease progression or histopathology (64). This discrepancy between the *in vitro* and *in vivo* models of PRRSV receptors indicates conflicting outcomes. These findings suggest that Sn primarily plays a role in binding PRRSV to the macrophage surface rather than facilitating viral internalization.

Vimentin (VIM) is a crucial component of the PRRSV receptor complex and plays a key role in the intracellular replication and metastasis of PRRSV (45, 46). It forms a polymer with other fine-cell bone frame microfilaments and interacts with the PRRSV nucleocapsid protein (47). Vimentin can render normally non-susceptible cell lines susceptible to PRRSV infection. This highlights its involvement in the viral receptor complex (45). Following PRRSV entry, vimentin undergoes reorganization facilitated by Serine 38 phosphorylation by calcium calmodulin-dependent protein kinase II gamma (48). As a result of this reorganization, cage-like structures form around PRRSV replication complexes within the nucleus.

Tetraspanin superfamily member CD151 is an RNA-binding protein that interacts with the 3'-UTR of the PRRSV genome and functions as an RNA-binding protein (49). By silencing the CD151 gene in MARC-145 cells, PRRSV infection decreases significantly, and antibodies against CD151 prevent it entirely (49). CD151 expression can be regulated by microRNAs (such as miR-506) that lead to a decrease in CD151 mRNA and protein levels, thereby resulting in the inhibition of PRRSV replication and viral release in MARC-145 cells

(50). CD151 possesses N-glycosylation and palmitoylation sites (65); their involvement in regulating PRRSV infection requires further investigation.

Non-muscle myosin heavy chain 9 (MYH9) plays various roles in cell adhesion, polarization, morphogenesis, and migration (66, 67). It interacts with PRRSV GP5, which is crucial for PRRSV internalization and intercellular spread. The C-terminal domain of MYH9 directly binds to the first ectodomain of viral GP5, and disruption of this interaction reduces PRRSV internalization (51). Specific amino acid residues within the MYH9 C-terminal domain are believed to be key binding sites for GP5 (52). Furthermore, MYH9 undergoes reorganization upon PRRSV infection, forming cage-like structures around the PRRSV replication complex (53). MYH9 co-expression with CD163 enhances PRRSV infection (51).

Heat shock protein member 8 (HSPA8) plays a role in various viral infections by regulating viral entry, replication, and assembly (68). Inhibition of endogenous HSPA8 reduces PRRSV replication by decreasing viral attachment and internalization (54). HSPA8 interacts with clathrin, and is involved in clathrin-mediated endocytosis (CME) (69). The PB domain of HSPA8 interacts with PRRSV GP4, and HSPA8 ATPase activity is required for PRRSV infection via CME (54). Moreover, HSPA8 co-localizes with PRRSV on the cell surface and facilitates viral fusion and entry (54). HSPA8-based therapies show promise in clinical trials and vaccine development for other diseases. For instance, recombinant HSPA8 fused with GP3 and GP4 boosts immune responses and confers protective effects against the highly pathogenic PRRSV infection in pigs (55). Therefore, HSPA8-based strategies have the potential for vaccine development.

The viral genome contains more than 10 ORFs. These ORFs encode nonstructural proteins crucial for viral replication. ORFs 2–7 encode structural proteins that play vital roles in viral formation, and are necessary for viral particle assembly. PRRSV uses multiple receptors for entry into host cells, including CD163, Sn, HS, VIM, MYH9, CD151, CD209, and HSPA8. Understanding the interactions

between PRRSV and these receptors offers potential targets to control and eradicate PRRSV outbreaks, and to develop vaccines and therapeutic strategies.

2.2. Different pig breeds show varying expression of PRRSV receptor genes in lung tissues upon PRRSV infection

Chinese Dapulian pigs (DPL) exhibit increased resistance to PRRSV when compared to commercial Duroc×Landrace×Yorkshire (DLY) crossbred pigs, as evidenced by lower rectal temperatures and serum PRRSV copy numbers (70). Analysis of lung tissue samples from PRRSV-uninfected DPL and DLY pigs show varied expression patterns of five PRRSV mediator genes (NMMHC-IIA, SIGLEC1, CD163, HSPG2, and VIM), with significantly higher mRNA expression levels of SIGLEC1, NMMHC-IIA, CD163, and VIM in DLY pigs than those in DPL pigs (70). Another study revealed that the mRNA level of CD163 in PAMs of Dingyuan pigs is significantly lower than that of Jiangquhai pigs within 24 h post-infection (hpi); this may account for the high resistance of Jiangquhai pigs to PRRSV (71). Moreover, Sn expression in PAMs from Dingyuan pigs increase at a faster rate than that in PAMs from Jiangquhai pigs following viral infection (71). This finding corresponds to the high PRRSV content in PAMs from Dingyuan pigs (71). The increased mRNA expression levels of CD163 and Sn may contribute to more rapid viral invasion and wider penetration sites *in vivo* and *in vitro* (72). Viral receptor expression varies among different pig breeds after PRRSV infection, and there are variations in the expression of PRRSV receptors (HS, Sn, CD163, CD151, and VIM) in the lung tissues of different pig breeds, even under normal physiological conditions (47, 71, 73).

Variations in receptor expression and RNA abundance can lead to activation or inhibition of various pathways, resulting in distinct responses to PRRSV infection in different pig breeds. Further exploration of the mechanisms underlying these susceptibility differences could pave the way for the development of innovative approaches to control PRRSV infection in swine populations.

3. Variation in manifestations in different pig breeds during PRRSV-infection

3.1. Symptoms and lesions after PRRSV infection

The clinical manifestations of PRRS are influenced by multiple factors, including the virus strain, age and immune status of the host, production environment, productive state, and specific PRRSV strains. The typical symptoms during the acute phase of the disease include loss of appetite, weakness, fever, and respiratory difficulties. Respiratory dyspnea is commonly observed across all the age groups of pigs, although infected pregnant sows may exhibit more severe symptoms.

Pregnant sows are highly susceptible to PRRSV infection and may exhibit various clinical symptoms. This includes loss of appetite, abortions, transient discoloration of the ears (commonly known as blue ear disease, which affects approximately 2% of sows), early farrowing, prolonged anestrus, delayed return to heat after weaning, coughing, and respiratory signs (74).

Symptoms in weaned and fattened piglets can be significant and may include hair loss, slight loss of appetite, mild respiratory problems (such as coughing), and localized skin redness. The mortality rate during this stage ranges from 10 to 20% and is influenced by hygiene and operational management. The presence of other microorganisms within a herd can increase mortality rates. Pigs aged 4–12 weeks born by infected sows exhibit clinical symptoms similar to those of suckling pigs, including loss of appetite, malabsorption, wasting, coughing, and pneumonia, and a 12% higher post-weaning mortality rate (75, 76). Secondary bacterial infections can lead to lung and systemic abscesses, abscess-related lameness, or poor growth (77, 78).

A range of clinical symptoms indicates potential issues in farrowing sows. These symptoms include anorexia, decreased water intake, reduced milk production, mastitis, premature delivery of piglets, discoloration of the skin (such as, verticillium wilt or blue vulva and ears), pressure sores, lethargy, respiratory symptoms (such as, coughing and pneumonia), mummified piglets, stillborn piglets, and weak piglets at birth (77, 79).

Severe respiratory diseases and decreased survival rates are the most common issues in piglets. Other clinical symptoms included eyelid swelling, conjunctivitis, listlessness, significant weight loss, diarrhea, rough and unkempt fur, purple ear discoloration, and abnormal behavior (76, 77).

3.2. Clinical features of PRRSV infected pigs

Artificial infection of TC pigs and LW pigs with HP-PRRSV results in similar symptoms of high fever. LW pigs have a temperature above 40.5°C from 0 to 3 days post-contact (dpc) and above 41.0°C from 4 to 7 dpc, while TC pigs have a temperature above 40.5°C from 1 to 3 dpc and above 41.0°C from 4 to 6 dpc (18). However, the clinical signs are less severe in TC pigs than those in LW pigs, showing changes in lying behavior, less depression, deep breathing, skin flushing, and reduced food intake. Furthermore, TC pigs have significantly less inflammatory exudation ($p < 0.01$) and alveolar wall thickening ($p < 0.05$) when compared with LW pigs. Post-mortem analysis revealed varying degrees of swelling and bleeding in the brain, liver, and spleen, with jagged edges in the spleen (18).

Similarly, a study involving 4–6-week-old piglets of Tibetan, ZangMei black (ZM), and LW piglets challenged with HP-PRRSV (JXA1) showed that LW piglets had a significant increase in rectal temperature from 2 dpi that remained elevated until 15 dpi ($40.4^{\circ}\text{C} \pm 0.55$). ZM piglets exhibit a significant increase in rectal temperature for 4 days (2–5 dpi) with no readings above 40°C, and Tibetan piglets did not show any rectal temperature readings above 40°C. Anorexia, sneezing, coughing, and diarrhea appeared in the affected ZM and LW piglets within 2–3 dpi; however, LW piglets experienced more severe symptoms, including increased shivering, hyperspasmia, and respiratory rates from 6 to 8 dpi. Some of the challenged LW piglets died at 9, 11, and 13 dpi, whereas Tibetan piglets did not exhibit typical signs or death throughout the 28-day period (80). The observed clinical signs were aligned with corresponding changes in temperature and body weight gain. LW piglets showed decreased body weight during the second week following challenge, ZM piglets experienced weight loss during the first week, and Tibetan piglets showed consistent weight gain throughout the 4 weeks (80).

Porcine reproductive and respiratory syndrome virus infection has a notable effect on the clinical presentation and growth

performance of pigs, which can significantly vary among breeds. For example, LW pigs experience weight loss and mortality after PRRSV infection, whereas ZM pigs show no weight changes. In contrast, Tibetan pigs (known for their robust disease resistance) continue to exhibit weight gain throughout the infection (80).

3.3. Viral load after PRRSV infection

TC pigs display significantly lower viral loads than LW pigs after artificial HP-PRRSV infection. Moreover, TC pigs display a reduced peak viral load and maintain a steady decline throughout the infection period. The maximum quantity of PRRSV particles in TC pigs is 0.4 times that found in LW pigs; this suggests a superior ability to control viral replication in TC pigs (18).

A study of 100 pigs from NEI (a Large White-Landrace composite population) and 100 pigs from a cross between Hampshire and Duroc line (HD) inoculated with PRRSV (97–7895 strain) indicated that the viremia titer was greater in HD pigs than that in NEI pigs on days 4, 7, and 14, whereas the viral titers in the lungs and bronchial lymph nodes were significantly higher in HD pigs (14).

A study involving seven Miniature (MI) pigs and eight commercial Pietrain (PI) pigs challenged with an attenuated PRRSV strain shows that viremia peaks at 6 dpi, with 100% viremia observed in PI pigs and at 12 dpi, with 87% viremia noted in MI pigs (81). MI pigs have a reduced duration of viremia. Different genetic susceptibilities to PRRSV may contribute to variations in antibody production (81).

Inoculation of eight purebred boars (two Landrace, three Yorkshire, and three Hampshire) with VR-2332 detected PRRSV RNA in the serum and PBMC between 4 and 11 dpi. The virus is not detected in the lymphoid tissues of Landrace pigs at 47 and 88 dpi, whereas Yorkshire and Hampshire pigs show varying viral loads in lymphoid tissues. Yorkshire and Hampshire boars exhibit higher resistance to PRRSV shedding in semen than Landrace boars (82).

In 2015, Tibetan, Zang Mei, and Large White piglets were challenged with HP-PRRSV (JXA1). During the challenge, the serum viral load in LW piglets peaked at 7 dpi, which gradually decreased until 28 dpi. Zang Mei piglets had their viral peak virus at 4 dpi, which decreased rapidly, resulting in significantly lower viral loads when compared to LW piglets at 14 and 21 dpi (80). Tibetan pigs consistently exhibited lower viral loads than the other two breeds throughout the challenge (80).

The virus titer and mRNA abundance in PAM supernatants following inoculation with PRRSV NJGC *in vitro* show similar trends among Landrace, Erhualian, Suzhong, Jiangquhuai, Dingyuan, and Meishan breeds (71).

Different breeds exhibit significant variations in clinical features, growth performance, and viral titers owing to genetic variations that ultimately affect their ability to combat PRRSV. Some breeds, such as Meishan and Tongcheng, demonstrate a genetic advantage in fighting the virus that results in a reduction in the duration of viremia.

4. Varied immune responses in different pig breeds infected by PRRSV

The innate immune response serves as the initial defense against PRRSV that is known for its ability to evade the host immune system by downregulating pattern recognition receptors (PRRs) (83). Despite

viral evasion strategies, the innate immune response plays a vital role in controlling viral spread, minimizing tissue damage, and initiating the adaptive immune response (84). Essential cytokines [including interleukin-1 (IL-1), interleukin-6 (IL-6), interleukin-10 (IL-10), and tumor necrosis factor-alpha (TNF- α)] have multifaceted roles in influencing the outcome of PRRSV infection (Table 2) (16, 85–91). These cytokines modulate inflammation, exert antiviral effects, and activate immune cells (92).

The adaptive immune system (including antigen-presenting cells) offers broader and more sophisticated recognition of antigens (93). It relies on the specific recognition of antigens by T and B cells that are generated through gene rearrangements during lymphocyte development, resulting in unique but limited specificity (93). The innate immune system is vital for eliminating viruses; however, it may not always be adequate for eradicating pathogens (93). Acquired immune functions are responsible for eliminating viruses and providing long-term immunity.

The adaptive immune response to PRRSV involves the activation of T and B cells, resulting in the production of targeted antibodies and development of cellular immune responses (94). These immune responses are crucial to eradicate the virus and protect against reinfection. The intricate mechanisms underlying the adaptive immune response to PRRSV were extensively explored in previous reviews (94, 95).

Differences in immune responses were observed among various pig breeds infected with PRRSV (14, 15, 17–19, 47, 82, 96–101). For instance, TC pigs demonstrate enhanced resistance to PRRSV with milder clinical symptoms, fewer lung lesions, and lower viremia levels when compared to other breeds, such as LW pigs. These distinctions can be attributed to genetic factors and variations in cytokine levels. TC pigs show higher serum levels of interferon-gamma (IFN- γ) that is associated with a T cell-mediated cellular immune response, whereas LW pigs show elevated levels of interleukin-10 (IL-10) that can inhibit viral clearance and impede the immune response (17, 18). These indicate the presence of genetic variations that influence viral resistance or susceptibility.

Further analysis of lymph nodes from TC and LW pigs infected with PRRSV revealed genetic differences in antigen presentation, metabolism, and immune activation; this suggests that genetic variations contribute to divergent immune responses (17). Integrated analysis of transcriptomic and metabolomic data provides additional insights into the immune response to PRRSV infection by highlighting the importance of immune activation, antigen recognition capacity,

TABLE 2 Summary of different virus strains affecting different cell cytokines.

Virus strain	Cell line	Cytokines	References
JX, HV, VR2332	PAM	IL6 \uparrow	(85)
CH-1a, HV	PAM	IL8 \uparrow	(86)
CH-1a	PAM	IL15 \uparrow	(87)
JXwn06, CH-1a	PAM	IL12p40 \uparrow	(88)
WuH3	MARC-145	TNF- α \uparrow	(16)
HV, CH-1a	PAM, MARC145	IL17 \uparrow	(89)
NVSL 97-7895	moDCs	IL10 \uparrow	(90)
PRRSV-23983	moDCs	IFN- α \uparrow	(91)

cell metabolism, and the cell cycle in the clearance of PRRSV. This analysis reveals differences in lipid metabolism and amino acid pathways between resistant and susceptible pigs, and further illustrates the impact of genetic factors on immune response (98).

A comparison of the innate immune responses of conventional and specific-pathogen-free (SPF) Yorkshire pigs to PRRSV shows that SPF pigs have elevated levels of pro-inflammatory cytokines, such as IL-1 β , IL-6, and TNF- β , and higher IFN- β concentrations when compared to conventional pig breeds (102). Furthermore, SPF pigs exhibit lower viral RNA levels and less severe clinical symptoms in response to PRRSV infections (102). Meanwhile, a study of the innate immune responses of LW and Meishan pigs to PRRSV revealed that the Meishan breed produces a higher concentration of IFN- α and has lower viral loads when compared to the LW breed; this suggests a greater resistance to PRRSV owing to differences in their innate immune response (16).

Additionally, the viral genomic diversity of PRRSV (including differences in immune epitopes) contributes to its ability to evade the immune system (22). Genetic variability among PRRSV strains affects the response of pig breeds to infections. Landrace, Large White, and Yorkshire breeds are more susceptible to PRRSV, whereas Pietrain, Meishan, and Hampshire breeds are relatively resistant owing to stronger innate immune responses (82, 103). Dendritic cells derived from Pietrain pigs elicit a more potent T cell response; this underscores the significance of innate immunity in adaptive immunity (104). The susceptibility of pig breeds to PRRSV infection is primarily determined by genetic factors rather than environmental or husbandry factors.

Variations in genes associated with the innate immune response and resistance to PRRSV are identified. For example, single-nucleotide polymorphisms (SNPs) in genes such as *EIF2AK2*, *CD163*, *CD169*, and *RGS16* are linked to increased resistance against PRRSV infection (105).

The differences in innate immunity observed among various pig breeds suggest disparities in their genetic makeup. Implementing breeding initiatives aimed at enhancing innate immunity may be a valuable strategy to boost the health and productivity of swine herds. Breeders and researchers can identify the genetic markers responsible for heightened innate immunity and increased resistance to PRRSV by delving into the mechanisms that regulate innate immunity,

5. Differential alternative splicing events triggered by PRRSV invasion in different pig breeds

Alternative splicing (AS) is a crucial mechanism for post-transcriptional RNA processing and is responsible for significant modification of transcript sequences (106, 107). It is a critical mechanism in the regulation of eukaryotic gene expression via transcriptional control that enhances the versatility and diversity of transcriptomes and proteomes (108–111). This results in various alternative splicing events (ASEs), including skipped exons (SE), retained introns (RI), alternative 5' and 3' splicing sites (A5SS and A3SS), and mutually exclusive events (ME) (112, 113).

Porcine reproductive and respiratory syndrome virus infection profoundly affects alternative splicing in pigs. Specifically, immune response-related genes (such as interferon-stimulated genes) exhibit alternative splicing following PRRSV infection (114). This suggests that alternative splicing may play a role in regulating the host response

to viral infections, such as PRRSV. Additionally, PRRSV infection can trigger widespread AS events in the spleen and inguinal lymph nodes (ILN) of TC and LW pigs. PRRSV infection resulted in 373 and 595 genes displaying differential ASEs in the spleen and ILN in TC pigs, respectively (114). Meanwhile, 458 and 560 genes exhibit differential ASEs in the spleen and ILN, respectively in LW pigs. Gene Ontology functional analysis revealed that these genes are important for immune responses, transcriptional regulation, metabolism, and apoptosis (114). Furthermore, the response to PRRSV in terms of alternative splicing significantly differed between the TC and LW pigs. This suggests a possible link between PRRSV infection and genetic variation in these two pig breeds.

6. Functions of host non-coding RNAs in PRRSV infection and replication

Non-coding RNAs (ncRNAs) play diverse roles in PRRSV infection and replication. PRRSV is an RNA virus possessing a long untranslated region (UTR) downstream of its open reading frame, 1ab (21). Research suggests that the 3'-UTR plays a significant role in modulating targeted mRNAs in animals (115, 116). This indicates that the extended UTR in PRRSV could potentially serve as a pool of targets for host miRNAs.

miRNAs play a critical role in regulating viral replication and the host immune response infection during PRRSV. For example, miR-181 inhibits PRRSV *in vivo* and *in vitro*, and therapeutic delivery of miR-181 alleviates symptoms and prolongs the survival of highly pathogenic PRRSV-infected pigs (117). Furthermore, it downregulates the PRRSV receptor CD163, effectively hindering PRRSV infection. The construction of an miR-181 target site-mutated PRRSV demonstrated that miR-181 effectively blocked wild-type PRRSV invasion in the late stage, suggesting its significant impact on PRRSV infection and replication *in vivo*. Additionally, cellular miR-23 inhibits PRRSV replication by directly targeting PRRSV RNA and potentially upregulating type I interferon (118). MiR-378 and miR-505 suppress PRRSV replication by directly targeting PRRSV RNA (118), whereas miR-10a-5p inhibits PRRSV replication by suppressing SRP14 expression (119).

In contrast, PRRSV-induced miR-142-5p significantly promotes viral replication by directly targeting FAM134B (120). Conversely, let-7 family miRNAs inhibit PRRSV replication by targeting the 3'-UTR of the PRRSV-2 genome and porcine IL-6 (121). MiR-146a expression increases in macrophages during PRRSV infection, and positively affects the immune response by regulating the expression of genes, such as *CIQTNF3* and *MAFB* (122). Notably, neither PRRSV-infected target cells nor host pigs induce the production of type I interferon (IFN) proteins *in vivo* or *in vitro* (123). MiRNAs can be induced or repressed by type I IFN, although they can also play key roles in regulating innate immune responses by modulating the production of type I IFN and other important molecular pathways (124). In particular, miR-331-3p/miR-210 is involved in lung inflammation by targeting ORF1b and downregulating STAT1/TNF- α (16).

Let-7b, miR-26a, miR-34a, and miR-145 directly target sequences within the porcine IFN- β 3' UTR regions at positions 160–181, 9–31, 27–47, and 12–32 bp, respectively, to inhibit the expression of IFN- β protein in primary PAMs (125). Moreover, it is suggested that PRRSV can suppress the post-transcriptional expression of IFN- β

protein by upregulating these four miRNAs in cultured PAMs (126). MiR-199a-3p downregulates the protein expression of CD151, a receptor utilized by PRRSV (125). Additionally, miR-199a-3p is differentially expressed in the lung tissues of different pig breeds (such as, Tongcheng and Landrace) in the control and infection groups; this suggests its crucial role in regulating PRRSV infection in pigs (127). Furthermore, miR-378 and miR-10a-5p are upregulated in the control group of Tongcheng pigs when compared to those in the control group of Landrace pigs, and both miRNAs showed inhibitory effects on PRRSV replication (126).

Numerous studies have explored the role of miRNAs in the PRRSV process, shedding light on their regulatory mechanisms in viral infection, and revealing variations in miRNA expression among different pig breeds. These findings provide novel insights into the interaction between PRRSV and the host, and present promising avenues to develop antiviral strategies against PRRSV infection.

7. Future perspectives

Future research should focus on several key areas to advance our understanding of PRRSV infections and drive the development of effective control strategies.

First, extensive studies are required to investigate the genetic factors underlying the varied responses to PRRSV infection among different pig breeds. Identifying specific genes and genetic markers associated with PRRSV resistance or susceptibility will provide valuable insights into targeted breeding programs and the development of precision medicine approaches. Through genetic improvement and selective breeding methods, it is possible to rear pig breeds that exhibit enhanced resistance to PRRSV. Leveraging modern genetic engineering technologies and selective breeding methods, individuals with robust immune responses can be selected for reproduction, thereby gradually improving the overall PRRSV resistance within the entire pig population.

Second, rapid advancements in single-cell transcriptome sequencing and spatial transcriptomics present opportunities to gain in-depth molecular insights into PRRSV infection. Further research in these areas can provide a comprehensive understanding of viral spread within tissues, the dynamics of host-virus interactions, and how various host cell types contribute to the pathogenesis and immune response against PRRSV.

Furthermore, the functional roles of ncRNAs in PRRSV infection and replication should be explored. Additional investigations into the regulatory mechanisms of host ncRNAs in modulating viral replication, immune responses, and disease outcomes could lead to the development of novel therapeutic interventions and identification of potential biomarkers for diagnostic purposes.

Additionally, incorporating multi-omics approaches (such as transcriptomics, genomics, proteomics, and epigenomics) will provide a more comprehensive understanding of the complex molecular interplay between PRRSV and the host. The integration of these omics datasets could uncover crucial interactions, pathways, and networks involved in PRRSV infection and host responses that ultimately lead to more effective preventive and therapeutic strategies.

Lastly, efforts should continue to focus on sustainable pig farming practices that reduce reliance on antibiotics and mitigate

environmental impacts. This includes integrating genetic information into breeding programs to select disease resistance traits, advancing precision farming technologies for early detection and intervention, and promoting biosecurity measures to minimize the risk of pathogen transmission.

In conclusion, future PRRSV studies should advance our understanding of the genetic and molecular mechanisms underlying host-virus interactions, develop targeted control strategies, and promote sustainable pig farming practices. Harnessing these insights will facilitate more effective prevention, management, and control of PRRSV that benefit swine health and productivity.

8. Conclusion

Overall, the findings of this review contribute to a comprehensive understanding of the genetic factors underlying the varied responses to PRRSV in different pig breeds to PRRSV infection. This knowledge can be used to formulate more effective control measures for PRRSV, such as designing breeding programs to select resistance traits and developing targeted vaccines. Additionally, exploring the potential of genetic-based interventions and further research into host-virus interactions at the molecular level holds promise for future developments in PRRSV control and prevention.

Author contributions

YP: Writing – original draft, Writing – review & editing. CL: Writing – original draft. HL: Writing – review & editing. ZF: Writing – original draft, Writing – review & editing.

Funding

The author(s) declare financial support was received for the research, authorship, and/or publication of this article. This research was funded by the Guangdong Basic and Applied Basic Research Foundation (2020B1515120016), Key Technologies R&D Program of Guangdong Province (2022B0202090001).

Conflict of interest

The authors declare that the research was conducted in the absence of any commercial or financial relationships that could be construed as a potential conflict of interest.

Publisher's note

All claims expressed in this article are solely those of the authors and do not necessarily represent those of their affiliated organizations, or those of the publisher, the editors and the reviewers. Any product that may be evaluated in this article, or claim that may be made by its manufacturer, is not guaranteed or endorsed by the publisher.

References

1. Wensvoort G, Terpstra C, Pol JMA, ter Laak EA, Bloemraad M, de Kluyver EP, et al. Mystery swine disease in the Netherlands: the isolation of Lelystad virus. *Vet Q.* (1991) 13:121–30. doi: 10.1080/01652176.1991.9694296
2. Benfield DA, Nelson E, Collins JE, Harris L, Goyal SM, Robison D, et al. Characterization of swine infertility and respiratory syndrome (SIRS) virus (isolate ATCC VR-2332). *J Vet Diagn Invest.* (1992) 4:127–33. doi: 10.1177/104063879200400202
3. Neumann EJ, Kliebenstein JB, Johnson CD, Mabry JW, Bush EJ, Seitzinger AH, et al. Assessment of the economic impact of porcine reproductive and respiratory syndrome on swine production in the United States. *J Am Vet Med Assoc.* (2005) 227:385–92. doi: 10.2460/javma.2005.227.385
4. Zhang Z, Li Z, Li H, Yang S, Ren F, Bian T, et al. The economic impact of porcine reproductive and respiratory syndrome outbreak in four Chinese farms: based on cost and revenue analysis. *Front Vet Sci.* (2022) 9:1024720. doi: 10.3389/fvets.2022.1024720
5. Renken C, Nathues C, Swam H, Fiebig K, Weiss C, Eddicks M, et al. Application of an economic calculator to determine the cost of porcine reproductive and respiratory syndrome at farm-level in 21 pig herds in Germany. *Porcine Health Manag.* (2021) 7:3. doi: 10.1186/s40813-020-00183-x
6. Dea S, Gagnon CA, Mardassi H, Pirzadeh B, Rogan D. Current knowledge on the structural proteins of porcine reproductive and respiratory syndrome (PRRS) virus: comparison of the north American and European isolates. *Arch Virol.* (2000) 145:659–88. doi: 10.1007/s007050050662
7. Murtaugh MP, Shi M, Brar MS, Leung FCC. Evolutionary diversification of type 2 porcine reproductive and respiratory syndrome virus. *J Gen Virol.* (2015) 96:1570–80. doi: 10.1099/vir.0.000104
8. Allende R, Lewis TL, Lu Z, Rock DL, Kutish GF, Ali A, et al. North American and European porcine reproductive and respiratory syndrome viruses differ in non-structural protein coding regions. *J Gen Virol.* (1999) 80:307–15. doi: 10.1099/0022-1317-80-2-307
9. Plagemann PG. Porcine reproductive and respiratory syndrome virus: origin hypothesis. *Emerg Infect Dis.* (2003) 9:903–8. doi: 10.3201/eid0908.030232
10. Su CM, Rowland RRR, Yoo D. Recent advances in PRRS virus receptors and the targeting of receptor-ligand for control. *Vaccines (Basel).* (2021) 9:354. doi: 10.3390/vaccines9040354
11. du T, Nan Y, Xiao S, Zhao Q, Zhou EM. Antiviral strategies against PRRSV infection. *Trends Microbiol.* (2017) 25:968–79. doi: 10.1016/j.tim.2017.06.001
12. Kick AR, Grete AF, Crisci E, Almond GW, Käser T. Testable candidate immune correlates of protection for porcine reproductive and respiratory syndrome virus vaccination. *Vaccines (Basel).* (2023) 11:594. doi: 10.3390/vaccines11030594
13. Li Z, Li L, Zhao S, Li J, Zhou H, Zhang Y, et al. Re-understanding anti-influenza strategy: attach equal importance to antiviral and anti-inflammatory therapies. *J Thorac Dis.* (2018) 10:2248–59. doi: 10.21037/jtd.2018.03.169
14. Petry DB, Holl JW, Weber JS, Doster AR, Osorio FA, Johnson RK. Biological responses to porcine respiratory and reproductive syndrome virus in pigs of two genetic populations. *J Anim Sci.* (2005) 83:1494–502. doi: 10.2527/2005.8371494x
15. Vincent AL, Thacker BJ, Halbur PG, Rothschild MF, Thacker EL. *In vitro* susceptibility of macrophages to porcine reproductive and respiratory syndrome virus varies between genetically diverse lines of pigs. *Viral Immunol.* (2005) 18:506–12. doi: 10.1089/vim.2005.18.506
16. You X, Qu Y, Zhang Y, Huang J, Gao X, Huang C, et al. Mir-331-3p inhibits PRRSV-2 replication and lung injury by targeting PRRSV-2 ORF1b and porcine TNF- α . *Front Immunol.* (2020) 11:547144. doi: 10.3389/fimmu.2020.547144
17. Liang W, Meng X, Zhen Y, Zhang Y, Hu X, Zhang Q, et al. Integration of transcriptome and proteome in lymph nodes reveal the different immune responses to PRRSV between PRRSV-resistant Tongcheng pigs and PRRSV-susceptible large white pigs. *Front Genet.* (2022) 13:800178. doi: 10.3389/fgene.2022.800178
18. Liang W, Li Z, Wang P, Fan P, Zhang Y, Zhang Q, et al. Differences of immune responses between Tongcheng (Chinese local breed) and large white pigs after artificial infection with highly pathogenic porcine reproductive and respiratory syndrome virus. *Virus Res.* (2016) 215:84–93. doi: 10.1016/j.virusres.2016.02.004
19. Bates JS, Petry DB, Eudy J, Bough L, Johnson RK. Differential expression in lung and bronchial lymph node of pigs with high and low responses to infection with porcine reproductive and respiratory syndrome virus. *J Anim Sci.* (2008) 86:3279–89. doi: 10.2527/jas.2007-0685
20. Snijder EJ, Meulenbergh JJ. The molecular biology of arteriviruses. *J Gen Virol.* (1998) 79:961–79.
21. Dokland T. The structural biology of PRRSV. *Virus Res.* (2010) 154:86–97. doi: 10.1016/j.virusres.2010.07.029
22. Huang C, Zhang Q, Feng WH. Regulation and evasion of antiviral immune responses by porcine reproductive and respiratory syndrome virus. *Virus Res.* (2015) 202:101–11. doi: 10.1016/j.virusres.2014.12.014
23. Matanin BM, Huang Y, Meng XJ, Zhang C. Purification of the major envelop protein GP5 of porcine reproductive and respiratory syndrome virus (PRRSV) from native virions. *J Virol Methods.* (2008) 147:127–35. doi: 10.1016/j.jviromet.2007.08.018
24. Johnson CR, Griggs TF, Gnanandarajah J, Murtaugh MP. Novel structural protein in porcine reproductive and respiratory syndrome virus encoded by an alternative ORF5 present in all arteriviruses. *J Gen Virol.* (2011) 92:1107–16. doi: 10.1099/vir.0.030213-0
25. Wu WH, Fang Y, Farwell R, Steffen-Bien M, Rowland RRR, Christopher-Hennings J, et al. A 10-kDa structural protein of porcine reproductive and respiratory syndrome virus encoded by ORF2b. *Virology.* (2001) 287:183–91. doi: 10.1006/viro.2001.1034
26. Lawson SR, Rossow KD, Collins JE, Benfield DA, Rowland RRR. Porcine reproductive and respiratory syndrome virus infection of gnotobiotic pigs: sites of virus replication and co-localization with MAC-387 staining at 21 days post-infection. *Virus Res.* (1997) 51:105–13. doi: 10.1016/S0168-1702(97)00086-5
27. Duan X, Nauwynck HJ, Pensaert MB. Virus quantification and identification of cellular targets in the lungs and lymphoid tissues of pigs at different time intervals after inoculation with porcine reproductive and respiratory syndrome virus (PRRSV). *Vet Microbiol.* (1997) 56:9–19. doi: 10.1016/S0378-1135(96)01347-8
28. Kim HS, Kwang J, Yoon IJ, Joo HS, Frey ML. Enhanced replication of porcine reproductive and respiratory syndrome (PRRS) virus in a homogeneous subpopulation of MA-104 cell line. *Arch Virol.* (1993) 133:477–83. doi: 10.1007/BF01313785
29. Calvert JG, Slade DE, Shields SL, Jolie R, Mannan RM, Ankenbauer RG, et al. CD163 expression confers susceptibility to porcine reproductive and respiratory syndrome viruses. *J Virol.* (2007) 81:7371–9. doi: 10.1128/JVI.00513-07
30. Stoian AMM, Rowland RRR. Challenges for porcine reproductive and respiratory syndrome (PRRS) vaccine design: reviewing virus glycoprotein interactions with CD163 and targets of virus neutralization. *Vet Sci.* (2019) 6:9. doi: 10.3390/vetsci6010009
31. Whitworth KM, Rowland RRR, Ewen CL, Triple BR, Kerrigan MA, Cino-Ozuna AG, et al. Gene-edited pigs are protected from porcine reproductive and respiratory syndrome virus. *Nat Biotechnol.* (2016) 34:20–2. doi: 10.1038/nbt.3434
32. Burkard C, Lillico SG, Reid E, Jackson B, Mileham AJ, Ait-Ali T, et al. Precision engineering for PRRSV resistance in pigs: macrophages from genome edited pigs lacking CD163 SRCR5 domain are fully resistant to both PRRSV genotypes while maintaining biological function. *PLoS Pathog.* (2017) 13:e1006206. doi: 10.1371/journal.ppat.1006206
33. Xu K, Zhou Y, Mu Y, Liu Z, Hou S, Xiong Y, et al. CD163 and pAPN double-knockout pigs are resistant to PRRSV and TGEV and exhibit decreased susceptibility to PDCoV while maintaining normal production performance. *elife.* (2020) 9:9. doi: 10.7554/eLife.57132
34. Stoian AMM, Rowland RRR, Brandariz-Nunez A. Mutations within scavenger receptor cysteine-rich (SRCR) protein domain 5 of porcine CD163 involved in infection with porcine reproductive and respiratory syndrome virus (PRRS). *J Gen Virol.* (2022) 103:001740. doi: 10.1099/jgv.0.001740
35. Guo CH, Wang M, Zhu Z, He S, Liu H, Liu X, et al. Highly efficient generation of pigs harboring a partial deletion of the CD163 SRCR5 domain, which are fully resistant to porcine reproductive and respiratory syndrome virus 2 infection. *Front Immunol.* (2019) 10:1846. doi: 10.3389/fimmu.2019.01846
36. Ye N, Wang B, Feng W, Tang D, Zeng Z. PRRS virus receptors and an alternative pathway for viral invasion. *Virus Res.* (2022) 320:198885. doi: 10.1016/j.virusres.2022.198885
37. Delputte PL, Vanderheijden N, Nauwynck HJ, Pensaert MB. Involvement of the matrix protein in attachment of porcine reproductive and respiratory syndrome virus to a heparinlike receptor on porcine alveolar macrophages. *J Virol.* (2002) 76:4312–20. doi: 10.1128/JVI.76.9.4312-4320.2002
38. Delputte PL, Costers S, Nauwynck HJ. Analysis of porcine reproductive and respiratory syndrome virus attachment and internalization: distinctive roles for heparan sulphate and sialoadhesin. *J Gen Virol.* (2005) 86:1441–5. doi: 10.1099/vir.0.80675-0
39. Delputte PL, van Breedam W, Delrue I, Oetke C, Crocker PR, Nauwynck HJ. Porcine arterivirus attachment to the macrophage-specific receptor sialoadhesin is dependent on the sialic acid-binding activity of the N-terminal immunoglobulin domain of sialoadhesin. *J Virol.* (2007) 81:9546–50. doi: 10.1128/JVI.00569-07
40. An TQ, Tian ZJ, He YX, Xiao Y, Jiang YF, Peng JM, et al. Porcine reproductive and respiratory syndrome virus attachment is mediated by the N-terminal domain of the sialoadhesin receptor. *Vet Microbiol.* (2010) 143:371–8. doi: 10.1016/j.vetmic.2009.11.006
41. Delrue I, van Gorp H, van Doorselaere J, Delputte PL, Nauwynck HJ. Susceptible cell lines for the production of porcine reproductive and respiratory syndrome virus by stable transfection of sialoadhesin and CD163. *BMC Biotechnol.* (2010) 10:48. doi: 10.1186/1472-6750-10-48
42. Xie J, Vereecke N, Theuns S, Oh D, Vanderheijden N, Trus I, et al. Comparison of primary virus isolation in pulmonary alveolar macrophages and four different continuous cell lines for type 1 and type 2 porcine reproductive and respiratory syndrome virus. *Vaccines (Basel).* (2021) 9:594. doi: 10.3390/vaccines9060594
43. Vanderheijden N, Delputte PL, Favoreel HW, Vandekerckhove J, van Damme J, van Woensel PA, et al. Involvement of sialoadhesin in entry of porcine reproductive and respiratory syndrome virus into porcine alveolar macrophages. *J Virol.* (2003) 77:8207–15. doi: 10.1128/JVI.77.15.8207-8215.2003
44. van Breedam W, van Gorp H, Zhang JQ, Crocker PR, Delputte PL, Nauwynck HJ. The M/GP(5) glycoprotein complex of porcine reproductive and respiratory syndrome virus binds the sialoadhesin receptor in a sialic acid-dependent manner. *PLoS Pathog.* (2010) 6:e1000730. doi: 10.1371/journal.ppat.1000730

45. Kim JK, Fahad AM, Shanmukhappa K, Kapil S. Defining the cellular target(s) of porcine reproductive and respiratory syndrome virus blocking monoclonal antibody 7G10. *J Virol.* (2006) 80:689–96. doi: 10.1128/JVI.80.2.689-696.2006
46. Wang WW, Zhang L, Ma XC, Gao JM, Xiao YH, Zhou EM. The role of vimentin during PRRSV infection of Marc-145 cells. *Bing Du Xue Bao.* (2011) 27:456–61. doi: 10.13242/j.cnki.bingduxuebao.002205
47. Shi C, Liu Y, Ding Y, Zhang Y, Zhang J. PRRSV receptors and their roles in virus infection. *Arch Microbiol.* (2015) 197:503–12. doi: 10.1007/s00203-015-1088-1
48. Zheng XX, Li R, Qiao S, Chen XX, Zhang L, Lu Q, et al. Vimentin rearrangement by phosphorylation is beneficial for porcine reproductive and respiratory syndrome virus replication *in vitro*. *Vet Microbiol.* (2021) 259:109133. doi: 10.1016/j.vetmic.2021.109133
49. Shanmukhappa K, Kim JK, Kapil S. Role of CD151, A tetraspanin, in porcine reproductive and respiratory syndrome virus infection. *Virol J.* (2007) 4:62. doi: 10.1186/1743-422X-4-62
50. Wu J, Peng X, Zhou A, Qiao M, Wu H, Xiao H, et al. MiR-506 inhibits PRRSV replication in MARC-145 cells via CD151. *Mol Cell Biochem.* (2014) 394:275–81. doi: 10.1007/s11010-014-2103-6
51. Gao J, Xiao S, Xiao Y, Wang X, Zhang C, Zhao Q, et al. MYH9 is an essential factor for porcine reproductive and respiratory syndrome virus infection. *Sci Rep.* (2016) 6:25120. doi: 10.1038/srep25120
52. Xue B, Hou G, Zhang G, Huang J, Li L, Nan Y, et al. MYH9 aggregation induced by direct interaction with PRRSV GP5 ectodomain facilitates viral internalization by permissive cells. *Front Microbiol.* (2019) 10:2313. doi: 10.3389/fmicb.2019.02313
53. Li L, Zhang L, Hu Q, Zhao L, Nan Y, Hou G, et al. MYH9 key amino acid residues identified by the anti-idiotypic antibody to porcine reproductive and respiratory syndrome virus glycoprotein 5 involve in the virus internalization by porcine alveolar macrophages. *Viruses.* (2020) 12:40. doi: 10.3390/v12010040
54. Wang L, Li R, Geng R, Zhang L, Chen XX, Qiao S, et al. Heat shock protein member 8 (HSPA8) is involved in porcine reproductive and respiratory syndrome virus attachment and internalization. *Microbiol Spectr.* (2022) 10:e0186021. doi: 10.1128/spectrum.01860-21
55. Li J, Jiang P, Li Y, Wang X, Cao J, Wang X, et al. HSP70 fused with GP3 and GP5 of porcine reproductive and respiratory syndrome virus enhanced the immune responses and protective efficacy against virulent PRRSV challenge in pigs. *Vaccine.* (2009) 27:285–32. doi: 10.1016/j.vaccine.2008.11.088
56. Stoian AMM, Rowland RRR, Brandariz-Núñez A. Identification of CD163 regions that are required for porcine reproductive and respiratory syndrome virus (PRRSV) infection but not for binding to viral envelope glycoproteins. *Virology.* (2022) 574:71–83. doi: 10.1016/j.virol.2022.07.012
57. Wei X, Li R, Qiao S, Chen XX, Xing G, Zhang G. Porcine reproductive and respiratory syndrome virus utilizes viral apoptotic mimicry as an alternative pathway to infect host cells. *J Virol.* (2020) 94:e00709–20. doi: 10.1128/JVI.00709-20
58. Segawa K, Nagata S. An apoptotic 'Eat Me' signal: phosphatidylserine exposure. *Trends Cell Biol.* (2015) 25:639–50. doi: 10.1016/j.tcb.2015.08.003
59. Cvetanovic M, Ucker DS. Innate immune discrimination of apoptotic cells: repression of proinflammatory macrophage transcription is coupled directly to specific recognition. *J Immunol.* (2004) 172:880–9. doi: 10.4049/jimmunol.172.2.880
60. Amara A, Mercer J. Viral apoptotic mimicry. *Nat Rev Microbiol.* (2015) 13:461–9. doi: 10.1038/nrmicro3469
61. Diaz-Griffero F, Jackson AP, Brojatsch J. Cellular uptake of avian leukosis virus subgroup B is mediated by clathrin. *Virology.* (2005) 337:45–54. doi: 10.1016/j.virol.2005.02.027
62. Mulloy B, Lever R, Page CP. Mast cell glycosaminoglycans. *Glycoconj J.* (2017) 34:351–61. doi: 10.1007/s10719-016-9749-0
63. Guo C, Zhu Z, Guo Y, Wang X, Yu P, Xiao S, et al. Heparanase upregulation contributes to porcine reproductive and respiratory syndrome virus release. *J Virol.* (2017) 91:e00625–17. doi: 10.1128/JVI.00625-17
64. Prather RS, Rowland RRR, Ewen C, Triple B, Kerrigan M, Bawa B, et al. An intact sialoadhesin (Sn/IGLEC1/CD169) is not required for attachment/internalization of the porcine reproductive and respiratory syndrome virus. *J Virol.* (2013) 87:9538–46. doi: 10.1128/JVI.00177-13
65. Hasegawa H, Watanabe H, Nomura T, Utsunomiya Y, Yanagisawa K, Fujita S. Molecular cloning and expression of mouse homologue of SFA-1/PETA-3 (CD151), a member of the transmembrane 4 superfamily. *Biochim Biophys Acta.* (1997) 1353:125–30. doi: 10.1016/S0167-4781(97)00095-X
66. Li L, Xue B, Sun W, Gu G, Hou G, Zhang L, et al. Recombinant MYH9 protein C-terminal domain blocks porcine reproductive and respiratory syndrome virus internalization by direct interaction with viral glycoprotein 5. *Antivir Res.* (2018) 156:10–20. doi: 10.1016/j.antiviral.2018.06.001
67. Vicente-Manzanares M, Ma X, Adelstein RS, Horwitz AR. Non-muscle myosin II takes Centre stage in cell adhesion and migration. *Nat Rev Mol Cell Biol.* (2009) 10:778–90. doi: 10.1038/nrm2786
68. Vega-Almeida TO, Salas-Benito M, de Nova-Ocampo MA, del Angel RM, Salas-Benito JS. Surface proteins of C6/36 cells involved in dengue virus 4 binding and entry. *Arch Virol.* (2013) 158:1189–207. doi: 10.1007/s00705-012-1596-0
69. Yu A, Shibata Y, Shah B, Calamini B, Lo DC, Morimoto RI. Protein aggregation can inhibit clathrin-mediated endocytosis by chaperone competition. *Proc Natl Acad Sci U S A.* (2014) 111:E1481–90. doi: 10.1073/pnas.1321811111
70. Jiang C, Xing F, Xing J, Jiang Y, Zhou E. Different expression patterns of PRRSV mediator genes in the lung tissues of PRRSV resistant and susceptible pigs. *Dev Comp Immunol.* (2013) 39:127–31. doi: 10.1016/j.dci.2012.01.003
71. Meng CH, Su L, Li Y, Zhu Q, Li J, Wang H, et al. Different susceptibility to porcine reproductive and respiratory syndrome virus infection among Chinese native pig breeds. *Arch Virol.* (2018) 163:2155–64. doi: 10.1007/s00705-018-3821-y
72. Wang F, Qiu H, Zhang Q, Peng Z, Liu B. Association of two porcine reproductive and respiratory syndrome virus (PRRSV) receptor genes, CD163 and SN with immune traits. *Mol Biol Rep.* (2012) 39:3971–6. doi: 10.1007/s11033-011-1177-4
73. You X, Li G, Lei Y, Xu Z, Zhang P, Yang Y. Role of genetic factors in different swine breeds exhibiting varying levels of resistance/susceptibility to PRRSV. *Virus Res.* (2023) 326:199057. doi: 10.1016/j.virusres.2023.199057
74. Nodelijk G. Porcine reproductive and respiratory syndrome (PRRS) with special reference to clinical aspects and diagnosis. *A review Vet Q.* (2002) 24:95–100. doi: 10.1080/01652176.2002.9695128
75. Salguero FJ, Frossard JP, Rebel MJM, Stadejek T, Morgan SB, Graham SP, et al. Host-pathogen interactions during porcine reproductive and respiratory syndrome virus 1 infection of piglets. *Virus Res.* (2015) 202:135–43. doi: 10.1016/j.virusres.2014.12.026
76. Cilverd H, Martín-Valls G, Li Y, Martín M, Cortey M, Mateu E. Infection dynamics, transmission, and evolution after an outbreak of porcine reproductive and respiratory syndrome virus. *Front Microbiol.* (2023) 14:1109881. doi: 10.3389/fmicb.2023.1109881
77. Done SH, Paton DJ. Porcine reproductive and respiratory syndrome: clinical disease, pathology and immunosuppression. *Vet Rec.* (1995) 136:32–5. doi: 10.1136/vr.136.2.32
78. Paiva RC, Moura CA, Thomas P, Haberl B, Greiner L, Rademacher CJ, et al. Risk factors associated with sow mortality in breeding herds under one production system in the midwestern United States. *Prev Vet Med.* (2023) 213:105883. doi: 10.1016/j.prevetmed.2023.105883
79. Pejsak Z, Stadejek T, Markowska-Daniel I. Clinical signs and economic losses caused by porcine reproductive and respiratory syndrome virus in a large breeding farm. *Vet Microbiol.* (1997) 55:317–22. doi: 10.1016/S0378-1135(96)01326-0
80. Kang RM, Ji G, Yang X, Lv X, Zhang Y, Ge M, et al. Investigation on host susceptibility of Tibetan pig to infection of porcine reproductive and respiratory syndrome virus through viral challenge study. *Vet Microbiol.* (2016) 183:62–8. doi: 10.1016/j.vetmic.2015.11.035
81. Reiner G, Willems H, Pesch S, Ohlinger VF. Variation in resistance to the porcine reproductive and respiratory syndrome virus (PRRSV) in Pietrain and miniature pigs. *J Anim Breed Genet.* (2010) 127:100–6. doi: 10.1111/j.1439-0388.2009.00818.x
82. Christopher-Hennings J, Holler LD, Benfield DA, Nelson EA. Detection and duration of porcine reproductive and respiratory syndrome virus in semen, serum, peripheral blood mononuclear cells, and tissues from Yorkshire, Hampshire, and landrace boars. *J Vet Diagn Investig.* (2001) 13:133–42. doi: 10.1177/104063870101300207
83. Fitzgerald KA, Kagan JC. Toll-like receptors and the control of immunity. *Cells.* (2020) 180:1044–66. doi: 10.1016/j.cell.2020.02.041
84. Ishii KJ, Koyama S, Nakagawa A, Coban C, Akira S. Host innate immune receptors and beyond: sensing of microbial infections. *Cell Host Microbe.* (2008) 3:352–63. doi: 10.1016/j.chom.2008.05.003
85. Xu Y, Wang H, Zhang X, Zheng X, Zhu Y, Han H, et al. Highly pathogenic porcine reproductive and respiratory syndrome virus (HP-PRRSV) induces IL-6 production through TAK-1/JNK/AP-1 and TAK-1/NF-kappaB signaling pathways. *Vet Microbiol.* (2021) 256:109061. doi: 10.1016/j.vetmic.2021.109061
86. Liu Y, du Y, Wang H, du L, Feng WH. Porcine reproductive and respiratory syndrome virus (PRRSV) up-regulates IL-8 expression through TAK-1/JNK/AP-1 pathways. *Virology.* (2017) 506:64–72. doi: 10.1016/j.virol.2017.03.009
87. du L, Liu Y, du Y, Wang H, Zhang M, du Y, et al. Porcine reproductive and respiratory syndrome virus (PRRSV) up-regulates IL-15 through PKCbeta1-TAK1-NF-kappaB signaling pathway. *Virology.* (2016) 496:166–74. doi: 10.1016/j.virol.2016.06.007
88. Yu Z, Huang C, Zhang Q, Feng WH. Porcine reproductive and respiratory syndrome virus (PRRSV) induces IL-12p40 production through JNK-AP-1 and NF-kappaB signaling pathways. *Virus Res.* (2016) 225:73–81. doi: 10.1016/j.virusres.2016.09.009
89. Wang H, du L, Liu F, Wei Z, Gao L, Feng WH. Highly pathogenic porcine reproductive and respiratory syndrome virus induces Interleukin-17 production via activation of the IRAK1-PI3K-p38MAPK-C/EBPbeta/CREB pathways. *J Virol.* (2019) 93:e01100–19. doi: 10.1128/JVI.01100-19
90. Flores-Mendoza L, Silva-Campa E, Reséndiz M, Osorio FA, Hernández J. Porcine reproductive and respiratory syndrome virus infects mature porcine dendritic cells and up-regulates interleukin-10 production. *Clin Vaccine Immunol.* (2008) 15:720–5. doi: 10.1128/0162-0224-07
91. Zhang H, Guo X, Nelson E, Christopher-Hennings J, Wang X. Porcine reproductive and respiratory syndrome virus activates the transcription of interferon alpha/beta (IFN-alpha/beta) in monocyte-derived dendritic cells (Mo-DC). *Vet Microbiol.* (2012) 159:494–8. doi: 10.1016/j.vetmic.2012.04.025

92. Bi J, Song S, Fang L, Wang D, Jing H, Gao L, et al. Porcine reproductive and respiratory syndrome virus induces IL-1 ss production depending on TLR4/MyD88 pathway and NLRP3 inflammasome in primary porcine alveolar macrophages. *Mediat Inflamm.* (2014) 2014:1–14. doi: 10.1155/2014/403515
93. Bonilla FA, Oettgen HC. Adaptive immunity. *J Allergy Clin Immunol.* (2010) 125:S33–40. doi: 10.1016/j.jaci.2009.09.017
94. Sang Y, Rowland RR, Blecha F. Interaction between innate immunity and porcine reproductive and respiratory syndrome virus. *Anim Health Res Rev.* (2011) 12:149–67. doi: 10.1017/S1466252311000144
95. Loving CL, Osorio FA, Murtaugh MP, Zuckermann FA. Innate and adaptive immunity against porcine reproductive and respiratory syndrome virus. *Vet Immunol Immunopathol.* (2015) 167:1–14. doi: 10.1016/j.vetimm.2015.07.003
96. Thanawongnuwech R, Halbur PG, Ackermann MR, Thacker EL, Royer RL. Effects of low (modified-live virus vaccine) and high (VR-2385)-virulence strains of porcine reproductive and respiratory syndrome virus on pulmonary clearance of copper particles in pigs. *Vet Pathol.* (1998) 35:398–406. doi: 10.1177/030098589803500509
97. Drigo M, Giacomini E, Lazzaro M, Pasotto D, Bilato D, Ruggeri J, et al. Comparative evaluation of immune responses of swine in PRRS-stable and unstable herds. *Vet Immunol Immunopathol.* (2018) 200:32–9. doi: 10.1016/j.vetimm.2018.04.007
98. Wu Q, Han Y, Wu X, Wang Y, Su Q, Shen Y, et al. Integrated time-series transcriptomic and metabolomic analyses reveal different inflammatory and adaptive immune responses contributing to host resistance to PRRSV. *Front Immunol.* (2022) 13:960709. doi: 10.3389/fimmu.2022.960709
99. Xu Y, Zhang Y, Sun S, Luo J, Jiang S, Zhang J, et al. The innate immune DNA sensing cGAS-STING signaling pathway mediates anti-PRRSV function. *Viruses.* (2021) 13:1829. doi: 10.3390/v13091829
100. Xu Y, Ye M, Zhang Y, Sun S, Luo J, Jiang S, et al. Screening of porcine innate immune adaptor signaling revealed several anti-PRRSV signaling pathways. *Vaccines (Basel).* (2021) 9:1176. doi: 10.3390/vaccines9101176
101. Zhu Z, Zhang X, Dong W, Wang X, He S, Zhang H, et al. TREM2 suppresses the proinflammatory response to facilitate PRRSV infection via PI3K/NF-kappaB signaling. *PLoS Pathog.* (2020) 16:e1008543. doi: 10.1371/journal.ppat.1008543
102. Eclercy J, Larcher T, Andraud M, Renson P, Bernard C, Bigault L, et al. PCV2 co-infection does not impact PRRSV MLV1 safety but enhances virulence of a PRRSV MLV1-like strain in infected SPF pigs. *Vet Microbiol.* (2020) 244:108656. doi: 10.1016/j.vetmic.2020.108656
103. Wang SJ, Liu WJ, Yang LG, Sargent CA, Liu HB, Wang C, et al. Effects of FUT1 gene mutation on resistance to infectious disease. *Mol Biol Rep.* (2012) 39:2805–10. doi: 10.1007/s11033-011-1039-0
104. Islam MA, Große-Brinkhaus C, Pröll MJ, Uddin MJ, Aqter Rony S, Tesfaye D, et al. PBMC transcriptome profiles identifies potential candidate genes and functional networks controlling the innate and the adaptive immune response to PRRSV vaccine in Pietrain pig. *PLoS One.* (2017) 12:e0171828. doi: 10.1371/journal.pone.0171828
105. Dong Q, Dunkelberger J, Lim KS, Lunney JK, Tuggle CK, Rowland RRR, et al. Associations of natural variation in the CD163 and other candidate genes on host response of nursery pigs to porcine reproductive and respiratory syndrome virus infection. *J Anim Sci.* (2021) 99:skab274. doi: 10.1093/jas/skab274
106. Fica SM, Nagai K. Cryo-electron microscopy snapshots of the spliceosome: structural insights into a dynamic ribonucleoprotein machine. *Nat Struct Mol Biol.* (2017) 24:791–9. doi: 10.1038/nsmb.3463
107. Papasaikas P, Valcarcel J. The spliceosome: the ultimate RNA chaperone and sculptor. *Trends Biochem Sci.* (2016) 41:33–45. doi: 10.1016/j.tibs.2015.11.003
108. Hu B, Li X, Huo Y, Yu Y, Zhang Q, Chen G, et al. Cellular responses to HSV-1 infection are linked to specific types of alterations in the host transcriptome. *Sci Rep.* (2016) 6:28075. doi: 10.1038/srep28075
109. Boudreault S, Martenon-Brodeur C, Caron M, Garant JM, Tremblay MP, Armero VES, et al. Global profiling of the cellular alternative RNA splicing landscape during virus-host interactions. *PLoS One.* (2016) 11:e0161914. doi: 10.1371/journal.pone.0161914
110. Bonenfant G, Meng R, Shotwell C, Badu P, Payne AF, Ciota AT, et al. Asian zika virus isolate significantly changes the transcriptional profile and alternative RNA splicing events in a neuroblastoma cell line. *Viruses.* (2020) 12:510. doi: 10.3390/v12050510
111. Fabozzi G, Oler AJ, Liu P, Chen Y, Minday S, Dolan MA, et al. Strand-specific dual RNA sequencing of bronchial epithelial cells infected with influenza A/H3N2 viruses reveals splicing of gene segment 6 and novel host-virus interactions. *J Virol.* (2018) 92:e00518–18. doi: 10.1128/JVI.00518-18
112. Ule J, Blencowe BJ. Alternative splicing regulatory networks: functions, mechanisms, and evolution. *Mol Cell.* (2019) 76:329–45. doi: 10.1016/j.molcel.2019.09.017
113. Baralle FE, Giudice J. Alternative splicing as a regulator of development and tissue identity. *Nat Rev Mol Cell Biol.* (2017) 18:437–51. doi: 10.1038/nrm.2017.27
114. Zhang Y, Xue L, Xu H, Liang W, Wu Q, Zhang Q, et al. Global analysis of alternative splicing difference in peripheral immune organs between Tongcheng pigs and large white pigs artificially infected with PRRSV *in vivo*. *Biomed Res Int.* (2020) 2020:4045204. doi: 10.1155/2020/4045204
115. Pasquinelli AE. NON-CODING RNA MicroRNAs and their targets: recognition, regulation and an emerging reciprocal relationship. *Nat Rev Genet.* (2012) 13:271–82. doi: 10.1038/nrg3162
116. Guo XK, Zhang Q, Gao L, Li N, Chen XX, Feng WH. Increasing expression of MicroRNA 181 inhibits porcine reproductive and respiratory syndrome virus replication and has implications for controlling virus infection. *J Virol.* (2013) 87:1159–71. doi: 10.1128/JVI.02386-12
117. Gao L, Guo XK, Wang L, Zhang Q, Li N, Chen XX, et al. MicroRNA 181 suppresses porcine reproductive and respiratory syndrome virus (PRRSV) infection by targeting PRRSV receptor CD163. *J Virol.* (2013) 87:8808–12. doi: 10.1128/JVI.00718-13
118. Zhang Q, Guo XK, Gao L, Huang C, Li N, Jia X, et al. MicroRNA-23 inhibits PRRSV replication by directly targeting PRRSV RNA and possibly by upregulating type I interferons. *Virology.* (2014) 450–451:182–95. doi: 10.1016/j.virol.2013.12.020
119. Zhao G, Hou J, Xu G, Xiang A, Kang Y, Yan Y, et al. Cellular microRNA miR-10a-5p inhibits replication of porcine reproductive and respiratory syndrome virus by targeting the host factor signal recognition particle 14. *J Gen Virol.* (2017) 98:624–32. doi: 10.1099/jgv.0.000708
120. Guan K, Su Q, Kuang K, Meng X, Zhou X, Liu B. MiR-142-5p/FAM134B Axis manipulates ER-Phagy to control PRRSV replication. *Front Immunol.* (2022) 13:842077. doi: 10.3389/fimmu.2022.842077
121. You X, Liu M, Liu Q, Li H, Qu Y, Gao X, et al. miRNA let-7 family regulated by NEAT1 and ARID3A/NF-kappaB inhibits PRRSV-2 replication *in vitro* and *in vivo*. *PLoS Pathog.* (2022) 18:e1010820. doi: 10.1371/journal.ppat.1010820
122. Hicks JA, Yoo D, Liu HC. Characterization of the microRNAome in porcine reproductive and respiratory syndrome virus infected macrophages. *PLoS One.* (2013) 8:e82054. doi: 10.1371/journal.pone.0082054
123. Forster SC, Tate MD, Hertzog PJ. MicroRNA as type I interferon-regulated transcripts and modulators of the innate immune response. *Front Immunol.* (2015) 6:1–9. doi: 10.3389/fimmu.2015.00334
124. Wang LL, Zhou L, Hu D, Ge X, Guo X, Yang H. Porcine reproductive and respiratory syndrome virus suppresses post-transcriptionally the protein expression of IFN-beta by upregulating cellular microRNAs in porcine alveolar macrophages *in vitro*. *Exp Ther Med.* (2018) 15:115–26. doi: 10.3892/etm.2017.5397
125. Zhen Y, Wang F, Liang W, Liu J, Gao G, Wang Y, et al. Identification of differentially expressed non-coding RNA in porcine alveolar macrophages from Tongcheng and large white pigs responded to PRRSV. *Sci Rep.* (2018) 8:15621. doi: 10.1038/s41598-018-33891-0
126. Li J, Chen Z, Zhao J, Fang L, Fang R, Xiao J, et al. Difference in microRNA expression and editing profile of lung tissues from different pig breeds related to immune responses to HP-PRRSV. *Sci Rep.* (2015) 5:9549. doi: 10.1038/srep09549
127. Li L, Gao F, Zheng H, Jiang Y, Tong W, Zhou Y, et al. Utilizing host endogenous microRNAs to negatively regulate the replication of porcine reproductive and respiratory syndrome virus in MARC-145 cells. *PLoS One.* (2018) 13:e0200029. doi: 10.1371/journal.pone.0200029



OPEN ACCESS

EDITED BY

Mengmeng Zhao,
Foshan University, China

REVIEWED BY

Bin Zhou,
Nanjing Agricultural University, China
Zhang Teng,
Nanyang Normal University, China

*CORRESPONDENCE

Aibing Wang

✉ bingaiwang@hunau.edu.cn

Jun Yao

✉ yaojun_joshua@hotmail.com

RECEIVED 10 October 2023

ACCEPTED 09 November 2023

PUBLISHED 27 November 2023

CITATION

Tan L, Wang K, Bai P, Zhang S, Zuo M, Shu X,
Wang A and Yao J (2023) Host cellular factors
involved in pseudorabies virus attachment and
entry: a mini review.
Front. Vet. Sci. 10:1314624.
doi: 10.3389/fvets.2023.1314624

COPYRIGHT

© 2023 Tan, Wang, Bai, Zhang, Zuo, Shu, Wang
and Yao. This is an open-access article
distributed under the terms of the [Creative
Commons Attribution License \(CC BY\)](#). The
use, distribution or reproduction in other
forums is permitted, provided the original
author(s) and the copyright owner(s) are
credited and that the original publication in this
journal is cited, in accordance with accepted
academic practice. No use, distribution or
reproduction is permitted which does not
comply with these terms.

Host cellular factors involved in pseudorabies virus attachment and entry: a mini review

Lei Tan^{1,2}, Kaixin Wang², Ping Bai³, Shuo Zhang³, Mengting Zuo⁴,
Xianghua Shu⁵, Aibing Wang^{2*} and Jun Yao^{6*}

¹College of Animal Science, Yangtze University, Jingzhou, China, ²College of Veterinary Medicine, Hunan Agricultural University, Changsha, China, ³Yunnan Southwest Agriculture and Animal Husbandry Group Co., Ltd, Kunming, China, ⁴Hunan Provincial Key Laboratory of the TCM Agricultural Biogenomics, Changsha Medical University, Changsha, Hunan, China, ⁵College of Animal Medicine, Yunnan Agricultural University, Kunming, China, ⁶Yunnan Tropical and Subtropical Animal Virus Diseases Laboratory, Yunnan Animal Science and Veterinary Institute, Kunming, China

Pseudorabies virus (PRV) belongs to the *Alphaherpesvirinae* subfamily and serves as an exceptional animal model for investigating the infection mechanism of Herpes simplex virus type 1. Notably, PRV has the capability to infect a wide range of mammals, including humans, highlighting its potential as an overlooked zoonotic pathogen. The attachment and entry steps of PRV into host cells are crucial to accomplish its life cycle, which involve numerous cellular factors. In this mini review, we offer a comprehensive summary of current researches pertaining to the role of cellular factors in PRV attachment and entry stages, with the overarching goal of advancing the development of novel antiviral agents against this pathogen.

KEYWORDS

pseudorabies virus, cellular factors, involvement, viral attachment and entry, antiviral strategies

Introduction

Pseudorabies virus (PRV), belonging to the subfamily *Alphaherpesvirinae*, is an enveloped double-stranded DNA virus (1). A variety of mammals, such as pigs, wild boars, goats, cattle, dogs, cats, and minks, are susceptible to the infection of PRV (2). Only pigs and wild boars are the unique nature hosts for PRV, clinical symptoms of pseudorabies (PR) caused by PRV in pigs are primarily characterized by central neural disorders in piglets with high morbidity, reproductive diseases in pregnant sows (2). Moreover, the prevalence of PRV also poses a huge threat to humans, with numerous of human encephalitis or endophthalmitis cases caused by PRV infection recently documented in China (3). Unfortunately, effective antiviral agents for treating PRV infections in both humans and animals remain limited.

Similar to other viruses, PRV infection involves multiple steps, including viral attachment, entry, replication, assembly, extracellular trafficking, and viral egress (4). Among these processes, viral attachment and entry are the initial steps in completing the virus's life cycle. Importantly, the virus could interact with or hijack various cellular factors to facilitate its attachment and entry efficiency. Thus, understanding the involvement of these cellular factors or their interactions with viral proteins during virus attachment and entry is critical for developing novel strategies to combat this pathogen. Numerous cellular proteins/factors have been reported to play roles in PRV attachment and entry stages, including Human HveC (Nectin-1) (5), Nectin-2 (6), Neuropilin-1 (NRP1) (7), Niemann-Pick1 (NPC1) (8, 9), porcine paired

immunoglobulin-like type 2 receptor α (PILR α) (10) and beta (PILR β) (11), etc. Meanwhile, a variety of cellular factors have been identified to inhibit viral attachment and entry, including the cholesterol 25-hydroxycholesterol (CH25H) (12), IFN-induced transmembrane protein 1 (IFITM1) (13), and IFITM2 (14).

In this mini review, we provide a comprehensive summary of the latest information focusing on cellular factors involved in PRV attachment and entry stages (Table 1; Figure 1). This summary aims to offer new insights for developing novel strategies against PRV infection, such as antiviral agents.

Cellular factors facilitating PRV attachment and entry

Viral attachment and entry steps are pivotal in establishing the virus life cycle within host cells, and they also partly determine the

TABLE 1 Function and antiviral strategies against cellular factors involved in PRV attachment and entry.

Factor	Function	Antiviral strategies
Nectin-1	Entry receptor Nectin-1 directly interacted with PRV gD (5)	Gene-modified mice (15, 16)
Nectin-2	Entry receptor? Knockout of nectin-2 suppressed PRV infection <i>in vitro</i> (6)	NA
NRP1	Attachment and entry receptor NRP1 directly interacted with the gB, gD, and gH (7)	NA
NPC1	Entry receptor? NPC1 inhibitor treatment blocked PRV entry <i>in vitro</i> and showed anti-PRV activity <i>in vivo</i> (mice) (5, 8)	Inhibitor (5, 8)
THBS3	Attachment and entry co-receptor THBS3 directly interacted with the PRV gD (17)	Antibody and soluble protein (17)
PILR α	Entry receptor? PILR α antibody blocked PRV entry (18)	Antibody (18)
PILR β	Attachment or entry receptor? PRV gB directly interacted with PILR β to mediate NK cells cytotoxicity (11)	NA
SM	Entry receptor? SM inhibitor suppressed PRV entry <i>in vitro</i> (19)	Inhibitor (19)
SMS1	Entry receptor? Knockout of SMS1 inhibited PRV entry <i>in vitro</i> (20)	NA

specificity of tissue or host cell infection (22, 23). These processes involve interactions between viral glycoproteins (e.g., gB, gC, gD, gH/gL, etc.) and cellular factors on the host cell membrane, facilitating the viral absorption and entry into host cells (23).

Nectin1 and nectin-2

Nectin-1 or nectin-2 are members of the nectin family, characterized by three Ig-like domains in the ectodomain (IgV-IgC-IgC), as well as transmembrane and cytoplasmic regions (24). These proteins are widely expressed in all tissues of mammals and involved in cell–cell adhesion (24). Growing evidence supports their roles as primary receptors for various *Alphaherpesvirus* infection *in vitro* and *in vivo*. For instance, Krummenacher et al. revealed that the C-terminal region of HSV-1 gD interacted with the N-terminal region of nectin-1, facilitating HSV-1 entry into host cells (25). Soluble nectin-1 protein treatment inhibited HSV-1 entry into different cell lines (5). Deletion of nectin-1 in animal experiments prevented viral infection and significantly alleviated clinical symptoms caused by HSV-1 or HSV-2 infection (26). Nectin-2 plays similar roles in HSV-1 infection compared to nectin-1 (27).

Both nectin-1 and nectin-2 are essential cellular factors for PRV infection. CHO-K1 cells, which lack *Alphaherpesvirus* receptors, are resistant to PRV infection. Li et al. found that over-expression of nectin-1 in CHO-K1 cells promoted PRV entry (5). Further investigation revealed that PRV gD directly interacted with both human and swine nectin-1, with higher binding affinity observed for human nectin-1 (5). Considering the high amino acid homology (96%) between porcine and human nectin-1, it is plausible that human nectin-1 may participate in PRV cross-transmission from pig to humans (5).

Another study generated nectin-1 or nectin-2 knockout (KO) PK15 cells via CRISPR/Cas9 technology, and found that these KO cells exhibited greater resistance to PRV infection compared with wild-type cells (6). Interestingly, further research showed that the deletion of nectin-1 or nectin-2 reduced the cell-to-cell spread ability of PRV, without affecting viral absorption and entry steps (6).

Moreover, nectin-1 mutant (F129A) mice presented milder clinical symptoms, decreased viral loads in tissue samples, and lower mortality rates when infected with PRV (16). Additionally, transgenic mice expressing soluble form of porcine nectin-1 protein were resistant to PRV infection (15). Consequently, nectin-1 represents an ideal target for combating PRV both *in vitro* and *in vivo*, through developing antibodies and chemical inhibitors against nectin-1, even generating nectin-1 gene-modified pigs, which may offer novel approaches against PRV infection in the future.

Neuropilin-1

NRP1 is a cell-surface receptor involved in a variety of biological processes, including angiogenesis, regulating vascular permeability, nervous system development, and tumorigenesis. NRP1 also acts as an essential co-receptor promoting the entry and replication stages of various viruses, such as Kaposi's sarcoma-associated herpesvirus (KSHV) (21), SARS-CoV-2 (28), Epstein–Barr virus (EBV) (29). However, a recent research showed that NRP1 was a restricting factor inhibiting HIV attachment of progeny virions to target cells (30).

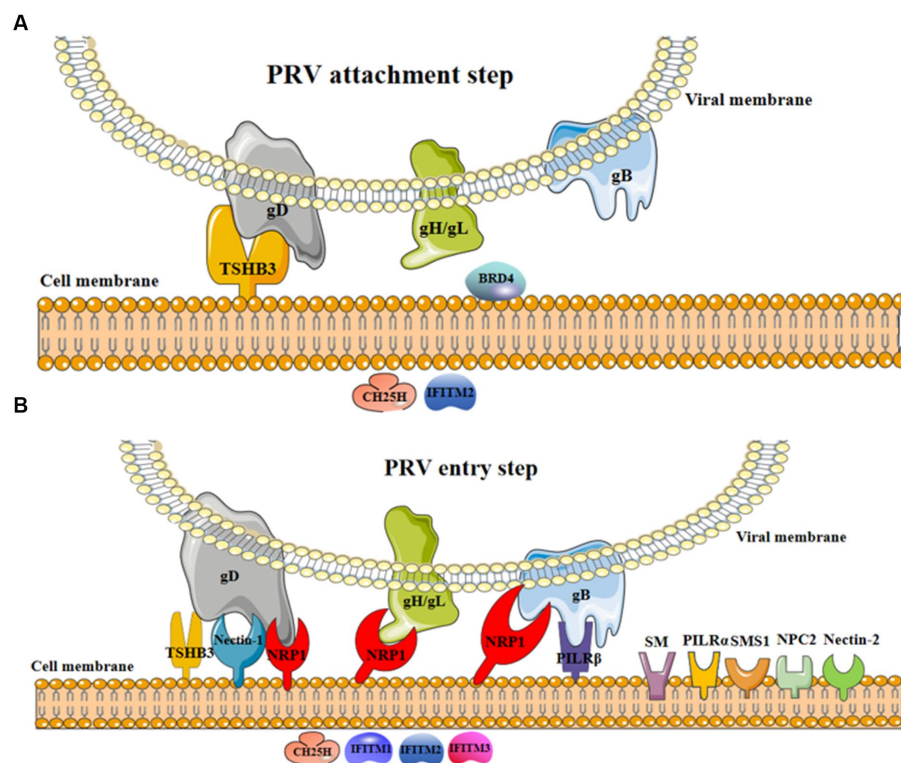


FIGURE 1

The involvement of cellular factors in PRV attachment and entry steps. **(A)** In the process of viral attachment, the interaction of cellular TSHB3 and PRV gD promoted viral attachment (17); BRD4 might promote viral attachment (21); CH25H and IFITM2 were restricted factors limiting viral attachment (12, 14). **(B)** In the process of viral entry, the interaction of cellular TSHB3 (gD) (17), nectin-1 (gD) (5), NRP1 (gD, gH/gL, and gB) (7), and PILR β (gB) (11) and PRV glycoproteins promote viral entry into host cells; nectin-2 (6), NPC1 (5, 8), PILR α (18), SM (19), and SMS1 (20) were potential factors promoting viral entry; CH25H (12) and IFITM1-3 (13, 14) were restricted factors inhibiting viral entry.

The involvement of NRP1 in PRV infection has been elucidated recently. Chen et al. first demonstrated that over-expression of NRP1 increased the production progeny viruses in PRV-infected cells, while inhibiting the endogenous expression of NRP1 suppressed viral replication in SK-N-SH cells (7). Further analysis revealed that over-expression of NRP1 enhanced viral attachment and entry efficiency into CHO cells, indicating that NRP1 might promote PRV entry (7). Furthermore, a cell-to-cell fusion assay revealed that NRP1 over-expression promoted viral glycoprotein-mediated cell-to-cell fusion (7). Co-immunoprecipitation (Co-IP) and BiFC assays indicated that NRP1 directly interacted with the gB, gD, and gH, suggesting that NRP1 promoted PRV attachment and entry by interacting with these viral glycoproteins (7). Moreover, PRV gB was found to accelerate NRP1 degradation via a lysosome-dependent pathway and this process was dependent on its furin-cleavage activity (7). Collectively, these findings underscore the essential roles of NRP1 in PRV attachment and entry into host cells, and suggest that NRP1 inhibitors could be effective agents for PRV prevention and treatment.

Niemann-pick C1

NPC1 belongs to the cholesterol family that is essential for the lysosomal cholesterol transport from late endosomes to cellular membrane (31). Abnormal expression of NPC1 is associated with

various cancers (32, 33). Recently, the contribution of NPC1 to virus infection has garnered attention, and the NPC1-specific inhibitor, U18666A, has been widely used to explore the potential roles of NPC1 in viral infection (34).

Li et al. first investigated the antiviral activities of inhibitors targeting proteins involved in lipid metabolism against PRV infection and found that U18666A inhibited PRV proliferation *in vitro* (8). Furthermore, viral replication ability was significantly suppressed in NPC1-knockout PK15 cells, while this effect was reversed by the over-expression of wild-type NPC1 in NPC1-knockout cells (8). However, no significant difference in PRV proliferation was observed between wide-type and NPC1-knockout cells after U18661A treatment, indicating that U18666A inhibited PRV infection via a NPC1-dependent pathway (8). Further investigation revealed that U18666A treatment primarily blocked viral entry by decreasing cholesterol aggregation in the plasma membrane, thus inhibiting the biological activities of clathrin-coated pits (8). Importantly, U18666A treatment improved the survival rates of PRV-infected mice by decreasing cytokines production and viral loads in different tissues (8). Overall, these results suggested that NPC1 is involved in PRV entry. However, another study suggested that U18666A treatment suppressed PRV infection by inhibiting the release of PRV particles (9). Thus, cellular NPC1 might participate in multiple stages of PRV life cycle, warranting further investigation.

Thrombospondin 3

Thrombospondin 3 (THBS3) is a member of the THBS family involved in cell–cell and cell–matrix interactions, and participating in the development of skeletal muscle. Additionally, the knockout of THBS3 in mice increases the stability and production of integrin membranes, providing protection against disease-causing stimuli for the heart (35).

Pan et al. first identified THBS3 as a novel co-receptor for PRV entry into cells (17). Following a strategy similar to the exploration of NPC1's role in PRV infection, Pan et al. investigated the effects of THBS3 knockdown, knockout, and over-expression on PRV proliferation. The results revealed that siRNA targeting THBS3 or THBS3 knockout effectively inhibited PRV-GFP (a recombinant PRV strain expressing GFP) infection in different cell lines (17). Moreover, both THBS3 antibody and soluble THBS3 protein treatment demonstrated similar antiviral activities against PRV-GFP infection, while THBS3 over-expression promoted PRV-GFP infection in PK15 cells (17).

Co-IP and pull-down assays demonstrated that both the N and C terminals of THBS3 directly interacted with PRV gD, but not gC and gB (17). And THBS3 over-expression promoted PRV binding/attachment to PK15 and CHO cells, with no impact on the expression and cellular location of nectin-1 (17). However, over-expression of THBS3 enhanced nectin-1 mediated viral fusion and entry efficiency (17). Considering the direct interaction between gD and THBS3 during PRV infection, and the multiple roles of THBS3 in viral infection, the potential of THBS3 as an antiviral target *in vivo* needs further exploration in the future.

Porcine paired immunoglobulin-like 2 receptor alpha and beta (PILR α and PILR β)

Porcine paired immunoglobulin-like 2 receptors (PILRs) belong to the member of the immunoglobulin superfamily, consist of two subtypes, PILR α and PILR β . The genetic sequences of PILR α and PILR β are conserved among different mammal species, yet their regulatory activities in the innate and adaptive immune systems differ. PILR α and PILR β are widely expressed in various immune system-related cells, including the dendritic cells, NK cells, monocytes, etc. Importantly, these receptors have drawn significant attention due to their involvements in *Alphaherpesvirus* infection.

Satoh et al. found that CHO-K1 cells with PILR α over-expression were effectively infected with HSV-1 and PRV, while the infection abilities of HSV-1 and PRV were completely inhibited after PILR α antibody treatment (10, 18). Further investigation revealed that PILR α participated in HSV-1 infection by interacting with gB during viral entry step (10).

Concerning PILR β , Pelsmaeker et al. found that expression of PRV gB accelerated the NK cell-mediated killing of gB-transfected swine kidney cells, which was also observed in PRV-infected cells (11). Further flow cytometric analysis demonstrated that PRV gB increased the binding activity of recombinant PILR β protein to the gB-transfected cells (11). These results underscore the essential roles of PILR β in PRV infection-mediated NK cell toxicity.

Sphingomyelin

Sphingomyelin (SM) is a primary component of the phospholipids found in the mammalian plasma membrane, actively contributing to the formation of lipid rafts in conjunction with the cholesterol (36). Pastenkos et al. made the noteworthy discovery that treatment with *Staphylococcus aureus*-derived sphingomyelinase (SMase) resulted in robust inhibition of PRV entry, as SMase treatment significantly reduced SM staining intensity, signifying the crucial role of SM in PRV entry (19). Furthermore, a recent study demonstrated that the knockout of sphingomyelin synthase 1 (SMS1) led to a significant inhibition of PRV entry into the rabbit PK13 cells (20).

Cellular factors inhibiting PRV attachment and entry

During viral entry, PRV glycoproteins (such as gB and gH) mediate membrane fusion processes that facilitate the penetration of viral capsid into the cytoplasm (37). Subsequently, the viral DNA genome is transported to the host nucleus, where it replicates, triggering host antiviral immune responses, as thoroughly summarized in recent reviews (38, 39). Some cellular factors involved in the innate immune response exhibit antiviral activities during PRV attachment or/and entry step.

IFN-induced transmembrane proteins

The IFITMs family, comprising five subtypes (IFITM1, IFITM2, IFITM3, IFITM5, and IFITM10) in humans, is conserved and mainly localized in the endo-lysosomal and plasma membranes. IFITMs are involved in various processes, including stem cell properties, DNA damage, and the activation of innate immune processes (40). Swine IFITMs family (IFITM1, IFITM2, and IFITM3) have been shown to inhibit multiple virus infections, including PRV (13, 14).

Wang et al. demonstrated that IFITM1 transcription was significantly up-regulated in PRV-infected cells (PK15 and 3D4/21 cells) (13). Knockdown of IFITM1, but not IFITM2 and IFITM3, enhanced PRV replication in PK15 cells, while over-expression of IFITM1 displayed antiviral activity (13). Further analysis revealed that IFITM1 knockdown promoted PRV entry into the target cells, suggesting that IFITM1 acts as a restricting factor limiting PRV entry, although its impact on PRV attachment requires further investigation (13).

Another study indicated that PRV infection significantly up-regulated the transcription of IFITM1, IFITM2, and IFITM3 at 12 h post-infection (hpi) and 24 hpi (14). Over-expression of IFITM1, IFITM2, or IFITM3 inhibited PRV replication, while knockdown of these IFITMs enhanced PRV replication efficiency (14). Further research demonstrated that all three IFITM subtypes restricted PRV entry into cells, with IFITM2 specifically interfering with PRV binding efficiency, a process that depends on cholesterol accumulation (14).

Cholesterol 25-hydroxylase

CH25H is a multi-transmembrane endoplasmic reticulum-associated enzyme responsible for catalyzing cholesterol into 25-hydrocholesterol (25HC) (41). CH25H belongs to the interferon-stimulated genes and broadly resists viral infection via different pathways (42).

Wang et al. reported that PRV infection increased the CH25H mRNA levels at 12 hpi and 24 hpi. Subsequent research showed that CH25H overexpression or 25HC treatment suppressed PRV replication (12). Further investigations, utilizing TCID₅₀ and western blot assays, revealed that 25HC treatment suppressed PRV attachment and entry steps (12). Collectively, the results suggest that CH25H negatively affected PRV replication by interfering with viral attachment and entry (12).

Bromodomain protein 4

Bromodomain protein 4 (BRD4), a member of the bromodomain and Extra-Terminal domain (BET) family, possesses a bromodomain that can bind to acetylated histones, participating in various cellular processes such as DNA repair, replication, and transcription (21). Moreover, the functions of BRD4 on PRV infection have received attention recently (21).

Wang et al. initially found that BRD4 inhibitors exhibited anti-PRV infection ability through GFP-reporter assays. Inhibition of BRD4 did not affect the transcription of viral genes but significantly suppressed PRV attachment (21). BRD4 inhibitor treatment or knockdown significantly inhibited PRV attachment, as revealed by RT-qPCR and western blot assays (21). Moreover, pre-treatment of JQ-1, a BRD4 inhibitor, increased the survival rate of PRV-infected mice compared to the control group (21). Mechanistically, BRD4 inhibitor treatment induced chromatin decompaction and double DNA damage, subsequently activating cGAS-dependent innate immune responses (21).

Perspective and concluding remarks

As of now, PRV continues to be a significant pathogen, causing substantial financial losses in the global swine industry. Furthermore, the potential for PRV transmission from pigs to other animal species has raised concerns, even prompting public alarm regarding the virus's potential risk to humans. Like other *Alphaherpesviruses*, PRV can establish latency in swine, thus making it challenging to eradicate through vaccination efforts.

Intracellular obligate pathogens, including viruses, depend on cellular components to accomplish their life cycles (8). Among the critical stages for viral infection, attachment and entry represent ideal targets for the development of antiviral strategies, akin to generating CD163 gene knockout pigs for PRRSV control (43). In the case of PRV, nectin-1 has been extensively studied as a cellular receptor for PRV entry and/or cell-to-cell spread, and genetic modification targeting nectin-1 holds promise for antiviral activities against PRV in mouse models. Thus, it is reasonable to expect that nectin-1 gene-edited pigs would be resistant to PRV infection, although ongoing monitoring of the clinical performance of these gene-edited pigs is

essential, given the multiple roles of nectin-1. Moreover, the development of antibodies and inhibitors against nectin-1 could be effective approach for PRV treatment, since the antiviral activity of antibodies against PRV or HSV-1 has been observed *in vitro* (39, 44).

Apart from nectin-1 and nectin-2, various cellular proteins involved in the promotion of PRV attachment and entry have been identified, partly due to the extensive research into the infection mechanisms of other *herpesviruses* and public concerns about PRV. However, it remains unclear which PRV-encoded proteins are involved in binding or interacting with the newly identified cellular factors, such as NPC1, SM, and SMS1 (8, 19, 20). Addressing these concerns will deepen our understanding of viral pathogenesis, and facilitate the development of vaccines and antiviral agents.

Additionally, this review has summarized four cellular factors negatively regulating PRV attachment and entry steps, including interferon-stimulated genes (IFITM1, IFITM2, and CH25H) and BRD4. However, several questions require clarification: (1) Further investigations should be performed to confirm the antiviral activities of these cellular factors against PRV *in vivo*. (2) It has been reported that PRV tegument proteins and glycoproteins can suppress the innate immune responses induced by virus infection (45). Such as PRV UL24, which can directly inhibit the transcription of multiple interferon-stimulated genes (e.g., OASL and ISG20 genes) (46). Therefore, further research is needed to determine whether PRV-encoded proteins can directly interact with or reduce the expression level of these cellular proteins (IFITM1, IFITM2, CH25H, and BRD4).

Functionally, cellular factors played similar roles in *Herpesvirus* infection, such as NRP1, which was identified as an entry factor promoting different *Herpesvirus* infection, including PRV (7), EBV (29), and KSHV (21). While NRP1 was recently identified as an antiviral agent inhibiting HIV infection, mainly via suppressing the infectivity of HIV-1 progeny virions and the viral transmission ability (30). NRP1 inhibitors effectively suppressed PRV infection *in vitro*, however, the co-infection of PRV and other pathogens were frequently detected in clinical samples (47). Further efforts will explore the roles of PRV attachment or entry-related cellular factors in other swine virus' infection, to comprehensively assess the possibility of these cellular factors in developing antiviral agents.

Conclusion

In summary, the prevalence of PRV remains a global concern, posing significant risks to human health. Recent researches have shed light on the roles of cellular factors in PRV attachment and entry steps, providing valuable insights for the development of novel antiviral approaches. However, our current understanding of PRV attachment and entry mechanisms is still incomplete. Therefore, further efforts are required to identify additional cellular factors involved in PRV attachment and entry, and explore their effects. Moreover, there is an urgent need to develop innovative antiviral agents such as chemical inhibitors, antibodies, and peptides, that can effectively target cellular factors like nectin-1 and nectin-2, which play crucial role in PRV attachment and entry. These advancements will undoubtedly contribute to the prevention and control of PRV in the future.

Author contributions

LT: Writing – original draft, Writing – review & editing. KW: Data curation, Writing – review & editing. PB: Manuscript revision & diagram preparation. SZ: Manuscript preparation, Review & Modification-polish. MZ: Writing – review & editing. XS: Funding acquisition, Writing – review & editing. AW: Funding acquisition, Writing – review & editing. JY: Funding acquisition, Writing – review & editing.

Funding

The author(s) declare financial support was received for the research, authorship, and/or publication of this article. This research was funded by the Major Specialized Projects of Yunnan Science and Technology (no. 202102AE090007) and Innovation Guidance and Technology-Based Enterprise Cultivation Program (no. 202304BI090003). Support was also provided by “Furong” Scholar funding to AW. Research and industrialization of large-scale and healthy pig farming technology (No. 202102AE090046).

References

1. Sun Y, Luo Y, Wang CH, Yuan J, Li N, Song K, et al. Control of swine pseudorabies in China: opportunities and limitations. *Vet Microbiol.* (2016) 183:119–24. doi: 10.1016/j.vetmic.2015.12.008
2. Tan L, Yao J, Yang Y, Luo W, Yuan X, Yang L, et al. Current status and challenge of pseudorabies virus infection in China. *Virol Sin.* (2021) 36:588–607. doi: 10.1007/s12250-020-00340-0
3. Liu Q, Wang X, Xie C, Ding S, Yang H, Guo S, et al. A novel human acute encephalitis caused by pseudorabies virus variant strain. *Clin Infect Dis.* (2020) 73:e3690–700. doi: 10.1093/cid/ciaa987
4. Pomeranz LE, Reynolds AE, Hengartner CJ. Molecular biology of pseudorabies virus: impact on neurovirology and veterinary medicine. *Microbiol Mol Biol Rev.* (2005) 69:462–500. doi: 10.1128/mmmbr.69.3.462-500.2005
5. Li A, Lu G, Qi J, Wu L, Tian K, Luo T, et al. Structural basis of nectin-1 recognition by pseudorabies virus glycoprotein D. *PLoS Pathog.* (2017) 13:e1006314. doi: 10.1371/journal.ppat.1006314
6. Huang Y, Li Z, Song C, Wu Z, Yang H. Resistance to pseudorabies virus by knockout of nectin1/2 in pig cells. *Arch Virol.* (2020) 165:2837–46. doi: 10.1007/s00705-020-04833-x
7. Chen M, Wang MH, Shen XG, Liu H, Zhang YY, Peng JM, et al. Neuropilin-1 facilitates pseudorabies virus replication and viral glycoprotein B promotes its degradation in a Furin-dependent manner. *J Virol.* (2022) 96:e0131822. doi: 10.1128/jvi.01318-22
8. Li G, Su B, Fu P, Bai Y, Ding G, Li D, et al. NPC1-regulated dynamic of clathrin-coated pits is essential for viral entry. *Sci China Life Sci.* (2022) 65:341–61. doi: 10.1007/s11427-021-1929-y
9. Song B. The cholesterol transport inhibitor U18666A interferes with pseudorabies virus infection. *Viruses.* (2022) 14:1539. doi: 10.3390/v14071539
10. Satoh T, Arai J, Suenaga T, Wang J, Kogure A, Uehori J, et al. PILRalpha is a herpes simplex virus-1 entry coreceptor that associates with glycoprotein B. *Cells.* (2008) 132:935–44. doi: 10.1016/j.cell.2008.01.043
11. De Pelsmaeker S, Dierick E, Klupp B, Mettenleiter TC, Cantoni C, Vitale M, et al. Expression of the pseudorabies virus gB glycoprotein triggers NK cell cytotoxicity and increases binding of the activating NK cell receptor PILRβ. *J Virol.* (2019) 93:e02107-18. doi: 10.1128/jvi.02107-18
12. Wang J, Zeng L, Zhang L, Guo ZZ, Lu SF, Ming SL, et al. Cholesterol 25-hydroxylase acts as a host restriction factor on pseudorabies virus replication. *J Gen Virol.* (2017) 98:1467–76. doi: 10.1099/jgv.0.000797
13. Wang J, Wang CF, Ming SL, Li GL, Zeng L, Wang MD, et al. Porcine IFITM1 is a host restriction factor that inhibits pseudorabies virus infection. *Int J Biol Macromol.* (2020) 151:1181–93. doi: 10.1016/j.ijbiomac.2019.10.162
14. Xie J, Bi Y, Xu S, Han Y, Idris A, Zhang H, et al. Host antiviral protein IFITM2 restricts pseudorabies virus replication. *Virus Res.* (2020) 287:198105. doi: 10.1016/j.virusres.2020.198105

Acknowledgments

We sincerely thank Xiaojie Huang and Lei Lei from Hunan Agricultural University for the assistance in data collection and diagram preparation.

Conflict of interest

The authors declare that the research was conducted in the absence of any commercial or financial relationships that could be construed as a potential conflict of interest.

Publisher's note

All claims expressed in this article are solely those of the authors and do not necessarily represent those of their affiliated organizations, or those of the publisher, the editors and the reviewers. Any product that may be evaluated in this article, or claim that may be made by its manufacturer, is not guaranteed or endorsed by the publisher.

15. Ono E, Tomioka Y, Taharaguchi S, Cherel P. Comparison of protection levels against pseudorabies virus infection of transgenic mice expressing a soluble form of porcine nectin-1/HveC and vaccinated mice. *Vet Microbiol.* (2006) 114:327–30. doi: 10.1016/j.vetmic.2005.12.011
16. Yang X, Yu C, Zhang Q, Hong L, Gu T, Zheng E, et al. A Nectin1 mutant mouse model is resistant to pseudorabies virus infection. *Viruses.* (2022) 14:874. doi: 10.3390/v14050874
17. Pan Y, Guo L, Miao Q, Wu L, Jing Z, Tian J, et al. Association of THBS3 with glycoprotein D promotes pseudorabies virus attachment, fusion, and entry. *J Virol.* (2023) 97:e0187122. doi: 10.1128/jvi.01871-22
18. Arai J, Uema M, Morimoto T, Sagara H, Akashi H, Ono E, et al. Entry of herpes simplex virus 1 and other alphaherpesviruses via the paired immunoglobulin-like type 2 receptor alpha. *J Virol.* (2009) 83:4520–7. doi: 10.1128/jvi.02601-08
19. Pastenkos G, Miller JL, Pritchard SM, Nicola AV. Role of sphingomyelin in alphaherpesvirus entry. *J Virol.* (2019) 93:e01547-18. doi: 10.1128/jvi.01547-18
20. Höpfer JE, Grey F, Baillie JK, Regan T, Parkinson NJ, Höpfer D, et al. A genome-wide CRISPR/Cas9 screen reveals the requirement of host sphingomyelin synthase 1 for infection with pseudorabies virus mutant gD(–)pass. *Viruses.* (2021) 13:1574. doi: 10.3390/v13081574
21. Lu ZZ, Sun C, Zhang X, Peng Y, Wang Y, Zeng Y, et al. Neuropilin 1 is an entry receptor for KSHV infection of mesenchymal stem cell through TGFBR1/2-mediated macropinocytosis. *Sci Adv.* (2023) 9:eadg1778. doi: 10.1126/sciadv.adg1778
22. Hu Y, Xie X, Yang L, Wang A. A comprehensive view on the host factors and viral proteins associated with porcine epidemic diarrhea virus infection. *Front Microbiol.* (2021) 12:762358. doi: 10.3389/fmicb.2021.762358
23. Ye N, Feng W, Fu T, Tang D, Zeng Z, Wang B. Membrane fusion, potential threats, and natural antiviral drugs of pseudorabies virus. *Vet Res.* (2023) 54:39. doi: 10.1186/s13567-023-01171-z
24. Samanta D, Almo SC. Nectin family of cell-adhesion molecules: structural and molecular aspects of function and specificity. *Cell Mol Life Sci.* (2015) 72:645–58. doi: 10.1007/s00108-014-1763-4
25. Krummenacher C, Supekár VM, Whitbeck JC, Lazear E, Connolly SA, Eisenberg RJ, et al. Structure of unliganded HSV gD reveals a mechanism for receptor-mediated activation of virus entry. *EMBO J.* (2005) 24:4144–53. doi: 10.1038/sj.emboj.7600875
26. Karaba AH, Kopp SJ, Longnecker R. Herpesvirus entry mediator and nectin-1 mediate herpes simplex virus 1 infection of the murine cornea. *J Virol.* (2011) 85:10041–7. doi: 10.1128/jvi.05445-11
27. Martinez WM, Spear PG. Structural features of nectin-2 (HveB) required for herpes simplex virus entry. *J Virol.* (2001) 75:11185–95. doi: 10.1128/jvi.75.22.11185-11195.2001
28. Cantuti-Castelvetri L, Ojha R, Pedro LD, Djannatian M, Franz J, Kuivanen S, et al. Neuropilin-1 facilitates SARS-CoV-2 cell entry and infectivity. *Science.* (2020) 370:856–60. doi: 10.1126/science.abd2985

29. Wang HB, Zhang H, Zhang JP, Li Y, Zhao B, Feng GK, et al. Neuropilin 1 is an entry factor that promotes EBV infection of nasopharyngeal epithelial cells. *Nat Commun.* (2015) 6:6240. doi: 10.1038/ncomms7240
30. Wang S, Zhao L, Zhang X, Zhang J, Shang H, Liang G. Neuropilin-1, a myeloid cell-specific protein, is an inhibitor of HIV-1 infectivity. *Proc Natl Acad Sci U S A.* (2022) 119:e2114884119. doi: 10.1073/pnas.2114884119
31. Ortega-Gonzalez P, Taylor G, Jangra RK, Tenorio R, Fernandez de Castro I, Mainou BA, et al. Reovirus infection is regulated by NPC1 and endosomal cholesterol homeostasis. *PLoS Pathog.* (2022) 18:e1010322. doi: 10.1371/journal.ppat.1010322
32. Fang Z, Li P, Shang L, Li F. Ebola viral receptor Niemann-pick C1 (NPC1) in human cancers: a potential biomarker and immunotherapeutic target. *Hum Cell.* (2022) 35:423–6. doi: 10.1007/s13577-021-00638-5
33. O'Neill KI, Kuo LW, Williams MM, Lind H, Crump LS, Hammond NG, et al. NPC1 confers metabolic flexibility in triple negative breast cancer. *Cancers (Basel).* (2022) 14:3543. doi: 10.3390/cancers14143543
34. Assefi M, Bijan Rostami R, Ebrahimi M, Altafi M, Tehrani PM, Zaidan HK, et al. Potential use of the cholesterol transfer inhibitor U18666A as an antiviral drug for research on various viral infections. *Microb Pathog.* (2023) 179:106096. doi: 10.1016/j.micpath.2023.106096
35. Schips TG, Vanhoutte D, Vo A, Correll RN, Brody MJ, Khalil H, et al. Thrombospondin-3 augments injury-induced cardiomyopathy by intracellular integrin inhibition and sarcolemmal instability. *Nat Commun.* (2019) 10:76. doi: 10.1038/s41467-018-08026-8
36. Komatsuya K, Kikuchi N, Hirabayashi T, Kasahara K. The regulatory roles of cerebellar glycosphingolipid microdomains/lipid rafts. *Int J Mol Sci.* (2023) 24:5566. doi: 10.3390/ijms24065566
37. Ben-Porat T, Rakusanova T, Kaplan AS. Early functions of the genome of herpesvirus. II. Inhibition of the formation of cell-specific polysomes. *Virology.* (1971) 46:890–9. doi: 10.1016/0042-6822(71)90089-4
38. Ye G, Liu H, Zhou Q, Liu X, Huang L, Weng C. A tug of war: pseudorabies virus and host antiviral innate immunity. *Viruses.* (2022) 14:547. doi: 10.3390/v14030547
39. Zhang R, Tang J. Evasion of I interferon-mediated innate immunity by pseudorabies virus. *Front Microbiol.* (2021) 12:801257. doi: 10.3389/fmicb.2021.801257
40. Friedlová N, Zavadil Kokáš F, Hupp TR, Vojtěšek B, Nekulová M. IFITM protein regulation and functions: far beyond the fight against viruses. *Front Immunol.* (2022) 13:1042368. doi: 10.3389/fimmu.2022.1042368
41. Xie T, Feng M, Zhang X, Li X, Mo G, Shi M, et al. Chicken CH25H inhibits ALV-J replication by promoting cellular autophagy. *Front Immunol.* (2023) 14:1093289. doi: 10.3389/fimmu.2023.1093289
42. Zhao J, Chen J, Li M, Chen M, Sun C. Multifaceted functions of CH25H and 25HC to modulate the lipid metabolism, immune responses, and broadly antiviral activities. *Viruses.* (2020) 12:727. doi: 10.3390/v12070727
43. Yang H, Zhang J, Zhang X, Shi J, Pan Y, Zhou R, et al. CD163 knockout pigs are fully resistant to highly pathogenic porcine reproductive and respiratory syndrome virus. *Antivir Res.* (2018) 151:63–70. doi: 10.1016/j.antiviral.2018.01.004
44. Wang C, Liang Q, Sun D, He Y, Jiang J, Guo R, et al. Nectin-1 and non-muscle myosin heavy chain-IIb: major mediators of herpes simplex Virus-1 entry into corneal nerves. *Front Microbiol.* (2022) 13:830699. doi: 10.3389/fmicb.2022.830699
45. Nie Z, Zhu S, Wu L, Sun R, Shu J, He Y, et al. Progress on innate immune evasion and live attenuated vaccine of pseudorabies virus. *Front Microbiol.* (2023) 14:1138016. doi: 10.3389/fmicb.2023.1138016
46. Chen X, Kong N, Xu J, Wang J, Zhang M, Ruan K, et al. Pseudorabies virus UL24 antagonizes OASL-mediated antiviral effect. *Virus Res.* (2021) 295:198276. doi: 10.1016/j.virusres.2020.198276
47. Li X, Chen S, Zhang LY, Niu GY, Zhang XW, Yang L, et al. Coinfection of porcine circovirus 2 and pseudorabies virus enhances immunosuppression and inflammation through NF- κ B, JAK/STAT, MAPK, and NLRP3 pathways. *Int J Mol Sci.* (2022) 23:4469. doi: 10.3390/ijms23084469



OPEN ACCESS

EDITED BY

Mengmeng Zhao,
Foshan University, China

REVIEWED BY

Tong-Qing An,
Chinese Academy of Agricultural Sciences,
China

Ruining Wang,
Henan University of Animal Husbandry and
Economy, China

*CORRESPONDENCE

Krisztián Bányai
✉ bkrota@hotmail.com

RECEIVED 25 October 2023

ACCEPTED 20 December 2023

PUBLISHED 08 January 2024

CITATION

Jakab S, Bálint Á, Cseri K, Bali K, Kaszab E,
Domán M, Halas M, Szarka K and
Bányai K (2024) Genome stability assessment
of PRRS vaccine strain with new ARTIC-style
sequencing protocol.

Front. Vet. Sci. 10:1327725.

doi: 10.3389/fvets.2023.1327725

COPYRIGHT

© 2024 Jakab, Bálint, Cseri, Bali, Kaszab,
Domán, Halas, Szarka and Bányai. This is an
open-access article distributed under the
terms of the [Creative Commons Attribution
License \(CC BY\)](#). The use, distribution or
reproduction in other forums is permitted,
provided the original author(s) and the
copyright owner(s) are credited and that the
original publication in this journal is cited, in
accordance with accepted academic
practice. No use, distribution or reproduction
is permitted which does not comply with
these terms.

Genome stability assessment of PRRS vaccine strain with new ARTIC-style sequencing protocol

Szilvia Jakab^{1,2}, Ádám Bálint³, Karolina Cseri^{4,5}, Krisztina Bali^{1,2},
Eszter Kaszab^{1,2,4}, Marianna Domán^{1,2}, Máté Halas⁶,
Krisztina Szarka^{4,5} and Krisztián Bányai^{1,2,7*}

¹Pathogen Discovery Group, HUN-REN Veterinary Medical Research Institute, Budapest, Hungary,

²National Laboratory for Infectious Animal Diseases, Antimicrobial Resistance, Veterinary Public Health and Food Chain Safety, Budapest, Hungary, ³Veterinary Diagnostic Directorate, National Food Chain Safety Office, Budapest, Hungary, ⁴One Health Institute, University of Debrecen, Debrecen, Hungary, ⁵Department of Metagenomics, University of Debrecen, Debrecen, Hungary, ⁶Prophyl Ltd., Mohács, Hungary, ⁷Department of Pharmacology and Toxicology, University of Veterinary Medicine, Budapest, Hungary

A tiling amplicon sequencing protocol was developed to analyse the genome sequence stability of the modified live PRRSV vaccine strain, Porcilis MLV. The backbone of the ARTIC-style protocol was formed by 34 individual primer pairs, which were divided into two primer pools. Primer pairs were designed to amplify 532 to 588 bp fragments of the corresponding genomic region. The amplicons are suitable for sequencing on Illumina DNA sequencers with available 600-cycle sequencing kits. The concentration of primer pairs in the pools was optimized to obtain a balanced sequencing depth along the genome. Deep sequencing data of three vaccine batches were also analysed. All three vaccine batches were very similar to each other, although they also showed single nucleotide variations (SNVs) affecting less than 1 % of the genome. In the three vaccine strains, 113 to 122 SNV sites were identified; at these sites, the minority variants represented a frequency range of 1 to 48.7 percent. Additionally, the strains within the batches contained well-known length polymorphisms; the genomes of these minority deletion mutants were 135 to 222 bp shorter than the variant with the complete genome. Our results show the usefulness of ARTIC-style protocols in the evaluation of the genomic stability of PRRS MLV strains.

KEYWORDS

porcine reproductive and respiratory syndrome virus, Porcilis MLV, genetic variability, single nucleotide variation, deep sequencing, tiling amplicon sequencing

1 Introduction

Porcine reproductive and respiratory syndrome (PRRS) remains one of the most devastating viral diseases in pig production systems, responsible for serious economic losses worldwide. The causative viral species, *Betaarterivirus suid 1* and *Betaarterivirus suid 2* (also known as PRRSV-1 and -2, respectively) are enveloped, positive-sense, single-stranded RNA viruses, with a genome of approximately 15 thousand nucleotides (nt) in length (1–3). PRRSV is characterized by high genetic diversity, posing challenges for disease control measures (4, 5).

Modified live virus (MLV) vaccines are widely used tools for the prevention and control of PRRS. These vaccines have been developed to reduce clinical severity and virus shedding, alleviating the disease-associated economic burden. Since their first introduction in 2000, Porcilis® PRRS (MSD Animal Health) vaccines against PRRSV-1 have been preferred vaccines

for the active immunisation of sows and growing pigs (6). In general, safety monitoring of vaccines is important during manufacturing, however, information on the genetic stability of vaccine strains in different batches is limited (7, 8). The quasispecies nature of live virus based vaccines poses additional challenges. To date, the whole virus genome sequence of four different Porcilis® PRRS MLV batches has been determined, showing that some deletion variants coexist in different vaccine batches (9). In addition to vaccine stability, another issue to consider is the loss of attenuation of MLV strains in the field that has already been confirmed for some commonly used PRRS MLVs (9–14). Regardless of the theoretic possibility of vaccine strain reversion, data indicate that Porcilis-derived field isolates are genetically more stable, at least based on ORF5 and ORF7 sequence analysis, than some other vaccines (15).

The genetic stability of live vaccines is a critical requirement for their development, production, and field use. Whole genome sequencing on next-generation sequencing platforms permits a more precise description of the population structure of vaccine strains. Tiling amplicon sequencing protocols could overcome sensitivity issues, as next-generation sequencing is preceded by targeted amplification of the genome using a large set of primer pairs. This approach has become very popular since the beginning of the SARS-CoV-2 pandemic. The ARTIC network has developed numerous protocols for direct amplification of virus genomes from clinical samples using tiled, multiplexed primers¹ (16). In 2020, Gohl and co-workers further developed the approach and established a tiled amplicon-based method for DNA library preparation and NGS sequencing (17). As the target-specific primers can be readily customized, this method can theoretically be adapted on any viral genomes, offering a rapid, sensitive and inexpensive approach to whole genome sequencing.

The aims of this study were the development of a tiled, tiling amplicon sequencing method specific for the Porcilis® PRRS MLV strain and the exploration of the genetic stability of commercial Porcilis® PRRS vaccine batches. This simple, fast, and cost-effective sequencing method could serve as a readily adaptable tool to affirm the quality of PRRS MLVs.

2 Materials and methods

2.1 Vaccines

Three different batches of Porcilis® PRRS vaccine (batch No. A220CE01, A220AD01, and A221AE01) were used to develop an ARTIC protocol and to compare the genetic stability of the Porcilis MLV strain.

2.2 RNA extraction and cDNA synthesis

Vaccine batches were diluted at 1:8 in PBS and then the viral RNA was isolated by the NucleoSpin RNA Virus Kit (Macherey-Nagel, Düren, Germany) according to the manufacturer's instruction.

Randomly primed reverse transcription was performed using the SuperScript™ IV VILO™ Master Mix (Thermo Fisher Scientific, Waltham, MA, United States) according to the manufacturer's instruction. The RT reaction mixture consisted of 4 µL Master Mix (with oligo (dT) 18 and random hexamer primers included), 11 µL nuclease free water and 5 µL RNA template was added. The thermal profile of the reaction was as follows: the denaturation step was performed at 65°C for 5 min, then annealing of primers, the reverse transcription and the inactivation of enzyme lasted 10 min at 25°C, 10 min at 50°C, and 5 min at 85°C, respectively.

2.3 Primer design

A tiling amplicon scheme was designed for whole genome amplification. Our aim was to create a robust primer set specific for the Porcilis vaccine strain and suitable for use in multiplex PCRs. Thus, we gathered whole genome records from the GenBank that showed >95% nucleotide sequence identity to the reference strain of Porcilis DV (accession no., KJ127878). This threshold was chosen based on the observation that Porcilis-derived strains display roughly this range of diversity when isolated under field conditions; in this respect, we expected that vaccine production conditions will not permit a high degree of diversification. Whole genome sequences were aligned by the MAFFT algorithm in Geneious Prime® (version 2022.2.2) software and the consensus sequence (threshold: 90%) was extracted and used for primer design. The primer set was designed on the PrimalScheme webserver giving the consensus sequence as input (16).

The amplicon size was adjusted to comply with the 2 × 300 base reading with any Illumina equipment where this option is available. Thus, the expected PCR product size ranged from 532 bp to 588 bp. Afterward, we individually inspected the resulting primer sequences with particular attention to self-, and cross-dimers and we also refined the oligos when needed. The process resulted in 68 primers equivalent to 34 amplicons that theoretically covered the full-length target genome (Table 1). All oligos contained the Illumina-compatible sequencing primer binding site Rd1 SP and Rd2 SP at the 5' end of the forward and reverse primer, in the following way:

forward: TCGTCGGCAGCGTCAGATGTGTATAAGAGACAG <PRRSV specific primer> and reverse: GTCTCGTGGGCTCGGAGATGTGTATAAGAGACAG <PRRSV specific primer>. Illumina-compatible forward and reverse indexing primers contained *part of the sequencing primer binding sites, i5 and i7 indices* (Nextera XT Index Kit v2 Set C) and the P5 and P7 adapters, respectively.

(F: 5'-AATGATACGGCGACCACCGAGATCTACACi5TCGTCGGCAGCGTC-3',

R: 5'-CAAGCAGAAGACGGCATACGAGATi7GTCTCGTGGGCTCGG-3').

To generate the primer pools, primers were resuspended to a stock concentration of 100 µM and then divided into two pools (poolAv1, from pool A1 and A2, respectively) by combining the same volume of odd and even numbered amplicons. Two other pooling schemes, poolAv2 and poolAv3, were prepared to adjust the relative proportions of primers, and consequently amplicons, to achieve a more balanced coverage of the genome.

¹ <https://artic.network/>

TABLE 1 Features of PRRSV primers tested in this study.

PRRSV specific primer and its sequence		Pool	Position*		Ratio of primers in different pooling schemes		
					v1	v2	v3
1_F	ATGATGTGTAGGGTATTCCCCCTAC	1	1	25	1	3	1.5
1_R	ACTTGGAGTTCACGAAGGTGTC	1	562	583	1	3	1.5
2_F	GCAATCACAACTTCCTCCAACG	2	490	511	1	1	1
2_R	CACGTCGGGGTYYTGACAA	2	1,015	1,034	1	1	1
3_F	TCTGYCCATTGAGGAGGCTCA	1	739	760	1	3	3
3_R	AGGCGAACRAATCTGGGGT	1	1,278	1,297	1	3	3
4_F	CTGTCTTGGCCCCRGCTCTGGATC	2	1,227	1,250	1	1	1
4_R	CTCACTCTACCTCCARTGAAC	2	1,710	1,732	1	1	1
5_F	CTTGYTCAGGCGATYCAATGTC	1	1,617	1,638	1	3	1.5
5_R	AARCACYCGTCCAGRGACACA	1	2,147	2,167	1	3	1.5
6_F	ARAAATGCGGTGCCACGGAA	2	2,020	2,039	1	1	1
6_R	GTGTTTGCTCTCTCACAAGGGT	2	2,562	2,583	1	1	1
7_F	CTCRGACYCCATGAAAGRAAAC	1	2,477	2,498	1	3	3
7_R	GCCTCGGTCAATTAAGGCTTG	1	3,030	3,050	1	3	3
8_F	ATGCTCCRGTTGGTTGAYGCC	2	2,923	2,942	1	3	3
8_R	TCACTCGACTARGAARATCCGG	2	3,462	3,483	1	3	3
9_F	TGAAGCAACTGGTGGCRCAG	1	3,316	3,335	1	1.5	1.5
9_R	AAAGTTGGCGCTGCTCAAGAG	1	3,868	3,888	1	1.5	1.5
10_F	GTTCTTGATGGCTTTTGCTGT	2	3,766	3,787	1	1.5	1.5
10_R	CATTTGAYRGCTGACTGGGAT	2	4,324	4,345	1	1.5	1.5
11_F	ATCAACRCACAAAAGCCCAT	1	4,240	4,261	1	1	1
11_R	GACACACAAAGTCGAGAGGAGC	1	4,771	4,792	1	1	1
12_F	TCAAGTGTGTGGCCGAGGAA	2	4,691	4,710	1	1	1
12_R	CAGTTAARGCAGCTCTCCGGAC	2	5,232	5,253	1	1	1
13_F	GACATCCACCAGTACACCTCTG	1	5,154	5,175	1	1	1
13_R	AGTTTGTGTTGAACCGGTGTGGA	1	5,692	5,713	1	1	1
14_F	GGAAGGGTTCGCCTTCTGTTTT	2	5,612	5,633	1	1	1
14_R	TGCGTAGAACGCCAGAGAAAAGC	2	6,143	6,164	1	1	1
15_F	TCTTTGTGCTTGCATGGGCC	1	6,061	6,080	1	3	1.5
15_R	GCATACGCTGCTCAATGTACTG	1	6,582	6,604	1	3	1.5
16_F	GTTGTCACAGGCTGACCTTGAT	2	6,494	6,515	1	1	1
16_R	ATCCGTGTAAAAGGTGTCACCG	2	7,040	7,061	1	1	1
17_F	GAGAGGATGAAGAAACAYTGTGT	1	6,957	6,979	1	5	3
17_R	CTCRGAAGTGACTTTTAGGTCTAAAG	1	7,512	7,537	1	5	3
18_F	GGCGGCYTRGTTGTGACTGAAA	2	7,442	7,463	1	5	3
18_R	ATTTACATCAGACACDGGGGC	2	7,967	7,988	1	5	3
19_F	TRCCTTACAAAACCTCTCAAGACA	1	7,899	7,922	1	1	1
19_R	ACTGAGCGCCGATCTGTGAGC	1	8,453	8,473	1	1	1
20_F	GTCAAGGAGAATTGGCAAACYGT	2	8,348	8,370	1	1	1.5
20_R	ACYAACATAGGCTGAATTTCAAGGA	2	8,892	8,916	1	1	1.5
21_F	ACTGTAATYTATGCCAGCAC	1	8,794	8,815	1	1.5	1.5
21_R	TGGCGGAAYTTYTTCCCTTCAT	1	9,324	9,345	1	1.5	1.5
22_F	AGGACCTCATCTGYGGTATTGC	2	9,222	9,243	1	1	1

(Continued)

TABLE 1 (Continued)

PRRSV specific primer and its sequence		Pool	Position*		Ratio of primers in different pooling schemes		
					v1	v2	v3
22_R	CTACTATGAACCTGCTGAGTAGYA	2	9,750	9,773	1	1	1
23_F	ATGGAGACTACCARGTGGTGC	1	9,678	9,698	1	5	3
23_R	ACAGGYCGGGTGGTAAAAAC	1	10,241	10,260	1	5	3
24_F	ACTATTACAGATTGGGCYCAACA	2	10,151	10,175	1	1	1
24_R	TRTCYGGGGAAAAGTAAAACCC	2	10,694	10,715	1	1	1
25_F	ACCCRAGGTGCAAGTCTCTCTT	1	10,608	10,629	1	1	1
25_R	AGAGTGCACACGGCTTTAGC	1	11,171	11,190	1	1	1
26_F	GGGGTGTGCATCACATYACATCAA	2	11,080	11,102	1	1	1
26_R	CAGTGTAGTCCTTGCCGTCATT	2	11,624	11,645	1	1	1
27_F	CGCAGTGGAAGATTTTGGGGTT	1	11,535	11,556	1	1	1
27_R	GGARACTCGCATGTGCCAAA	1	12,079	12,098	1	1	1
28_F	ACTATCGAAGGTCCTATGAARGCTT	2	11,995	12,019	1	1	1
28_R	TGATGGTYAGCTCGAATGATGT	2	12,530	12,551	1	1	1
29_F	TGTGGCTTCATCTGTTACCTTGT	1	12,440	12,462	1	1	1.5
29_R	CGAACGCCTCAGAAACCATGA	1	12,989	13,009	1	1	1.5
30_F	AATAGACGGGGGCAATTGGTTC	2	12,916	12,937	1	1	1
30_R	CAATGGTTGTAGCCCACCTCAT	2	13,444	13,465	1	1	1
31_F	CCAACATACCCAGCAGCATCAT	1	13,374	13,395	1	1	1
31_R	TGAAGTTGGTAAACCGGGTACG	1	13,911	13,932	1	1	1
32_F	CTTTCGCAGCGYTCGTATGTT	2	13,846	13,866	1	1	1
32_R	GGCAACACAATCTGCATCTGGA	2	14,372	14,393	1	1	1
33_F	CACCAACCGTGTGCGAYTTAC	1	14,284	14,304	1	1	1
33_R	CGTCTGGATCGATTGCAAGCAG	1	14,822	14,843	1	1	1
34_F	TCTAGTACCAGGACTTCGGAGC	2	14,521	14,542	1	1	1
34_R	TTAATTTCCGGTCACATGGTTCCTGC	2	15,076	15,100	1	1	1

*Relative to reference genome KF991509.

2.4 Library preparation and next generation sequencing

Whole genome amplification connected with library preparation consisted of a two-step PCR protocol. Both PCR rounds (PCR-1 and PCR-2) were performed using Q5U® Hot Start High-Fidelity DNA Polymerase (NEB, Frankfurt, Germany) according to the manufacturer's instruction. Separate PCR-1 reactions for the multiplex primer set of pool A1 and A2 were composed of 15.46 µL nuclease-free water, 5 µL 5X Q5U Reaction Buffer, 0.5 µL dNTP Mix (10 mM), 1.29 µL primer pool A1 or A2 (10 µM, final concentration of 0.015 µM per primer), 0.25 µL Q5U Hot Start High-Fidelity DNA Polymerase and 2.5 µL cDNA template. PCR cycling was performed at 98°C for 30 s, followed by 30 cycles of 98°C for 15 s and 65°C for 5 min, then held at 4°C. PCR-1 products were analysed on 1% agarose gel, the bands were excised at 600 bp, or so, and the DNA were purified from gel slices with the Gel/PCR DNA Fragments Extraction Kit (Favorgen, Ping Tung, Taiwan). After gel extraction, pool A1 and A2 were combined then diluted 1:100 for each sample. During the second PCR, Illumina specific adapters and indices were added to the PCR-1 products. PCR-2 composed of 11.75 µL nuclease-free water, 5 µL 5X

Q5U Reaction Buffer, 0.5 µL dNTP Mix (10 mM), 1.25–1.25 µL forward and reverse indexing primers (10 µM), 0.25 µL Q5U Hot Start High-Fidelity DNA Polymerase and 5 µL pooled and diluted DNA template of PCR-1. PCR cycling was performed at 98°C for 30 s, 30 cycles of 98°C for 20 s, 55°C for 15 s and 72°C for 1 min, the final extension lasted for 5 min at 72°C, then held at 4°C. Again, PCR-2 products were analysed on 1% agarose gel, the bands were excised at ~600 bp, and the gel slices were isolated with Gel/PCR DNA Fragments Extraction Kit (Favorgen, Ping Tung, Taiwan).

The concentrations of DNA libraries were measured using a Qubit equipment and then diluted to 4 nM. This pool was denatured and then diluted to 20 pM, spiked with 35% PhiX, and sequenced on an Illumina Miseq sequencer using the Reagent Kit v3 (600-cycle) (Illumina, San Diego, CA, United States).

2.5 Sequence data analysis

First, the Illumina sequence reads were trimmed as follows: sequence reads under 75 bp were discarded, the PRRSV specific primer sequences and low-quality bases (minimum Phred score of 10)

were removed at both ends using BBDuk plugin in Geneious Prime®. Second, genome assembly was performed in Geneious Prime® with the built-in Geneious algorithm, or if necessary, with the Minimap2 assembler, implementing reference mapping to a Porcilis DV strain (accession no., KF991509).

Intra-strain sequence variability was analysed from the short-read data of poolAv3. For the analysis of single nucleotide variants (SNVs) the sequence reads under 75 bp were discarded, the PRRSV specific primer sequences and low-quality bases (minimum Phred score of 30) were removed at both ends using BBDuk plugin in Geneious Prime®. We used the built-in algorithm of Geneious Prime® for variant calling with minimum variant frequency of 1%. Only SNVs that were identified on parallel sequencing runs were accepted.

3 Results and discussion

3.1 Assay evaluation

In this study, we developed and tested a tiling amplicon sequencing protocol specific for a widely used PRRSV vaccine strain, Porcilis MLV. The workflow was based on a two-step PCR library preparation method. We first examined whether the designed primer set successfully amplifies different batches of Porcilis MLV. In this respect, we encountered an immediate obstacle, as the study was launched after Hungary was declared PRRS-free and the Porcilis MLV vaccine was available in limited quantities on the market. Next to the evaluation of individual primer combinations, we focused on the improvement of primer balance in individual primer pools to achieve better sequence coverage across the genome.

In the first step of the test development, our results showed that all 34 primer pairs generated PCR products of the expected size in the separate reactions (Figure 1). These PCR products were then pooled to obtain equimolar ratios for each amplicon (1 to 34) and then subjected these pools to sequencing. The overall sequencing depth ranged from 9,251x to 13,889x and the assembled contig covered the full-length genome (Figure 2). These data indicated that the assay design met our expectations. However, because it was not practical to use the primer pairs in separate reaction tubes, the primers were pooled. In this practice, we followed the protocols previously

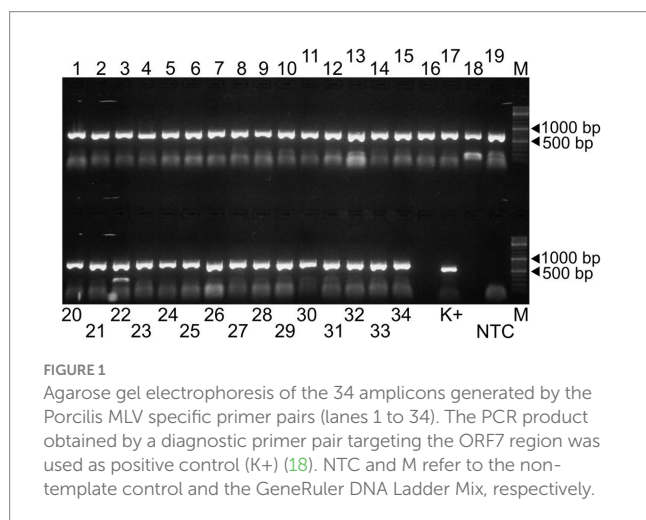
established for other viruses and combined the even and odd primer pairs in separate reaction tubes (poolAv1) (16, 17). Thus, two primer pool mixtures were prepared and the cDNA templates were amplified under same conditions in these two reaction tubes during the PCR-1 round.

Sequencing the Porcilis vaccine strain from different batches was successful with poolAv1 (Figure 2). Genome coverage, depending on the vaccine batch, approached or reached 100%, while sequencing depth varied within and between all vaccine batches. We observed a reduction of the sequencing depth at amplicons 1, 3, 5, 7, 8, 15, 17, 21, 23, and 29 for A220CE01, at amplicons 8, 18 and 23 for A220AD01, and at amplicons 1, 7, 8, 9, 15, 17, 18, and 23 for A221AE01, respectively (Figure 2). Thus, 7 out of 12 primer pairs resulted in reduced amount of their respective PCR products in at least two distinct vaccine batches. Moreover, in case of amplicon 23, no reads were generated in A220CE01. To better evaluate the efficiency of the primer pairs, we calculated the mean sequencing depth per amplicon and per vaccine sample by excluding overlapping amplicon regions. The mean sequencing depth was 9,944x, 11,069x, and 1799x, whereas the range of sequencing depths ranged between 3x and 39,624x, 290x and 37,921x, and 12x and 18,107x for A220CE01, A220AD01, and A221AE01, respectively. The varying efficiencies of primer pairs used in equimolar ratio prompted us to optimize the assay.

To improve the primer balance we modified the working concentration of selected primers in the reaction mixtures and prepared two distinct experimental primer concentrations (Table 1). As such, we prepared two other variations of poolA, designated as v2 and v3. Figure 2 shows the coverage and sequencing depth achieved by using primer pools with different concentration ratios of individual primers. By using poolAv2 and poolAv3, we reached a more balanced sequencing depth along the entire genome, compared to the poolAv1. For example, the differences between the minimum and maximum depth per amplicon achieved by poolAv3 for the three vaccine batches was 14- to 16-fold compared to the 131- to 14,151-fold difference observed when primers were used in equimolar ratios (poolAv1). Overall, the primer concentration optimization resulted in a significant decrease of the number of low depth regions and simultaneously diminished regions without sequence reads. As a result, we achieved a more balanced sequencing depth for the entire genome. The need to optimize primer concentrations was already demonstrated for other tiling amplicon based whole genome sequencing protocols, for example, for the widely used SARS-CoV-2 ARTIC primers (19).

3.2 Vaccine strain variability

When comparing consensus sequences generated by the four different pooling approaches, such as the separate PCR-1 with 34 primer pairs and poolA with the three different pooling schemes, we identified some nucleotide differences in the assembled consensus genome sequences. In the consensus genome of A220CE01 from poolAv1 and 1–34, in A220AD01 from poolAv2, and in A221AE01 from poolAv1 we identified, respectively, 6 nt and 2 nt, 1 nt, and 5 nt differences from the others of the given batches. Among these, 1 (A220CE01), 1 (A220AD01), and 3 (A221AE01) mutations corresponded to the identified SNV sites. To further explore the



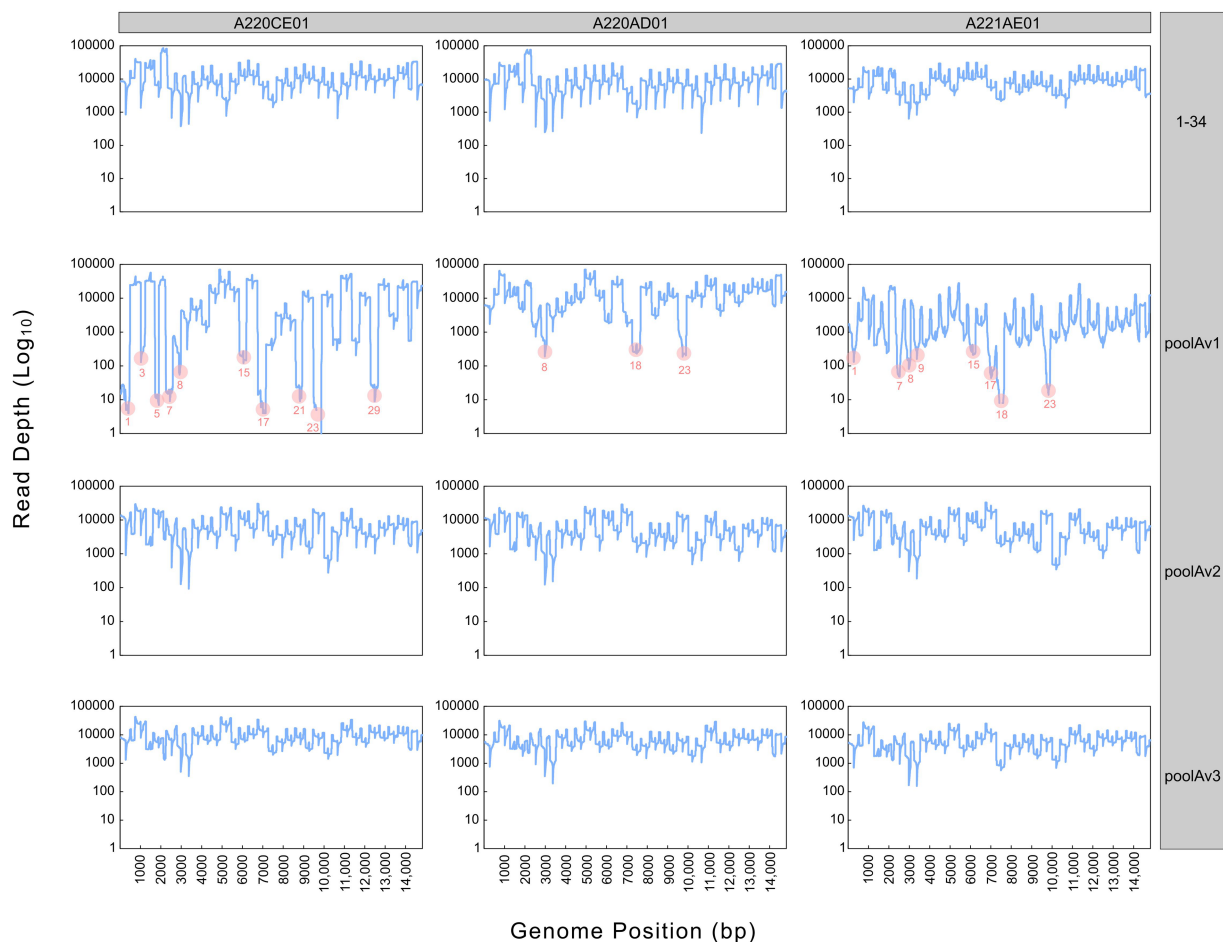


FIGURE 2

Sequencing depth derived from different pooling approaches (1–34, poolAv1, poolAv2, poolAv3) as determined for the three vaccine batches (A220CE01, A220AD01, A221AE01). In the plots linked to poolAv1, the drop-off amplicons are highlighted.

vaccine strain variation, short-read sequences generated by the poolAv3 were used for genomic analyses.

Previously, three different deletion variants of the Porcilis strain were found in some vaccine batches; these were designated as LONG-DEL, SHORT-DEL, and SHIFT-DEL. The difference among the three variants were seen in the genomic regions 2,216 to 2,437 for LONG-DEL, 2,231 to 2,365 for SHORT-DEL, 2,344 to 2,435 and 2,446 to 2,506 for SHIFT-DEL (9). When analysing data from poolAv3, beside the FULL-LENGTH variant, we could also detect all deletion variants in the three vaccine batches, and we estimated that the LONG-DEL variant was the most abundant form of the Porcilis vaccine strain, a finding that corresponds to previously published results (9). Downstream genetic analyses were conducted with the LONG-DEL variant. In brief, all three assembled LONG-DEL genomic variants of the Porcilis vaccine strain were 14,853 nt long.

Sites 1_F (5'-ATGATGTGTAGGGTAT'TCCCCCCCCCCC TAC-3') and 34_R (5'-TTAATTTCGGTCACATGGTTCCTGC-3') at the 5' and 3' ends of the genome, respectively, were excluded from the assembly, as no overlapping amplicons were generated in this region.

The complete genomes derived from the three vaccine batches were nearly identical, only one polymorph site was detected at position

1,519 (the position is relative to the Porcilis DV strain; accession no., KF991509). The pairwise nucleotide identity of all available Porcilis complete genomes from different vaccine batches, including the strains of this study, varied between 99.9 and 100% (the deleted region at nt position 2,215–2,506 was excluded from the alignment and the calculations). When the vaccine strains were compared to the wild-type DV strain (accession no., KJ127878) the nucleotide identity values were as high as 99.1%. In fact, we observed a total of 126 nt difference between vaccine strains and the wild-type DV strain. These mutations accumulated chiefly within the 5' end of the ORF1 region and the ORF2a region (Figure 3).

Based on the analyses of amplicon deep sequencing, we detected high genetic complexity. Our analyses of intra-strain variability showed that 122, 115, and 113 SNV positions were present in the Porcilis PRRS batches of A220CE01, A220AD01, and A221AE01, respectively (Figure 3). Most of the minor variants (a total of 104 sites) in these assemblies were identical in all three vaccine batches. The mean frequency of SNV bases in the minor variants, calculated from duplicated amplicon libraries, varied between 1.1 to 48.7%, 1 to 47.2%, and 1.3 to 48.1%, respectively, for the three batches (Supplementary Figure S1). The majority of SNVs was found in the

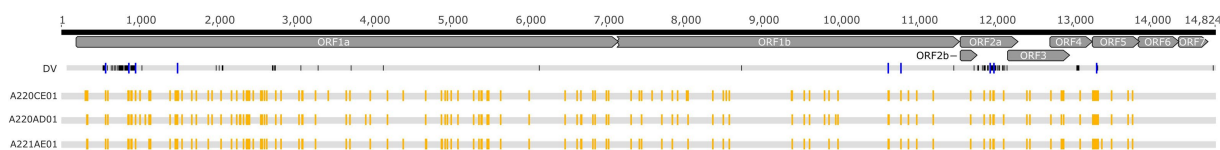


FIGURE 3

Schematic alignment of the Porcilis DV strain and the vaccine batches investigated in our study. Yellow squares show the SNV distribution within the vaccine batches whereas blue squares display SNV sites that correspond to the nucleotide differences between the DV and the vaccine batches.

ORF1a of all three genomes (55.4 to 60.9%), while no SNVs were detected at all in the ORF6 and ORF7 regions. The number of SNVs across the whole genome found in our vaccine batches was much lower than in some field strains, including a PRRSV-2 MLV-like strain (20, 21). Altogether we observed a maximum of 15 nt difference between our vaccine batches and previously sequenced Porcilis strains, and 7 of these differences were identified as minor variants in our SNV analysis, suggesting that the quasispecies structure partly contributes to the identified inter-vaccine-vial diversity (Supplementary Figure S2).

The intra-strain variability of the Porcilis MLV vaccine was determined directly from vaccine vials. According to previous studies the uneven distribution and the accumulation of SNVs in the ORF1a region is very typical and it is irrelevant whether the study strain is a vaccine derivative, or, a wild-type PRRSV strain (20–22). The absence of SNVs in the ORF6 and ORF7 regions was not unexpected, as these coding regions are highly conserved, even though some field strains harbour measurable mutant spectra at these sites (20–23). Importantly, the pattern of SNVs in the Porcilis vaccine strains did not entirely correspond with sites that differ between the DV strain these sites; a total of 9 minor variants were shared between them, six in ORF1a, two in ORF2a and one in ORF5 (Figure 3).

4 Conclusion

ARTIC-style protocols suitable for the amplification of whole viral genomes have become a keystone for some years to describe genetic diversity and to support molecular epidemiological investigations. In our study, we developed and evaluated an ARTIC-style sequencing method for PRRSV. Our assay was designed to be able to assess the genetic stability of vaccine strains of Porcilis MLV, but we anticipate that the assay can be readily adapted to other PRRSV MLVs. Further efforts are needed to demonstrate the potential field application of this protocol, as frequent recombination events between vaccine and wild-type PRRSVs in the field may pose a challenge to the successful design and implementation of broad-range ARTIC methods. Such leaps in viral genome evolution could erroneously undermine the value of these assays if common evolutionary mechanisms are not taken into account when evaluating the obtained sequence data.

Data availability statement

The datasets presented in this study can be found in online repositories. The names of the repository/repositories and accession number(s) can be found at: <https://www.ncbi.nlm.nih.gov/genbank/>, PRJNA1026488.

Author contributions

SJ: Formal analysis, Methodology, Writing – original draft, Writing – review & editing. AB: Resources, Supervision, Writing – review & editing. KC: Methodology, Writing – review & editing. KBL: Formal analysis, Methodology, Writing – review & editing. EK: Formal analysis, Methodology, Writing – review & editing. MD: Methodology, Validation, Writing – review & editing. MH: Resources, Supervision, Writing – review & editing. KS: Methodology, Supervision, Writing – review & editing. KBn: Conceptualization, Funding acquisition, Supervision, Writing – review & editing.

Funding

The author(s) declare financial support was received for the research, authorship, and/or publication of this article. This work was supported by the National Laboratory for Infectious Animal Diseases, Antimicrobial Resistance, Veterinary Public Health and Food Chain Safety, RRF-2.3.1-21-2022-00001. The work was prepared with the professional support of the Doctoral Student Scholarship Program of the Co-operative Doctoral Program of the Ministry of Innovation and Technology, financed from the National Research, Development and Innovation Fund. The funding bodies had no role in the design of the study, in the collection, analysis, and interpretation of data, and in writing the manuscript.

Conflict of interest

MH is employed by Prophyl Ltd.

The remaining authors declare that the research was conducted in the absence of any commercial or financial relationships that could be construed as a potential conflict of interest.

Publisher's note

All claims expressed in this article are solely those of the authors and do not necessarily represent those of their affiliated organizations, or those of the publisher, the editors and the reviewers. Any product that may be evaluated in this article, or claim that may be made by its manufacturer, is not guaranteed or endorsed by the publisher.

Supplementary material

The Supplementary material for this article can be found online at: <https://www.frontiersin.org/articles/10.3389/fvets.2023.1327725/full#supplementary-material>

References

- Brinton MA, Gulyaeva A, Balasuriya UBR, Dunowska M, Faaberg KS. ICTV virus taxonomy profile: Arteriviridae 2021. *J Gen Virol.* (2021) 102:001632. doi: 10.1099/jgv.0.001632
- Dokland T. The structural biology of PRRSV. *Virus Res.* (2010) 154:86–97. doi: 10.1016/j.virusres.2010.07.029
- Snijder EJ, Kikkert M, Fang Y. Arterivirus molecular biology and pathogenesis. *J Gen Virol.* (2013) 94:2141–63. doi: 10.1099/vir.0.056341-0
- Murtaugh MP, Stadejek T, Abrahante JE, Lam TTY, Leung FCC. The ever-expanding diversity of porcine reproductive and respiratory syndrome virus. *Virus Res.* (2010) 154:18–30. doi: 10.1016/j.virusres.2010.08.015
- Stadejek T, Stankevicius A, Murtaugh MP, Oleksiewicz MB. Molecular evolution of PRRSV in Europe: current state of play. *Vet Microbiol.* (2013) 165:21–8. doi: 10.1016/j.vetmic.2013.02.029
- Chae C. Commercial PRRS modified-live virus vaccines. *Vaccine.* (2021) 9:185. doi: 10.3390/vaccines9020185
- Legnardi M, Cecchinato M, Homonnay Z, Dauphin G, Koutoulis KC. Viral subpopulation variability in different batches of infectious bronchitis virus (IBV) vaccines based on GI-23 lineage: implications for the field. *Virus Res.* (2022) 319:198877. doi: 10.1016/j.virusres.2022.198877
- Serrão de Andrade AA, Soares AER, Paula de Almeida LG, Ciapina LP. Testing the genomic stability of the Brazilian yellow fever vaccine strain using next-generation sequencing data. *Interface Focus.* (2021) 11:20200063. doi: 10.1098/rsfs.2020.0063
- Eclercy J, Renson P, Hirschaud E, Andraud M, Beven V. Phenotypic and genetic evolutions of a porcine reproductive and respiratory syndrome modified live vaccine after limited passages in pigs. *Vaccine.* (2021) 9:392. doi: 10.3390/vaccines9040392
- Botner A, Strandbygaard B, Sørensen KJ, Have P, Madsen KG. Appearance of acute PRRS-like symptoms in sow herds after vaccination with a modified live PRRS vaccine. *Vet Rec.* (1997) 141:497–9. doi: 10.1136/vr.141.19.497
- Jiang YF, Xia TQ, Zhou YJ, Yu LX, Yang S, Huang QF. Characterization of three porcine reproductive and respiratory syndrome virus isolates from a single swine farm bearing strong homology to a vaccine strain. *Vet Microbiol.* (2015) 179:242–9. doi: 10.1016/j.vetmic.2015.06.015
- Storgaard T, Oleksiewicz M, Botner A. Examination of the selective pressures on a live PRRS vaccine virus. *Arch Virol.* (1999) 144:2389–401. doi: 10.1007/s007050050652
- Wang J, Zhang M, Cui X, Gao X, Sun W, Ge X. Attenuated porcine reproductive and respiratory syndrome virus regains its fatal virulence by serial passaging in pigs or porcine alveolar macrophages to increase its adaptation to target cells. *Microbiol Spectr.* (2022) 10:e0308422. doi: 10.1128/spectrum.03084-22
- Zhang Z, Zhou L, Ge X, Guo X, Han J, Yang H. Evolutionary analysis of six isolates of porcine reproductive and respiratory syndrome virus from a single pig farm: MLV-evolved and recombinant viruses. *Infect Genet Evol.* (2018) 66:111–9. doi: 10.1016/j.meegid.2018.09.024
- Bálint Á, Molnár T, Kecskeméti S, Kulcsár G, Soós T, Szabó PM. Genetic variability of PRRSV vaccine strains used in the National Eradication Programme. *Hungary Vaccines.* (2021) 9:849. doi: 10.3390/vaccines9080849
- Quick J, Grubaugh ND, Pullan ST, Claro IM, Smith AD, Gangavarapu K. Multiplex PCR method for MinION and Illumina sequencing of Zika and other virus genomes directly from clinical samples. *Nat Protoc.* (2017) 12:1261–76. doi: 10.1038/nprot.2017.066
- Gohl DM, Garbe J, Grady P, Daniel J, Watson RHB. A rapid, cost-effective tailed amplicon method for sequencing SARS-CoV-2. *BMC Genomics.* (2020) 21:863. doi: 10.1186/s12864-020-07283-6
- Balka G, Hornyák Á, Bálint Á, Kiss I, Kecskeméti S. Genetic diversity of porcine reproductive and respiratory syndrome virus strains circulating in Hungarian swine herds. *Vet Microbiol.* (2008) 127:128–35. doi: 10.1016/j.vetmic.2007.08.001
- Lambisia AW, Mohammed KSMakori TO, Ndwiga L. Optimization of the SARS-CoV-2 ARTIC network V4 primers and whole genome sequencing protocol. *Front Med.* (2022) 9:836728. doi: 10.3389/fmed.2022.836728
- Brar MS, Shi M, Hui RK-H, Leung FC-C. Genomic evolution of porcine reproductive and respiratory syndrome virus (PRRSV) isolates revealed by deep sequencing. *PLoS One.* (2014) 9:88807. doi: 10.1371/journal.pone.0088807
- Xing J, Zheng Z, Cao X, Wang Z, Xu Z, Gao H, et al. Whole genome sequencing of clinical specimens reveals the genomic diversity of porcine reproductive and respiratory syndrome viruses emerging in China. *Transbound Emerg Dis.* (2022) 69:e2530–40. doi: 10.1111/tbed.14597
- Clilverd H, Martín-Valls G, Li Y, Martín M, Cortey M, Mateu E. Infection dynamics, transmission, and evolution after an outbreak of porcine reproductive and respiratory syndrome virus. *Front Microbiol.* (2023) 14:1109881. doi: 10.3389/fmicb.2023.1109881
- Jakab S, Bali K, Freytag C, Pataki A, Fehér E, Halas M. Deep sequencing of porcine reproductive and respiratory syndrome virus ORF7: a promising tool for diagnostics and epidemiologic surveillance. *Animals.* (2023) 13:3223. doi: 10.3390/ani13203223



OPEN ACCESS

EDITED BY

Mengmeng Zhao,
Foshan University, China

REVIEWED BY

Alfonso Rosamilia,
Experimental Zooprophyllactic Institute of
Lombardy and Emilia Romagna (IZSLER), Italy
Peter Oba,
International Livestock Research Institute,
Uganda

*CORRESPONDENCE

Umberto Molini
✉ u.molini76@gmail.com

RECEIVED 18 October 2023

ACCEPTED 08 December 2023

PUBLISHED 15 January 2024

CITATION

Molini U, Coetzee LM, Hemberger MY,
Chiwome B, Khaiseb S, Dundon WG and
Franzo G (2024) First detection and molecular
characterization of porcine reproductive and
respiratory syndrome virus in Namibia, Africa.
Front. Vet. Sci. 10:1323974.
doi: 10.3389/fvets.2023.1323974

COPYRIGHT

© 2024 Molini, Coetzee, Hemberger,
Chiwome, Khaiseb, Dundon and Franzo. This
is an open-access article distributed under
the terms of the [Creative Commons
Attribution License \(CC BY\)](https://creativecommons.org/licenses/by/4.0/). The use,
distribution or reproduction in other forums is
permitted, provided the original author(s) and
the copyright owner(s) are credited and that
the original publication in this journal is cited,
in accordance with accepted academic
practice. No use, distribution or reproduction
is permitted which does not comply with
these terms.

First detection and molecular characterization of porcine reproductive and respiratory syndrome virus in Namibia, Africa

Umberto Molini^{1,2*}, Lauren M. Coetzee^{2,3},
Maria Y. Hemberger¹, Bernard Chiwome¹, Siegfried Khaiseb²,
William G. Dundon⁴ and Giovanni Franzo⁵

¹School of Veterinary Medicine, Faculty of Health Sciences and Veterinary Medicine, University of Namibia, Windhoek, Namibia, ²Central Veterinary Laboratory (CVL), Windhoek, Namibia, ³Faculty of Veterinary Medicine, University of Teramo, Teramo, Italy, ⁴Animal Production and Health Laboratory, Animal Production and Health Section, Department of Nuclear Sciences and Applications, Joint FAO/IAEA Division, International Atomic Energy Agency, Vienna, Austria, ⁵Department of Animal Medicine, Production and Health, University of Padova, Legnaro, Legnaro, Italy

Introduction: The swine sector in Africa plays an important role in local economies, contributing to poverty alleviation and community subsistence. In addition, intensive farming is progressively becoming more important in the region. Therefore, any disease affecting swine populations can have detrimental effects on local communities. Porcine Reproductive and Respiratory Syndrome (PRRS) is among the most important infectious diseases affecting swine worldwide, but information on its epidemiology in Africa is extremely limited.

Material and methods: In the present study, 147 healthy butchered pigs, originating from 15 Namibian intensive and rural farms were tested by RT-PCR and the ORF7 genes of positive samples were sequenced for further genetic characterization and phylogenetic analysis. Additionally, 55 warthogs were also evaluated using the same approach.

Results: Overall, 7 out of 147 pigs (4.76%) tested positive, all originating from 3 rural farms (with a within-herd detection frequency higher than 14%) characterized by strong epidemiological links. All industrial pig and warthog samples were negative. Sequence analysis revealed that all strains belonged to the *Betaarterivirus suid1* species, previously known as PRRSV type I, and were likely imported from Europe at least 6 years ago, evolving independently thereafter. When and how the first introduction occurred could not be determined due to the absence of other African sequences for comparison.

Discussion: The present work provides the first detection and characterization of PRRSV molecular epidemiology in Namibia. Based on the present findings, the presence of the PRRSV appears marginal and limited to backyard farms. While biosecurity measures applied in industrial farms appear to be effective in preventing viral introduction, PRRSV circulation in rural settings still represents a potential threat, and considering the socio-economical implication of livestock diseases decreasing animal performances in rural areas, active monitoring should be encouraged to promptly act against emerging menaces and guarantee the welfare of local pig populations.

KEYWORDS

PRRSV, Namibia, Africa, molecular epidemiology, phylogenetics, virus

1 Introduction

The swine industry is experiencing significant growth in several African countries, mirroring an increase in internal demand. Approximately 5% of pigs worldwide are raised in Africa, mostly in sub-Saharan region. Pig production in Namibia, although not the largest on the continent, has an important role in local society and economy (1). Large commercial farms are scattered throughout the country and characterised by advanced management and biosecurity measures, especially targeted at the prevention of African Swine Fever (ASF) introduction (2). However, the majority of local pig production is based on smallholder activities. Pig production contributes significantly to poverty alleviation, female and youth employment and guarantees family and community subsistence and welfare in rural and peri-urban settings (3, 4). According to the data provided by the Namibia Agricultural Union (NAU), local pork production in Namibia accounts for between 45 and 50% of consumption, with the deficit being covered by imports from Europe, Germany and Spain being the main sources. Imports from South Africa have been banned due to the foot-and-mouth disease in August 2022. A total of 14,752 pigs were slaughtered in Namibia between January and April 2023. There is an approximate population of 40,000 pigs in Namibia, primarily located in three districts: Mariental, Windhoek, and Tsumeb.

No African country has yet begun to export pork meat, although a reasonable trade of live animals and pig-derived products is known to occur at regional levels.

The impact of diseases on pigs can result in huge economic consequences for farmer livelihoods and income generation both at the household, community, and regional levels. The impact of diseases results in losses of income to the farmers, and possible closure of markets (4).

The presence and wide circulation of several swine pathogens have been documented in Namibia (5–8). Nevertheless, no information is available on one of the most devastating viral diseases affecting the swine industry in high-income countries: Porcine Reproductive and Respiratory Syndrome (PRRS) (9, 10). PRRS is caused by two viral species, *Betaarterivirus suis* 1 and *Betaarterivirus suis* 2, belonging to the genus *Betaarterivirus*, family *Arteriviridae*.¹ These viruses were previously known as porcine reproductive and respiratory syndrome virus 1 (PRRSV-1), or European type, and porcine reproductive and respiratory syndrome virus 2 (PRRSV-2), or American type (11). They are characterized by a single-stranded, positive-sense RNA [ssRNA(+)] genome of approximately 15 kb. About three-quarters of the genome is occupied by open-reading frame (ORF) 1a and ORF1ab, which encode 14 non-structural proteins, while the terminal region consists of eight partially overlapping ORFs (ORF2a, ORF2b, ORF3, ORF4, ORF5, ORF5a, ORF6 and ORF7) coding for the structural proteins (12). Like other RNA viruses, PRRSV shows a high evolutionary and recombination

rate causing the continuous emergence of new variants on which genetic drift and selective pressures can act, leading to the observed genetic, phenotypic and biological heterogeneity of circulating strains (13–15). Because of this high variability and rapid evolution, the sequencing of relatively short genomic regions is enough to provide useful information on the molecular epidemiology of these viruses. Among the different ORFs, ORF5 and ORF7 are the most commonly used to reconstruct epidemiological links among pig farms, commercial producers, regions, countries, etc. (16–18).

PRRSV infection is responsible for reproductive disorders in sows, respiratory signs, decreased average daily gain, and mortality in growing/fattening animals although the impact can vary depending on the viral species and strain and the overall host condition and immune status. Costs associated with PRRSV disease management also include antimicrobial costs related to increased susceptibility to secondary infections, control strategies and vaccination (19).

Despite the relevance of this infection, only limited data are available from Africa (20). No information on PRRSV was available from Namibia prior to this study. Namibia hosts a remarkable biodiversity, including several wild species that can come in contact with infected domestic animals. In addition to domestic pigs, wild boar is the only other host shown to be susceptible to PRRSV infection although the impact of PRRSV in wildlife is generally considered to be limited. However, no information is currently available on the impact of PRRSV on African wild species especially those that have been shown to be susceptible to infections by other swine pathogens (5–7).

To fill this information gap, several samples were collected from both rural and commercial pig populations, and from wild warthogs, to evaluate the presence of the PRRSV in Namibia and to genetically characterize any strains that might be detected.

2 Materials and methods

2.1 Sample collection and processing

Samples (tonsils or lymph nodes) were collected from 147 healthy butchered pigs (5–6 months of age, approximately 75–100 kg) between March 2018 and May 2023. All of the animals originated from 15 piggeries, comprising 3 industrial facilities and 12 backyard operations. These piggeries were located in six different regions of Namibia: Khomas, Hardap, Kunene, Omaheke, Otjozondjupa, and Erongo. All of the backyard piggeries involved in the study consisted of 30 to 100 animals and observed a medium level of biosecurity. In contrast, the three industrial piggeries maintained herds of approximately 1,400 animals and adhered to a high and strict level of biosecurity.

Additionally, the tonsils of 55 warthogs, living in the area owned by four livestock farms in the Khomas and Otjozondjupa regions, and undergoing periodic hunting campaigns, were collected at slaughter between June 2019 and June 2023, and included in the study.

Sampling collection was conducted by a veterinarian with a specialization in Veterinary Public Health during the post-mortem

¹ <https://ictv.global/taxonomy>

inspection at the abattoir. All samples were collected in sterile and properly labeled airtight containers. The tissues were removed from the carcasses using sterile disposable scalpels and metal forceps, which were carefully flamed with a portable Bunsen burner for each sample. After collection, all the samples were transported refrigerated to the laboratory (+4°C). The tonsils or lymph nodes were homogenized in 1 mL of sterile phosphate-buffered saline (PBS) using the TissueLyser LT (Qiagen, Germany). Total RNA was extracted from the homogenized samples using the High Pure Viral Nucleic Acid Kit (Hoffman-La Roche, Switzerland) with an elution volume of 100 µL, following the manufacturer's instructions.

ORF7 from each sample was amplified using a one-step RT-PCR method as described by Oleksiewicz et al. (21). In brief, ORF7 was amplified using the primer pair ORF7F (5' GCC CCT GCC CAG CAC G 3') and ORF7R (5' TCG CCC TAA TTG AAT AGG TGA 3'), resulting in an amplicon of 637 bp (21). The following thermal profile was applied: reverse transcription at 50°C for 30 min, initial denaturation at 94°C for 2 min, followed by 40 cycles of denaturation at 94°C for 15 s, annealing at 55°C for 20 s, and elongation at 68°C for 50 s. This was followed by a final elongation step at 68°C for 10 min.

2.2 Sequencing and phylogenetic analysis

Amplicons of positive samples were purified using a Wizard SV Gel and PCR Clean-Up System (Promega) and sequenced commercially by LGC Genomics (Berlin, Germany). The sequences of the positive samples were edited and assembled using the Staden software package version 2.0.0b8. All obtained sequences were submitted to the GenBank database under accession numbers OR604620-OR604626.

ORF7 sequences were preliminarily analyzed using BLAST (22) and thereafter a collection of one thousand related sequences was downloaded and aligned to the Namibian ones using MAFFT (23). A maximum-likelihood phylogenetic tree was reconstructed using IQ-TREE (24) selecting the substitution model with the lowest Akaike information criterion (AIC), calculated by JModelTest (25). Ten thousand ultrafast bootstrap replicates were performed to assess clade reliability.

The time passed between the Namibian clade origin and its detection was estimated by performing a serial coalescent analysis using BEAST 1.10 (26), selecting the relaxed lognormal (27) and the Skygrid (28) as molecular clock and viral population size parameter, respectively. For each analysis, an independent run of 100 million generations was performed. Results were analyzed using Tracer 1.7 (29) after the removal of a burn-in of 20% and accepted only if the estimated sample size (ESS) was greater than 200 and the convergence and mixing were adequate. Parameter estimation was summarized in terms of mean and 95% highest posterior density (95HPD). Maximum clade credibility (MCC) trees were constructed and annotated using TreeAnnotator (BEAST package).

3 Results

Seven out of 147 pigs (4.76%; Table 1) coming from 3 of the 15 piggeries involved in the study tested positive for PRRSV by RT-PCR. The ORF7 gene was successfully sequenced in all of the positive samples. None of the 55 warthog samples tested positive for PRRSV. Among the 15 piggeries, only three backyard facilities located

in the Hardap Region tested positive for PRRSV with a within-herd prevalence ranging from 14.29 to 30%, while none of the industrial piggeries showed evidence of PRRSV.

BLAST analysis demonstrated that the sequences were from viruses that belonged to the *Betaarterivirus suis* species, with a percentage of identity of approximately 95% with the most closely related sequence.

The phylogenetic analysis confirmed the Namibian strains as being part of a long branch stemming from a European cluster, including viruses collected, in particular, from Italy (Figure 1).

Based on the genetic distance and the estimated evolutionary rate (i.e., $6.029 \cdot 10^{-3}$ [95HPD, $5.188 \cdot 10^{-3}$ – $6.922 \cdot 10^{-3}$] substitution/site/year), an independent evolution lasting for at least 5.961 years was calculated (mean = 8.011; [95HPD, 5.961–9.743]; Figure 2).

4 Discussion

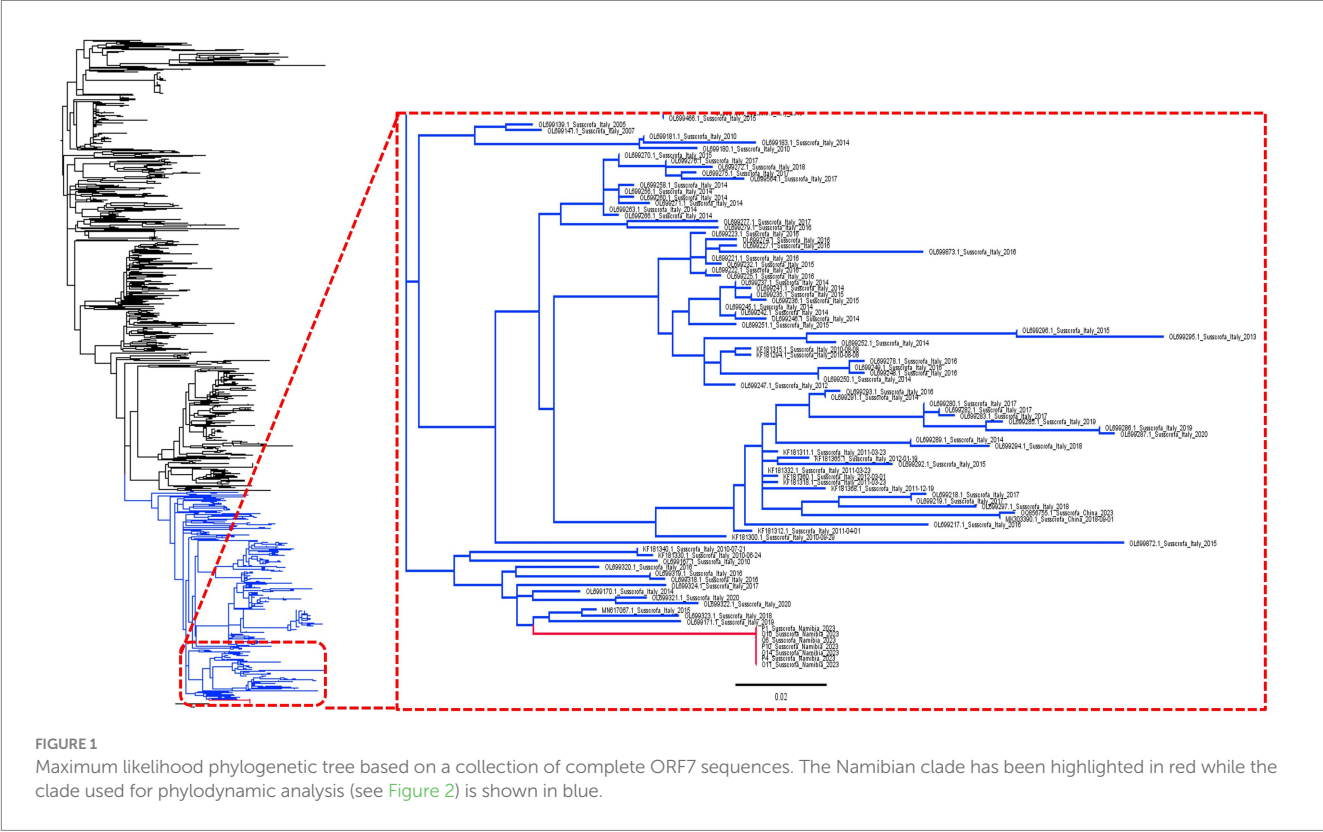
PRRS is one of the most important swine diseases globally, causing an enormous economic burden on the pig industry (19). Although African intensive swine farming only has a marginal impact on the global scenario, both commercial and backyard farms play a significant role in local society, with implications on population welfare and sustenance that goes beyond mere economic relevance (4). High-quality protein source, poverty alleviation, female empowerment are some examples of the multifaceted benefits of pig production in several African countries, Namibia included. Therefore, any disease damaging this sector can have severe detrimental effects on a broader scale. Despite the impact of PRRSV, information on PRRSV epidemiology in Africa is almost absent. The first report of the virus dates back to 2004 from South Africa, followed by a second outbreak in 2007 (20). Some more recent studies have revealed a high detection frequency of PRRSV in Uganda and Nigeria, by serological and molecular methods (30–33). A frequency of PRRSV type 1 and type 2 of 24.65 and 2.73%, respectively, was reported using a commercial real-time RT-PCR assay in Uganda between April 2018 and December 2019 (33).

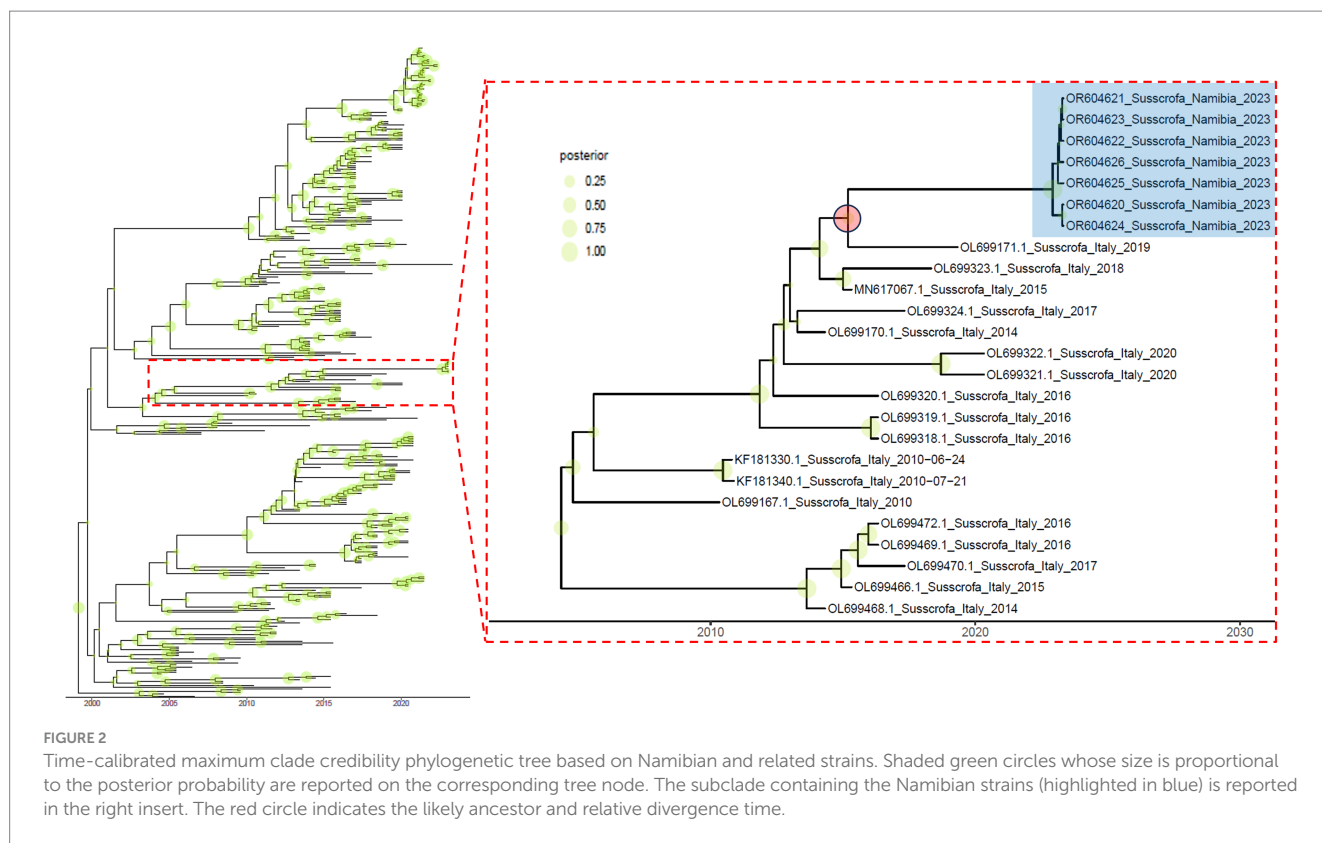
The present study reports the presence of PRRSV in the Namibian swine population for the first time and, more significantly, the first genetic characterization of African strains.

The overall prevalence was significantly lower than that reported in high-income countries and the previous Ugandan study. None of the tested samples originating from industrial farms were positive, which suggests the effectiveness of biosecurity measures applied to control ASF but also preventing PRRSV introduction (8, 34). This finding confirms what has already been reported for PCV-3 in Namibia. On the other hand, three rural farms were shown to be infected, with a within-farm detection frequency higher than 14%. The identified strains were genetically identical. Because of the high evolutionary rate (i.e., $6.029 \cdot 10^{-3}$ [95HPD: $5.188 \cdot 10^{-3}$ – $6.922 \cdot 10^{-3}$] substitution/site/year) of PRRSV estimated herein and in agreement with previous studies (15), this finding suggests an extremely recent introduction. The three farms had strong epidemiological links between them due to the sharing of some boars for breeding purposes, a routine that should thus be strongly discouraged and replaced by the use of certified semen. Therefore, the rapid spread of the identified strain is highly plausible and fits well with the remarkable diffusion potential of PRRSV already demonstrated in intensive farms in high-income countries.

TABLE 1 Metadata of the samples included in the study.

Species	Samples	Number	Farm ID	Type of farm	Region	Collection date	PRRSV positive	Sequences obtained
Domestic Pig	Lymph node	9	A	Rural	Khomas	March 2018	0	0
Domestic Pig	Lymph node	5	B	Rural	Khomas	May 2018	0	0
Domestic Pig	Lymph node	21	C	Industrial	Otjozondjupa	August 2018	0	0
Domestic Pig	Lymph node	7	D	Rural	Omaheke	October 2018	0	0
Domestic Pig	Tonsils	15	E	Industrial	Hardap	September 2019	0	0
Domestic Pig	Tonsils	15	F	Industrial	Hardap	November 2019	0	0
Domestic Pig	Tonsils	10	G	Rural	Kunene	November 2019	0	0
Domestic Pig	Tonsils	15	H	Rural	Khomas	May 2020	0	0
Domestic Pig	Tonsils	5	I	Rural	Khomas	August 2022	0	0
Domestic Pig	Tonsils	3	L	Rural	Hardap	February 2023	0	0
Domestic Pig	Tonsils	4	M	Rural	Khomas	February 2023	0	0
Domestic Pig	Tonsils	4	N	Rural	Erongo	February 2023	0	0
Domestic Pig	Tonsils	14	O	Rural	Hardap	May 2023	2	2
Domestic Pig	Tonsils	10	P	Rural	Hardap	May 2023	3	3
Domestic Pig	Tonsils	10	Q	Rural	Hardap	May 2023	2	2
Warthog	Tonsils	35	R	Rural	Khomas	June 2019 – June 2023	0	0
Warthog	Tonsils	11	S	Rural	Khomas	September 2019	0	0
Warthog	Tonsils	3	T	Rural	Khomas	June 2022	0	0
Warthog	Tonsils	6	U	Rural	Otjozondjupa	May 2022	0	0





When compared to the international scenario, no closely related sequence could be detected. Based on the estimated PRRSV evolutionary rate at least 6 years of independent evolution can be hypothesized. The closest related sequences were part of an Italian clade of PRRV type I. However, it must be stressed that Italy was largely overrepresented in the ORF7 sequence dataset. Therefore, such findings must be evaluated with caution since no trade of pigs or related products, occurs between Italy and Namibia. On the other hand, PRRSV circulation among European countries is significant (14). Therefore, an introduction of European strains can be proposed with a higher confidence, as already seen for several other animal pathogens including those of swine. Importation from other continents, Asia in particular, often described for other pathogens (35–38), was not observed but should nevertheless be considered and investigated with more extensive studies.

Namibian importation of semen and live animals from Europe and South Africa for breeding purposes has been forbidden since 2019. Nevertheless, a preceding introduction from Europe fits well with the long, independent evolution estimated for the present clade. Where and how this introduction event occurred cannot be determined due to the absence of any comparable molecular data from other African countries. The report of PRRSV type I in Uganda (33) may suggest that PRRSV was introduced into other African countries that have a more developed swine industry and that it then spread to Namibia through transboundary animal movements. However, a direct introduction in Namibia cannot be excluded either. More intensive sampling and sequencing of PRRSVs in other African countries should be performed to better understand the molecular epidemiology of the virus on the continent, and understand its population dynamics, introduction and spreading patterns.

Only a few farms, located in a restricted geographical area and with strong epidemiological links between each other were shown to be infected, in the absence of detectable clinical signs. This evidence, combined with the PRRSV-free status of intensive farms, suggests a limited circulation of the virus in Namibia. Unfortunately, despite efforts, funding and farmer compliance prevented a more extensive investigation in the current study. Similarly, the inclusion of more Namibian regions would be useful to increase the representativeness of the obtained data. Further studies are therefore needed to gain a more comprehensive understanding of the epidemiological scenario, characterization of risk factors and calculation of actual economic impact.

Finally, no evidence of the presence of PRRSV in warthogs was found, supporting the restricted host tropism of this virus. Alternatively, the apparently low levels of PRRSV circulation in Namibia may also explain why the virus has not been detected in other species.

The present work is the first step in the study and characterization of PRRSV molecular epidemiology in Africa. Although the presence of PRRSV type I strains, most likely originating from Europe, has been shown in Namibia, its relevance seems marginal and limited to backyard farms. While biosecurity measures such as limited access for people and vehicles, the regular cleaning and disinfection of facilities, the maintenance of a closed herd, farm compartmentalization, the presence of fences around the facilities and the daily inspection of animals applied in industrial farms appear effective in preventing viral introduction, PRRSV circulation in rural farms still represents a potential threat to industrial ones, as has been previously shown in high-income countries (17). Moreover, because of the socio-economical implication of livestock diseases decreasing animal performances even in rural areas, active monitoring should be suggested to promptly act against emerging menaces and guarantee local population welfare.

Data availability statement

The datasets presented in this study can be found in online repositories. The names of the repository/repositories and accession number(s) can be found at: <https://www.ncbi.nlm.nih.gov/genbank/>, OR604620, OR604621, OR604622, OR604623, OR604624, OR604625, OR604626.

Ethics statement

The animal studies were approved by Neudamm Decentralized Ethics Committee. The studies were conducted in accordance with the local legislation and institutional requirements. Written informed consent was not obtained from the owners for the participation of their animals in this study because the samples used for the research activity “first detection and molecular characterization of porcine reproductive and respiratory virus (PRRSV) in Namibia, Africa” were secondary samples obtained from domestic pigs and warthogs, which were originally collected during previous research projects conducted in Namibian pig abattoirs and authorized by the Neudamm Decentralized Ethics Committee of the University of Namibia. Therefore, no specific ethical approval for this study was required.

Author contributions

UM: Conceptualization, Funding acquisition, Investigation, Resources, Supervision, Writing – original draft, Writing – review & editing. LC: Data curation, Formal analysis, Writing – review & editing. MH: Data curation, Writing – review & editing. BC: Data curation, Writing – review & editing. SK: Data curation, Project administration, Writing – review & editing. WD: Funding acquisition,

Methodology, Resources, Writing – review & editing. GF: Conceptualization, Data curation, Formal analysis, Methodology, Software, Writing – original draft, Writing – review & editing.

Funding

The author(s) declare financial support was received for the research, authorship, and/or publication of this article. This work was supported by the Department of Animal Medicine, Production and Health, University of Padua [grant number BIRD225455/22] and by the IAEA Peaceful Uses Initiative (PUI) VETLAB Network. The sequences were generated through the Sequencing Services of the Animal Production and Health sub-programme of the Joint Food and Agricultural Organization of the United Nations/International Atomic Energy Agency (IAEA) Division.

Conflict of interest

The authors declare that the research was conducted in the absence of any commercial or financial relationships that could be construed as a potential conflict of interest.

Publisher's note

All claims expressed in this article are solely those of the authors and do not necessarily represent those of their affiliated organizations, or those of the publisher, the editors and the reviewers. Any product that may be evaluated in this article, or claim that may be made by its manufacturer, is not guaranteed or endorsed by the publisher.

References

- Mary Louise Penrith. Demographics of pigs in Africa In: *Regional Training Course (Africa) Import Risk Analysis for African Swine Fever*. World Organisation for Animal Health (WOAH). (2021).
- Fasina F. *An Overview of Swine Production and Marketing Value Chains, West and Central Africa*. World Organisation for Animal Health (WOAH). (2021).
- Okai E. K. (2019). Big Opportunities for Pig Farmers in West Africa. Available at: <https://www.thepigsite.com/articles/big-opportunities-for-pig-farmers-in-west-africa> (Accessed October 10, 2023).
- Weka R, Bwala D, Adedeji Y, Ifende I, Davou A, Ogo N, et al. Tracing the domestic pigs in Africa In: G Kušec and ID Kušec, editors. *Tracing the Domestic Pig*. Rijeka: IntechOpen (2021).
- Molini U, Coetzee LM, Hemberger MY, Khaibab S, Cattoli G, Dundon WG. Evidence indicating transmission of porcine parvovirus 1 between warthogs and domestic pigs in Namibia. *Vet Res Commun*. (2023) 47:981–5. doi: 10.1007/s11259-022-10038-1
- Molini U, Franco G, Gous L, Moller S, Hemberger YM, Chiwome B, et al. Three different genotypes of porcine circovirus 2 (PCV-2) identified in pigs and warthogs in Namibia. *Arch Virol*. (2021) 166:1723–8. doi: 10.1007/s00705-021-05035-9
- Molini U, Franco G, Settypalli TBK, Hemberger MY, Khaibab S, Cattoli G, et al. Viral co-infections of warthogs in Namibia with African swine fever virus and porcine parvovirus 1. *Animals*. (2022) 12:1697. doi: 10.3390/ani12131697
- Molini U, Marruchella G, Matheus F, Hemberger YM, Chiwome B, Khaibab S, et al. Molecular investigation of porcine circovirus type 3 infection in pigs in Namibia. *Pathogens*. (2021) 10:585. doi: 10.3390/pathogens10050585
- Nieuwenhuis N, Duinhof TF, Van Nes A. Papers: economic analysis of outbreaks of porcine reproductive and respiratory syndrome virus in nine sow herds. *Vet Rec*. (2012) 170:225. doi: 10.1136/vr.100101
- Segalés J, Mateu E. One world, one health: the threat of emerging and re-emerging viral infections of pigs. *Transbound Emerg Dis*. (2012) 59:1–2. doi: 10.1111/J.1865-1682.2011.01303.X
- Ruedas-Torres I, Rodríguez-Gómez IM, Sánchez-Carvajal JM, Larenas-Muñoz F, Pallarés FJ, Carrasco L, et al. The jigsaw of PRRSV virulence. *Vet Microbiol*. (2021) 260:109168. doi: 10.1016/J.VETMIC.2021.109168
- Dokland T. The structural biology of PRRSV. *Virus Res*. (2010) 154:86–97. doi: 10.1016/j.virusres.2010.07.029
- Duffy S. Why are RNA virus mutation rates so damn high? *PLoS Biol*. (2018) 16:e3000003. doi: 10.1371/journal.pbio.3000003
- Franzo G, Faustini G, Legnardi M, Cecchinato M, Drigo M, Tucciarone CM. Phylogenetic and phylogeographic reconstruction of porcine reproductive and respiratory syndrome virus (PRRSV) in Europe: patterns and determinants. *Transbound Emerg Dis*. (2022) 69:e2175–84. doi: 10.1111/tbed.14556
- Stadejek T, Stankevicius A, Murtaugh MP, Oleksiewicz MB. Molecular evolution of PRRSV in Europe: current state of play. *Vet Microbiol*. (2013) 165:21–8. doi: 10.1016/j.vetmic.2013.02.029
- Balka G, Podgórska K, Brar MS, Bálint Á, Cadar D, Celer V, et al. Genetic diversity of PRRSV 1 in Central Eastern Europe in 1994–2014: origin and evolution of the virus in the region. *Sci Rep*. (2018) 8:7811. doi: 10.1038/s41598-018-26036-w
- Franzo G, Barbierato G, Pesente P, Legnardi M, Tucciarone CM, Sandri G, et al. Porcine reproductive and respiratory syndrome (Prs) epidemiology in an integrated pig company of northern Italy: a multilevel threat requiring multilevel interventions. *Viruses*. (2021) 13:2510. doi: 10.3390/v13122510
- Shi M, Lemey P, Singh Brar M, Suchard MA, Murtaugh MP, Carman S, et al. The spread of type 2 porcine reproductive and respiratory syndrome virus (PRRSV) in North America: a phylogeographic approach. *Virology*. (2013) 447:146–54. doi: 10.1016/j.virol.2013.08.028
- Montaner-Tarbes S, del Portillo HA, Montoya M, Fraile L. Key gaps in the knowledge of the porcine respiratory reproductive syndrome virus (PRRSV). *Front Vet Sci*. (2019) 6:435543. doi: 10.3389/FVETS.2019.00038/BIBTEX

20. Beltran-Alcrudo D, Lubroth J, Njeumi F, Pinto J, DeLaRocque S, Martin V, et al. Porcine reproductive and respiratory syndrome (PRRS) regional awareness. *FAO*. (2007) 2. doi: 10.1002/9781119506287.ch26
21. Oleksiewicz MB, Bøtner A, Madsen KG, Storgaard T. Sensitive detection and typing of porcine reproductive and respiratory syndrome virus by RT-PCR amplification of whole viral genes. *Vet Microbiol.* (1998) 64:7–22. doi: 10.1016/S0378-1135(98)00254-5
22. Madden T. The BLAST sequence analysis tool In: *The BLAST Sequence Analysis Tool*. USA: National Center for Biotechnology Information (2013). 1–17.
23. Standley K. MAFFT multiple sequence alignment software version 7: improvements in performance and usability (outlines version 7). *Mol Biol Evol.* (2013) 30:772–80. doi: 10.1093/molbev/mst010
24. Nguyen LT, Schmidt HA, Von Haeseler A, Minh BQ. IQ-TREE: a fast and effective stochastic algorithm for estimating maximum-likelihood phylogenies. *Mol Biol Evol.* (2015) 32:268–74. doi: 10.1093/molbev/msu300
25. Darriba D, Taboada GL, Doallo R, Posada D. JModelTest 2: more models, new heuristics and parallel computing. *Nat Methods.* (2012) 9:772. doi: 10.1038/nmeth.2109
26. Suchard MA, Lemey P, Baele G, Ayres DL, Drummond AJ, Rambaut A. Bayesian phylogenetic and phylodynamic data integration using BEAST 1.10. *Virus Evol.* (2018) 4:vey016. doi: 10.1093/ve/vey016
27. Drummond AJ, Ho SYW, Phillips MJ, Rambaut A. Relaxed phylogenetics and dating with confidence. *PLoS Biol.* (2006) 4:e88–e710. doi: 10.1371/journal.pbio.0040088
28. Hill V, Baele G. Bayesian estimation of past population dynamics in BEAST 1.10 using the Skygrid coalescent model. *Mol Biol Evol.* (2019) 36:2620–8. doi: 10.1093/molbev/msz172
29. Rambaut A, Drummond AJ, Xie D, Baele G, Suchard MA. Posterior summarization in Bayesian phylogenetics using tracer 1.7. *Syst Biol.* (2018) 67:901–4. doi: 10.1093/sysbio/syy032
30. Aiki-Raji CO, Adebisi AI, Abiola JO, Oluwayelu DO. Prevalence of porcine reproductive and respiratory syndrome virus and porcine parvovirus antibodies in commercial pigs, Southwest Nigeria. *Beni Suef Univ J Basic Appl Sci.* (2018) 7:80–3. doi: 10.1016/j.bjbas.2017.07.006
31. Dione M, Masembe C, Akol J, Amia W, Kungu J, Lee HS, et al. The importance of on-farm biosecurity: Sero-prevalence and risk factors of bacterial and viral pathogens in smallholder pig systems in Uganda. *Acta Trop.* (2018) 187:214–21. doi: 10.1016/j.actatropica.2018.06.025
32. Meseko C, Oluwayelu D. Evidence of porcine reproductive and respiratory syndrome virus antibodies in commercial pig husbandry in Nigeria: a preliminary study. *Trop Vet.* (2014) 32:97–103. doi: 10.4314/TV.V32I3-4
33. Oba P, Dione MM, Erume J, Wieland B, Mutisya C, Ochieng L, et al. Molecular characterization of porcine reproductive and respiratory syndrome virus (PRRSv) identified from slaughtered pigs in northern Uganda. *BMC Vet Res.* (2022) 18:176–8. doi: 10.1186/s12917-022-03272-x
34. Mutua F, Dione M. The context of application of biosecurity for control of African swine fever in smallholder pig systems: current gaps and recommendations. *Front Vet Sci.* (2021) 8:1–11. doi: 10.3389/fvets.2021.689811
35. Franzo G, De Villiers L, De Villiers M, Ravandi A, Gyani K, Van Zyl L, et al. Molecular epidemiology of canine parvovirus in Namibia: introduction pathways and local persistence. *Prev Vet Med.* (2022) 209:105780. doi: 10.1016/j.prevetmed.2022.105780
36. Franzo G, Dundon WG, De Villiers M, De Villiers L, Coetzee LM, Khaïseb S, et al. Phylodynamic and phylogeographic reconstruction of beak and feather disease virus epidemiology and its implications for the international exotic bird trade. *Transbound Emerg Dis.* (2022) 69:e2677–87. doi: 10.1111/tbed.14618
37. Franzo G, Settypalli TBK, Agusi ER, Meseko C, Minoungou G, Ouoba BL, et al. Porcine circovirus-2 in Africa: identification of continent-specific clusters and evidence of independent viral introductions from Europe, North America and Asia. *Transbound Emerg Dis.* (2022) 69:e1142–52. doi: 10.1111/tbed.14400
38. Franzo G, Zerbo HL, Ouoba BL, Dji-Tombo AD, Kindo MG, Sawadogo R, et al. A phylogeographic analysis of porcine parvovirus 1 in Africa. *Viruses.* (2023) 15:207. doi: 10.3390/V15010207



OPEN ACCESS

EDITED BY

Mengmeng Zhao,
Foshan University, China

REVIEWED BY

Nanhua Chen,
Yangzhou University, China
Bo Wan,
Henan Agricultural University, China

*CORRESPONDENCE

Fuxiao Liu

✉ laudawn@126.com

Xiaoxiao Duan

✉ dxx45@163.com

†These authors have contributed equally to this work

RECEIVED 17 December 2023

ACCEPTED 15 January 2024

PUBLISHED 24 January 2024

CITATION

Li Y, Liu T, Zhang Y, Duan X and Liu F (2024) RNA recombination: non-negligible factor for preventing emergence or reemergence of Senecavirus A. *Front. Vet. Sci.* 11:1357179. doi: 10.3389/fvets.2024.1357179

COPYRIGHT

© 2024 Li, Liu, Zhang, Duan and Liu. This is an open-access article distributed under the terms of the [Creative Commons Attribution License \(CC BY\)](https://creativecommons.org/licenses/by/4.0/). The use, distribution or reproduction in other forums is permitted, provided the original author(s) and the copyright owner(s) are credited and that the original publication in this journal is cited, in accordance with accepted academic practice. No use, distribution or reproduction is permitted which does not comply with these terms.

RNA recombination: non-negligible factor for preventing emergence or reemergence of Senecavirus A

Yan Li^{1,2†}, Tianyu Liu^{1†}, Youming Zhang³, Xiaoxiao Duan^{2*} and Fuxiao Liu^{1*}

¹College of Veterinary Medicine, Qingdao Agricultural University, Qingdao, China, ²Qingdao Center for Animal Disease Control and Prevention, Qingdao, China, ³State Key Laboratory of Microbial Technology, Shandong University, Qingdao, China

KEYWORDS

Senecavirus A, RNA recombination, copy-choice recombination, evolution, infection

Introduction

As an emerging virus, Senecavirus A (SVA) induces the vesicular disease in pigs. Clinical cases initially show mild signs characterized by lethargy and lameness, usually followed by the development of vesicles on the snout, dewclaw or (and) coronary band. SVA-elicited signs are generally indistinguishable from those of other vesicular diseases (1). In addition, SVA may cause epidemic transient neonatal losses in swine (2, 3). Although SVA infection was initially found at a Canada market in 2007 (4), the viral prototype had been recognized as a contaminant in culture of PER.C6 cells in 2002 (5). A retrospective study unexpectedly exhibited that SVA was circulating in the pig population of the United States as early as 1988, or even earlier (6). To date, SVA has been found in several countries, including Canada (4), the United States (7), Brazil (8), China (9), Thailand (10), Vietnam (11) and more recently Chile (12), therefore attracting a great deal of attention from the pig industry worldwide.

SVA belongs to the genus *Senecavirus* in the family *Picornaviridae*. Its virion is an icosahedral particle, approximately 30 nm in diameter. Its genome is a positive-sense, single-stranded and non-segmented RNA, approximately 7 300 nt in length, with a 3' poly(A) tail but without 5'-end capped structure. The genome contains 5' and 3' untranslated regions, and a long encoding region of polyprotein precursor. After SVA infection in a susceptible cell, the viral polyprotein precursor will be translated in the cytoplasm, and then progressively cleaved into 12 polypeptides, namely L, VP4, VP2, VP3, VP1, 2A, 2B, 2C, 3A, 3B, 3C and 3D (5). The VP1 to VP4 are four structural proteins. Their 60 copies form an icosahedral capsid with the typical architecture of picornavirus. The other proteins are non-structural proteins, involved in viral genome replication, host cell metabolism, and immune evasion (13). Mutual replication between genome and antigenome is catalyzed by a picornavirus-encoded RNA-dependent RNA polymerase (RdRp), also termed 3D polymerase (14).

Selective pressure prompting SVA evolution

Understanding the origin and evolution of SVA is important for its prevention and surveillance. It is speculated that SVA originates from the United States in the 1980s, subsequently spreading to other countries and regions (15). To date, SVA has evolved into eight distinct lineages, including Clade Ancestor and Clade I to VII (16). Genomic

differentiation progressively emerged with the continuous SVA evolution. Due to the low-fidelity characteristics of SVA RdRp, SVA displays a relatively high mutation rate during serial passaging *in vitro*, as demonstrated by our previous study (17). Therefore, SVA can rapidly enhance its own adaptive ability *via* synonymous codon bias evolution (18). Indeed, the codon preference analysis has indicated that natural selection is a primary driving force that affects the codon usage bias in SVA (15). Selection pressure analysis has additionally exhibited that the SVA polyprotein has been undergoing selection, with four amino acid residues located in the VP1, 2A, 3C, and 3D encoding regions that are under positive/diversifying selection (19).

SVA intra-species recombination

Picornaviral members possess a typical feature, i.e., intra-species recombination, whereby viral progenies are produced from more than one parental genome (20). Such a recombination pattern can help picornaviruses adapt to a new environment, such as counteracting an error catastrophe within the viral genome (21). The intra-species recombination event has been demonstrated to occur in a population of picornaviruses, like enterovirus, aphthovirus and cardiovirus (22). Recently, it has been also reported that RNA recombination events have arisen among different SVA strains (23–29). Out of these reports, the earliest one characterized an SVA isolate (HeN-1/2018) from China in detail by the SimPlot analysis. The result revealed two breakpoints separating the viral genome into three regions, of which two fragments were independently derived from two genetically related variants of another country (23).

The intra-species recombination is an unpredictable event (30). Liu et al. (29) showed that two China variants (CH-GDZS-2019 and CH-GDMZ-2019), albeit isolated from the same province in 2019, had different results of recombination analysis. The CH-GDZS-2019 was genetically derived from USA-IA44662–2015-P1 and USA-GBI29–2015, both of which were isolated from the USA in 2015, while the CH-GDMZ-2019 was genetically derived from two China isolates (29). More recently, Wu et al. (27) collected a total of 238 SVA complete genomes from GenBank for recombination analysis by means of bioinformatic tools. The result showed that five isolates were identified as recombinants. Each of them was genetically derived from two or three isolates, which were suggested as the representatives of its putative parental lineages.

Copy-choice recombination pattern

Intra-species recombination is a dominant genetic feature of picornaviruses, because these viruses exhibit remarkable structural or functional plasticity of their genomes (22). A typical model indicates that the picornaviral RdRp can switch a template during anti-genome (or genome) synthesis, causing occurrence of RNA recombination between two different individuals. Such a model was referred to as copy-choice recombination (20). The copy-choice recombination is responsible for the formation of recombinant RNA molecules through the RdRp switching from one template to another during genome/antigenome replication. For a given

picornavirus, some special sequences are prone to occurrence of copy-choice recombination within them. These recombination-prone sequences are also known as recombination hotspots, which are associated both with RNA secondary structures and with nucleotide base composition (31). Determining recombination-prone sequences will uncover the existence of significant biases in the production of specific recombinant forms. Characterizing recombination-prone sequences will provide insight into a molecular mechanism involved in template switching (32). In addition, the RdRp plays an essential role in SVA replicative recombination, as evidenced by two RdRp variants (S460L and I212/S460L) that can reduce SVA recombination capacity (33).

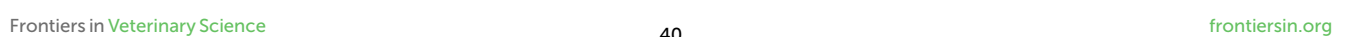
As mentioned above, SVA has been continually evolving, and even recombining with one another (23–29). Unfortunately, the conclusion of recombination events was only deduced by the analysis using bioinformatic tools. We recently used reverse genetics technique to confirm experimentally that the copy-choice recombination could indeed occur inside a cell. We found that two lethal SVA cDNA clones, if independently transfected into cells, had no ability of virus recovery. However, their co-transfection led to the replication-competent virus successfully rescued from a cell monolayer. Sanger sequencing indicated the rescued virus with a wild-type genotype, implying that the copy-choice recombination event made the recombinant SVA avoid lethal mutations (34).

Model of copy-choice recombination between SVAs

If two different strains, SVA-A and -B, infect the same cell, copy-choice recombination may occur during genome/antigenome replication. Figure 1 schematically represents a series of events involved in how two different SVA virions infect a single cell, and more importantly how two genomes recombine with each other via the copy-choice pattern. In an SVA-A and -B-infected cell, the viral RdRp slides along the SVA-A genome for synthesizing its antigenome. If hindered by a physical barrier (e.g., a high-order RNA structure) during the replication of antigenome, the RdRp may detach from the genome template (Figure 1, step V), and then drag a nascent incomplete antigenome to search for an alternative template. The step VI briefly shows the process of template switching. The copy-choice recombination finally results in one recombinant that simultaneously harbors SVA-A and -B-derived sequences. If both SVA-A and -B harbor detrimental mutations but at two different positions in their genomes, the recombinant will “cleverly” evade these detrimental mutations, consequently achieving higher adaptability to a new environment.

Copy-choice recombination improving virus fitness

Copy-choice recombination makes the progeny genome derive from more than one parental genome. This reproductive mode in virology is referred to as sexual replication (35), which can create considerable changes in the viral genome, allowing for antigenic shifts, host jumps, and fitness alteration. For example, copy-choice recombination of chikungunya virus can give rise



to genome diversification, and even generate emerging variants that are positively selected in mosquitoes, thereby allowing chikungunya virus to overcome “tight” genetic bottlenecks or even providing an advantage in the improvement of viral fitness (36). The accumulation of mutations in viral RNA genomes perhaps leads to an error catastrophe, lethal to virus growth. However, poliovirus was demonstrated to be able of utilizing copy-choice recombination to evade the ribavirin-induced error catastrophe, therefore drastically enhancing its own fitness (21). Using defined imprecise recombinant viruses with Oxford Nanopore and Illumina next generation sequencing technologies, Bentley et al. (37) have drawn a conclusion that viruses undergo frequent and continuous recombination events over a prolonged period until the fittest viruses, predominantly those with wild-type length genomes, dominate the population.

RNA recombination: non-negligible factor for preventing SVA infection

Although the emergence of viral variants is often involved in site mutations a given long-term selective pressure causes, both intra- and inter-species RNA recombination events would even directly cause the emergence or reemergence of positive-stranded RNA viruses. This is definitely a non-negligible issue for the prevention of emerging and reemerging diseases. As mentioned above, RNA recombination events continuously occur especially among intra-species individuals. For example, high recombination rates in the spike gene have been demonstrated to cause the emergence of lethal canine enteric coronaviruses (38). Similarly, porcine epidemic diarrhea virus has also revealed genetic changes in its spike gene, perhaps giving rise to the emergence of highly virulent variants in the field (39, 40). Enteroviruses, aphthoviruses and teschoviruses have shown phylogenetic segregation by serotype only in the structural region. Lack of segregation elsewhere has been proven to be attributable to extensive inter-serotype recombination (41).

Viral RNA recombination facilitates the ontogeny of viral variants with increased virulence and pathogenesis. The recombinant may resist immune responses, confer pathogenic effects in hosts, or (and) make itself be more transmissible in susceptible populations (30). Indeed, Bai et al. (2) showed that an SVA isolate from Shandong province in China was a putative recombinant, able to confer low fever, blisters, and lameness in pigs. More recently, another putative recombinant, also isolated from Shandong province, could elicit obvious clinical signs in pigs, and was capable of transmission to contact-exposed individuals (28). Therefore, the virulence enhancement is an adverse consequence SVA recombinants confer. This is the first non-negligible consequence resulting from the RNA recombination. Another key issue is a given SVA recombinant may be less virulent than its progenitor to hosts, causing the latent virus transmission in a population of pigs. If so, such a SVA recombinant would be a potential risk factor in hosts. It will gradually evolve along with common behavior of hosts, such as movement, mating and production. If there are changes in the herd environment, the SVA recombinant

would possibly revert back to a status as highly virulent as that of its progenitor. This is the second non-negligible issue for preventing SVA infection. Last but not least, there is a potential risk, namely, RNA recombination that perhaps makes virus recombinants break through the host-range limitation. Although SVA infection is not regarded as zoonosis now, SVA has potent oncolytic activities in some human tumor cells (42). If SVA recombines with a human-derived virus, the emerging recombinant would have a potential in infecting humans, even inducing a severe zoonosis.

Conclusions and future perspectives

Although SVA was found in the 1980s, how SVA originated was still unclear. SVA has been continually evolving via point mutations and RNA recombination. Compared with that of point mutations, the molecular mechanism of RNA recombination is greatly complicated. Moreover, compared with point mutations, although a map of RNA recombination can be represented by analysis using bioinformatic tools, the recombination process is not easily confirmed through an experiment. Therefore, RNA recombination among different SVAs is often neglected, consequently remaining a potential threat to the pig industry or even the public health. The pattern of copy-choice recombination makes SVA simultaneously acquire genomic sequences from two even more parental strains. This pattern randomly occurs in theory, and is unpredictable during the SVA evolution.

The outbreak of SVA infection was not frequently reported worldwide in recent 3 years. However, in order to prevent emergence or reemergence of SVA, RNA recombination should not be neglected by practitioners. Broad-spectrum antiviral agents should not be abused, because they possibly exert selection pressures on the SVA evolution. It is necessary now for taking action on continuous detection and surveillance for SVA recombination. Elucidation of the recombination-related mechanism will enable us to learn more about the relationship between RNA recombination and natural selection. Both epidemiological survey and phylogenetic analysis will contribute to the construction of a model for predicting major trends of SVA evolution in future.

Author contributions

YL: Writing—original draft. TL: Writing—original draft. YZ: Writing—review & editing. XD: Writing—review & editing. FL: Writing—review & editing.

Funding

The author(s) declare financial support was received for the research, authorship, and/or publication of this article. This work

was supported by the Qingdao Demonstration Project for People-benefit from Science and Techniques (Grant no. 23-2-8-xdny-14-nsh) and the Open Project Fund of State Key Laboratory of Microbial Technology (M2023-03).

Conflict of interest

The authors declare that the research was conducted in the absence of any commercial or financial relationships

that could be construed as a potential conflict of interest.

Publisher's note

All claims expressed in this article are solely those of the authors and do not necessarily represent those of their affiliated organizations, or those of the publisher, the editors and the reviewers. Any product that may be evaluated in this article, or claim that may be made by its manufacturer, is not guaranteed or endorsed by the publisher.

References

- Fernandes MHV, de Lima M, Joshi LR, Diel DG. A virulent and pathogenic infectious clone of Senecavirus A. *J Gen Virol.* (2021) 102:001643. doi: 10.1099/jgv.0.001643
- Bai J, Fan H, Zhou E, Li L, Li S, Yan J, et al. Pathogenesis of a senecavirus A isolate from swine in Shandong Province, China. *Vet Microbiol.* (2020) 242:108606. doi: 10.1016/j.vetmic.2020.108606
- Oliveira TES, Michelazzo MMZ, Fernandes T, de Oliveira AG, Leme RA, Alfieri AF, et al. Histopathological, immunohistochemical, and ultrastructural evidence of spontaneous Senecavirus A-induced lesions at the choroid plexus of newborn piglets. *Sci Rep.* (2017) 7:16555. doi: 10.1038/s41598-017-16407-0
- Pasma T, Davidson S, Shaw SL. Idiopathic vesicular disease in swine in Manitoba. *Can Vet J.* (2008) 49:84–5.
- Hales LM, Knowles NJ, Reddy PS, Xu L, Hay C, Hallenbeck PL. Complete genome sequence analysis of Seneca Valley virus-001, a novel oncolytic picornavirus. *J Gen Virol.* (2008) 89:1265–75. doi: 10.1099/vir.0.83570-0
- Knowles NJ, Hales LM, Jones BH, Landgraf JG, House JA, Skele KL, et al. Epidemiology of Seneca Valley Virus: Identification and Characterization of Isolates from Pigs in the United States. In: *Northern Lights EUROPE 2006: XIVth Meeting of the European Study Group on the Molecular Biology of Picornaviruses*. Saarisekä, Inari, Finland (2006).
- Singh K, Corner S, Clark S, Scherba G, Fredrickson R. Seneca valley virus and vesicular lesions in a pig with idiopathic vesicular disease. *J Vet Sci Technol.* (2012) 3:1–3. doi: 10.4172/2157-7579.1000123
- Leme RA, Zotti E, Alcantara BK, Oliveira MV, Freitas LA, Alfieri AF, et al. Senecavirus A: an emerging vesicular infection in Brazilian pig herds. *Trans Emerg Dis.* (2015) 62:603–11. doi: 10.1111/tbed.12430
- Wu Q, Zhao X, Bai Y, Sun B, Xie Q, Ma J. The first identification and complete genome of senecavirus A affecting pig with idiopathic vesicular disease in China. *Transbound Emerg Dis.* (2017) 64:1633–40. doi: 10.1111/tbed.12557
- Saeng-Chuto K, Rodtian P, Temeeyasen G, Wegner M, Nilubol D. The first detection of Senecavirus A in pigs in Thailand, 2016. *Transbound Emerg Dis.* (2018) 65:285–8. doi: 10.1111/tbed.12654
- Arzt J, Bertram MR, Vu LT, Pauszek SJ, Hartwig EJ, Smoliga GR, et al. First detection and genome sequence of Senecavirus A in Vietnam. *Microbiol Resour Annu.* (2019) 8:e01247–18. doi: 10.1128/MRA.01247-18
- Bennett B, Urzúa-Encina C, Pardo-Roa C, Ariyama N, Lecocq C, Rivera C, et al. First report and genetic characterization of Seneca Valley virus (SVV) in Chile. *Transbound Emerg Dis.* (2022) 69:e3462–e8. doi: 10.1111/tbed.14747
- Wang Q, Meng H, Ge D, Shan H, Geri L, Liu F. Structural and nonstructural proteins of Senecavirus A: recent research advances, and lessons learned from those of other picornaviruses. *Virology.* (2023) 585:155–63. doi: 10.1016/j.virol.2023.06.004
- Kok CC, McMinn PC. Picornavirus RNA-dependent RNA polymerase. *Int J Biochem Cell Biol.* (2009) 41:498–502. doi: 10.1016/j.biocel.2008.03.019
- Zeng W, Yan Q, Du P, Yuan Z, Sun Y, Liu X, et al. Evolutionary dynamics and adaptive analysis of Seneca Valley virus. *Infect Genet Evol.* (2023) 113:105488. doi: 10.1016/j.meegid.2023.105488
- Gao H, Chen YJ, Xu XQ, Xu ZY, Xu SJ, Xing JB, et al. Comprehensive phylogeographic and phylodynamic analyses of global Senecavirus A. *Front Microbiol.* (2022) 13:980862. doi: 10.3389/fmicb.2022.980862
- Liu F, Huang Y, Wang Q, Li J, Shan H. Rescue of Senecavirus A to uncover mutation profiles of its progenies during 80 serial passages *in vitro*. *Vet Microbiol.* (2021) 253:108969. doi: 10.1016/j.vetmic.2020.108969
- Zhao S, Cui H, Hu Z, Du L, Ran X, Wen X. Senecavirus A enhances its adaptive evolution via synonymous codon bias evolution. *Viruses.* (2022) 14:1055. doi: 10.3390/v14051055
- Joshi LR, Mohr KA, Gava D, Kutish G, Buysse AS, Vannucci FA, et al. Genetic diversity and evolution of the emerging picornavirus Senecavirus A. *J Gen Virol.* (2020) 101:175–87. doi: 10.1099/jgv.0.001360
- Kirkegaard K, Baltimore D. The mechanism of RNA recombination in poliovirus. *Cell.* (1986) 47:433–43. doi: 10.1016/0092-8674(86)90600-8
- Kempf BJ, Watkins CL, Peersen OB, Barton DJ. Picornavirus RNA recombination counteracts error catastrophe. *J Virol.* (2019) 93:e00652–19. doi: 10.1128/JVI.00652-19
- Lukashev AN. Recombination among picornaviruses. *Rev Med Virol.* (2010) 20:327–37. doi: 10.1002/rmv.660
- Wang Z, Zhang X, Yan R, Yang P, Wu Y, Yang D, et al. Emergence of a novel recombinant Seneca Valley virus in Central China, 2018. *Emerg Microbes Infect.* (2018) 7:180. doi: 10.1038/s41426-018-0183-1
- Liu J, Zha Y, Li H, Sun Y, Wang F, Lu R, et al. Novel recombinant seneca valley virus isolated from slaughtered pigs in Guangdong Province. *Virol Sin.* (2019) 34:722–4. doi: 10.1007/s12250-019-00139-8
- Guo Z, Chen XX, Ruan H, Qiao S, Deng R, Zhang G. Isolation of three novel senecavirus A strains and recombination analysis among senecaviruses in China. *Front Vet Sci.* (2020) 7:2. doi: 10.3389/fvets.2020.00002
- Dong J, Rao D, He S, Jiao F, Yi B, Chen B, et al. Emergence of a novel recombinant USA/GB129/2015-like strain of Seneca Valley virus in Guangdong Province, 2018. *Can J Vet Res.* (2021) 85:224–8.
- Wu H, Li C, Ji Y, Mou C, Chen Z, Zhao J. The evolution and global spatiotemporal dynamics of senecavirus A. *Microbiol Spectr.* (2022) 10:e0209022. doi: 10.1128/spectrum.02090-22
- Li C, Wu X, Wang X, Shi J, Liu C, Peng Z, et al. Complete genome and pathogenesis of a novel recombinant Senecavirus A isolate in PR China. *J Gen Virol.* (2022) 103:1788. doi: 10.1099/jgv.0.001788
- Liu J, Guo Q, Li H, Yu X, Liu B, Zhao B, et al. Genomic diversity and recombination of Seneca Valley viruses emerged in pig herds in Guangdong Province during 2019. *Virus Genes.* (2020) 56:642–5. doi: 10.1007/s11262-020-01769-x
- Wang H, Cui X, Cai X, An T. Recombination in positive-strand RNA viruses. *Front Microbiol.* (2022) 13:870759. doi: 10.3389/fmicb.2022.870759
- Runckel C, Westesson O, Andino R, DeRisi JL. Identification and manipulation of the molecular determinants influencing poliovirus recombination. *PLoS Path.* (2013) 9:e1003164. doi: 10.1371/journal.ppat.1003164
- Moumen A, Polomack L, Roques B, Buc H, Negroni M. The HIV-1 repeated sequence R as a robust hot-spot for copy-choice recombination. *Nucleic Acids Res.* (2001) 29:3814–21. doi: 10.1093/nar/29.18.3814
- Li C, Wang H, Shi J, Yang D, Zhou G, Chang J, et al. Senecavirus-specific recombination assays reveal the intimate link between polymerase fidelity and RNA recombination. *J Virol.* (2019) 93:e00576–19. doi: 10.1128/JVI.00576-19
- Liu F, Wang Q, Meng H, Zhao D, Hao X, Zhang S, et al. Experimental evidence for occurrence of putative copy-choice recombination between two Senecavirus A genomes. *Vet Microbiol.* (2022) 271:109487. doi: 10.1016/j.vetmic.2022.109487
- Chao L. Evolution of sex and the molecular clock in RNA viruses. *Gene.* (1997) 205:301–8. doi: 10.1016/S0378-1119(97)00405-8
- Filomatori CV, Bardossy ES, Merwaiss F, Suzuki Y, Henrion A, Saleh MC, et al. RNA recombination at Chikungunya virus 3' UTR as

- an evolutionary mechanism that provides adaptability. *PLoS Path.* (2019) 15:e1007706. doi: 10.1371/journal.ppat.1007706
37. Bentley K, Alnaji FG, Woodford L, Jones S, Woodman A, Evans DJ. Imprecise recombinant viruses evolve via a fitness-driven, iterative process of polymerase template-switching events. *PLoS Path.* (2021) 17:e1009676. doi: 10.1371/journal.ppat.1009676
 38. Licitra BN, Duhamel GE, Whittaker GR. Canine enteric coronaviruses: emerging viral pathogens with distinct recombinant spike proteins. *Viruses.* (2014) 6:3363–76. doi: 10.3390/v6083363
 39. Vlasova AN, Marthaler D, Wang Q, Culhane MR, Rossow KD, Rovira A, et al. Distinct characteristics and complex evolution of PEDV strains, North America, May 2013–February 2014. *Emerg Infect Dis.* (2014) 20:1620–8. doi: 10.3201/eid2010.140491
 40. Jarvis MC, Lam HC, Zhang Y, Wang L, Hesse RA, Hause BM, et al. Genomic and evolutionary inferences between American and global strains of porcine epidemic diarrhea virus. *Prev Vet Med.* (2016) 123:175–84. doi: 10.1016/j.prevetmed.2015.10.020
 41. Simmonds P. Recombination and selection in the evolution of picornaviruses and other Mammalian positive-stranded RNA viruses. *J Virol.* (2006) 80:11124–40. doi: 10.1128/JVI.01076-06
 42. Luo D, Wang H, Wang Q, Liang W, Liu B, Xue D, et al. Senecavirus A as an oncolytic virus: prospects, challenges and development directions. *Front Oncol.* (2022) 12:839536. doi: 10.3389/fonc.2022.839536



OPEN ACCESS

EDITED BY
Mengmeng Zhao,
Foshan University, China

REVIEWED BY
Yan-Dong Tang,
Chinese Academy of Agricultural Sciences,
China
Hai Li,
Xi'an Jiaotong University, China

*CORRESPONDENCE
Liangyu Yang
✉ 1993009@ynau.edu.cn
Bin Xiang
✉ 2021060@ynau.edu.cn

[†]These authors have contributed equally to this work

RECEIVED 14 April 2024

ACCEPTED 27 May 2024

PUBLISHED 12 June 2024

CITATION

Xu Y, Yi H, Kuang Q, Zheng X, Xu D, Gong L, Yang L and Xiang B (2024) Nucleotide metabolism-related host proteins RNA polymerase II subunit and uridine phosphorylase 1 interacting with porcine epidemic diarrhea virus N proteins affect viral replication.
Front. Vet. Sci. 11:1417348.
doi: 10.3389/fvets.2024.1417348

COPYRIGHT

© 2024 Xu, Yi, Kuang, Zheng, Xu, Gong, Yang and Xiang. This is an open-access article distributed under the terms of the [Creative Commons Attribution License \(CC BY\)](#). The use, distribution or reproduction in other forums is permitted, provided the original author(s) and the copyright owner(s) are credited and that the original publication in this journal is cited, in accordance with accepted academic practice. No use, distribution or reproduction is permitted which does not comply with these terms.

Nucleotide metabolism-related host proteins RNA polymerase II subunit and uridine phosphorylase 1 interacting with porcine epidemic diarrhea virus N proteins affect viral replication

Yifan Xu^{1,2†}, Heyou Yi^{2,3†}, Qiyuan Kuang², Xiaoyu Zheng², Dan Xu², Lang Gong², Liangyu Yang^{1*} and Bin Xiang^{1,2*}

¹College of Veterinary Medicine, Yunnan Agricultural University, Kunming, China, ²College of Veterinary Medicine, South China Agricultural University, Guangzhou, China, ³Key Laboratory of Animal Pathogen Infection and Immunology of Fujian Province, College of Animal Sciences, Fujian Agriculture and Forestry University, Fuzhou, China

Porcine epidemic diarrhea virus (PEDV) is a highly infectious pathogen that targets pig intestines to cause disease. It is globally widespread and causes huge economic losses to the pig industry. PEDV N protein is the protein that constitutes the core of PEDV virus particles, and most of it is expressed in the cytoplasm, and a small part can also be expressed in the nucleus. However, the role of related proteins in host nucleotide metabolic pathways in regulating PEDV replication have not been fully elucidated. In this study, PEDV-N-labeled antibodies were co-immunoprecipitated and combined with LC-MS to screen for host proteins that interact with N proteins. Bioinformatics analyses showed that the selected host proteins were mainly enriched in metabolic pathways. Moreover, co-immunoprecipitation and confocal microscopy confirmed that the second-largest subunit of RNA polymerase II (RPB2) and uridine phosphorylase 1 (UPP1) interacted with the N protein. RPB2 is the main subunit of RNA polymerase II and plays an important role in eukaryotic transcription. UPP1 is an enzyme that catalyzes reversible phosphorylation of uridine to uracil and ribo-1-phosphate to promote catabolism and bio anabolism. RPB2 overexpression significantly promoted viral replication, whereas UPP1 overexpression significantly inhibited viral replication. Studies on interactions between the PEDV N and host proteins are helpful in elucidating the pathogenesis and immune escape mechanism of PEDV.

KEYWORDS

porcine epidemic diarrhea virus, N protein, RPB2, UPP1, protein interaction

1 Introduction

Porcine epidemic diarrhea is an acute, highly contagious disease of pigs caused by the porcine epidemic diarrhea virus (PEDV). Newborn piglets infected with PEDV exhibit diarrhea, dehydration, vomiting, and high mortality (1). PEDV was first reported in the United Kingdom in 1971 and has since become globally widespread in the pig industry. After

a large-scale outbreak of PEDV variant strains in China in 2010, huge economic losses were incurred by the pig industry (2–5).

PEDV belongs to the coronavirus family and is a plus-stranded RNA virus with a total genome length of approximately 28 kb. It encodes 16 nonstructural and four structural proteins: spike (S protein), membrane (M protein), envelope (E protein), and nuclear (N protein) proteins, as well as one helper protein (ORF3) (6). The structural N protein is the core protein of the virion, which wraps around the RNA genome of the virus and forms a helical ribonucleoprotein with an RNA chaperone activity (7, 8). The N protein is localized in microparticles throughout the cytoplasm of coronavirus-infected cells and can also be localized in the nucleolus of some cells (9). N proteins may also stabilize the envelope assembly complex during VLP assembly by interacting with M proteins (10). Studies have shown that the coronavirus N protein can regulate host protein expression. The SARS-CoV N protein can up-regulate the host COX2 protein, causing inflammation through multiple COX-2 signaling cascades (11, 12). The PEDV N protein interacts with the host autophagy pathway to degrade HNRNPA1, FUBP3, HNRNPK, PTBP1, and TARDBP proteins, thereby promoting PEDV replication (13). The PEDV N protein can degrade STAT1 and prevent its phosphorylation, thus inhibiting interferon-stimulated gene expression, which is conducive to self-replication (14). The PEDV N protein interacts with host p53 protein to induce S-phase arrest, thereby promoting viral replication (15). The PEDV N protein promotes the cyclization of viral mRNA carried by the N protein through interactions with PABPC1 and eIF4F proteins, thus promoting viral transcription and replication (13, 16). However, the role of related proteins in host nucleotide metabolic pathways in regulating PEDV replication is still unknown. RNA polymerase II largest subunit (RPB2) and uridine phosphorylase 1 (UPP1) are key proteins in the nucleotide metabolic pathway. RPB2 regulates the activity of RNA polymerase (17) and UPP1 regulates the activity of thymidine phosphorylase (18). In this study, co-immunoprecipitation (Co-IP) and LC-MS were used to screen and identify host protein profiles that interact with PEDV-N. It was found that PEDV N protein interacts with host proteins RPB2 and UPP1, which are related to nucleotide metabolism, aiming to supplement the function of the PEDV N protein, and to further understand the infection mechanism of PEDV to provide a scientific basis for the development of PED prevention and control strategies.

2 Materials and methods

2.1 Cells, viruses, and plasmids

Vero-E6 cells and HEK293T cells were cultured in DMEM (Gibco, Guangzhou, China) with 10% serum (Gibco, Guangzhou, China) at 37°C and 5% CO₂. The PEDV used in this study was the newly isolated and identified FS202201 strain (19), which was maintained in infected cells in DMEM containing 7 µg/mL trypsin (Gibco, Guangzhou, China).

Abbreviations: Co-IP, Co-immunoprecipitation; PEDV, Porcine epidemic diarrhea virus; RPB2, RNA polymerase II subunit; UPP1, Uridine phosphorylase 1; BP, Biological process; CC, Cellular component; MF, Molecular function; HSV, Herpes simplex virus; IAV, Influenza A virus; CHIKV, Chikungunya virus; SFV, Semliki Forest viruses.

The Fastagen kit (Fastagen, Shanghai, China) was used to extract whole genome RNA from PEDV and Vero-E6 cells, according to the manufacturer's instructions, and GenStar reverse transcriptase (Genstar, Guangzhou, China) used to reverse-transcribe the RNA into cDNA, which was used as a template to amplify the target gene fragment via PCR. The primers used are listed in Table 1. PCAGGS-N-HA and PCAGGS-RPB2/UPP1-Flag plasmids were constructed using the recombinant enzyme (C112) (Vazyme, China, Shanghai) from the target gene and pCAGGS vector cut by the enzyme. All plasmids were verified using sequencing.

2.2 Reagents and antibodies

Lipofectamine 2000 (11668500) was purchased from Thermo Fisher Scientific (Shanghai, China). GAPDH, Flag, and the mouse anti-HA monoclonal antibodies (M20003) were purchased from Abmart (Shanghai, China), and CoraLite 594-conjugated goat anti-mouse IgG (H+L) and CoraLite 488-conjugated goat anti-rabbit IgG (H+L) antibodies obtained from Proteintech (Proteintech, Guangzhou, China). Anti-PEDV N protein mouse monoclonal antibody was prepared in our laboratory. The endonuclease sites used for plasmid construction are ECoRI (Thermo, FD0274) and SacI (Thermo, FD1134).

2.3 Immunoprecipitation

Vero-E6 cells were inoculated into a 10 cm cell culture dish and transfected with the pCAGGS-N-HA plasmid using Lipofectamine 2000. Proteins were extracted 24 h later using RIPA lysis buffer (P0013B Biotronix) containing a protease phosphatase inhibitor mixture (P1048 Biotronix). The proteins were incubated at 4°C for 15 min, centrifuged at 15,000×g for 10 min, and the supernatant thereafter removed. The cell lysate was added to HA-labeled magnetic beads that were washed with TBS and thereafter incubated in a 4°C shaker for 12 h. The samples were then subjected to mass spectrometry (MS) analysis.

2.4 LC-MS analysis

The magnetic beads were centrifuged and the supernatant discarded. The magnetic beads were washed twice with 200 µL 1× PBS. A 100 µL volume of a 50 mmol/L NH₄HCO₃ solution was added to resuspend the magnetic beads. The final concentration of DTT

TABLE 1 Primer sequences used to construct plasmids.

Primers	Sequences (5'–3')
pCAGGS-N-HA-F	ATGGCTTCTGTCAGCTTCCA
pCAGGS-N-HA-R	AATTAAAGGACATAGCTTCTA
pCAGGS-RPB2-Flag-F	ATGTCCACTCCCCAGCCACCG
pCAGGS-RPB2-Flag-R	AATGTGAGAGTGCAGTGCAGTCTT
pCAGGS-UPP1-Flag-F	AGACTCCCTATGAGCTTCACCT
pCAGGS-UPP1-Flag-R	AAAACCTGTCACGAAAATTA

solution was 10 mmol/L, and the solution reduced in a water bath at 56°C for 1 h. The final concentration of the IAA solution was 50 mmol/L, and the reaction incubated in the dark for 40 min. Trypsin was added according to the mass ratio of trypsin to substrate (1:100), and the enzyme added at 37°C for 4 h. The enzyme was further added according to the mass ratio (1:100), and the enzyme digestion reaction left overnight at 37°C for 16 h. After digestion, the peptides were desalted using a self-filling column, and the solvent dried in a vacuum centrifuge concentrator at 45°C. The peptide was dissolved with the sample solution (0.1% formic acid, 2% acetonitrile), then fully oscillated in a vortex, centrifuged at 13,200 rpm for 10 min at 4°C, and the supernatant thereafter transferred to the upper sample tube for mass spectrometry analysis. The samples were detected by a Q Exactive Hybrid Quadrupole-Orbitrap Mass Spectrometer (Thermo Fisher Scientific), and the relevant parameters are shown in Table 2. The mass spectrometry proteomics data have been deposited to the ProteomeXchange Consortium via the PRIDE (20) partner repository with the dataset identifier PXD052564.

2.5 Biological information analysis

Raw MS files were analyzed and searched against the target protein database based on the sample species using MaxQuant (1.6.2.10). OmicsBean software¹ was used to annotate functional classifications of the proteins. KEGG pathway annotations were analyzed using Kobas 3.0.

2.6 Co-immunoprecipitation assay

HEK293T cells were inoculated into a 10 cm cell culture dish and co-transfected with the pCAGGS-N-HA and targeted host gene expression plasmids (pCAGGS-RPB2-Flag, pCAGGS-UPP1-Flag) using Lipofectamine 2000. Proteins were extracted 24 h later, as described in section 2.3. The proteins were incubated at 4°C for 15 min, then centrifuged at 15,000 × g for 10 min, whereafter the supernatant was removed. The cell lysate was added to HA-labeled magnetic beads that were washed with TBS and incubated in a 4°C shaker for 12 h. The beads were washed four times with cold PBST, and 1× SDS loading buffer diluted with cell lysate was added and heated in a metal bath at 100°C for 5 min, whereafter SDS-PAGE was performed.

2.7 Transfection

Vero-E6 cells and HEK293T cells were seeded onto 12-well plates and transfected when they reached 80% confluency. A 100 µL volume of serum-free Opti-MEM medium and 2 µg plasmid were added into a 1.5 mL EP tube and gently mixed. In another 1.5 mL EP tube, 200 µL serum-free Opti-MEM medium and 6 µL Lipofectamine 2000 transfection reagent were added and gently mixed. After incubation at 25°C for 5 min, the contents of both tubes were gently mixed and

TABLE 2 Parameters used for mass spectrometry analysis.

Mass spectrometry	
Spray voltage	2.2 kV
Capillary temperature	270°C
MS resolution	70,000 at 400 <i>m/z</i>
MS precursor <i>m/z</i> range	300.0–1800.0
Product ion scan range	start from <i>m/z</i> 100
Activation type	CID
Min. signal required	1500.0
Isolation width	3.00
Normalized coll. energy	40.0
Default charge state	6
Activation Q	0.250
Activation time	30.000
Data dependent MS/MS	Up to top 20 most intense peptide ions from the preview scan in the Orbitrap

incubated at 25°C for 15 min. The culture medium was discarded, the cells gently washed with PBS once, and the incubated mixture added and incubated in a cell incubator at 37°C with 5% CO₂ for 6 h. Thereafter, the culture medium was replaced with 1 mL DMEM containing 2% FBS (Gibco) and incubated in a cell incubator at 37°C with 5% CO₂ for 24 h.

2.8 Immunofluorescence assay

When Vero-E6 cells reached 80% confluency, they were co-transfected with the pCAGGS-N-HA and targeted host gene expression plasmids (pCAGGS-RPB2-Flag, pCAGGS-UPP1-Flag) for 24 h, whereafter they were fixed with 4% paraformaldehyde at 25°C for 15 min and permeated with 0.2% Triton X-100 at 25°C for another 15 min. The cells were incubated with specific antibodies at 4°C overnight or at 37°C for 1 h. Thereafter, they were incubated with CoraLite 488-conjugated goat anti-mouse and CoraLite 594-conjugated goat anti-rabbit secondary antibodies diluted with PBS at 37°C for 45 min, and their nuclei stained with DAPI for 5 min at 25°C. The cells were cleaned with PBS three times before each operation. Cells were observed under a fluorescence microscope (Leica, Wetzlar, Germany).

2.9 Western blotting

Proteins were separated on a 10% SDS-PAGE gel (Vazyme, Shanghai, China) and transferred to polyvinylidene fluoride membranes. We used 5% skim milk powder enclosed in a shaker at 25°C for 1 h to prevent nonspecific binding. The specific PEDV N protein, HA, Flag and GAPDH primary antibodies were incubated at 25°C for 1 h, and thereafter incubated with the corresponding IRDye 800CW secondary antibody at 25°C for 1 h. After closure, samples were washed with TBST buffer three times before each step. The results were observed using a Sapphire RGBNIR Biomolecular Imager (Azure Biosystems, Dublin CA, United States).

¹ <http://www.omicsbean.cn>

2.10 Prediction site analysis

The tertiary structure of the PEDV N protein (GenBank: WMT38788.1) was predicted using AlphaFold2. The N protein model with the highest accuracy was selected according to the predicted local distance difference test, and HADDOCK 2.4 used to predict the interaction between the two host proteins, RNA polymerase II (RPB2) (GenBank: EHH53784.1) and uridine phosphorylase 1 (UPP1) (GenBank: EHH52134.1). Host protein sequences were obtained from the PDB database. The optimal interaction model was selected based on docking parameters, including the affinity index of the protein-ligand complex, contact residue ratio, and van der Waals force, as well as the electrostatic, confinement, and dissolution energies. The types of polar bonds, accessible and buried surface areas, and folding free energies of potential amino acid interaction sites in the interaction model were predicted using PDBEPIA. PyMOL was used to demonstrate the three-dimensional structure of the interaction model, in which the polar bond between the 5A viral and host proteins was selected for amino acid interactions, and the interaction site with the highest confidence obtained according to the PDBEPIA results.

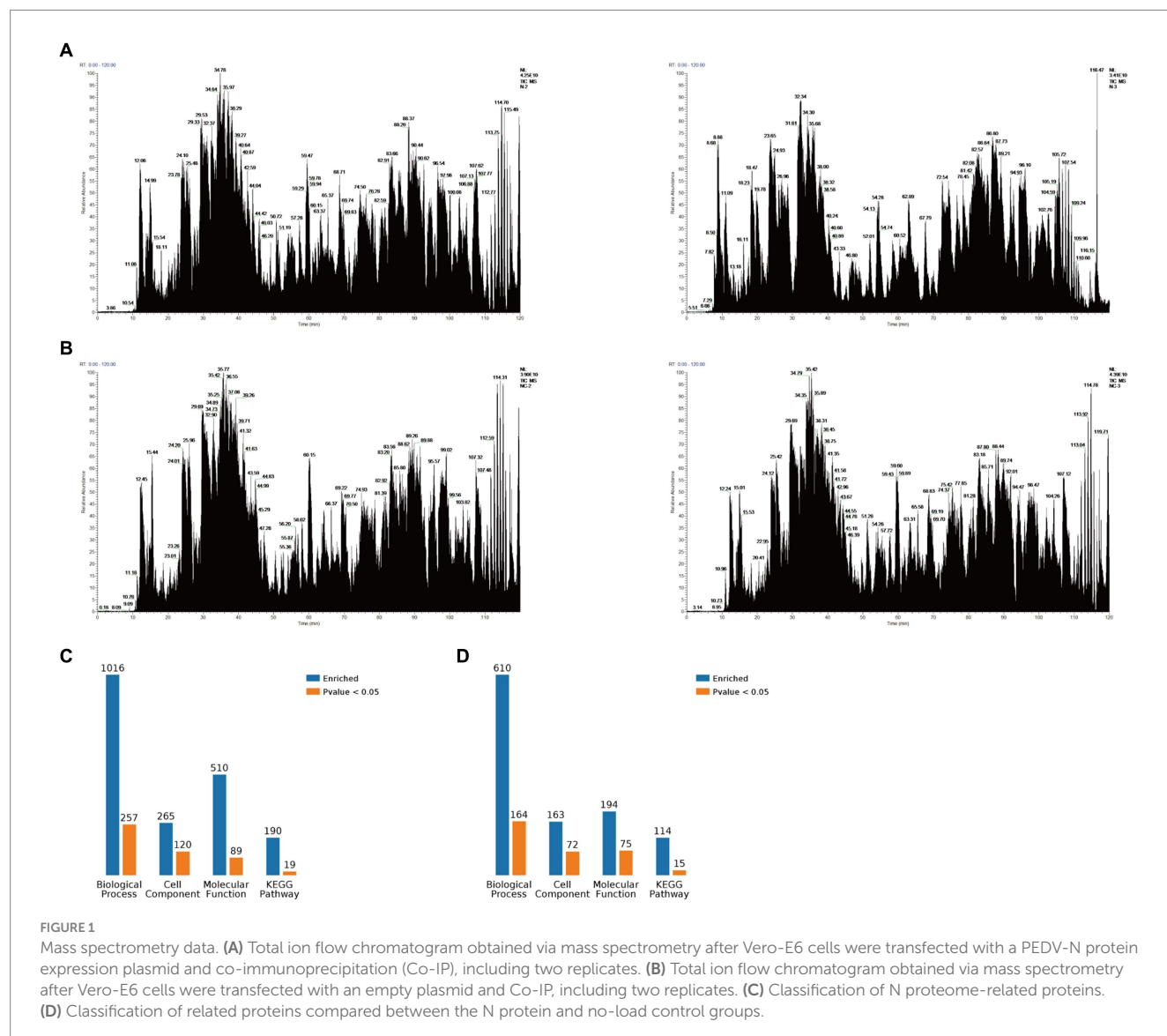
2.11 Statistical analysis

Data were analyzed using GraphPad Prism 7.0, and all data expressed as the mean \pm standard deviation. Student's *t*-test was used to determine whether differences between the mean values were statistically significant ($p < 0.05$).

3 Results

3.1 Co-IP-MS analysis of the PEDV N protein

The PEDV N protein expression and no-load plasmids were transfected into Vero-E6 cells, and the PEDV N protein pulled down via Co-IP for Co-IP-MS detection. The treated samples were analyzed using LC-MS; the raw file of the original mass spectrometry results was obtained, and the total ion flow chromatogram (Figures 1A,B) generated after analysis using MaxQuant (1.6.2.10). The total ion flow diagram showed that the number of peaks was large and the peak width small,



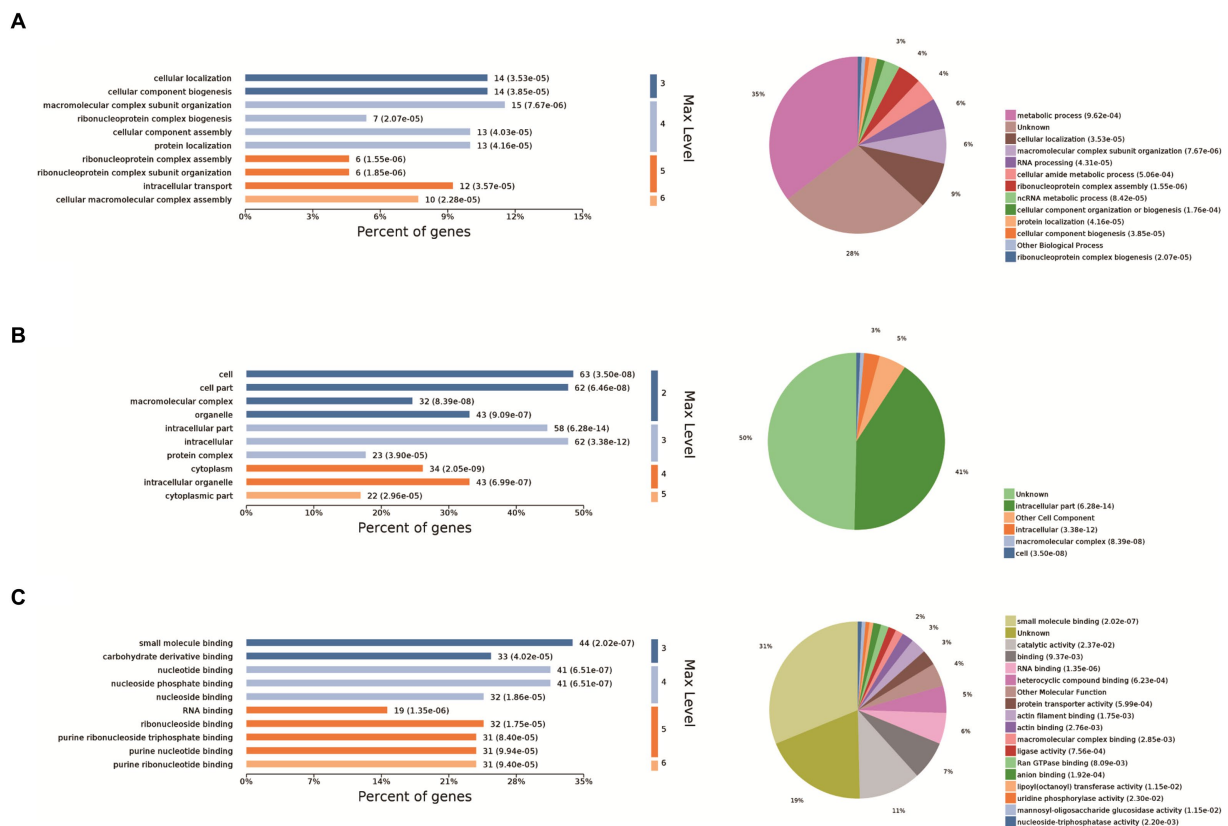


FIGURE 2

GO analysis. The 10 most significant GO nodes are shown, and the biological processes that each protein is most likely to participate in were counted and represented as pie charts. The horizontal coordinate of the bar chart in the figure is the percentage of enriched proteins, and the number after each bar is the number of proteins in that classification. Pie charts are the biological processes that each protein is most likely to be involved in based on a p -value. (A) Biological process, (B) cellular component, and (C) molecular function categories of the proteins.

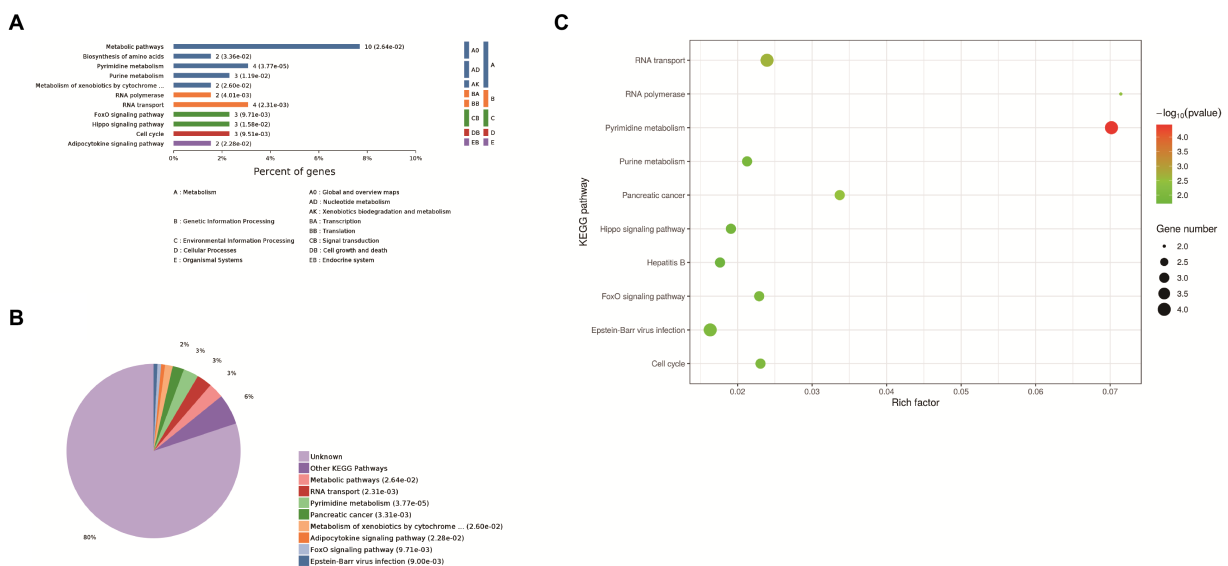


FIGURE 3

KEGG analysis. (A) Enrichment category of the KEGG pathway. The horizontal coordinate is the percentage of enriched protein, and the vertical coordinate is the largest level from smallest to largest. Different levels are shown in different colors, and the number behind each column is the number of proteins in that category. (B) Classification and statistics of the KEGG pathway of expressed proteins. (C) Bubble map of the KEGG pathway of differentially expressed proteins. Top-10 Kyoto Encyclopedia of Genes and Genomes (KEGG) enriched pathways of differentially expressed genes (DEGs) between Control group and PEDV N protein overexpression group. In the figure, the horizontal coordinate KEGG Term represents the name of the pathway in which the protein is enriched. The ordinate rich factor represents the enrichment factor, and the larger the rich factor, the higher the enrichment degree. Protein number on the right side of the legend indicates the number of proteins enriched by the pathway.

which indicates that the separation efficiency of liquid chromatography was good, the mass spectrometry data collection normal, and the parallelism good. Compared with the control group, 791 different proteins were enriched, of which 144 were significantly differentially expressed proteins. These differential proteins were enriched by KEGG pathway to 114 pathways, 11 of which were significant differences, including metabolic pathways, biosynthesis of amino acids, pyrimidine metabolism, purine metabolism, metabolism of xenobiotics by cytochrome P450, RNA polymerase, RNA transport, FoxO signaling pathway, Hippo signaling pathway, cell cycle, adipocytokine signaling pathway. At the same time, the differential proteins were subjected to Gene Ontology (GO) functional enrichment analysis based on biological process (BP), cellular component (CC), and molecular function (MF). The results showed significant enrichment in BP related ribonucleoprotein complex assembly, ribonucleoprotein complex subunit organization, macromolecular complex subunit organization, ribonucleoprotein complex biogenesis, cellular macromolecular complex assembly, cellular localization, intracellular transport, cellular component biogenesis, cellular component assembly, protein localization. CC related intracellular part, intracellular, cytoplasm, cell, cytoplasm, macromolecular complex, intracellular organelle, organelle, cytoplasmic part, protein complex. MF related small molecule binding, nucleotide binding, nucleoside phosphate binding, RNA binding, ribonucleoside binding, nucleoside binding, carbohydrate derivative binding, purine ribonucleoside triphosphate binding, purine ribonucleotide binding, purine nucleotide binding (Figures 1C,D). The LC-MS data was derived from previous research (21).

3.2 GO functional enrichment analysis of PEDV N-interacting proteins

The 10 most significant GO functions at different maximum levels were selected in the biological process, cellular component, and molecular function categories, and the number and percentage of proteins related to each function represented by bar charts. Based on the *p*-value, the biological process in which each protein was most likely to

be involved was determined, and pie charts drawn based on the results to clearly determine the percentage of different proteins in each group. Compared with the control group, there were 610 biological processes, most of which were related to metabolic processes. It also enriched ribonucleoprotein complex assembly, ribonucleoprotein complex subunit organization and macromolecular complex subunit organization, ribonucleoprotein complex biogenesis, cellular macromolecular complex assembly, cellular localization, intracellular transport, cellular component biogenesis, cellular component assembly, protein localization. Biological processes also have the largest percentage of proteins involved in metabolic processes (35%), cellular localization (9%), macromolecular complex subunit organization (6%), RNA processing (6%), cellular amide metabolic process (4%), ribonucleoprotein complex assembly (4%), ncRNA metabolic process (3%) (Figure 2A). The cell components were enriched to 163 related nodes, among which the intracellular part was the most important. In addition, there were significant differences in intracellular organelle, cytoplasm, cell, cytoplasm, macromolecular complex, intracellular organelle, organelle, cytoplasmic part, protein complex. Most of the proteins were associated with the intracellular part (41%), other cell component (5%), and intracellular (3%) (Figure 2B). The molecular function is enriched to 194 nodes, and small molecule binding is the most important node. In addition, there are significant differences in nucleotide binding, nucleoside phosphate binding, RNA binding, ribonucleoside binding and nucleoside binding, carbohydrate derivative binding, purine ribonucleoside triphosphate binding, purine ribonucleotide binding, purine nucleotide binding. Small molecule binding was associated with the most proteins (31%), catalytic activity (11%), binding (7%), RNA binding (6%), heterocyclic compound binding (5%), other molecular function (4%), protein transporter activity (3%), actin filament binding (3%), and actin binding (2%) (Figure 2C).

3.3 KEGG pathway enrichment analysis of PEDV N-interacting proteins

Eleven enrichment classes of the KEGG pathways with the most significant differences were shown. These include Metabolic pathways,

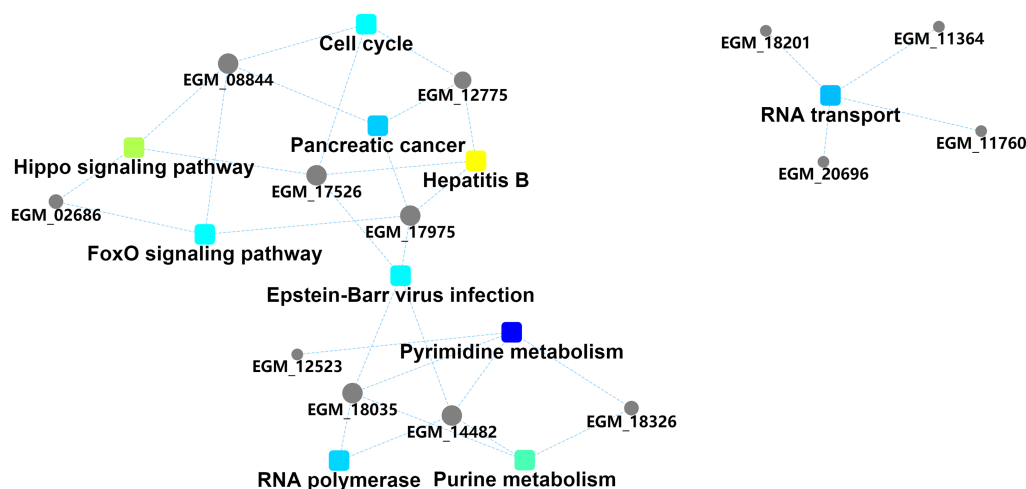


FIGURE 4
Protein-protein interaction information. Squares represent GO/KEGG terms and circles represent genes/proteins.

biosynthesis of amino acids, pyrimidine metabolism, purine metabolism, and metabolism of xenobiotics by cytochrome P450, RNA polymerase, RNA transport, FoxO signaling pathway, Hippo signaling pathway, cell cycle, adipocytokine signaling pathway (Figure 3A). Based on the *p*-value, we determined the biological process in which each protein was most likely involved. It mainly includes metabolic pathways, RNA transport, pyrimidine metabolism, pancreatic cancer and metabolism of xenobiotics by cytochrome P450, FoxO signaling pathway, Epstein–Barr virus infection, adipocytokine signaling pathway (Figure 3B). We found that host proteins that interact with N proteins are mainly involved in RNA transport, RNA transport, Pyrimidine metabolism, and Purine metabolism. Finally, according to the bubble map, the pyrimidine and urine metabolism pathways (Figure 3C) were selected based on the

p-value, degree of enrichment, and number of proteins enriched in the pathway.

3.4 Protein–protein interaction network analysis of PEDV N-interacting proteins

The interaction diagram of the differentially expressed proteins demonstrated the importance of pyrimidine and purine metabolism, which could interact with four and three host proteins, respectively, and are thus associated with other biological processes (Figure 4). Pyrimidine and purine metabolism mainly involves the anabolism of pyrimidine and purine nucleotides. These results suggest that the PEDV N protein may create favorable conditions for viral

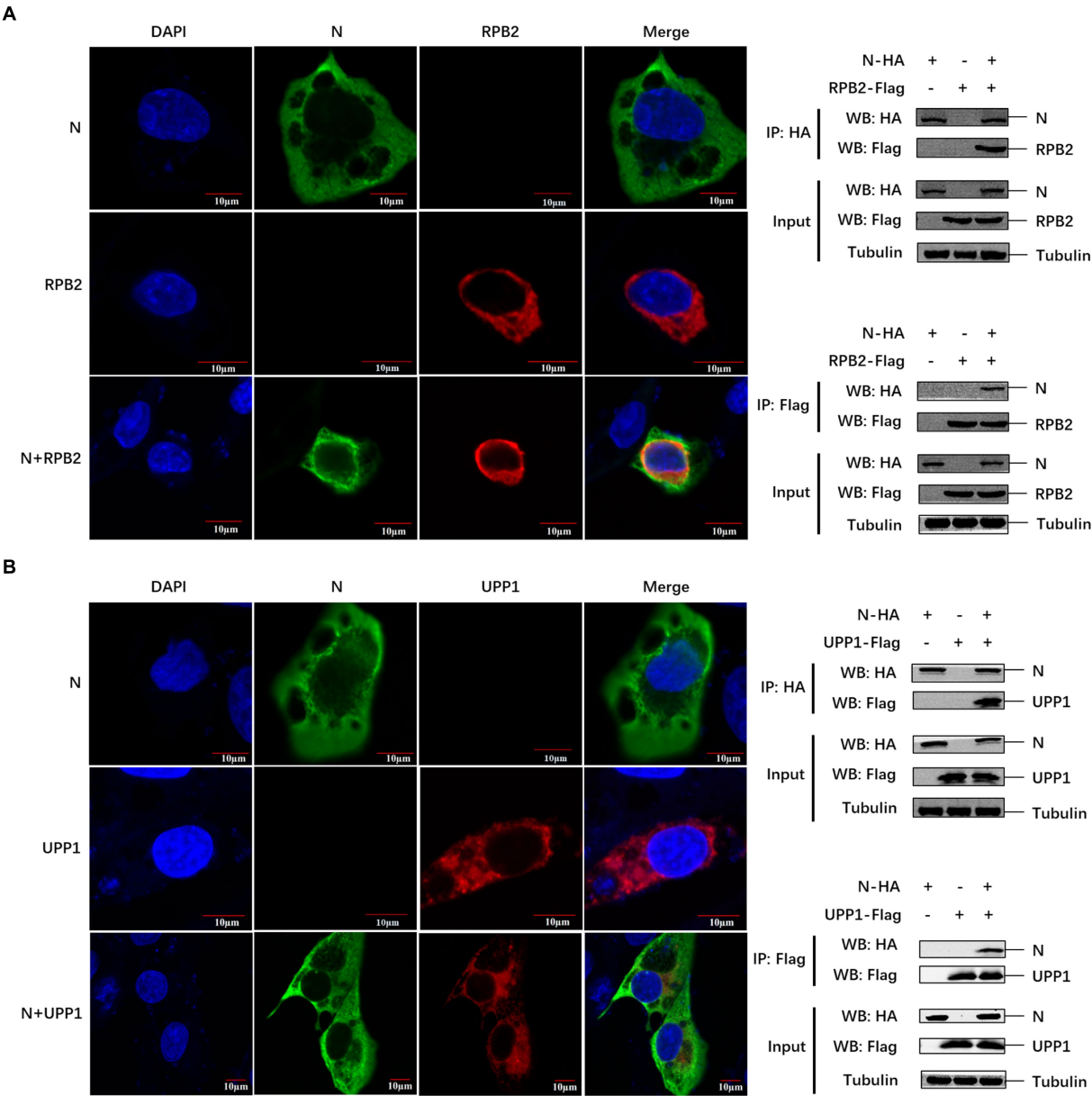


FIGURE 5
The PEDV N protein interacts with RPB2 and UPP1 host proteins. **(A,B)** The subcellular localization of PEDV N protein and host protein RPB2 and UPP1 in Vero-E6 cells was detected by confocal. The interaction between PEDV N protein and host protein RPB2 and UPP1 was detected by Co-IP.

replication and proliferation by regulating host nucleotide metabolic pathways.

3.5 Verification of the interaction between PEDV N and two host proteins

We further verified the relationship between the PEDV N protein and the two identified pathways. Known proteins in the two pathways (RBP2 and UPP1) were selected to verify their interaction with the PEDV N protein. Confocal microscopy was used to detect the colocalization between PEDV N and host RBP2 and UPP1 proteins, and the results showed that there was a colocalization phenomenon between in Vero-E6 cells, which was further demonstrated via Co-IP in HEK293T cells that PEDV N interacts with RBP2 and UPP1, respectively (Figures 5A,B).

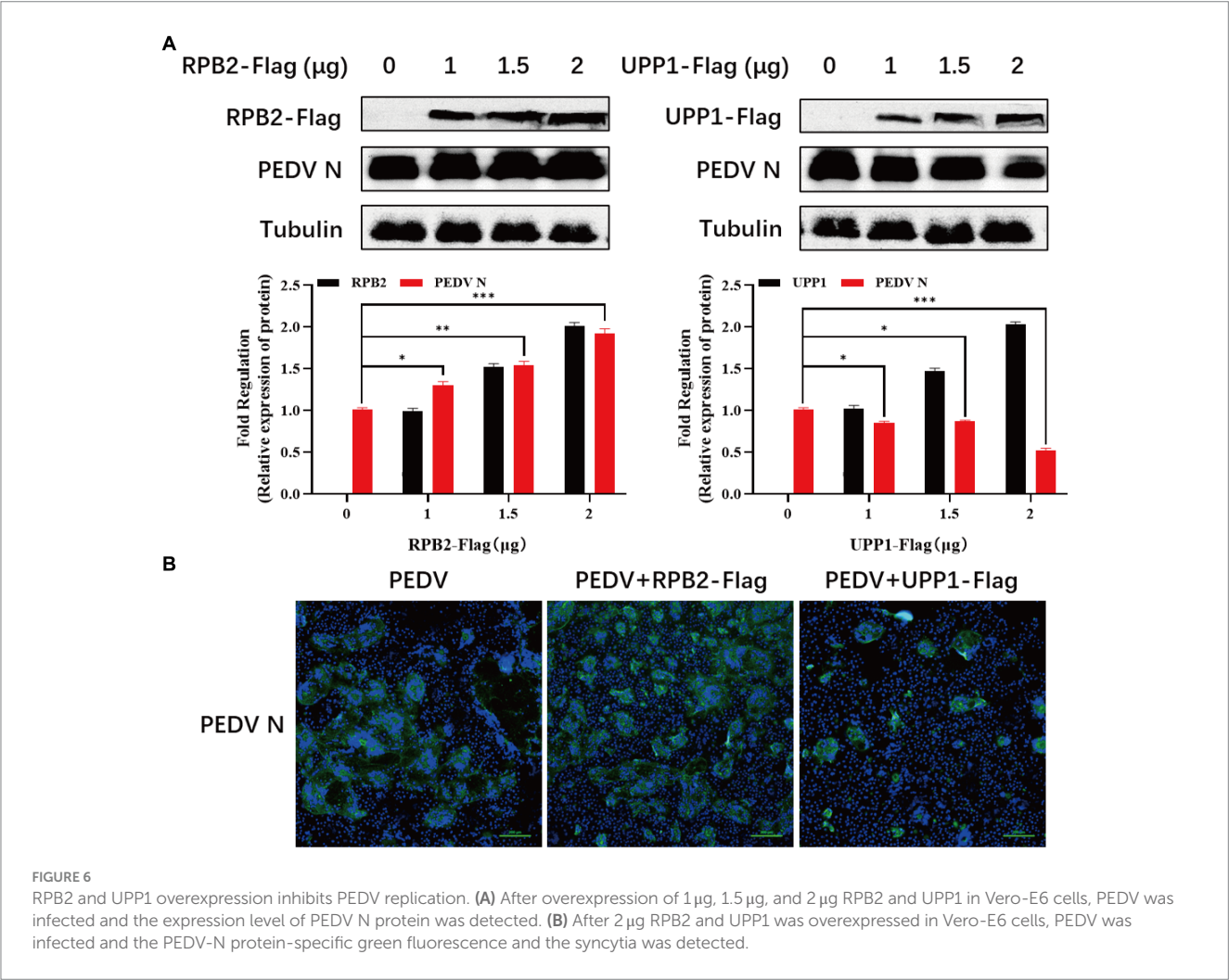
3.6 RBP2 and UPP1 participates the regulation of virus replication

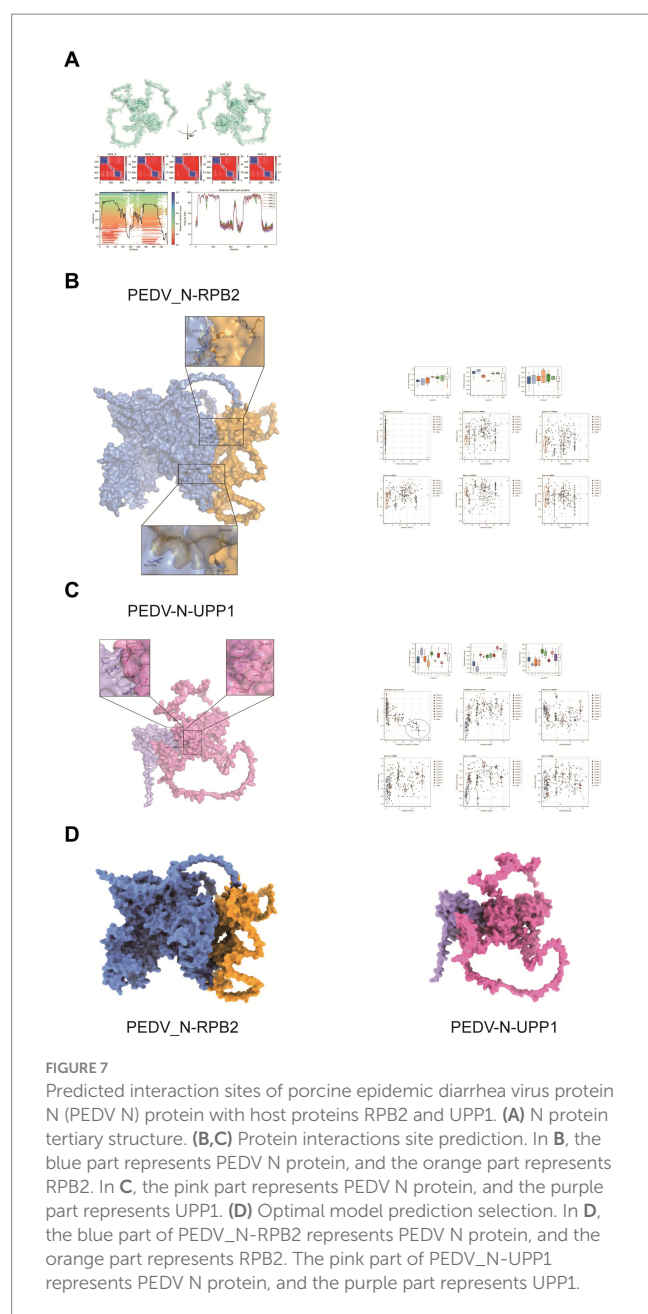
The RBP2 and UPP1 plasmids were overexpressed in PEDV-inoculated Vero-E6 cells to determine the effect of RBP2 and UPP1 on

PEDV replication, and the viral replication level detected via IFA and Western blotting. The results showed that, compared with PEDV infection alone, after RBP2 overexpression, the expression levels of the PEDV N protein increased (Figure 6A), the PEDV-N protein-specific green fluorescence and the syncytia were increased (Figure 6B). As for UPP1, after overexpression, the expression levels of the PEDV N protein downregulated (Figure 6A), the PEDV-N protein-specific green fluorescence and the syncytia were also downregulated (Figure 6B).

3.7 Prediction of the interaction sites between PEDV N and the two host proteins

Interaction sites between the PEDV N and host RBP2 and UPP1 proteins remain unclear. Hence, in pursuit of a comprehensive perception regarding the intricate interaction mechanisms exhibited between the PEDV N protein and host proteins RBP2 and UPP1, it is crucial to embark on advanced research. HADDOCK was used for model interaction prediction. The cluster was classified according to the affinity index, Van der Waals forces, proportion of contacting residues, restraints energy, and other parameters in the molecular docking of viral and host





proteins. N protein tertiary structure was shown in Figure 7A. The results showed the optimal prediction models for the PEDV N and host RPB2 and UPP1 proteins were Cluster_4 and Cluster_1, respectively (Figures 7B,C). As claimed by the ultimate interaction model in HADDOCK, PDBEPIA and PyMOL were carried out for interaction site selection. In the PDBEPIA table, Structure refers to the amino acid residues and their corresponding positions, while HSDC represents the polar bond of the amino acid residue interaction, and ASA as well as BSA denote to the accessible surface area and the buried surface area separately, with ΔG corresponding to the folding free energy. At the interaction interface, both the ASA and BSA attain significant elevated score, indicating that the surface area exposed to the solvent and the hidden surface area were substantial. Consequently, the folding state of the protein was relatively stable and the folding free energy negative, which also

indicates the flexibility and dynamics of the structure and corresponding region.

The predicted sites of amino acid interactions of PEDV N protein with host RPB2 and UPP1 were PEDV_N-RPB2: ARG-11 vs. GLY-53 and ARG-219 vs. GLU-504, PEDV_N-UPP1: ASP-27/ARG-60/GLU-68 vs. LYS-230 and ARG-63 vs. GLU-237 (Figures 7B,C). Figure 7D shows the conformational display of the 3D model of PEDV N protein interactions with host RPB2 and UPP1 proteins, providing a basis for studying interactions between the virus and host proteins.

4 Discussion

PED first broke out in the United Kingdom in 1971 and has become the primary cause of diarrheal diseases in pigs (22). PEDV N protein plays an important role in the process of virus infection. The PEDV N protein has been reported to play a role in recruiting the E3 ubiquitin ligase, COP1, and inhibiting COP1 self-ubiquitination and protein degradation, thus enhancing COP1 mediated p53 degradation and promoting viral replication (23). The PEDV N protein can degrade STAT1 by inhibiting ACE2 promoter activity and preventing its phosphorylation, thus inhibiting interferon-stimulated gene expression (14). Previous studies have explored how PEDV hijacks PABPC1 and eIF4F proteins related to the host transcription translation system to promote viral proliferation, and promotes cyclization of viral mRNA carried by N protein, thus promoting viral transcription and promoting viral replication (13, 16). In this study, we explored the influence of PEDV N protein interaction with pyrimidine and purine metabolism pathway related proteins RPB2 and UPP1 on virus replication. LC-MS analysis and verification showed that RPB2 and UPP1 interact with PEDV N protein, and overexpression of RPB2 can promote PEDV replication, while overexpression of UPP1 can inhibit PEDV replication.

Eukaryotic RNA polymerase II comprises 12 subunits (RPB1-RPB12), of which RPB1 and RPB2 are the main subunits that constitute its catalytic center. They also play an important role in eukaryotic transcription (24). RPB affects gene expression levels through transcription initiation, transcription rate, transcription termination, and regulatory complex assembly. Viruses interact with factors associated with the host cell transcription system to regulate the extent of infection, further expansion, or suppression (17, 25). Herpes simplex virus (HSV) infection is known to promote complex formation of the RPB1 protein (26). BET inhibitors were reported to promote the recruitment of bromodomain-containing protein 4 and the CDK9/RPB1 complex to the HSV gene promoter, thus enhancing viral replication (27). The viral RNA-dependent RNA polymerase (FluPol) of the influenza A virus (IAV) binds to the regulatory CTD domain of RPB1 and interacts with RPB4 to initiate host transcription and secondary transcription of RPB4 (28). Nonstructural protein 2 of Chikungunya viruses (CHIKV) and Semliki Forest viruses (SFV) inhibits the IFN response by inducing the degradation of RPB1 (29, 30). In the purine and pyrimidine metabolism pathways enriched by host proteins that interacted with the PEDV N protein, as screened in this study, the RPB2 protein was present in both of them; thus, its influence on PEDV replication could be verified further. The PEDV N protein interacted with the host RPB2 protein, and overexpression of RPB2 was conducive to viral replication. It is speculated that the PEDV N protein may regulate the activity and stability of the RNA polymerase complex through interaction with RPB2

and improve its catalytic efficiency to promote viral self-replication. However, this hypothesis warrants further study.

UPP1 catalyzes the reversible phosphorylation of uridine (or 2'-deoxyuridine) to uracil and ribo-1-phosphate (or deoxyribo-1-phosphate) (18). It is mainly associated with immune and inflammatory responses, particularly T-cell activation (31). Studies have shown that berberine treatment inhibits pro-inflammatory and IRF8-IFN- γ signaling axis-related genes, including UPP1, *in vitro* and *in vivo* (32). In terms of energy metabolism, UPP1 can release uridine-derived ribose and promote central carbon metabolism, and its expression affects uridine utilization by cells (33). In the present study, we found that the PEDV N protein interacted with the host UPP1 protein, and UPP1 overexpression inhibited PEDV replication, which may be related to the regulation of host cell energy metabolism and the antiviral immune response by UPP1.

In summary, 144 host proteins that might interact with PEDV N proteins were screened using Co-IP and LC/MS-MS analyses. These host proteins were mainly concentrated in metabolic pathways, of which pyrimidine and urine metabolism were the most significant. In this study, two host proteins involved in pyrimidine and urine metabolism (RBP2 and UPP1) were verified, and the results showed that both proteins interacted with the PEDV N protein. Overexpression of RBP2 was found to promote PEDV replication, whereas overexpression of UPP1 inhibited PEDV replication. In addition, the predicted sites of amino acid interactions of PEDV N protein with host RBP2 and UPP1 were PEDV_N-RBP2: ARG-11 vs. GLY-53 and ARG-219 vs. GLU-504, PEDV_N-UPP1: ASP-27/ARG-60/GLU-68 vs. LYS-230 and ARG-63 vs. GLU-237. Overall, this study elucidated the interaction between two host proteins RBP2 and UPP1 related to nucleotide metabolism and PEDV N protein, which provided a theoretical basis for further exploring the pathogenesis and prevention of PEDV.

Data availability statement

The datasets presented in this study can be found in online repositories. The names of the repository/repositories and accession number(s) can be found at: <https://www.ebi.ac.uk/pride/archive/projects/PXD052564>.

References

- Pensaert MB, de Bouck P. A new coronavirus-like particle associated with diarrhea in swine. *Arch Virol.* (1978) 58:243–7. doi: 10.1007/BF01317606
- Park S, Kim S, Song D, Park B. Novel porcine epidemic diarrhea virus variant with large genomic deletion, South Korea. *Emerg Infect Dis.* (2014) 20:2089–92. doi: 10.3201/eid2012.131642
- Tan L, Li Y, He J, Hu Y, Cai X, Liu W, et al. Epidemic and genetic characterization of porcine epidemic diarrhea virus strains circulating in the regions around Hunan, China, during 2017–2018. *Arch Virol.* (2020) 165:877–89. doi: 10.1007/s00705-020-04532-7
- Vidal A, Martín-Valls GE, Tello M, Mateu E, Martín M, Darwich L. Prevalence of enteric pathogens in diarrheic and non-diarrheic samples from pig farms with neonatal diarrhea in the North East of Spain. *Vet Microbiol.* (2019) 237:108419. doi: 10.1016/j.vetmic.2019.108419
- Vlasova AN, Marthaler D, Wang Q, Culhane MR, Rossow KD, Rovira A, et al. Distinct characteristics and complex evolution of PEDV strains, North America, May 2013–February 2014. *Emerg Infect Dis.* (2014) 20:1620–8. doi: 10.3201/eid2010.140491
- Duarte M, Gelfi J, Lambert P, Rasschaert D, Laude H. Genome organization of porcine epidemic diarrhoea virus. *Adv Exp Med Biol.* (1993) 342:55–60. doi: 10.1007/978-1-4615-2996-5_9
- de Haan CAM, Rottier PJM. Molecular interactions in the assembly of coronaviruses. *Adv Virus Res.* (2005) 64:165–230. doi: 10.1016/S0065-3527(05)64006-7
- Zúñiga S, Sola I, Moreno JL, Sabella P, Plana-Durán J, Enjuanes L. Coronavirus nucleocapsid protein is an RNA chaperone. *Virology.* (2007) 357:215–27. doi: 10.1016/j.virol.2006.07.046
- Shi D, Lv M, Chen J, Shi H, Zhang S, Zhang X, et al. Molecular characterizations of subcellular localization signals in the nucleocapsid protein of porcine epidemic diarrhea virus. *Viruses.* (2014) 6:1253–73. doi: 10.3390/v6031253
- Arndt AL, Larson BJ, Hogue BG. A conserved domain in the coronavirus membrane protein tail is important for virus assembly. *J Virol.* (2010) 84:11418–28. doi: 10.1128/JVI.01131-10
- Kopecky-Bromberg SA, Martínez-Sobrido L, Frieman M, Baric RA, Palese P. Severe acute respiratory syndrome coronavirus open reading frame (ORF) 3b, ORF 6, and nucleocapsid proteins function as interferon antagonists. *J Virol.* (2007) 81:548–57. doi: 10.1128/JVI.01782-06
- Yan X, Hao Q, Mu Y, Timani KA, Ye L, Zhu Y, et al. Nucleocapsid protein of SARS-CoV activates the expression of cyclooxygenase-2 by binding directly to regulatory elements for nuclear factor-kappa B and CCAAT/enhancer binding protein. *Int J Biochem Cell Biol.* (2006) 38:1417–28. doi: 10.1016/j.biocel.2006.02.003

Author contributions

YX: Conceptualization, Data curation, Validation, Writing – original draft. HY: Software, Writing – original draft, Conceptualization. QK: Formal analysis, Methodology, Software, Writing – original draft. XZ: Writing – review & editing, Conceptualization, Formal analysis. DX: Writing – review & editing, Investigation. LG: Writing – review & editing, Resources. LY: Writing – review & editing, Project administration, Supervision. BX: Funding acquisition, Visualization, Writing – review & editing.

Funding

The author(s) declare that financial support was received for the research, authorship, and/or publication of this article. This research was funded by Academician (Expert) Workstation of Yunnan Province Program (202305AF150127) and Yunnan Ten Thousand Talents Plan leading Talents of Industrial Technology Project of China (YNWR-CYJS-2019-020).

Conflict of interest

The authors declare that the research was conducted in the absence of any commercial or financial relationships that could be construed as a potential conflict of interest.

Publisher's note

All claims expressed in this article are solely those of the authors and do not necessarily represent those of their affiliated organizations, or those of the publisher, the editors and the reviewers. Any product that may be evaluated in this article, or claim that may be made by its manufacturer, is not guaranteed or endorsed by the publisher.

13. Zhai X, Kong N, Zhang Y, Song Y, Qin W, Yang X, et al. N protein of PEDV plays chess game with host proteins by selective autophagy. *Autophagy*. (2023) 19:2338–2352. doi: 10.1080/15548627.2023.2181615
14. Li Z, Chen X, Ma C, Du X, Zhang Y. Angiotensin converting enzyme 2 does not facilitate porcine epidemic diarrhea virus entry into porcine intestinal epithelial cells and inhibits it-induced inflammatory injury by promoting STAT1 phosphorylation. *Virus Res*. (2023) 340:199300. doi: 10.1016/j.virusres.2023.199300
15. Su M, Shi D, Xing X, Qi S, Yang D, Zhang J, et al. Coronavirus porcine epidemic diarrhea virus nucleocapsid protein interacts with p53 to induce cell cycle arrest in S-phase and promotes viral replication. *J Virol*. (2021) 95:e0018721–1. doi: 10.1128/JVI.00187-21
16. Zhai H, Qin W, Dong S, Yang X, Zhai X, Tong W, et al. PEDV N protein capture protein translation element PABPC1 and eIF4F to promote viral replication. *Vet Microbiol*. (2023) 284:109844. doi: 10.1016/j.vetmic.2023.109844
17. Gulyas L, Glaunsinger BA. RNA polymerase II subunit modulation during viral infection and cellular stress. *Curr Opin Virol*. (2022) 56:101259. doi: 10.1016/j.coviro.2022.101259
18. Cao D, Pizzorno G. Uridine phosphorylase: an important enzyme in pyrimidine metabolism and fluoropyrimidine activation. *Drugs Today*. (2004) 40:431–43. doi: 10.1358/dot.2004.40.5.850491
19. Sun Y, Gong T, Wu D, Feng Y, Gao Q, Xing J, et al. Isolation, identification, and pathogenicity of porcine epidemic diarrhea virus. *Front Microbiol*. (2023) 14:1273589. doi: 10.3389/fmicb.2023.1273589
20. Perez-Riverol Y, Bai J, Bandla C, Hewapathirana S, García-Seisdedos D, Kamatchinathan S, et al. The PRIDE database resources in 2022: a hub for mass spectrometry-based proteomics evidences. *Nucleic Acids Res*. (2022) 50:D543–52. doi: 10.1093/nar/gkab1038
21. Gao Q, Weng Z, Feng Y, Gong T, Zheng X, Zhang G, et al. KPNA2 suppresses porcine epidemic diarrhea virus replication by targeting and degrading virus envelope protein through selective autophagy. *J Virol*. (2023) 97:e0011523. doi: 10.1128/jvi.00115-23
22. Zhang H, Zou C, Peng O, Ashraf U, Xu Q, Gong L, et al. Global dynamics of porcine enteric coronavirus PEDV epidemiology, evolution, and transmission. *Mol Biol Evol*. (2023) 40:msad052. doi: 10.1093/molbev/msad052
23. Dong W, Cheng Y, Zhou Y, Zhang J, Yu X, Guan H, et al. The nucleocapsid protein facilitates p53 ubiquitination-dependent proteasomal degradation via recruiting host ubiquitin ligase COP1 in PEDV infection. *J Biol Chem*. (2024) 300:107135. doi: 10.1016/j.jbc.2024.107135
24. Osman S, Cramer P. Structural biology of RNA polymerase II transcription: 20 years on. *Annu Rev Cell Dev Biol*. (2020) 36:1–34. doi: 10.1146/annurev-cellbio-042020-021954
25. Haas DA, Meiler A, Geiger K, Vogt C, Preuss E, Kochs G, et al. Viral targeting of TFIIB impairs de novo polymerase II recruitment and affects antiviral immunity. *PLoS Pathog*. (2018) 14:e1006980. doi: 10.1371/journal.ppat.1006980
26. Ren K, Zhang W, Chen X, Ma Y, Dai Y, Fan Y, et al. An epigenetic compound library screen identifies BET inhibitors that promote HSV-1 and -2 replication by bridging P-TEFb to viral gene promoters through BRD4. *PLoS Pathog*. (2016) 12:e1005950. doi: 10.1371/journal.ppat.1005950
27. Dai W, Tian R, Yu L, Bian S, Chen Y, Yin B, et al. Overcoming therapeutic resistance in oncolytic herpes virotherapy by targeting IGF2BP3-induced NETosis in malignant glioma. *Nat Commun*. (2024) 15:131. doi: 10.1038/s41467-023-44576-2
28. Morel J, Sedano L, Lejal N, Da Costa B, Batsché E, Muchardt C, et al. The influenza virus RNA-polymerase and the host RNA-polymerase II: RPB4 is targeted by a PB2 domain that is involved in viral transcription. *Viruses*. (2022) 14:518. doi: 10.3390/v14030518
29. Frolova EI, Fayzulin RZ, Cook SH, Griffin DE, Rice CM, Frolov I. Roles of nonstructural protein nsP2 and alpha/beta interferons in determining the outcome of Sindbis virus infection. *J Virol*. (2002) 76:11254–64. doi: 10.1128/JVI.76.22.11254-11264.2002
30. Fros JJ, van der Maten E, Vlak JM, Pijlman GP. The C-terminal domain of Chikungunya virus nsP2 independently governs viral RNA replication, cytopathicity, and inhibition of interferon signaling. *J Virol*. (2013) 87:10394–400. doi: 10.1128/JVI.00884-13
31. Wang J, Xu S, Lv W, Shi F, Mei S, Shan A, et al. Uridine phosphorylase 1 is a novel immune-related target and predicts worse survival in brain glioma. *Cancer Med*. (2020) 9:5940–7. doi: 10.1002/cam4.3251
32. Yan M, Wang H, Sun J, Liao W, Li P, Zhu Y, et al. Expression of IRF8 in gastric epithelial cells confers protective innate immunity against *Helicobacter pylori* infection. *J Immunol*. (2016) 196:1999–2003. doi: 10.4049/jimmunol.1500766
33. Nwosu ZC, Ward MH, Sajjakulnukit P, Poudel P, Ragulan C, Kasperek S, et al. Uridine-derived ribose fuels glucose-restricted pancreatic cancer. *Nature*. (2023) 618:151–8. doi: 10.1038/s41586-023-06073-w



OPEN ACCESS

EDITED BY

Mengmeng Zhao,
Foshan University, China

REVIEWED BY

Pan Hu,
Jilin University, China
Jianfa Wang,
Heilongjiang Bayi Agricultural University,
China

*CORRESPONDENCE

Fuxiao Liu
✉ laudawn@126.com

[†]These authors have contributed equally to this work

RECEIVED 13 May 2024

ACCEPTED 10 June 2024

PUBLISHED 25 June 2024

CITATION

Li Y, Chu H, Jiang Y, Li Z, Wang J and Liu F (2024) Comparative transcriptomics analysis on Senecavirus A-infected and non-infected cells.
Front. Vet. Sci. 11:1431879.
doi: 10.3389/fvets.2024.1431879

COPYRIGHT

© 2024 Li, Chu, Jiang, Li, Wang and Liu. This is an open-access article distributed under the terms of the [Creative Commons Attribution License \(CC BY\)](#). The use, distribution or reproduction in other forums is permitted, provided the original author(s) and the copyright owner(s) are credited and that the original publication in this journal is cited, in accordance with accepted academic practice. No use, distribution or reproduction is permitted which does not comply with these terms.

Comparative transcriptomics analysis on Senecavirus A-infected and non-infected cells

Yan Li^{1,2†}, Huanhuan Chu^{1,3†}, Yujia Jiang^{1,4}, Ziwei Li¹, Jie Wang¹ and Fuxiao Liu^{1*}

¹College of Veterinary Medicine, Qingdao Agricultural University, Qingdao, China, ²Qingdao Center for Animal Disease Control and Prevention, Qingdao, China, ³College of Veterinary Medicine, Northwest A&F University, Yangling, China, ⁴Qingdao Zhongren-OLand Bioengineering Co., Ltd., Qingdao, China

Senecavirus A (SVA) is an emerging virus that causes the vesicular disease in pigs, clinically indistinguishable from other high consequence vesicular diseases. This virus belongs to the genus *Senecavirus* in the family *Picornaviridae*. Its genome is a positive-sense, single-stranded RNA, approximately 7,300 nt in length, with a 3' poly(A) tail but without 5'-end capped structure. SVA can efficiently propagate in different cells, including some non-pig-derived cell lines. A wild-type SVA was previously rescued from its cDNA clone using reverse genetics in our laboratory. In the present study, the BSR-T7/5 cell line was inoculated with the passage-5 SVA. At 12 h post-inoculation, SVA-infected and non-infected cells were independently collected for the analysis on comparative transcriptomics. The results totally showed 628 differentially expressed genes, including 565 upregulated and 63 downregulated ones, suggesting that SVA infection significantly stimulated the transcription initiation in cells. GO and KEGG enrichment analyses demonstrated that SVA exerted multiple effects on immunity-related pathways in cells. Furthermore, the RNA sequencing data were subjected to other in-depth analyses, such as the single-nucleotide polymorphism, transcription factors, and protein-protein interactions. The present study, along with our previous proteomics and metabolomics researches, provides a multi-omics insight into the interaction between SVA and its hosts.

KEYWORDS

Senecavirus A, RNA-seq, transcriptomics, differentially expressed gene, enrichment analysis, immunity, pathway

1 Introduction

Senecavirus A (SVA), as an emerging virus, has been demonstrated to be a causative agent for vesicular disease in swine (1–5). SVA-infected pigs develop vesicular lesions mainly on the snout, dewclaw or (and) coronary band. Other signs include lameness, anorexia, lethargy, cutaneous hyperemia, and fever (6, 7). The SVA-induced signs are clinically indistinguishable from those of other vesicular diseases in pigs (8). The outbreak of SVA infection has been recently reported in several countries, including Canada, the United States, Brazil, China, Thailand, Vietnam and Chile. The transmission risk of SVA has attracted a great deal of attention from the pig industry around the world.

SVA is the only member of the genus *Senecavirus* in the family *Picornaviridae* (9). The virion is a typical icosahedral particle without envelope. It harbors a positive-sense, single-stranded RNA

genome, approximately 7,300 nt in length, composed of 5' untranslated region (UTR), long encoding region and 3' UTR. Like those of other picornaviruses, the 5' terminus of SVA genome does not contain a cap structure. In contrast, a short peptide (VPg) is covalently linked to the 5' terminus, and plays an essential role in synthesizing the SVA genome. The 5' UTR bears a type-IV internal ribosome entry site (10), structurally and functionally similar to those of pestiviruses (11), allowing for the initiation of polyprotein translation in a cap-independent manner. The 3' UTR is approximately 70 nt in length, followed by a variable-length poly(A) tail (12). The encoding region of SVA polyprotein follows the standard "L-VP4-VP2-VP3-VP1-2A-2B-2C-3A-3B-3C-3D" layout. After SVA infection, the viral polyprotein will be translated in cytoplasm, and then gradually cleaved into 12 proteins, namely, L, VP4, VP2, VP3, VP1, 2A, 2B, 2C, 3A, 3B, 3C and 3D (13). The VP4, VP2, VP3 and VP1 as structural proteins participate in viral morphogenesis. The others are nonstructural proteins, albeit uninvolved in the package of virion, playing a crucial role in viral replication (14–16).

RNA sequencing (RNA-seq) is a technique that uses next-generation sequencing to reveal the presence and quantity of RNA molecules in a biological sample, providing a snapshot of gene expression in the sample, also known as transcriptome. A transcriptome is the full range of mRNA molecules expressed by an organism. The RNA-seq technique contributes to identifying a transcriptome in a given population, even in a single cell (17). Comparative transcriptomics facilitates the elucidation of differentiation between two groups (populations, species and so on) in their alternative gene spliced transcripts, post-transcriptional modifications, gene fusion, single-nucleotide polymorphism (SNP) and changes in gene expression over time (18). Large DNA viruses, such as human cytomegalovirus and African swine fever virus, contained very long genomes. Each of these viruses itself has a complicated transcriptome (19, 20) in virus-infected cells. In contrast, some small RNA viruses, such as picornavirus, only have a simple "transcriptome," i.e., one single RNA genome. Therefore, it is meaningless to uncover a picornaviral "transcriptome" only based on a given picornavirus itself.

SVA can trigger a variety of metabolic and biochemical changes in cells through virus-specific or -nonspecific mechanisms (21–23). For example, SVA 2C protein can target mitochondria and cause release of cytochrome C into cytoplasm, which activates caspase-9 and -3 in a series of signaling cascades to induce the onset of apoptosis (24). In addition, SVA infection is able to affect the level of transcription in hosts. For example, SVA 2C protein can block the transcription of interferon-stimulated gene 56 and interferon- β to weaken the innate immunity in hosts (21). We have demonstrated that SVA infection can lead to significant changes in cellular proteome and metabolome, even at an early stage of infection (25, 26). Virus-caused differentiation of cellular proteome is closely related to the change in cellular transcriptome. Therefore, a comparative transcriptomics analysis was conducted here to uncover a profile of SVA-induced changes in cellular transcriptome at the early stage of infection.

2 Materials and methods

2.1 Cell line and virus

The BSR-T7/5 cell line, derived from the baby hamster kidney cell, was kindly provided by the China Animal Health and Epidemiology

Center. This cell line was cultured at 37°C with 5% CO₂ in Dulbecco's modified Eagle's medium (DMEM), supplemented with 4% fetal bovine serum (VivaCell, Shanghai, China), penicillin (100 U/mL), streptomycin (100 µg/mL) and amphotericin B (0.25 µg/mL). The wild-type SVA was rescued previously from a full-length cDNA clone (27), genetically derived from an SVA isolate, CH-LX-01-2016 (28).

2.2 Sample preparation

BSR-T7/5 cells were seeded into six T25 flasks for culture at 37°C. When the cells were 90% confluent, three flasks were randomly selected for incubation with the passage-5 SVA at an MOI (multiplicity of infection) of 2.5. The other flasks, as non-infected controls, were not treated. There were three SVA-infected samples (S1, S2 and S3) and three non-infected controls (C1, C2 and C3). Supernatants were separately removed from the six flasks at 12 h post-inoculation (hpi). Cell monolayers were gently washed with PBS three times, followed by the extraction of total RNAs using the TRIzol reagent (Thermo Fisher, Waltham, MA, United States), as per the manufacturer's instructions. The concentration, quality and integrity of total RNAs were determined using the NanoDrop spectrophotometer (Thermo Fisher, Waltham, MA, United States). Three µg of RNA was used as input material to prepare RNA sample for each group.

2.3 RNA-seq analysis

The preparation of sequencing libraries was carried out as described previously with modifications (29). The mRNAs were purified from total RNAs using poly-T oligo-attached magnetic beads, further fragmented, and then used as templates to produce cDNAs. The first strand cDNA was synthesized using a system with random hexamer primers and the reverse transcriptase. The second strand cDNA was synthesized via the first strand with dNTP, buffer solution, DNA polymerase I and RNase H. Remaining overhangs were converted into blunt ends through exonuclease/polymerase activities. After adenylation of the 3' ends of DNA fragments, Illumina paired-end adapter oligonucleotides were ligated to prepare for hybridization. The cDNA fragments of 400 to 500 bp were preferentially size-selected using the AMPure XP system (Beckman Coulter, Beverly, United States). DNA fragments with ligated adaptor molecules on both ends were selectively enriched using Illumina PCR Primer Cocktail in a 15-cycle PCR reaction. Products were purified using the AMPure XP system, and then quantified by the Agilent high sensitivity DNA assay on the Agilent 2,100 Bioanalyzer (Agilent Technologies, CA, United States). The sequencing libraries were subjected to sequencing on the NovaSeq 6,000 platform (Illumina, CA, United States) for obtaining image files.

2.4 Quality control and reads mapping

The image files were transformed by the software of sequencing platform. The original data was generated in a FASTQ format (raw data). Sequencing data contained a number of connectors and low-quality reads. The Cutadapt (v1.15) software was used to filter the sequencing data (30), subsequently obtaining high-quality sequences (clean data) for further analysis. Two reference genomes were those of the golden

hamster (Genbank No.: PRJNA77669) and the SVA CH-LX-01-2016 (Genbank No.: KX751945). The filtered reads were separately mapped to both reference genomes using the HISAT2 (v2.0.5) program (31).

2.5 Analysis of differential expression

The analysis of differentially expressed genes (DEGs) was performed as described previously with modifications (32). The HTSeq (v0.9.1) was used to compare the Read Count values on each gene as the original gene expression (33). Gene expression was standardized through the FPKM (Fragments Per Kilobase of transcript per Million mapped reads). DEGs were determined by the DESeq (v1.30.0) with screening parameters as follows: the fold change (FC) > 2 (or < 0.5) and the significant *p* value < 0.05 (34). The bi-directional clustering analysis of all DEGs was performed by the Pheatmap (v1.0.8) package. The heatmap was drawn according to the expression level of the same gene in different groups and the expression patterns of different genes in the same group, with the Euclidean method for calculating the distance, and the complete linkage method for clustering.

2.6 Analyses of GO and KEGG enrichments

All genes were mapped to terms in the database of gene ontology (GO). Differentially enriched genes were calculated for each term. The topGO package was designed to perform the GO enrichment analysis on the DEGs. The *p* value was calculated by the hypergeometric distribution method. The *p* value < 0.05 was determined as the standard of significant enrichment. The GO terms were found with significantly differentially enriched genes, all of which were further classified to determine the main biological functions. The ClusterProfiler (v3.4.4) software was used to carry out the enrichment analysis of DEGs on the KEGG (Kyoto Encyclopedia of Genes and Genomes) pathways. The *p* value < 0.05 was determined as the standard of significant enrichment (35).

2.7 Other analyses on RNA-seq data

2.7.1 Analysis of new transcripts

On the basis of the existing reference genome, the software StringTie (<http://ccb.jhu.edu/software/stringtie/>) was used to assemble the mapped reads (36). The assembling results were compared with the known transcripts for obtaining unannotated transcripts.

2.7.2 Analysis of alternative splicing events

The rMATS (v3.2.5) software was used to uncover alternative splicing events (37). The main types of alternative splicing events included skipped exon (SE), retained intron (RI), alternative 5' splice site (A5SS), alternative 3' splice site (A3SS), and mutually exclusive exons (MXE).

2.7.3 Analysis of SNP sites

The Varscan program was used to obtain SNP sites (38). The filtering criteria were: (i) SNP site base Q > 20, (ii) the number of reads

covering the site > 8, (iii) the number of reads supporting the mutation site > 2, and (4) the *p* value of SNP locus < 0.01.

2.7.4 Prediction of transcription factors

Transcription factors and their own families were predicted via the comparison with the Animal Transcription Factor Database (AnimalTFDB) (39), a comprehensive database including classification and annotation of genome-wide transcription factors, transcription co-factors and chromatin remodeling factors in numerous animal genomes.

2.7.5 Analysis of differential exon usage

The DEXSeq package was used to analyze the RNA-seq data for identifying the differential exon usage, as described previously (40).

2.7.6 Interaction analysis in protein network

The STRING database (<https://string-db.org/>) was used to unveil putative protein–protein interactions (PPI) (41), contributing to clarifying the relationship among genes of interest.

2.8 Validation of gene expression by RT-qPCR

Four representative genes, namely, SVA genome, Nfkbia, Phlda2 and Txnip, were selected for validating the profile of gene expression. The GAPDH (glyceraldehyde-3-phosphate dehydrogenase) gene was used as an internal reference control. Gene-specific primers were listed in [Supplementary file 18](#) for RT-qPCR validation. The RT-qPCR analysis was performed with three technical repeats, using the AceQ qPCR SYBR Green Master Mix (Vazyme, Nanjing, China) based on the LightCycler 480® Real-time PCR System (Roche, Rotkreuz, Switzerland), as per the manufacturer's instructions. The RT-qPCR results were analyzed through the $2^{-\Delta\Delta C_t}$ method for relatively quantifying the four genes of interest (42). The GraphPad Prism (v8.0) was used for statistical analysis by two-tailed Student's *t*-test with Welch's correction. Data were shown as means \pm standard deviations of three independent experiments.

3 Results

3.1 Sequencing for *de novo* transcriptome assembly

The BSR-T7/5 cell monolayers showed no obvious cytopathic effect (CPE) at 12 hpi ([Figure 1](#)). Cells were separately collected from SVA-infected and non-infected groups to extract total RNAs for the construction of high-quality cDNA libraries. The primary library-related data were listed in [Supplementary file 1](#). The cDNA libraries were subjected to sequencing to obtain image files, subsequently transformed into raw data for statistical classification, as shown in [Table 1](#). Because the raw data contained a number of connectors and low-quality reads, the Cutadapt (v1.15) software was used to filter the raw data for obtaining high-quality clean sequences, as listed in [Supplementary file 2](#). There were three key parameters, namely, base mass, base content, and average mass of reads. Their distributions were independently shown in [Supplementary 3, 4 and 5](#).

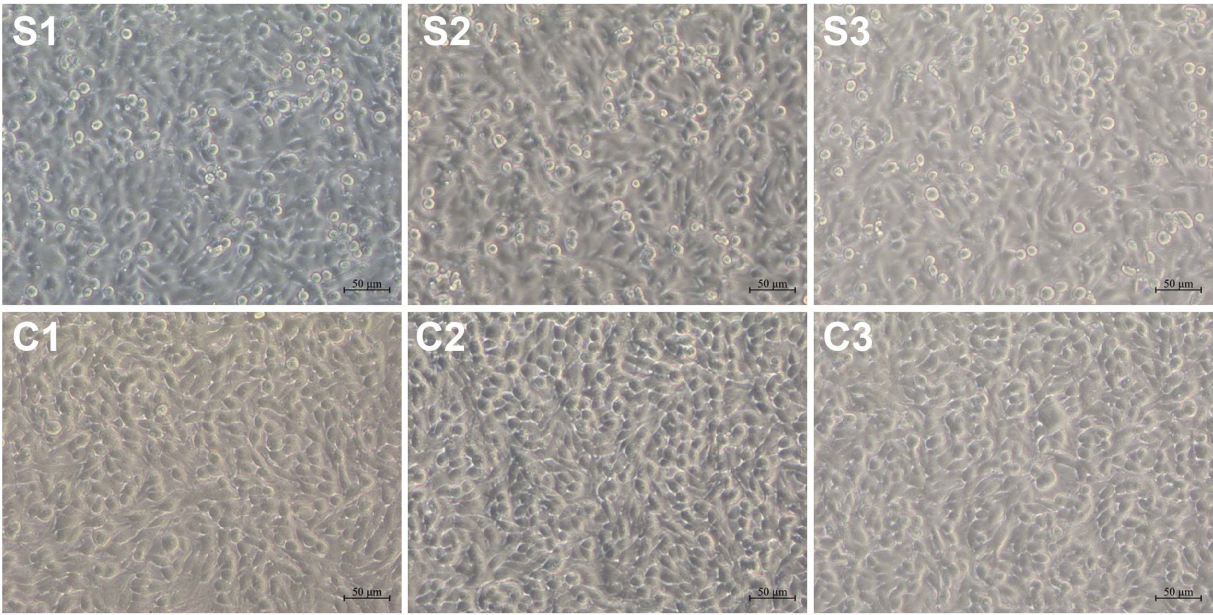


FIGURE 1
SVA-infected and non-infected cell monolayers at 12 hpi. S1, S2, and S3: SVA-infected groups; C1, C2 and C3: non-infected controls.

TABLE 1 Statistic data of RNA-seq for all six groups.

Sample name	Reads No.	Bases (bp) No.	Q30 (bp)	N (%)	Q20 (%)	Q30 (%)
S1	45,327,558	6,844,461,258	6,647,043,638	0.012777	99.00	97.12
S2	53,263,406	8,042,774,306	7,823,495,397	0.012671	99.06	97.27
S3	39,688,814	5,993,010,914	5,820,866,532	0.012943	99.02	97.13
C1	42,486,048	6,415,393,248	6,235,364,335	0.012489	99.01	97.19
C2	53,252,482	8,041,124,782	7,800,962,620	0.012589	98.95	97.01
C3	57,220,586	8,640,308,486	8,385,089,387	0.013141	98.96	97.05

Reads No.: the total number of reads; Bases (bp) No.: the total number of bases; Q30 (bp): the total number of bases with base recognition accuracy more than 99.9%; N (%): the percentage of ambiguous bases; Q20 (%) or Q30 (%): the percentage of Q20 or Q30 bases with base recognition accuracy more than 99%.

3.2 Transcriptomic mapping

The filtered reads were mapped to both reference genomes, those of the golden hamster and the SVA CH-LX-01-2016, using the HISAT2 (v2.0.5) program. The results of RNA-seq mapping were listed in Table 2. The global profile of reads was subjected to the further statistical analysis on the distribution of reads mapped to both genomes, in which genetic elements included coding sequence, intron, intergenic spacer, and UTR. The mapping results were listed in Table 3, and shown in Supplementary file 6. Supplementary file 7 exhibited the coverage distributions of reads mapped to genes. To sum up, a high-quality dataset of RNA-Seq was harvested here, meeting a standard for the further bioinformatics analysis.

3.3 Profile of gene expression

A total of 20,374 genes were identified in all six groups (Supplementary file 8), but these genes contained more than 3,000

components with FPKM value = 0. FPKM was a simple method for normalizing the read count data, based on gene length and the total number of mapped reads. The FPKM-normalized expression level was divided into different intervals (Supplementary file 9) for the six groups, as shown in Supplementary file 10. The number of genes, either co-identified in different groups or recognized in a single group, was shown in Figure 2A. The density distribution of FPKM values was displayed in Figures 2B,C, as two different forms. To validate whether the sequencing depth of RNA-seq was sufficient for the analysis of gene expression, the saturation analysis was performed for all six groups, as shown in Supplementary file 11. The correlation analysis of gene expression, based on calculation of Pearson's correlation coefficients, was carried out among the six groups (Figure 2D). The closer to 1.0 the correlation coefficient was, the higher the similarity of expression pattern was among the six groups. Principal component analysis made it possible to project a high-dimensional dataset onto two or three dimensions, as shown in Figure 2E. The closer the distance was, the higher the similarity was among groups.

TABLE 2 Statistical data of RNA-seq mapping.

Sample name	Clean reads	Total mapped (Rate)	Multiple mapped (Rate)	Uniquely mapped (Rate)
S1	44,738,448	40,444,421 (90.40%)	770,019 (1.90%)	39,674,402 (98.10%)
S2	52,647,920	47,570,136 (90.36%)	904,976 (1.90%)	46,665,160 (98.10%)
S3	39,219,782	35,252,668 (89.88%)	643,266 (1.82%)	34,609,402 (98.18%)
C1	41,942,238	36,798,807 (87.74%)	902,042 (2.45%)	35,896,765 (97.55%)
C2	52,501,164	45,940,744 (87.50%)	1,092,548 (2.38%)	44,848,196 (97.62%)
C3	56,437,286	49,541,887 (87.78%)	1,183,403 (2.39%)	48,358,484 (97.61%)

Clean reads: the number of sequences used for mapping; Total mapped (Rate): the number of sequences successfully mapped (Total mapped/Clean reads); Multiple Mapped (Rate): the number of sequences mapped to multiple regions (Multiple mapped/Total mapped); Uniquely Mapped (Rate): the number of sequences mapped to a single region (Uniquely mapped/Total mapped).

TABLE 3 Distribution of read-mapped regions.

Sample name	Map events	Mapped to gene (Rate)	Mapped to intergene (Rate)	Mapped to exon (Rate)
S1	39,674,402	36,731,507 (92.58%)	2,942,895 (7.42%)	34,599,182 (94.19%)
S2	46,665,160	42,794,501 (91.71%)	3,870,659 (8.29%)	39,814,657 (93.04%)
S3	34,609,402	31,712,144 (91.63%)	2,897,258 (8.37%)	29,532,363 (93.13%)
C1	35,896,765	32,161,772 (89.60%)	3,734,993 (10.40%)	29,444,837 (91.55%)
C2	44,848,196	39,799,780 (88.74%)	5,048,416 (11.26%)	35,909,925 (90.23%)
C3	48,358,484	43,583,502 (90.13%)	4,774,982 (9.87%)	40,133,590 (92.08%)

Map events: the number of mapping events; Mapped to gene (Rate): the number of reads mapped to genetic regions (Mapped to gene/Map events); Mapped to InterGene: the number of reads mapped to intergenic spacers (Mapped to intergene/Map events); Mapped to exon (Rate): the number of reads mapped to exons (Mapped to exon/Mapped to gene).

3.4 Analysis of differential expression

DEGs were determined by the DESeq (v1.30.0) with screening parameters, $|\log_2FC| > 1$ and the significant p value < 0.05 . A total of 628 DEGs, including 565 upregulated (Supplementary file 12) and 63 downregulated (Supplementary file 13) components, were identified here. The basemean was described as the “mean of normalized counts of all samples.” The basemean values of DEGs, corresponding to the group C and S, were exhibited in Figures 3A,B, respectively. The distributions of sequence length, p value and \log_2FC were exhibited in Figures 3C–H. A single asterisk in Figures 3G,H indicated the exclusion of positive or negative infinity (“Inf” in

Supplementary files 12, 13), respectively. The distribution and degree of differential expression were graphically shown in a volcano plot and a heatmap, respectively.

The volcano plot (Figure 3I), drawn by the GraphPad Prism software, revealed the p value versus the FC for all identified genes. The threshold values were set as $|\log_2FC| > 1$ and p value < 0.05 . The upregulated, downregulated and stably-expressed genes were indicated by red, green and grey circles, respectively. The R language Pheatmap (1.0.8) software package was used for the bi-directional clustering analysis to draw the heatmap (Figure 3J), which provided a visual depiction for hierarchical clustering of all 628 DEGs from the six groups. The red and green labels represented the upregulated and downregulated DEGs, respectively. The intensity of color reflected the degree of differentiation in gene expression. All 628 DEGs, based on their differences in expression patterns, were classified into nine different clusters (Figure 3K), in which grey lines indicated expression patterns, and each blue line represented the average value in each cluster.

3.5 GO enrichment analysis

The topGO package was used for performing the GO enrichment analysis on DEGs. The GO terms were found with significantly differentially enriched genes. The numbers of category BP, CC and MF were 3,093, 357 and 644, respectively. The complete GO data were listed in Supplementary file 14 in detail. Figure 4A displayed the top-10 statistically significant GO terms for each GO category. The false discovery rate (FDR), ranging from 0 to 1, was associated with the degree of GO enrichment. The lower the FDR was, the more significant the enrichment degree was. The GO terms with the top-20 lowest FDRs were shown in a bubble plot (Figure 4B). Each GO category was organized further as a directed acyclic graph (Figures 4C–E), in which parental terms described more general functional categories than their next-generation terms. GO terms with the top-10 lowest FDRs were framed with rectangles, and the others were indicated by ellipses. The more statistically significant a GO term was, the darker its color was.

3.6 KEGG enrichment analysis

The analysis of KEGG pathway enrichment was performed to uncover DEG-related pathways. The result showed that DEGs were enriched in a total of 275 KEGG pathways (Supplementary file 15). Figure 4F displayed the top-30 statistically significant KEGG pathways (p value < 0.05), classified into four categories, namely, environmental information processing, human diseases, metabolism, and organismal systems. According to the result of KEGG enrichment, the degree of enrichment was evaluated through the rich factor, FDR, and the number of DEGs enriched in a given pathway. The higher the rich factor was, the more significant the enrichment degree was. The lower the FDR was, the more significant the enrichment degree was. The KEGG pathways with the top-20 lowest FDRs were shown in a bubble plot (Figure 4G).

3.7 Other analyses on RNA-seq data

The StringTie was used to assemble the mapped reads. The assembling results were compared with the known transcripts to

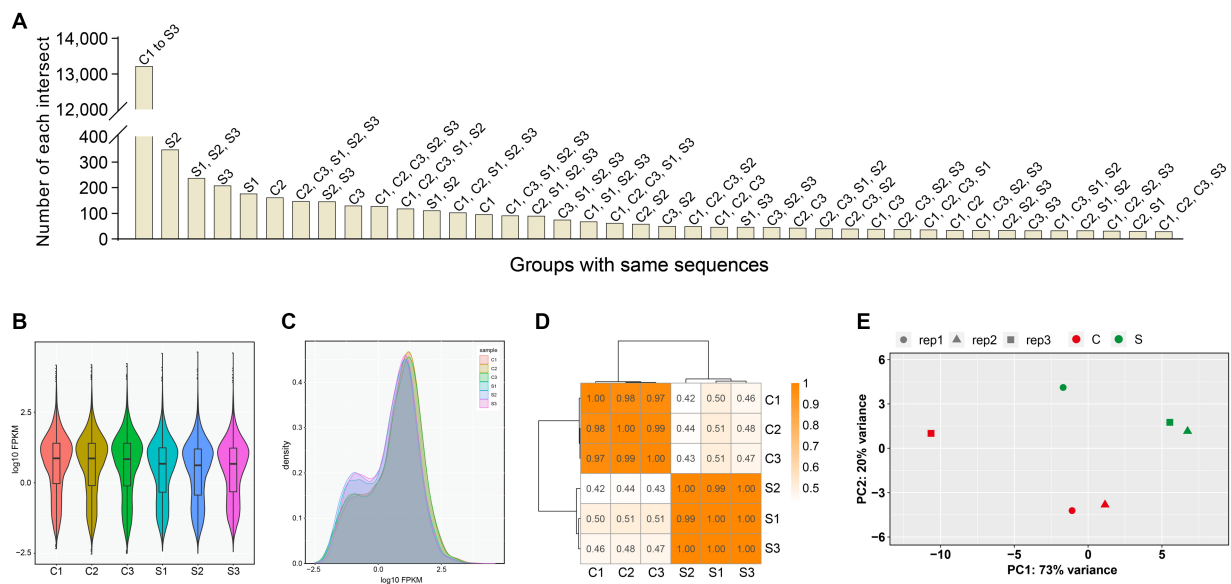


FIGURE 2

Profile of gene expression in all groups. The numbers of genes that are either co-identified in different groups or recognized in a single group (A). Violin plot of FPKM distributions in all groups (B). Distributions of FPKM densities in all groups (C). The correlation analysis of gene expression via the calculation of Pearson's correlation coefficients (D). Principal component analysis on all groups (E). PC1: principal component 1. PC2: principal component 2.

obtain unannotated transcripts. The transcripts from class codes j, i, u, and x, regarded as new transcripts, were functionally annotated and listed in [Supplementary file 16](#). The proportion of each class code was shown in [Figure 5A](#). Five types of alternative splicing events were analyzed by the rMATS (v3.2.5) software. The SE and RI exhibited the most and the least alternative splicing events, respectively ([Figure 5B](#)). The SNP sites were analyzed by the Varscan program. The numbers of heterozygous and homozygous variants were shown in [Figure 5C](#). Transcription factors and their own families were predicted through the comparison with those in the AnimalTFDB. [Figure 5D](#) showed the number of transcription factors in each family. Out of the identified families, 20 were demonstrated to contain upregulated, downregulated or both components ([Figure 5E](#)). The DEXSeq package was used to analyze the RNA-seq data for identifying the differential exon usage, as shown in [Supplementary file 17](#). [Figure 5F](#) revealed a representative gene with differential exon usage. DEGs were comprehensively analyzed in the STRING database to unveil potential PPIs (Score > 0.95) for constructing a PPI network, which including 26 nodes and 17 edges ([Figure 5G](#)). Red and green nodes indicated upregulated and downregulated genes, respectively.

3.8 Validation of gene expression by RT-qPCR

Three upregulated and one downregulated DEGs were selected for validating the profile of gene expression through RT-qPCR. The three upregulated genes included SVA genome, Nfkbia and Phlda2 ([Supplementary file 12](#)); the downregulated gene was Txnip ([Supplementary file 13](#)). The RT-qPCR detection demonstrated that the expression trend of DEGs was consistent with the result of RNA-seq analysis ([Figure 6](#)). Due to the group C without SVA inoculation, the expression differentiation of SVA genome was

extremely significant between both groups ([Figure 6](#), Left upper). There was no need for the statistical analysis on it.

4 Discussion

The *Picornaviridae* is a well-characterized family within the plus-strand RNA viruses. SVA is a typical picornavirus. Its genome is only a positive-sense, single-stranded mRNA, harboring a 3' poly(A) tail but no 5' capped structure. In other words, an SVA virion has a single mRNA, which however is not the viral transcript. Picornaviruses, albeit structurally simple, possibly have significant effects on physiological functions in their hosts. After entrance of virion into a cell, a picornaviral genome will be released into cytosol. This genome either relies on the host translation machinery to initiate the translation of polyprotein, or serves as a template to synthesize an antigenome, which will be used as a template for synthesizing another genome. The nascent genome can be used as a template for the next round of translation or replication, and alternatively is packaged into a virion ([43](#)). Therefore, although SVA as such has no concept of viral transcriptome, its infection may exert a significant impact on the cellular transcriptome. This prompted us to conduct the present study for uncovering the transcriptomic change in SVA-infected cells.

A replication-competent SVA was previously rescued from its cDNA clone in our laboratory ([27](#)). The passage-5 SVA was used here as a model virus. Despite SVA inoculation with MOI of 2.5, three cell monolayers showed no visible CPE at 12 hpi ([Figure 1](#)). Because we demonstrated previously that SVA infection led to significant cellular changes both in proteomic and in metabolomic profiles at 12 hpi, it could be postulated that the cellular transcriptome would be also affected at 12 hpi to some extent. The RNA-seq recognized totally 20,374 genes in the six groups, but containing more than 3,000 genes with FPKM value = 0. The correlation of gene expression is an

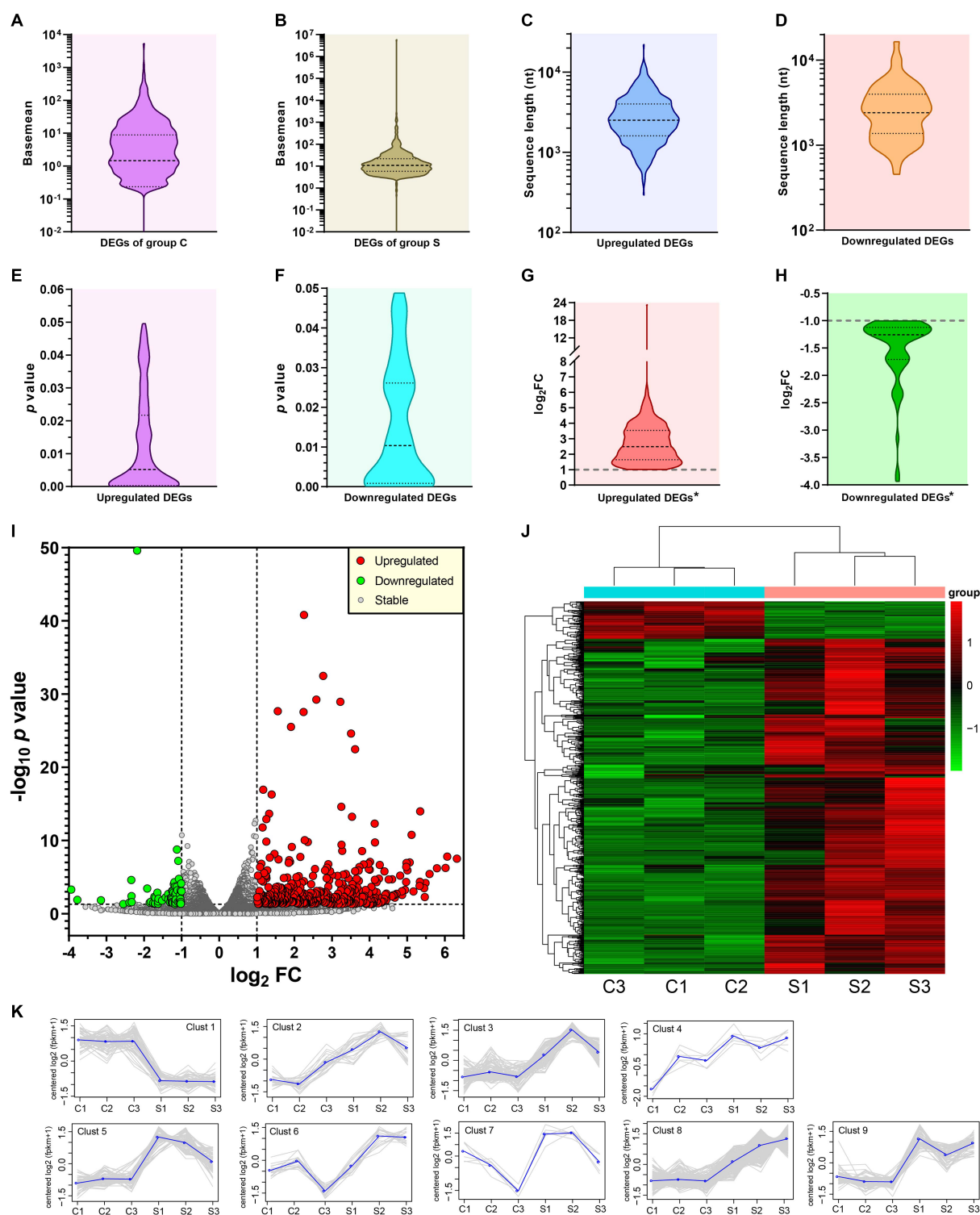


FIGURE 3

Profile and analysis of DEGs. Distribution of basemean values in group C (A) and S (B). Distributions of sequence lengths of upregulated (C) and downregulated (D) DEGs. Distributions of p values of upregulated (E) and downregulated (F) DEGs. Distributions of $\log_2 FC$ values of upregulated (G) and downregulated (H) DEGs. *Excluding the SVA-related data. Volcano plot of p value versus FC for all identified genes but excluding outliers (I). The threshold values are set as $|\log_2 FC| > 1$ and p value < 0.05 . Heatmap based on bi-directional clustering analysis of all DEGs (J). Clustering analysis on expression patterns of DEGs (K). Grey lines indicate expression patterns. Each blue line represents the average value in each cluster.

important indicator to demonstrate the reliability of experiment, and the reasonability of samples. A certain correlation coefficient, if between 0.8 and 1.0, would indicate the extremely strong correlation

between two groups. The current correlation analysis displayed the extremely strong intra-group correlation, but the weak inter-group correlation (Figure 2D), implying the RNA-seq data that were reliable.

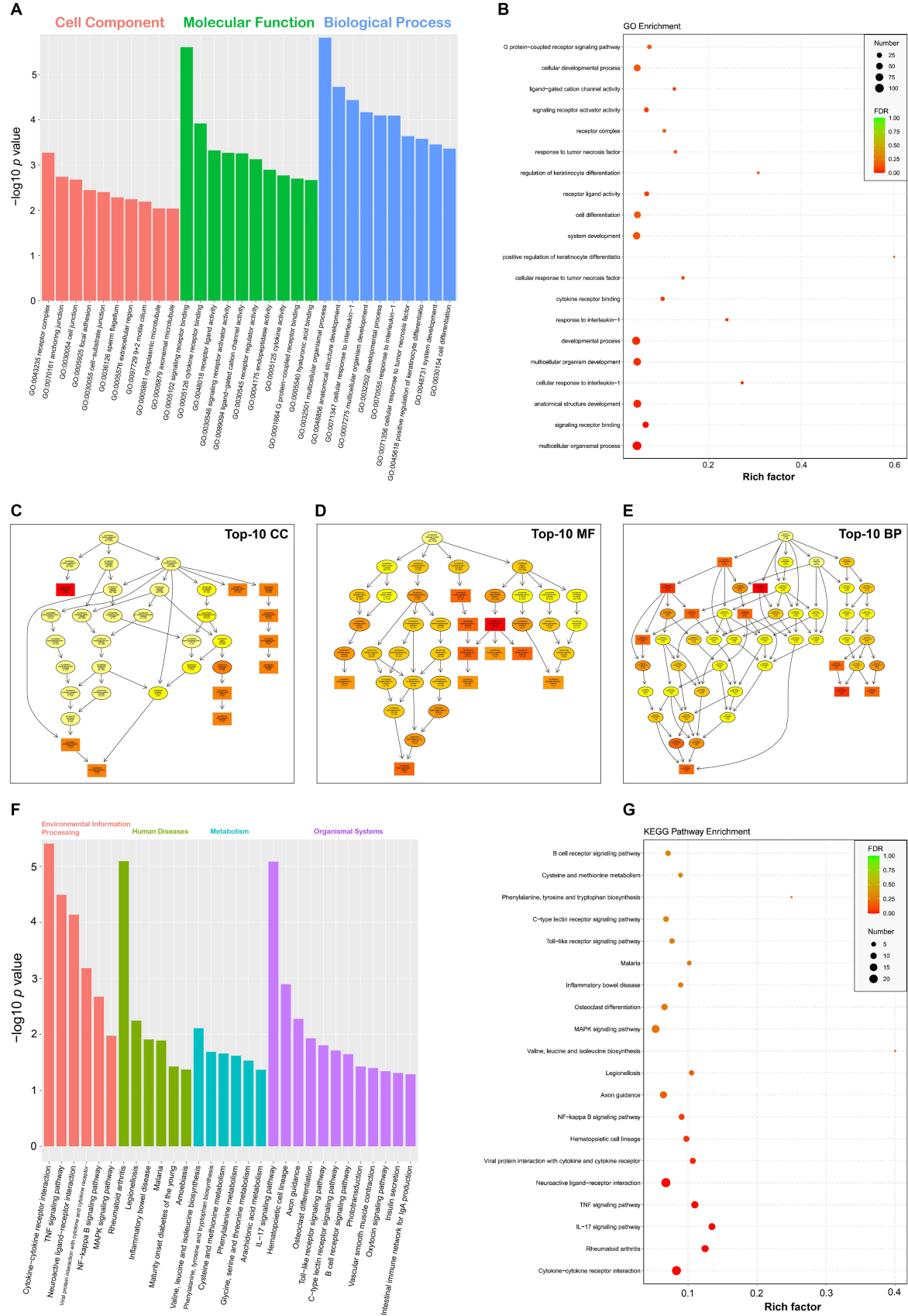


FIGURE 4
GO and KEGG enrichment analyses of DEGs. Top-10 statistically significant GO terms of three categories (A). Bubble plot of top-20 statistically significant GO terms (B). Directed acyclic graphs of top-10 statistically significant GO categories (C–E). GO terms with the top-10 lowest FDRs are framed with rectangles, and the others are indicated by ellipses. The more statistically significant a GO term is, the darker its color is. Top-30 statistically significant KEGG pathways, classified into four categories (F). Bubble plot of top-20 statistically significant KEGG pathways (G).

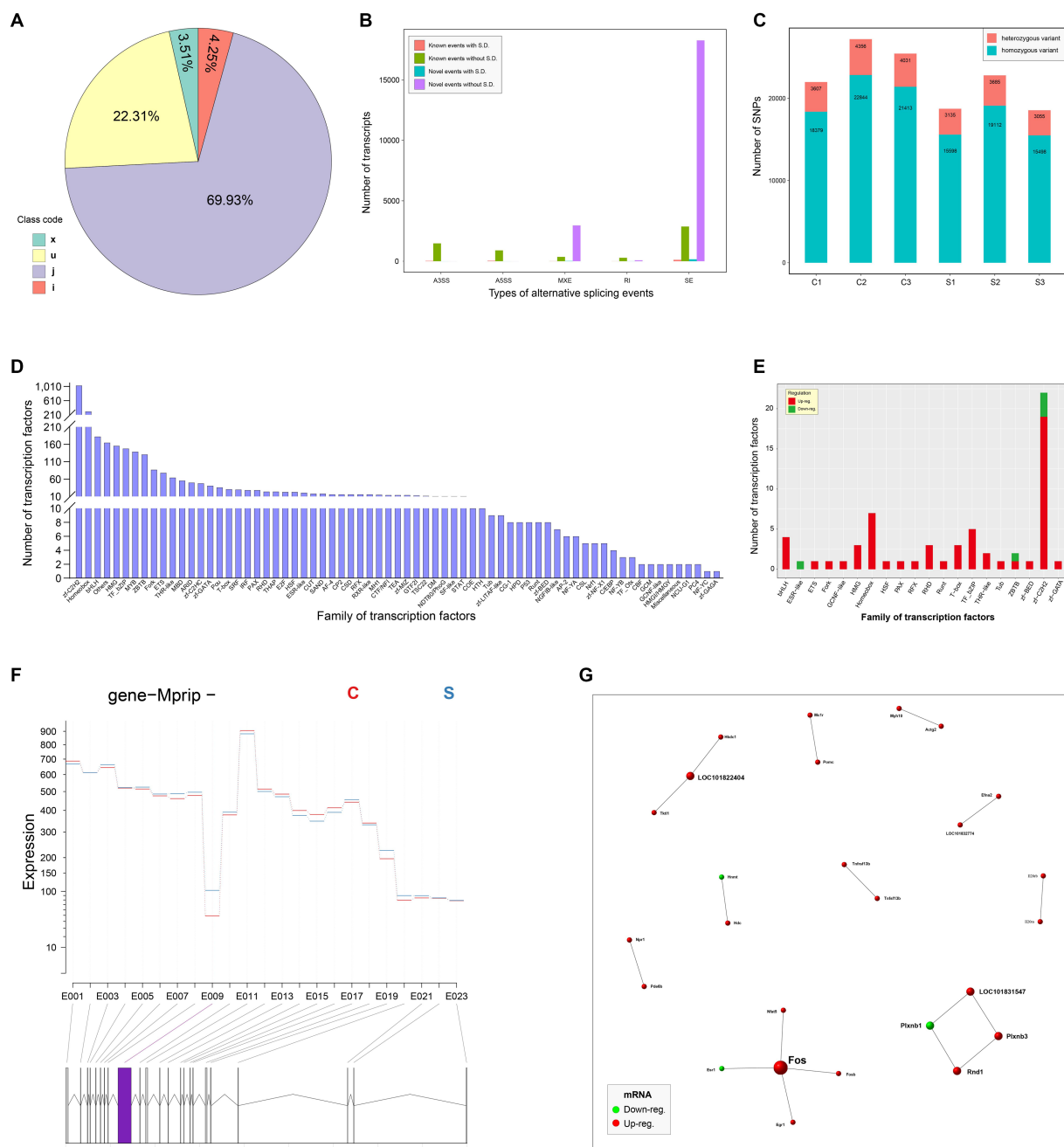


FIGURE 5

In-depth analysis of RNA-seq data. Pie chart of new transcripts (A). All new transcripts are classified into four categories, x, u, j and i. Analysis of alternative splicing events (B). X and Y axes indicate the types of alternative splicing events, and the number of new transcripts, respectively. S.D.: significant differentiation. The numbers of SNP sites in all groups (C). Profile of transcription factor families (D). The Y axis indicates the number of transcription factors in each family. Transcription factor families with significantly differential transcription factors (E). A representative gene with differential exon usage (F). The differential exon usage is marked with a purple rectangle. PPI network with 26 nodes and 17 edges (G). The score of PPI is set to be more than 0.95. Red and green nodes indicate upregulated and downregulated genes, respectively.

RNA-seq data were subjected to the further analysis on the differentiation expression. The result totally recognized 565 upregulated and 63 downregulated DEGs here. Out of these DEGs, five representative genes (three upregulated and two downregulated genes) were selected out for RT-qPCR analysis to validate preliminarily the profile of DEGs. Except the downregulated DEG, Tcta gene (data not shown), the other four showed their expression trends consistent with the result of RNA-seq analysis (Figure 6). In our previous study

on comparative proteomics between SVA-infected and non-infected cells, we identified totally 305 upregulated and 56 downregulated DEPs (differentially expressed proteins) (25). Regardless of the present or the previous study, the number of upregulated components was much higher than that of downregulated ones. Such a result was consistent with our postulation that DEGs shared a similar regulation trend with DEPs between SVA-infected and non-infected groups. Out of the identified DEGs in group S, the SVA genome was most

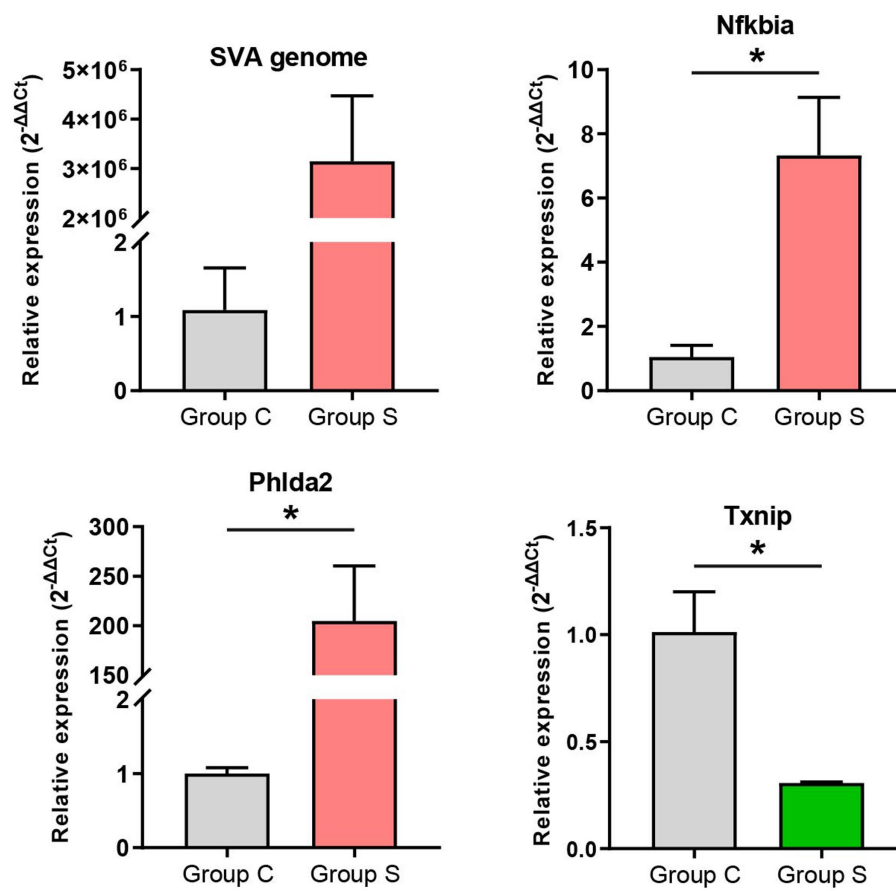


FIGURE 6

RT-qPCR validation of gene expression. The $2^{-\Delta\Delta C_t}$ method is used for relative quantification. The GAPDH gene is an internal control for normalization. Data are shown as means \pm standard deviations of three independent experiments. Statistical significance is determined by two-tailed Student's *t*-test with Welch's correction. **p* < 0.05.

statistically significant in the expression level (Supplementary file 12). Due to the group C without SVA inoculation, both GO and KEGG enrichment analyses excluded the data of SVA genome, and others with positive or negative infinity (Supplementary files 12, 13). The KEGG enrichment analysis showed that several DEGs were significantly enriched in many immunity-related pathways, such as TNF signaling pathway, IL-17 signaling pathway, Toll-like receptor signaling pathway, and B cell receptor signaling pathway (Figure 4F). The GO enrichment analysis also revealed a few statistically significant terms associated with immune responses, e.g., the response to interleukin-1 and the cellular response to tumor necrosis factor (Figure 4A). Like the conclusion drawn in a previous report (44), the current results also suggest that SVA infection may be able to induce significantly immune responses, especially the innate immune response, in hosts at an early stage of infection.

Further, RNA-seq data were subjected to the in-depth analyses, concerning SNPs, transcription factors, PPI and so on. The analysis of SNP events indicated that there was no significant differentiation in the number of SNP events between group C and S (Figure 5C), implying that SVA infection had no ability of inducing the occurrence of SNP events in the host genome. It is worth noting that out of the 20 statistically significant families of transcription factors, most of them only contain upregulated components (Figure 5E). This result implies

that SVA infection can notably stimulate multiple transcriptional pathways, resulting in upregulated DEGs far more than downregulated DEGs. The STRING database was used here to unravel putative PPIs in SVA-infected cells. The result revealed no formation of complicated interaction network among 26 putative DEPs (Figure 5G). Although the 26 DEPs include no SVA-related protein, the possibility that SVA-related proteins interact with cellular proteins cannot be ruled out, because the information of SVA proteins has not been deposited in the STRING database.

SVA emerged in many countries and regions over the past 20 years. It has been still considered as an emerging virus. Natural selection has been a primary evolutionary force affecting SVA codon usage bias (45). Multi-omics analysis provides an integrated approach to facilitate in-depth studies on the virology, especially on the interaction of viruses with their hosts. Based on our previous researches on proteomics and metabolomics, it was demonstrated that SVA infection could lead to significant changes in cellular intrinsic components even at an early stage of infection (25, 26). In order to comparatively analyze transcriptomic profiles between SVA-infected and non-infected cells, we conducted the present study. To sum up, the current results revealed that most of the DEGs were upregulated genes, indicating that SVA infection positively stimulated the transcription initiation in cells. GO and KEGG enrichment analyses

demonstrated that SVA could markedly affect immunity-related pathways in cells, whereas the mechanism remained to be elucidated.

Data availability statement

The data presented in the study are deposited in the NCBI repository, accession number PRJNA1100277.

Author contributions

YL: Writing – original draft, Methodology, Formal analysis. HC: Writing – original draft, Methodology, Investigation, Data curation. YJ: Writing – review & editing, Formal analysis. ZL: Writing – review & editing, Investigation. JW: Writing – review & editing, Software. FL: Writing – review & editing, Writing – original draft, Supervision, Conceptualization.

Funding

The author(s) declare that financial support was received for the research, authorship, and/or publication of this article. This work was supported by the National Natural Science Foundation of China (Grant No. 32273000), the Qingdao Demonstration Project for People-benefit from Science and Techniques (Grant No. 24-2-8-xdny-4-nsh), and the Postgraduate Innovation Program of Qingdao Agricultural University (QNYCX24043).

References

1. Pasma T, Davidson S, Shaw SL. Idiopathic vesicular disease in swine in Manitoba. *Can Vet J.* (2008) 49:84–5.
2. Singh K, Corner S, Clark S, Scherba G, Fredrickson R. Seneca Valley virus and vesicular lesions in a pig with idiopathic vesicular disease. *J. Vet. Sci. Technol.* (2012) 3:1–3. doi: 10.4172/2157-7579.1000123
3. Leme RA, Zotti E, Alcantara BK, Oliveira MV, Freitas LA, Alfieri AF, et al. Senecavirus a: an emerging vesicular infection in Brazilian pig herds. *Transbound Emerg Dis.* (2015) 62:603–11. doi: 10.1111/tbed.12430
4. Sun D, Vannucci F, Knutson TP, Corzo C, Marthaler DG. Emergence and whole-genome sequence of Senecavirus a in Colombia. *Transbound Emerg Dis.* (2017) 64:1346–9. doi: 10.1111/tbed.12669
5. Wu Q, Zhao X, Bai Y, Sun B, Xie Q, Ma J. The first identification and complete genome of Senecavirus a affecting pig with idiopathic vesicular disease in China. *Transbound Emerg Dis.* (2017) 64:1633–40. doi: 10.1111/tbed.12557
6. Leme RA, Alfieri AF, Alfieri AA. Update on Senecavirus infection in pigs. *Viruses.* (2017) 9:170. doi: 10.3390/v9070170
7. Leme RA, Oliveira TE, Alcantara BK, Headley SA, Alfieri AF, Yang M, et al. Clinical manifestations of Senecavirus a infection in neonatal pigs, Brazil, 2015. *Emerg Infect Dis.* (2016) 22:1238–41. doi: 10.3201/eid2207.151583
8. Fernandes MHV, de Lima M, Joshi LR, Diel DG. A virulent and pathogenic infectious clone of Senecavirus a. *J Gen Virol.* (2021) 102:001643. doi: 10.1099/jgv.0.001643
9. Oliveira TES, Leme RA, Agnol AMD, Gerez JR, Pelaquim IF, Miyabe FM, et al. Seneca Valley virus induces immunodepression in suckling piglets by selective apoptosis of B lymphocytes. *Microb Pathog.* (2021) 158:105022. doi: 10.1016/j.micpath.2021.105022
10. Hellen CU, de Breyne S. A distinct group of hepacivirus/pestivirus-like internal ribosomal entry sites in members of diverse picornavirus genera: evidence for modular exchange of functional noncoding RNA elements by recombination. *J Virol.* (2007) 81:5850–63. doi: 10.1128/JVI.02403-06
11. Willcocks MM, Locker N, Gomwalk Z, Royall E, Bakhshesh M, Belsham GJ, et al. Structural features of the Seneca Valley virus internal ribosome entry site (IRES)

Acknowledgments

We gratefully thank the Shanghai Bioprofile Biotechnology Co., Ltd. (Shanghai, China) for providing technical assistance in RNA-seq. We also thank Xianggan Cui for his help in technical support.

Conflict of interest

YJ was employed by the Qingdao Zhongren-OLand Bioengineering Co., Ltd.

The remaining authors declare that the research was conducted in the absence of any commercial or financial relationships that could be construed as a potential conflict of interest.

Publisher's note

All claims expressed in this article are solely those of the authors and do not necessarily represent those of their affiliated organizations, or those of the publisher, the editors and the reviewers. Any product that may be evaluated in this article, or claim that may be made by its manufacturer, is not guaranteed or endorsed by the publisher.

Supplementary material

The Supplementary material for this article can be found online at: <https://www.frontiersin.org/articles/10.3389/fvets.2024.1431879/full#supplementary-material>

- element: a picornavirus with a pestivirus-like IRES. *J Virol.* (2011) 85:4452–61. doi: 10.1128/JVI.01107-10
12. Zhao D, Li Y, Li Z, Zhu L, Sang Y, Zhang H, et al. Only fourteen 3'-end poly(a)s sufficient for rescuing Senecavirus a from its cDNA clone, but inadequate to meet requirement of viral replication. *Virus Res.* (2023) 328:199076. doi: 10.1016/j.virusres.2023.199076
13. Liu F, Wang Q, Huang Y, Wang N, Shan H. A 5-year review of Senecavirus a in China since its emergence in 2015. *Front Vet Sci.* (2020) 7:567792. doi: 10.3389/fvets.2020.567792
14. Choudhury SM, Ma X, Zeng Z, Luo Z, Li Y, Nian X, et al. Senecavirus a 3D interacts with NLRP3 to induce IL-1 β production by activating NF- κ B and Ion Channel signals. *Microbiol Spectr.* (2022) 10:e0209721. doi: 10.1128/spectrum.02097-21
15. Liu H, Li K, Chen W, Yang F, Cao W, Zhang K, et al. Senecavirus a 2B protein suppresses type I interferon production by inducing the degradation of MAVS. *Mol Immunol.* (2022) 142:11–21. doi: 10.1016/j.molimm.2021.12.015
16. Zhao K, Guo XR, Liu SF, Liu XN, Han Y, Wang LL, et al. 2B and 3C proteins of Senecavirus a antagonize the antiviral activity of DDX21 via the caspase-dependent degradation of DDX21. *Front Immunol.* (2022) 13:951984. doi: 10.3389/fimmu.2022.951984
17. Duhan L, Kumari D, Naime M, Parmar VS, Chhillar AK, Dangi M, et al. Single-cell transcriptomics: background, technologies, applications, and challenges. *Mol Biol Rep.* (2024) 51:600. doi: 10.1007/s11033-024-09553-y
18. Maher CA, Kumar-Sinha C, Cao X, Kalyana-Sundaram S, Han B, Jing X, et al. Transcriptome sequencing to detect gene fusions in cancer. *Nature.* (2009) 458:97–101. doi: 10.1038/nature07638
19. Zeng J, Cao D, Yang S, Jaiyan DK, Liu X, Wu S, et al. Insights into the transcriptome of human cytomegalovirus: a comprehensive review. *Viruses.* (2023) 15:1703. doi: 10.3390/v15081703
20. Deb R, Sengar GS, Sonowal J, Pegu SR, Das PJ, Singh I, et al. Transcriptome signatures of host tissue infected with African swine fever virus reveal differential expression of associated oncogenes. *Arch Virol.* (2024) 169:54. doi: 10.1007/s00705-023-05959-4

21. Wen W, Yin M, Zhang H, Liu T, Chen H, Qian P, et al. Seneca Valley virus 2C and 3C inhibit type I interferon production by inducing the degradation of RIG-I. *Virology*. (2019) 535:122–9. doi: 10.1016/j.virol.2019.06.017
22. Hou L, Dong J, Zhu S, Yuan F, Wei L, Wang J, et al. Seneca valley virus activates autophagy through the PERK and ATF6 UPR pathways. *Virology*. (2019) 537:254–63. doi: 10.1016/j.virol.2019.08.029
23. Li L, Bai J, Fan H, Yan J, Li S, Jiang P. E2 ubiquitin-conjugating enzyme UBE2L6 promotes Senecavirus A proliferation by stabilizing the viral RNA polymerase. *PLoS Path.* (2020) 16:e1008970. doi: 10.1371/journal.ppat.1008970
24. Liu T, Li X, Wu M, Qin L, Chen H, Qian P. Seneca Valley virus 2C and 3C(pro) induce apoptosis via mitochondrion-mediated intrinsic pathway. *Front Microbiol.* (2019) 10:1202. doi: 10.3389/fmicb.2019.01202
25. Liu F, Ni B, Wei R. Comparative proteomic profiling: cellular metabolisms are mainly affected in Senecavirus A-inoculated cells at an early stage of infection. *Viruses*. (2021) 13:1036. doi: 10.3390/v13061036
26. Liu F, Ni B, Wei R. Senecavirus A- and non-infected cells at early stage of infection: comparative Metabolomic profiles. *Front Cell Infect Microbiol.* (2022) 11:736506. doi: 10.3389/fcimb.2021.736506
27. Liu F, Huang Y, Wang Q, Li J, Shan H. Rescue of Senecavirus A to uncover mutation profiles of its progenies during 80 serial passages *in vitro*. *Vet Microbiol.* (2021) 253:108969. doi: 10.1016/j.vetmic.2020.108969
28. Zhao X, Wu Q, Bai Y, Chen G, Zhou L, Wu Z, et al. Phylogenetic and genome analysis of seven senecavirus A isolates in China. *Transbound Emerg Dis.* (2017) 64:2075–82. doi: 10.1111/tbed.12619
29. Ding L, Li Q, Chakrabarti J, Munoz A, Faure-Kumar E, Ocádiz-Ruiz R, et al. MiR130b from Schlafen4(+) MDSCs stimulates epithelial proliferation and correlates with preneoplastic changes prior to gastric cancer. *Gut*. (2020) 69:1750–61. doi: 10.1136/gutjnl-2019-318817
30. Martin M. Cutadapt removes adapter sequences from high-throughput sequencing reads. *EMBnet J.* (2011) 17:10–2. doi: 10.14806/ej.17.1.200
31. Kim D, Paggi JM, Park C, Bennett C, Salzberg SL. Graph-based genome alignment and genotyping with HISAT2 and HISAT-genotype. *Nat Biotechnol.* (2019) 37:907–15. doi: 10.1038/s41587-019-0201-4
32. Qiao J, Li H, Li Y. Dietary *Clostridium butyricum* supplementation modifies significantly the liver transcriptomic profile in weaned piglets. *J Anim Physiol Anim Nutr.* (2020) 104:1410–23. doi: 10.1111/jpn.13326
33. Anders S, Pyl PT, Huber W. HTSeq—a Python framework to work with high-throughput sequencing data. *Bioinformatics* (2015) 31:166–169. doi: 10.1093/bioinformatics/btu638, HTSeq—a Python framework to work with high-throughput sequencing data
34. Li D, Zand MS, Dye TD, Goniewicz ML, Rahman I, Xie Z. An evaluation of RNA-seq differential analysis methods. *PLoS One*. (2022) 17:e0264246. doi: 10.1371/journal.pone.0264246
35. Yu G, Wang LG, Han Y, He QY. clusterProfiler: an R package for comparing biological themes among gene clusters. *OMICS*. (2012) 16:284–7. doi: 10.1089/omi.2011.0118
36. Kovaka S, Zimin AV, Pertea GM, Razaghi R, Salzberg SL, Pertea M. Transcriptome assembly from long-read RNA-seq alignments with StringTie2. *Genome Biol.* (2019) 20:278. doi: 10.1186/s13059-019-1910-1
37. Shen S, Park JW, Lu ZX, Lin L, Henry MD, Wu YN, et al. rMATS: robust and flexible detection of differential alternative splicing from replicate RNA-Seq data. *Proc Natl Acad Sci USA*. (2014) 111:E5593–601. doi: 10.1073/pnas.1419161111
38. Koboldt DC, Chen K, Wylie T, Larson DE, McLellan MD, Mardis ER, et al. VarScan: variant detection in massively parallel sequencing of individual and pooled samples. *Bioinformatics*. (2009) 25:2283–5. doi: 10.1093/bioinformatics/btp373
39. Zhang HM, Chen H, Liu W, Liu H, Gong J, Wang H, et al. AnimalTFDB: a comprehensive animal transcription factor database. *Nucleic Acids Res.* (2012) 40:D144–9. doi: 10.1093/nar/gkr965
40. Anders S, Reyes A, Huber W. Detecting differential usage of exons from RNA-seq data. *Genome Res.* (2012) 22:2008–17. doi: 10.1101/gr.133744.111
41. Szklarczyk D, Morris JH, Cook H, Kuhn M, Wyder S, Simonovic M, et al. The STRING database in 2017: quality-controlled protein-protein association networks, made broadly accessible. *Nucleic Acids Res.* (2017) 45:D362–8. doi: 10.1093/nar/gkw937
42. Livak KJ, Schmittgen TD. Analysis of relative gene expression data using real-time quantitative PCR and the 2(-Delta Delta C(T)) method. *Methods*. (2001) 25:402–8. doi: 10.1006/meth.2001.1262
43. Kinobe R, Wiyatno A, Artika IM. Insight into the enterovirus A71: a review. *Rev Med Virology*. (2022) 32:e2361. doi: 10.1002/rmv.2361
44. Wang J, Mou C, Wang M, Pan S, Chen Z. Transcriptome analysis of senecavirus A-infected cells: type I interferon is a critical anti-viral factor. *Microb Pathog.* (2020) 147:104432. doi: 10.1016/j.micpath.2020.104432
45. Zeng W, Yan Q, Du P, Yuan Z, Sun Y, Liu X, et al. Evolutionary dynamics and adaptive analysis of Seneca Valley virus. *Infect Genet Evol.* (2023) 113:105488. doi: 10.1016/j.meegid.2023.105488



OPEN ACCESS

EDITED BY

Lingxue Yu,
Chinese Academy of Agricultural Sciences,
China

REVIEWED BY

Qin Zhao,
Northwest A&F University, China
Wenliang Li,
Jiangsu Academy of Agricultural Sciences
(JAAS), China
Tao Lin,
Elpiscience, China

*CORRESPONDENCE

Yanhua Li
✉ 007206@yzu.edu.cn
Anping Wang
✉ wap4017@163.com

RECEIVED 18 May 2024

ACCEPTED 12 June 2024

PUBLISHED 26 June 2024

CITATION

Guo J, Li C, Lu H, Wang B, Zhang L, Ding J,
Jiao X, Li Q, Zhu S, Wang A and Li Y (2024)
Reverse genetics construction and
pathogenicity of a novel recombinant
NADC30-like PRRSV isolated in China.
Front. Vet. Sci. 11:1434539.
doi: 10.3389/fvets.2024.1434539

COPYRIGHT

© 2024 Guo, Li, Lu, Wang, Zhang, Ding, Jiao,
Li, Zhu, Wang and Li. This is an open-access
article distributed under the terms of the
[Creative Commons Attribution License](#)
(CC BY). The use, distribution or reproduction
in other forums is permitted, provided the
original author(s) and the copyright owner(s)
are credited and that the original publication
in this journal is cited, in accordance with
accepted academic practice. No use,
distribution or reproduction is permitted
which does not comply with these terms.

Reverse genetics construction and pathogenicity of a novel recombinant NADC30-like PRRSV isolated in China

Jinyao Guo¹, Chenxi Li^{1,2,3}, Huipeng Lu⁴, Bin Wang¹,
Linjie Zhang¹, Jingjing Ding¹, Xue Jiao¹, Qingyu Li¹,
Shanyuan Zhu⁴, Anping Wang^{4*} and Yanhua Li^{1,2,3*}

¹College of Veterinary Medicine, Yangzhou University, Yangzhou, Jiangsu, China, ²Comparative Medicine Research Institute, Yangzhou University, Yangzhou, Jiangsu, China, ³Jiangsu Co-Innovation Center for Prevention and Control of Important Animal Infectious Diseases and Zoonoses, Yangzhou, Jiangsu, China, ⁴Jiangsu Agri-animal Husbandry Vocational College, Jiangsu Key Laboratory for High-Tech Research and Development of Veterinary Biopharmaceuticals, Taizhou, China

China has the largest pig herd in the world which accounts for more than 50% of the global pig population. Over the past three decades, the porcine reproductive and respiratory syndrome virus (PRRSV) has caused significant economic loss to the Chinese swine industry. Currently, the prevalent PRRSV strains in the field are extremely complicated, and the NADC30-like strains, NADC34-like strains, and novel recombinant viruses have become a great concern to PRRS control in China. In this study, a novel NADC30-like PRRSV, named GS2022, was isolated from the lung of a dead pig collected from a farm that experienced a PRRS outbreak. The complete genome of GS2022 shares the highest identity with the NADC30 strain and contains a discontinuous deletion of 131 aa in nsp2. Novel deletion and insertion have been identified in ORF7 and 3'UTR. Recombination analysis revealed that the GS2022 is a potential recombinant of NADC30-like and JXA1-like strains. Both inter-lineage and intra-lineage recombination events were predicted to be involved in the generation of the GS2022. An infectious cDNA clone of GS2022 was assembled to generate the isogenic GS2022 (rGS2022). The growth kinetics of rGS2022 were almost identical to those of GS2022. The pathogenicity of the GS2022 and rGS2022 was evaluated using a nursery piglet model. In the infection groups, the piglets exhibited mild clinical symptoms, including short periods of fever and respiratory diseases. Both gross lesions and histopathological lesions were observed in the lungs and lymph nodes of the infected piglets. Therefore, we reported a novel recombinant NADC30-like PRRSV strain with moderate pathogenicity in piglets. These results provide new information on the genomic characteristics and pathogenicity of the NADC30-like PRRSV in China.

KEYWORDS

PRRSV, NADC30-like, RNA recombination, reverse genetics, pathogenicity

1 Introduction

Porcine reproductive and respiratory syndrome (PRRS) is one of the most economically important infectious diseases to the pig industry worldwide. The characteristic symptoms of this disease are reproductive failure in pregnant pigs and severe respiratory syndrome in piglets. It was first reported in North America in 1987 and almost simultaneously reported in

Europe, and now is widely spread globally except in Australia, New Zealand, Scandinavia, Switzerland and some South American countries.¹ PRRSV, the etiological agent of PRRS, is a member of the genus *Betaarterivirus* in the family *Arteriviridae* in the order *Nidovirales*. PRRSV can be divided into two species, *Betaarterivirus suis* 1 and *Betaarterivirus suis* 2, which were also, respectively, called PRRSV-1 and PRRSV-2 (1). The prototype strains for those two species are the Lelystad and VR-2332 strains (2, 3). The single-stranded positive-sense RNA genome of PRRSV is around 15 kb in length, and the cap structure and polyadenylation tail can be found at its 5' and 3' ends. Two large polyproteins encoded by ORF1a and ORF1b at the 5' end of the genome are further proteolytic processed into nonstructural proteins (nsp1 α / β , nsp2~nsp6, nsp7 α / β , and nsp8~nsp12) (4). Besides, nsp2TF and nsp2N, two additional nonstructural proteins, are translated through a dual-programmed ribosomal frameshift mechanism in the nsp2-coding region (5, 6). These nonstructural proteins play key roles in viral RNA replication and modulation of host antiviral immune responses (7, 8). At least 8 open reading frames (ORFs) at the 3' end of the genome encode the structural proteins, including ORF2a/b, ORF3~7, and ORF5a (9).

Since the nsp2-coding region and ORF5 are the most variable regions in the PRRSV genome, their nucleotide sequences are usually used for phylogenetic analysis. A panel of unique deletion patterns has been identified in the nsp2 protein sequences of PRRSV-2, such as a discontinuous deletion of 30 amino acids (aa) in HP-PRRSV strains, a continuous deletion of 100 aa in NADC34-like strains, and a discontinuous deletion of 131 aa in NADC30-like strains (10). Based on the sequence diversity of ORF5, PRRSV-2 can be divided into nine lineages (L1~L9) (11). In China, the majority of prevalent PRRSV-2 strains belong to L1, L3, L5, and L8. Since 2013, many PRRSV strains that share significantly high sequence identity with NADC30 strain reported in the US were frequently detected in south-central China and were named NADC30-like PRRSV (12–14). In 2017, two novel PRRSV strains containing a 100 aa continuous deletion in nsp2 were reported in China and termed NADC34-like PRRSV (15). In recent years, NADC30-like PRRSV and NADC34-like PRRSV have become the dominant strains circulating in pig herds in China (16). The pathogenicity of those strains varies significantly, although they are much less pathogenic to pigs than HP-PRRSV (13, 17–20). To date, the mechanism leading to the difference in pathogenicity is largely unknown.

The extremely high mutation rate and RNA recombination are the main driving forces behind the rapid evolution of PRRSV (10, 21). Recently, a large number of recombinant PRRSV strains have been reported in different regions of China, and most of the strains were generated with the NADC30-like or NADC34-like PRRSV strains as parental viruses. Consistently, PRRSV strains in lineage 1 were found to serve as parental strains in the majority of the recombination events of PRRSV-2 according to a recombination analysis of PRRSV strains from China and the US (10). However, the mechanism behind the RNA recombination and variable pathogenicity of NADC30-like PRRSV is not well understood. In this study, a novel recombinant NADC30-like PRRSV strain GS2022 was isolated from a pig lung collected from a farm experiencing PRRS outbreak in 2022 and

characterized *in vitro*. An infectious cDNA clone of this strain was generated. The pathogenicity of the wild-type virus and cloned virus in piglets was further investigated.

2 Materials and methods

2.1 Cells, viruses, and antibodies

MARC-145 cells (ATCC) for PRRSV infection were cultured in Modified Eagle Medium (MEM; Sig-ma-Aldrich, St. Louis, MO, United States) supplemented 10% fetal bovine serum (FBS; Sig-ma-Aldrich, St. Louis, MO, United States) and 1% penicillin–streptomycin (Thermo Fisher Scientific, Waltham, MA, United States). BHK-21 cells (ATCC) for the recovery of recombinant PRRSV were maintained in Dulbecco's modified eagle medium (DMEM; ThermoFisher Scientific, Waltham, MA, United States) supplemented with 10% FBS (Vazyme Biotech, Nanjing, China) and 1% penicillin–streptomycin (Thermo Fisher Scientific, Waltham, MA, United States). Porcine alveolar macrophages (PAMs) isolated from the lung lavage fluid of 4-week-age PRRSV-negative piglets were cultured in RPMI-1640 medium (Cytiva, Logan, UT, United States) containing 10% FBS (Sigma-Aldrich, St. Louis, MO, United States) and 2% penicillin–streptomycin. All cells were cultured at 37°C with 5% CO₂ in a humidified incubator (ThermoFisher Scientific, Waltham, MA, United States). An HP-PRRSV TA-12 strain described previously was used in this study (22). A monoclonal antibody against PRRSV N for the immunofluorescence assay was purchased from MEDIAN Diagnostics, Korea.

2.2 Sample collection and virus isolation

In 2022, in a pig farm within Gansu province in China, about 60 dead piglets that had exhibited typical clinical symptoms of PRRS, including high fever, coughing, and depression, were diagnosed to be PRRSV infection by qRT-PCR (23). We further isolated a PRRSV strain with one of the PRRSV-positive lung tissues. The lung tissue was homogenized in MEM, and centrifugation was conducted to collect the virus supernatant. The supernatant was then filtrated through a 0.22 μ m filter to remove bacteria contaminations. Porcine alveolar macrophages (PAMs) and MARC-145 cells were, respectively, incubated with the virus supernatant for 2 h and maintained with MEM medium supplemented with 2% FBS (Sigma-Aldrich, St. Louis, MO, United States) and 2% pen-streptomycin at 37°C. The cells were monitored daily for cytopathic effects (CPE). Virus supernatant was collected when 80% of cells exhibited obvious CPE, and cells were fixed for indirect immunofluorescence assay (IFA) with a monoclonal antibody to detect PRRSV N protein as described previously. If no CPE was observed until 5 days post-inoculation, cells were also fixed for IFA detection of PRRSV N protein. The isolated PRRSV was named as GS2022 strain and further confirmed by full-length genome sequencing.

2.3 Immunofluorescence assay

MARC-145 cells or PAMs were infected with the GS2022 or TA-12 viruses, respectively. At 3 dpi, cells were fixed with ice-cold

¹ <https://prpsccontrol.com/>

methanol at -20°C for 10 min and then air-dry for immunofluorescence assay detection of PRRSV N protein. Briefly, cell monolayers were blocked with 1% BSA (Solarbio Life Sciences, Beijing, China) in $1\times$ PBS buffer for 30 min at room temperature, and then incubated with a monoclonal antibody against PRRSV N protein for 1 h at 37°C . After extensive washes with $1\times$ PBS to remove unbound primary antibody, cell monolayers were incubated with an Alexa 488-conjugated goat anti-mouse secondary antibody (Jackson ImmunoResearch Inc., West Grove, PA, United States) for 45 min at 37°C . Cell nuclei were counterstained with 4',6-diamidino-2-phenylindole (DAPI) solution (Solarbio Life Sciences, Beijing, China). After extensive washes with $1\times$ PBS, fluorescent images of the cell monolayers were captured with an IX73 epifluorescence microscope (Olympus).

2.4 Complete genome sequencing of PRRSV GS2022 strain

To obtain the whole genomic sequence of the GS2022 strain, four pairs of primers were designed to amplify the viral genome as listed in Table 1. Viral genomic RNA was extracted from the isolated virus and the homologous of the original lung tissue using a viral nucleic extraction kit (TIANGEN Biotech, China), respectively. The cDNA generated with a HiScript III 1st Strand cDNA Synthesis Kit (Vazyme Biotech, Nanjing, China) was used for PCR amplification using the Phanta Max Super-Fidelity DNA Polymerase (Vazyme Biotech, Nanjing, China). Four DNA fragments amplified for each sample were gel-purified with a FastPure Gel DNA Extraction Mini Kit and subjected to DNA

sequencing in the facility of GENEWIZ (Suzhou, China). Two consensus full-length genomes were assembled using the SnapGene software version 4.3.6 for the isolated virus and the virus contained in the lung tissue, respectively. The complete genome of GS2022 was submitted to the Genbank under Accession No. PP235415.1.

2.5 Sequence alignment and phylogenetic analysis

24 PRRSV genomic sequences which represent the four most prevalent PRRSV-2 lineages were downloaded for sequence alignment and phylogenetic analysis. Sequence alignment was performed with the CLC Genomic Workbench 20.0.4 (QIAGEN) for the complete genomes, nsp2-coding sequences, and ORF5 sequences of the representative PRRSV strains and GS2022 strain. Based on the aligned sequences, three phylogenetic trees were constructed, respectively, by MEGA-X using the Maximum Likelihood method and the Tamura-Nei model (24).

2.6 Recombinant analysis

Recombination events between PRRSV strains were detected by the Simplot software v.3.5.1 and the boot scanning analysis was performed with a window size of 400 bp and a step size of 50 bp. Furthermore, seven different algorithms (RDP, GENECONV, Bootscan, MaxChi, Chimera, SiScan, and Phylpro) included in RDP 4.0 software (25) were used to identify the potential recombination events and breakpoints in the GS2022 genome.

TABLE 1 A list of primers for full-length genome sequencing and reverse genetics construction.

Name	Sequence (5'-3')	Usage
PRRSV-seq-F1	ATGACGTATAGGTGTTGG	RT-PCR amplify four overlapping genomic fragments of PRRSV
PRRSV-seq-R1	AGAAGCTCAAAAGAATGAAG	
PRRSV-seq-F2	GGTGATTGGGGYTTTGC	
PRRSV-seq-R2	TAAGGTATGTCYCCAAACCT	
PRRSV-seq-F3	ACTAAAGAGGAAGTYGCAC	
PRRSV-seq-R3	TCATTGTAATCCTCCCATC	
PRRSV-seq-F4	AAGGAATCAGTYGCGGT	
PRRSV-seq-R4	TTTTTTTTTTTAATTACGGCCG	
GS-vec-F	GGCCGGCATGGTCCCAGCCT	PCR amplify vector
GS-vec-R	CTATTTAAATAGCTCTGCTTATATAGACCTCC	
GS-F1-F	GTCTATATAAGCAGAGCTATTTAAATATAGCATGACGTATAGGTGTTGGC	PCR amplify three overlapping genomic fragments of the GS2022
GS-F1-R	CAACCAGGTGAGTGGTTCC	
GS-F2-F	GTTTGGGAACCACTCACC	
GS-F2-R	GACCATAGACATAAGTTGTCTCTG	
GS-F3-F	ATAAGCAGAGCTATTTAAATAGACAAACTTATGTCTATGGTCAAC	
GS-F3-R	GGAGGCTGGGACATGCCGGCCTTTTTTTTTTTTTTTTTTTTAATTACGGCC	
GS-dnoti-F	ACGGGGAGGTCGCTGGTACCC	Inactivate the <i>NotI</i> site in the nsp1 α region
GS-dnoti-R	GGGTACCAGCGACCTCCCCGTTCTGTAA	

2.7 Construction of a full-length cDNA clone of the GS2022 strain

The passage 2 virus stock of GS2022 collected at 36 h post-infection (hpi) from infected PAMs was used for the construction of a full-length cDNA clone. Two rounds of homologous recombination were conducted to assemble this cDNA clone as described previously (22) with minor modifications. Viral RNA was extracted with a TIANamp Virus RNA kit (TIANGEN, Beijing, China) per the manufacturer's instructions. Viral RNA was used as a template to synthesize cDNA using a HiScript III 1st Strand cDNA Synthesis Kit (Vazyme Biotech, Nanjing, China) using primers GS-F3-R and GS-F2-R, respectively. Three fragments (F1~F3) covering the complete genome of GS2022 were PCR amplified using the Phanta Max Super-Fidelity DNA Polymerase (Vazyme Biotech, Nanjing, China), while the backbone vector was amplified using pCMV-TA-12 (22) as a template. To facilitate *in vitro* homologous recombination, the neighboring individual DNA fragments share around 20 nucleotide acids at both terminuses. Initially, the F3 fragment was inserted into the vector through homologous recombination using the NEBuilder HiFi DNA Assembly Master Mix (NEB, Ipswich, MA, United States), and the shuttle plasmid was designated as pCMV-GS2022-F3. Next, the remaining two fragments were assembled with the pCMV-GS2022-F3 which was linearized with the *Swa*I restriction enzyme using the NEBuilder HiFi DNA Assembly Master Mix (NEB, Ipswich, MA, United States). To distinguish the rescued virus from the wild-type (WT) virus, a genetic marker (two silent mutations of C564A and C567T) was introduced to disrupt the *Not*I restriction site within the nsp1 α -coding region. A full-length cDNA clone of GS2022 verified by DNA sequencing was designated as pCMV-GS2022-M.

2.8 Recovery of the recombinant virus

DNA transfection of BHK-21 cells was performed to rescue the recombinant PRRSV. Briefly, when the BHK-21 cell monolayer in a

12-well culture plate reached about 70~80% confluence, cells were transfected with 1 μ g of a full-length cDNA clone using Lipofectamine 3,000 transfection reagent (ThermoFisher Scientific, Waltham, MA, United States) according to the manufacturer's instructions. At 2 days post-transfection (dpt), culture supernatant was harvested to infect PAMs seeded in a 12-well culture plate 12 h ahead, and BHK-21 cells were fixed with ice-cold methanol for 20 min and stained with a mAb against N protein. PAMs were monitored daily for the appearance of cytopathic effect (CPE) under an IX73 epifluorescence microscope (Olympus). Around 3 days post-infection (dpi), the culture supernatant was harvested as passage 1 (P1) virus and stored at -80°C , and then further passaged in PAMs.

2.9 Viral growth kinetics

The growth kinetics of the recombinant GS2022 (rGS2022) in PAMs were characterized by viral growth curves using the P3 virus. Briefly, PAMs seeded in a 24-well tissue culture plate were inoculated with GS2022 and rGS2022 at a multiplicity of infection (MOI) of 0.01, respectively. At 2 hpi, the viral inoculums were changed with fresh infection medium, MEM supplemented with 2% FBS (Sigma-Aldrich, St. Louis, MO, United States) and 2% pen-streptomycin. At the indicated time points post-infection (0, 12, 24, 36, 48 hpi), culture supernatants were harvested for viral titration and viral titers were calculated as TCID₅₀/mL. For each time point, two replicates were included. Viral growth curves were plotted with viral titers using GraphPad Prism 9.

2.10 Animal study

All animal experiments received approval from the Institutional Animal Care and Use Committee of the Jiangsu Key Laboratory for High-Tech Research and Development of

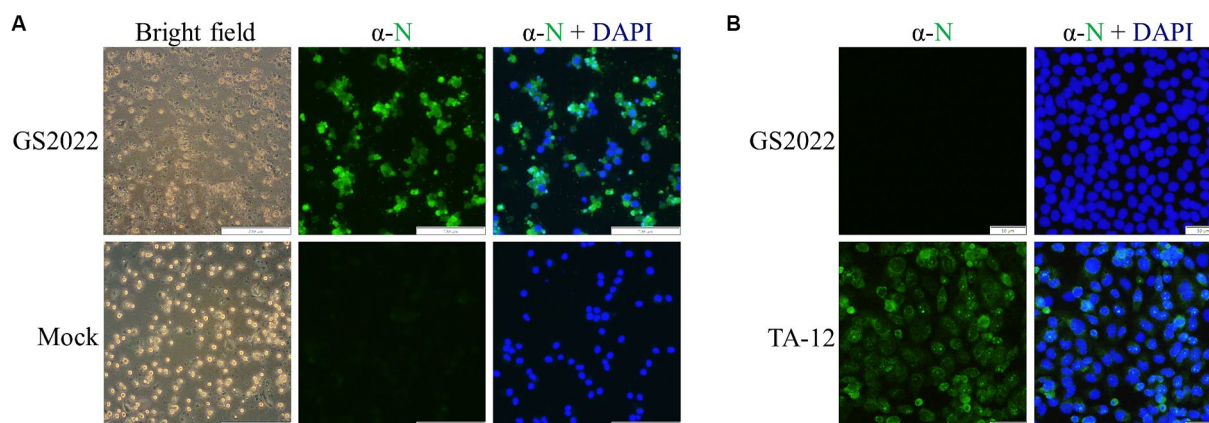


FIGURE 1

Virus isolation of GS2022 from a lung sample of a fatal piglet. (A) The GS2022 strain was isolated using PAMs. CPE caused by the inoculation of the lung suspension was observed at ~48 hpi. The expression of PRRSV N protein was further detected by IFA. The scale bars for bright field and fluorescent pictures are 200 μ m and 100 μ m. (B) The GS2022 virus cannot establish infection in Marc-145 cells. MARC-145 was inoculated with the isolated GS2022 and HP-PRRSV TA-12 strain, respectively. At 48 hpi, IFA detection of N protein was conducted to monitor viral replication. The scale bar is 50 μ m.

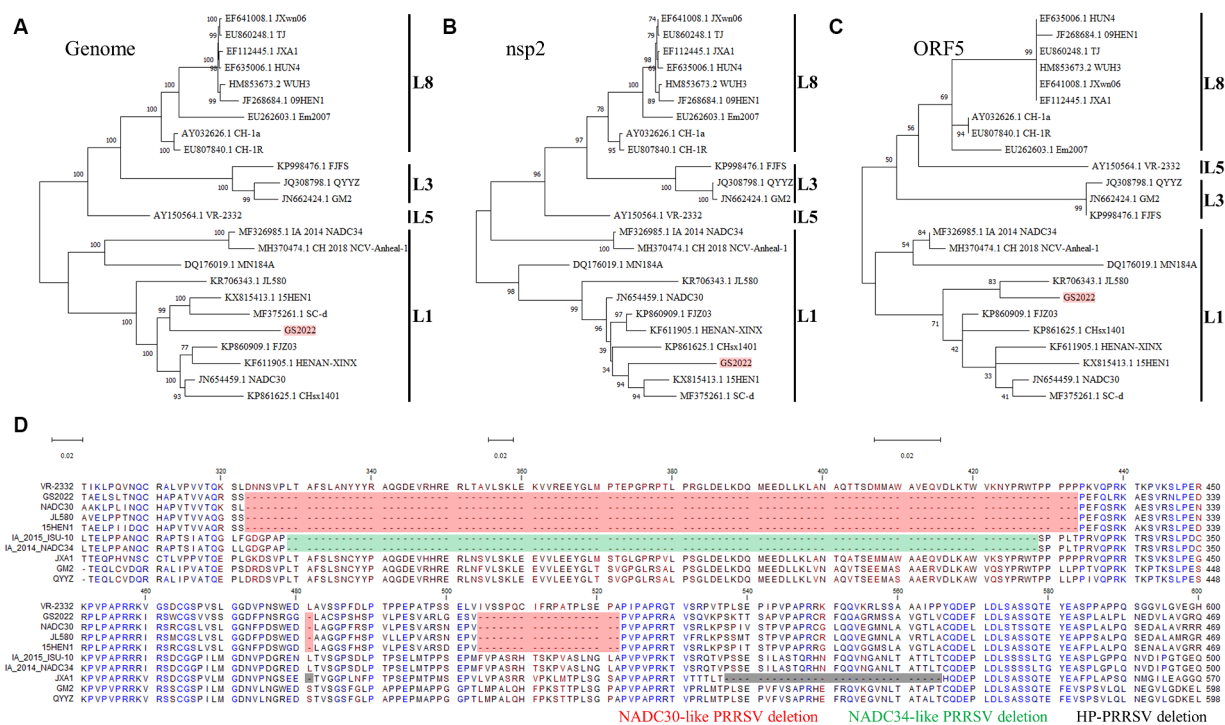


FIGURE 2

Complete genomic sequence analysis of the GS2022 strain. (A–C) Phylogenetic trees based on the complete genome, nsp2-coding region, and ORF5. A total of 24 complete genomes of the representative strains in lineages 1, 3, 5, and 8 were downloaded from the GenBank database for phylogenetic analysis. Sequence alignment was performed with CLC Genomic Workbench 20 (QiaGen). Based on the aligned sequences, phylogenetic trees were constructed, respectively, by MEGA-X using the Maximum Likelihood method and the Tamura-Nei model. (D) Sequence analysis of nsp2 protein. The nsp2 protein of GS2022 contains a characteristic deletion pattern of 131 discontinuous amino acids at positions 323–433, 483, and 508–526. The deletion patterns specific for the NADC30-like PRRSV strain, NADC34-like PRRSV strain, and HP-PRRSV were highlighted, respectively, with colors of red, green, and black.

Veterinary Biopharmaceuticals, Jiangsu Agri-animal Husbandry Vocational College (protocol code jsahvc-2023-32) and strictly adhered to conventional animal welfare regulations and standards. Fifteen 4-week-old healthy piglets were purchased from a pig farm that had no previous history of PRRS outbreaks or PRRSV vaccination. These pigs were free of PRRSV, PCV2, CSFV, and PRV based on the detection of antibodies against those viruses. PRRSV-free status of these pigs was also confirmed by qRT-PCR. All pigs were randomly divided into 3 groups ($n = 5$) and housed separately in an isolated environment. Piglets in group 1 and group 2 were infected with GS2022 or rGS2022 at a dose of 10^6 TCID₅₀/mL per pig via intranasal (1 mL) and intramuscular (1 mL) routes simultaneously. The piglets of group 3 received an equivalent volume of DMEM via the same routes as the placebo. Following viral infection, the piglets underwent daily monitoring for their rectal temperature and clinical signs that were graded using a scoring system as previously reported (26), including lethargy, anorexia, skin discoloration, sneezing, coughing, labored and abdominal breathing, and respiratory rate (Supplementary Table S1). At 0, 3, 7 and 10 dpi, their body weights and blood samples were collected for further analysis. All animals were euthanized humanely at the end of the study (10 dpi). During necropsy, tissues including lung, tonsil, and submandibular lymph nodes were checked for gross lesions and collected for viral load quantification and histopathology analysis.

2.11 Viral RNA quantification

Viremia and viral loads in tissues were quantified by reverse-transcription quantitative PCR (RT-qPCR) assay using a primer/probe set targeting the ORF6 of PRRSV-2 (23). A standard curve generated using a serially 10-fold diluted (10^8 to 10^3 copies/ μ L) plasmid containing the ORF6 was used for absolute quantification. For the tissue samples (including lung, submandibular lymph nodes, and tonsils), approximately 0.5 g of tissue was homogenized with 1 mL of DMEM. The supernatant was collected after centrifugation at $12000 \times g$ for 10 min at 4°C to remove residual tissue debris. For each supernatant or serum sample, 140 μ L was used for viral RNA extraction using the TIANamp Virus RNA kit (TIANGEN, Beijing, China), and 50 μ L viral RNA was eluted. RT-qPCR reactions were assembled with 5 μ L viral RNA and the HiScript II One Step qRT-PCR Probe Kit (Vazyme Biotech, Nanjing, China) according to the manufacturer's instructions. Viral RNA loads in serum and tissues were calculated according to the standard curve.

2.12 Serological test

A commercial ELISA kit (NECVB, Harbin, China) was used to measure antibody response to PRRSV infection using the serum samples collected at 0, 3, 7, and 10 dpi according to the manufacturer's instructions. The PRRSV-specific antibody titers were reported as

sample-to-positive (S/P) ratios. The serum samples with an S/P ratio of 0.38 or higher were considered positive.

2.13 Histopathology

The tissues collected at necropsy, including the lung, lymph nodes, and tonsils were fixed in 10% buffered neutral formalin. The hematoxylin and eosin (H&E) staining were performed for pathological examination by the Servicebio (Wuhan, China).

3 Results

3.1 The isolation and characterization of the GS2022 strain

A piglet lung with a high viral RNA load of PRRSV was selected for viral isolation using PAMs and MARC-145 cells. After filtration through a 0.22 μm syringe filter, the lung suspension was serially diluted for inoculation. Typical CPE characterized by irregular cell margins and cell destruction was observed at 48 hpi for PAMs with inoculation but not the mock (Figure 1A), while no CPE was observed for MARC-145 cells with inoculation until 5 dpi. This isolated PRRSV strain was designated

as GS2022. To confirm the success of viral isolation, IFA was further conducted to detect the expression of viral protein using a monoclonal antibody against N protein. As expected, N protein expression in PAMs overlapped with cells that exhibited CPE (Figure 1A). In addition, we confirmed that the isolated virus was not able to infect MARC-145, while the HP-PRRSV TA-12 strain as a control can replicate in MARC-145 cells indicated by N protein expression (Figure 1B). Thus, the GS2022 strain can only infect the primary macrophages.

3.2 Sequence analysis of the complete genome of the GS2022 strain

We downloaded all complete genomes of PRRSV-2 in the Genbank and made sequence alignment to find highly conserved regions within the PRRSV-2 genomes. Four pairs of primers (Table 1) anchoring these highly conserved regions were designed for RT-PCR amplification of the complete PRRSV genome. Four PCR products covering the full-length genome of GS2022 were purified for DNA sequencing using a panel of primers listed in Table 1. Two consensus complete genomes of GS2022 for isolated virus and lung suspension assembled with the SnapGene software were identical. Based on the BLAST-N search, GS2022 shares the highest sequence identity with two NADC30-like strains (NADC30, 91%; 15HEN1, 90.68%), but low

TABLE 2 Sequence identities between GS2022 and the representative PRRSV strains.

	NADC30		15HEN1		JXA1		NADC34		VR2332	
	nt	aa	nt	aa	nt	aa	nt	aa	nt	aa
Genome	91.00%		90.68%		84.44%		84.08%		84.87%	
5'UTR	89.42%		88.89%		95.77%		89.84%		90.43%	
nsp1α	89.63%	93.33%	88.52%	92.22%	89.44%	92.78%	85.37%	92.22%	88.52%	93.33%
nsp1β	89.66%	83.74%	88.51%	81.28%	79.31%	74.38%	78.16%	74.38%	80.30%	75.86%
nsp2	89.73%	86.85%	89.61%	86.01%	74.99%	69.67%	76.24%	71.80%	77.97%	72.37%
nsp3	88.26%	94.78%	94.76%	98.69%	85.88%	93.01%	85.88%	92.58%	85.44%	92.58%
nsp4	82.86%	92.16%	95.59%	97.55%	94.61%	97.06%	83.66%	92.65%	88.40%	93.14%
nsp5	88.63%	92.94%	94.12%	95.29%	92.94%	94.12%	82.16%	89.41%	87.25%	92.35%
nsp7α	93.29%	93.96%	85.01%	91.95%	84.56%	92.62%	83.67%	91.95%	87.25%	94.63%
nsp7β	92.12%	92.73%	76.97%	74.55%	78.48%	76.36%	80.00%	80.91%	83.33%	80.00%
nsp8	94.07%	95.56%	84.44%	93.33%	82.96%	91.11%	89.36%	95.56%	86.67%	91.11%
nsp9	90.60%	97.08%	88.75%	96.35%	89.73%	96.20%	86.85%	95.33%	89.00%	96.20%
nsp10	94.63%	98.19%	93.20%	97.51%	83.90%	93.65%	89.27%	97.05%	85.34%	95.24%
nsp11	91.78%	95.96%	90.88%	95.96%	87.59%	97.31%	84.60%	95.96%	87.00%	94.62%
nsp12	94.37%	96.73%	92.86%	94.12%	87.88%	94.77%	83.55%	89.54%	87.01%	92.81%
GP2a	93.39%	93.75%	93.26%	93.36%	84.44%	84.77%	85.73%	83.59%	86.64%	88.67%
GP3	90.98%	90.94%	89.15%	88.19%	81.70%	79.13%	85.10%	83.07%	83.79%	81.89%
GP4	93.30%	95.51%	90.13%	92.15%	87.50%	87.08%	91.81%	96.07%	87.34%	88.20%
GP5	93.27%	89.50%	91.54%	88.50%	84.41%	82.50%	87.89%	88.50%	84.08%	80.50%
M(6)	95.05%	95.40%	95.62%	96.55%	88.76%	94.25%	92.57%	92.53%	88.95%	93.10%
N(7)	95.12%	97.54%	93.22%	94.26%	89.10%	89.34%	93.77%	96.72%	89.70%	91.80%
3'UTR	97.35%		98.01%		90.67%		94.70%		91.39%	

Bold value means the highest sequence identities to the corresponding genomic regions of the GS2022 strain.

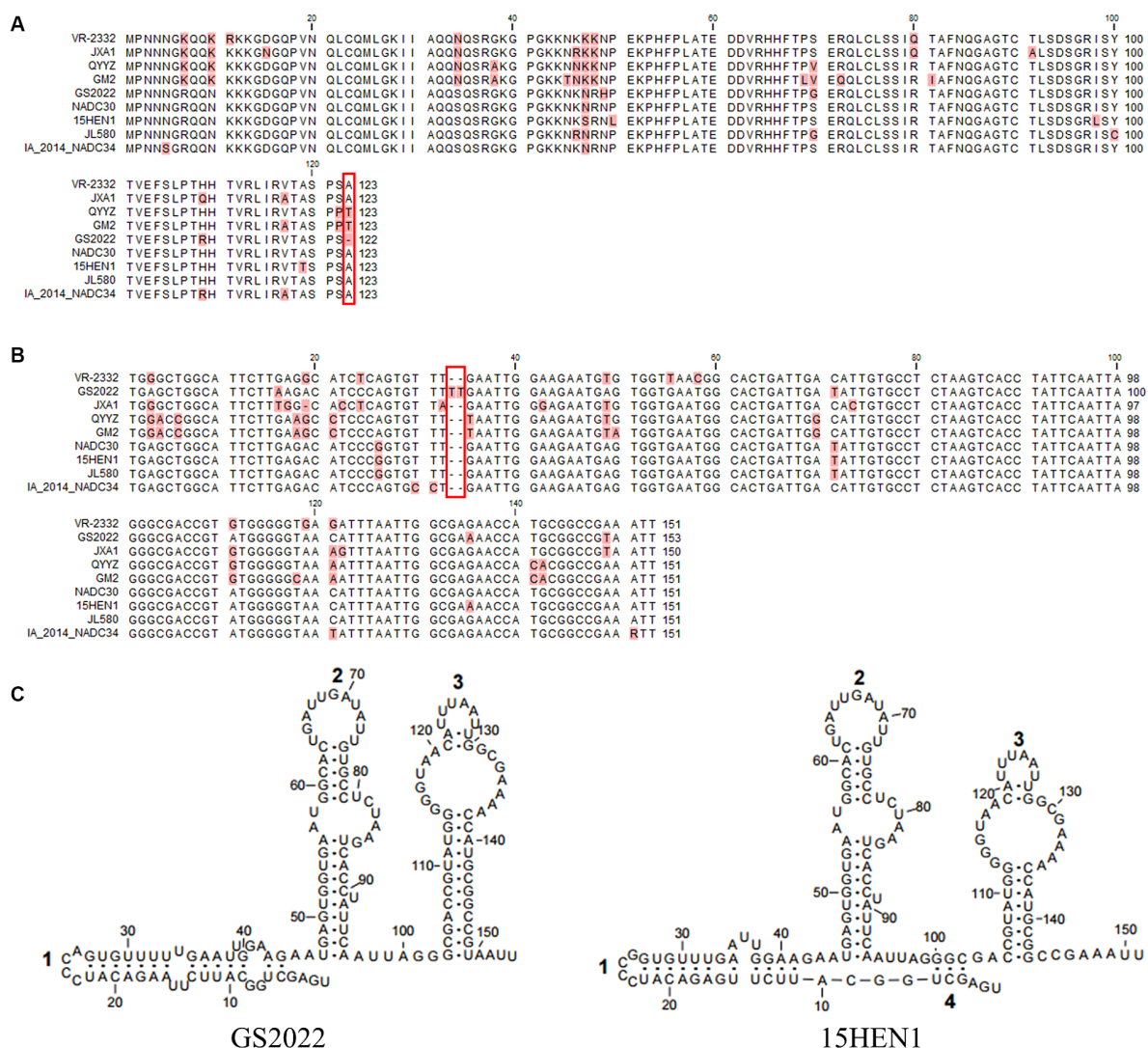


FIGURE 3

The unique deletion or insertion in ORF7 and 3'UTR of the GS2022 strain. (A) The N protein of GS2022 contains a deletion of the 123rd amino acid. The deletion was highlighted with a rectangle in red. (B) Two uridines-insertion in 3'UTR of the GS2022 strain. In the sequence alignment of 3'UTR, two uridines inserted between the 33rd and 34th positions of GS2022 3'UTR were highlighted with a rectangle in red. (C) The predicted RNA structures of 3'UTR. The RNA structures were predicted with the Mfold web server (27) and modified with Rnaviz 2.0.3 (28).

sequence identities with the other prevalent strains in China, such as JXA1 strain (84.44%), NADC34 strain (84.08%), and VR-2332 strain (84.87%). To determine the genetic evolutionary relationship between the GS2022 strain and other representative PRRSV isolates, phylogenetic trees based on the complete PRRSV genome, nsp2-coding region, and ORF5 were constructed with 24 representative PRRSV strains that belong to the lineages of 1, 3, 5, and 8. As illustrated in Figures 2A–C, the GS2022 strain is consistently claded with the NADC30-like PRRSV strains in lineage 1. As expected, GS2022 nsp2 protein contains a characteristic deletion pattern of 131 amino acids (111+1+19) which is shared by the NADC30-like PRRSV strains (Figure 2D). Thus, the GS2022 strain is a NADC30-like PRRSV, although it shares quite low sequence identities with the other NADC30-like strains.

Next, the untranslated regions and individual coding regions of the GS2022 genome were further compared with the corresponding regions of the representative PRRSV-2 strains, respectively. As shown in Table 2, the regions of nsp1~nsp2 and nsp7α~3'UTR share the

highest sequence identity with NADC30 strain at the levels of nucleotide and amino acid, the nsp3~nsp5 is more similar to the corresponding region of the 15HEN1 strain, and the 5'UTR is more similar to that of the JXA1 strain. These results suggested that the GS2022 strain might be a recombinant virus via genomic exchange between NADC30-like PRRSV and JXA1-like PRRSV.

Besides the deletion in nsp2, a deletion of the 123rd residue of N protein was found in the GS2022 strain (Figure 3A). Through a BLAST search in the GenBank, this deletion has not been observed in any PRRSV strains reported before. Two uridines were inserted between the 33rd and 34th nucleotides in the 3'UTR of the GS2022 genome (Figure 3B). Since the secondary structure of 3'UTR may play an important role in PRRSV replication, we further compared the predicted secondary structures of the 3'UTR of the GS2022 strain and the 15HEN1 strain. Based on the prediction by Mfold (Figure 3C), the structure of GS2022 3'UTR is very similar to that of 15HEN1 3'UTR, although the stem of stem-loop 1 in GS2022 is longer than that of 15HEN1.

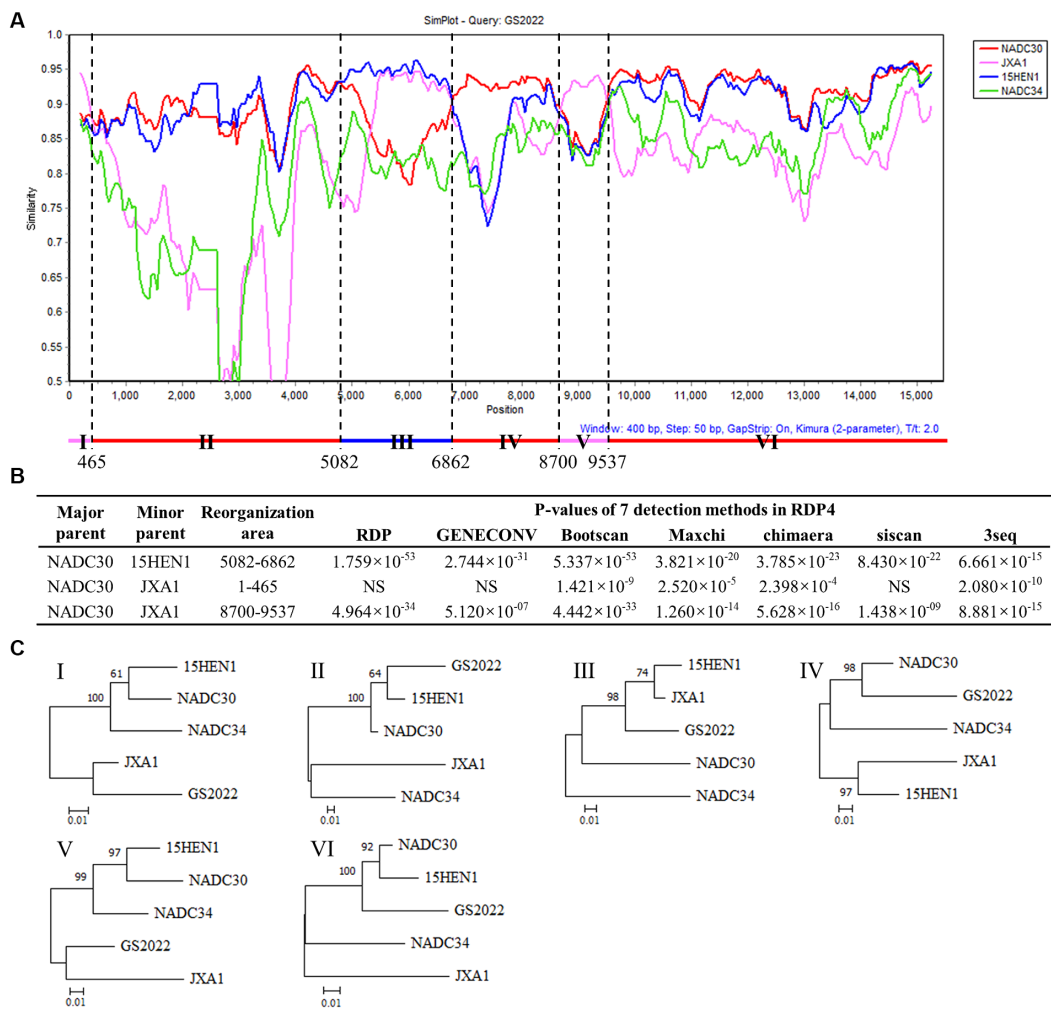


FIGURE 4 Recombination analysis of the GS2022 strain. **(A)** Recombination analysis of GS2022 was performed with Simplot v.3.5.1 software. Based on the sequence identities listed in Table 2, four representative PRRSV-2 strains were selected as the potential parental viruses for analysis, including NADC30 (JN654459), JXA1 (EF112445), 15HEN1 (KX815413.1), and NADC34 (MF326985.1). The parameters of the sliding window and step size were set as 400 bp and 50 bp, respectively. The Y-axis showed the similarity between the GS2022 and the individual representative strain. **(B)** Three recombination events of the GS2022 genome were predicted with 7 detection methods in RDP4.0. **(C)** Phylogenetic trees were constructed based on six genomic fragments divided by the predicted breakpoints.

3.3 GS2022 is a recombinant virus generated by inter-lineage and intra-lineage recombinations

Since the low sequence identities shared by GS2022 with the other strains in lineage 1, we speculated that GS2022 is a recombinant virus with its genomic fragments derived from multiple parental strains. Based on the sequence identities listed in Table 2, we selected four representative strains as potential parental viruses to predict recombination events of the GS2022 genome using the SimPlot software and RDP4.0. As shown in Figure 4A, the GS2022 genome is divided into six fragments by five breakpoints at nucleotide positions 465 in nsp1 α , 5,082 in nsp3, 6,862 nsp7 β , 8,700 nsp9, and 9,537 nsp10, which was predicted by at least 4 of 7 algorithms in RDP4.0 (Figure 4B). Based on this prediction, the GS2022 strain was generated by three crossovers among the parental viruses, NADC30 served as the major parental virus, and 15HEN1 and JXA1 served as the minor parental viruses. The predicted recombination events were further confirmed by phylogenetic analysis of six individual

genomic fragments (Figure 4C). Thus, sequence analysis suggested that the GS2022 strain is a recombinant strain generated through three crossovers among NADC30, 15HEN1, and JXA1 strains.

3.4 Reverse genetics of the GS2022 strain

To generate a tool to study the GS2022 strain, we constructed reverse genetics of this strain through *in vitro* homologous recombination as illustrated in Figure 5A. A full-length cDNA clone of the GS2022 was verified by DNA sequencing. As shown in Supplementary Table S2, in comparison to the wild-type virus, ten mutations were identified in this cDNA clone, including 6 silent nucleotide substitutions and 4 amino acid mutations in nsp1 β , nsp9, and N protein. The recombinant virus, rGS2022, was rescued by DNA transfection of BHK-21 cells with this cDNA clone and inoculation of PAMs. At 3 dpi, PAMs exhibited typical CPE, which was confirmed by IFA detection of N protein (Figure 5B). To rule out

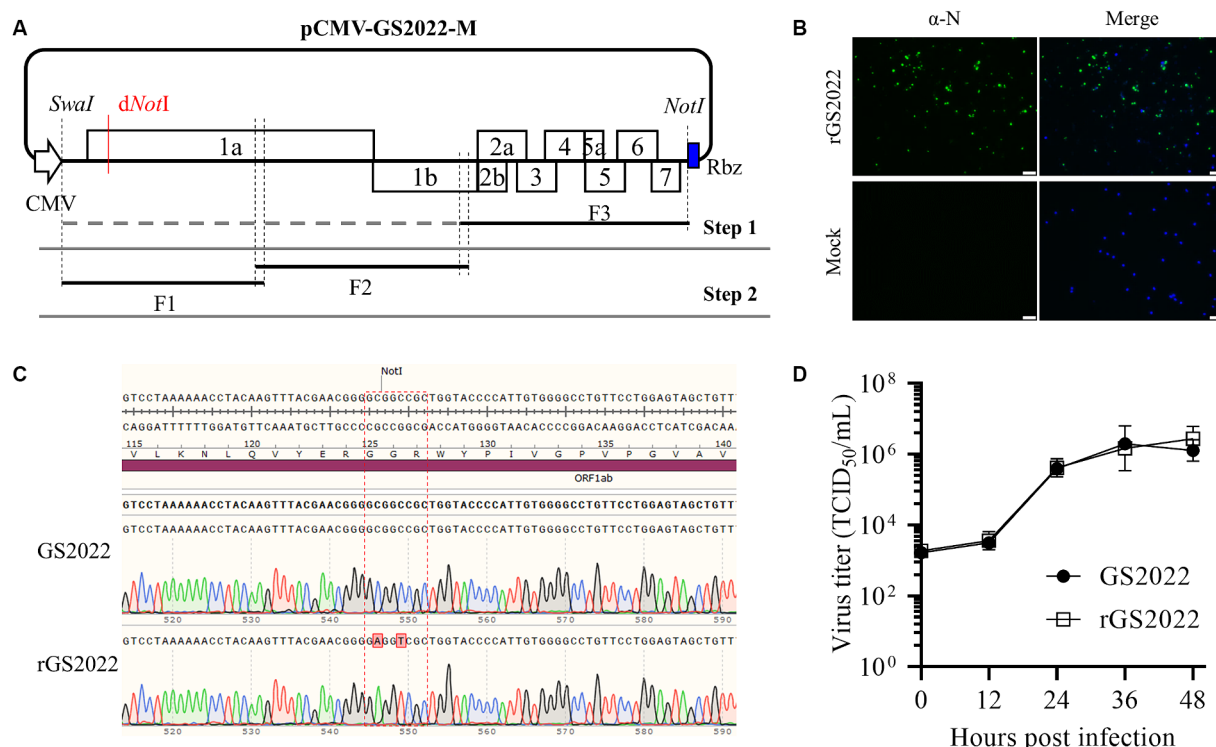


FIGURE 5

Construction of a reverse genetics of the GS2022 strain. **(A)** A schematic diagram of the construction strategy of a full-length cDNA clone. A three-step cloning strategy based on homologous recombination *in vitro* was applied to assemble a full-length cDNA clone containing a genetic marker. The complete genome of the GS2022 strain was divided into three fragments F1 ~ F3. In the first step, a human cytomegalovirus immediate-early promoter (CMV), a unique restriction enzyme site of SwaI, the F3, and a hepatitis D virus ribozyme (HDV Rbz) were inserted into the backbone vector to generate the shuttle plasmid pCMV-GS2022-F3. In the second step, the F2 and F3 were assembled with the linearized shuttle plasmid. Finally, the restriction enzyme site of NotI in the nsp1α-coding region was removed by two silent mutations. **(B)** Recovery and *in vitro* characterization of the recombinant viruses. BHK-21 cells in a 12-well plate were transfected with 1.5 μg cDNA clone plasmid per well using lipofectamine 3,000 transfection reagent according to the manufacturer's instructions. At 48 hpt, culture supernatant was harvested to inoculate PAMs. When typical CPE was observed, N protein expression was confirmed by IFA detection. The nucleus was counterstained with DAPI. The scale bar is 50 μm. **(C)** The genetic marker carried by rGS2022 was confirmed by sequencing the P0 virus. **(D)** The growth curves of GS2022 and rGS2022 in PAMs. PAMs were infected with the indicated viruses at an MOI of 0.01. At the indicated time points, culture supernatants were harvested and subjected to titration in PAMs. The data points represent the means ± standard deviation (SD).

the possibility of wild-type virus contamination, the genetic marker in nsp1α of rGS2022 was confirmed by DNA sequencing (Figure 5C). The growth kinetics of rGS2022 were characterized by a viral growth curve using the P3 virus. The virus titers of rGS2022 at all time points post-infection were almost identical to those of GS2022 (Figure 5D). Thus, the reverse genetics of the GS2022 strain established here can be a useful tool for future investigation of this virus.

3.5 Clinical symptom and pathological lesion of GS2022-inoculated and rGS2022-inoculated piglets

The nursery piglets were challenged with GS2022 or rGS2022 to study the pathogenicity of GS2022. A short period of fever was observed in both infection groups indicated by rectal temperatures at 1 dpi, and the rectal temperatures of pigs in the infection groups were consistently higher than those of the control group (Figure 6A). All pigs infected with GS2022 or rGS2022 showed typical clinical signs including fever, coughing, sneezing, depression, and shivering, while no obvious clinical signs were observed in the control group. The clinical signs were scored as listed in Supplementary Table S1. Since

inoculation, the clinical sign scores of pigs in infection groups were gradually increasing, but not in the control group (Figure 6B). The body weight gain of the rGS2022 infection group was significantly less than that of the control group (Figure 6C). All animals survived from PRRSV challenge.

In line with the results of the clinical symptoms, pigs with PRRSV infection showed different degrees of interstitial pneumonia. The lung tissues of the pigs in PRRSV infection groups exhibited moderate levels of macroscopic lesions, including pulmonary consolidation, edema, and hemorrhage (Figure 7A). Obvious microscopic lung lesions were observed in PRRSV infection groups, such as alveolar interstitial thickening and inflammatory cell infiltration (Figure 7B). Acute hemorrhage and infiltration of neutrophils were observed in submandibular lymph nodes (Figure 7C). In contrast, no pathological lesions were observed in the lung and submandibular lymph nodes of pigs in the control group (Figure 7).

3.6 Viremia and viral load in tissues

To evaluate the replication of the GS2022 strain in piglets, viremia and viral load in tissues were determined by quantitative RT-PCR. The

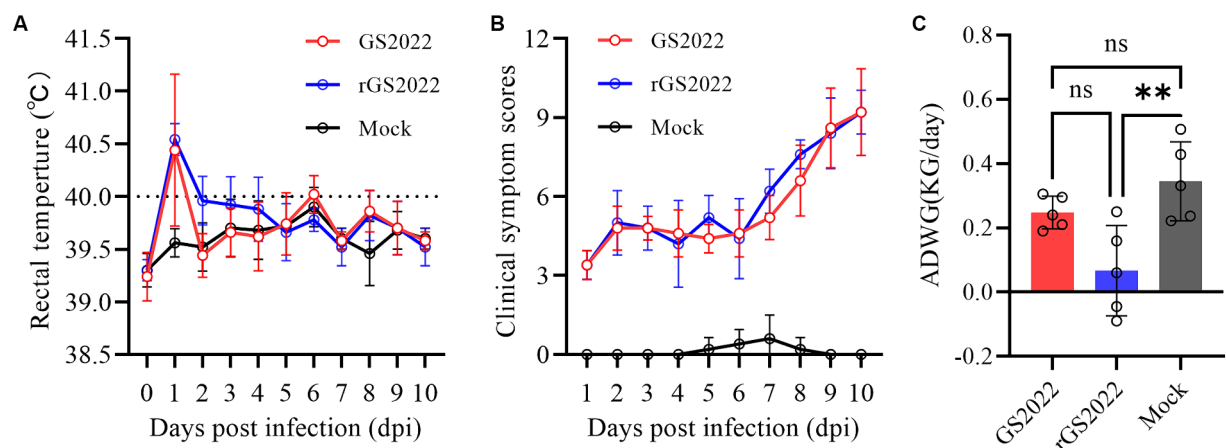


FIGURE 6
The rectal temperature, clinical sign scores, and weight gain of the piglets. **(A)** Rectal temperatures of piglets were measured daily. The clinical fever cut-off value was set at 40.0°C. **(B)** The clinical signs of each piglet were monitored daily and scored according to [Supplementary Table S1](#). **(C)** Average daily weight gain of the piglets during the experiment (ns, $p > 0.05$, **, $p < 0.01$).

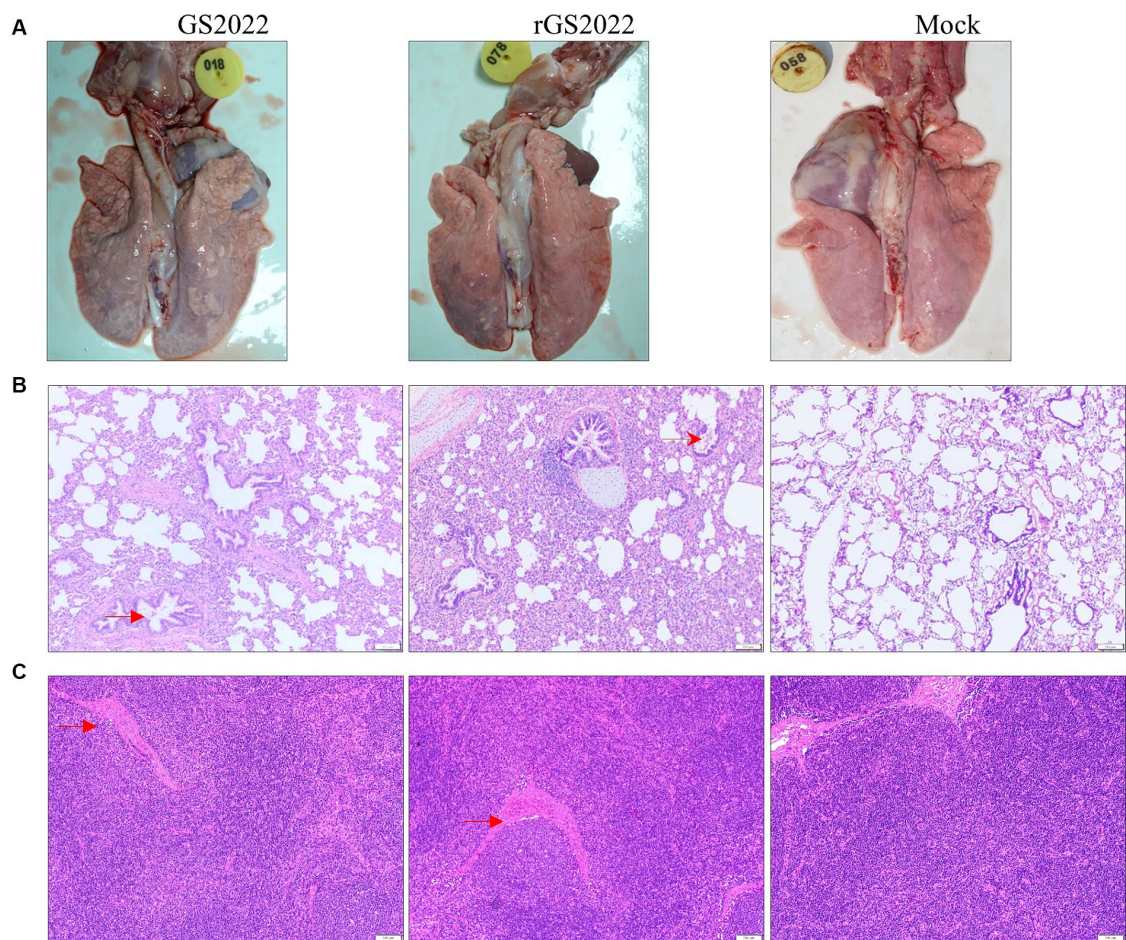


FIGURE 7
Pathological lesions in tissues. **(A)** The macroscopic lesion of the lungs. Interstitial pneumonia in the lung with thickening of alveolar septa accompanied by infiltration of immune cells hyperplasia was observed in the lungs in the PRRSV infection group. **(B)** The microscopic lesion of the lungs. H&E staining indicated the presence of interstitial pneumonia signs in the lungs of the PRRSV infection groups, such as interval thickening and inflammatory infiltration. By contrast, the alveoli of the piglets in the control group were normal. **(C)** The microscopic lesion of the submandibular lymph nodes. Vascular dilatation and infiltration of neutrophils were observed in the PRRSV infection groups. Arrows in red color were used to highlight the lesions.

viremia of the infected pigs increased sharply from 3 dpi and peaked at 7 dpi ($1 \sim 3 \times 10^7$ copies/mL) (Figure 8A), while no viremia was detected in the control group throughout the experimental period. Besides, viral RNA was also detected in the lung, tonsil, and lymph node tissues of pigs with infection at 10 dpi. Similar levels of viral RNA in lung tissues were detected in both infection groups (Figure 8B). In tonsil tissues, viral RNA was detected in 3/5 of pigs in the GS2022 infection group and 5/5 of pigs in the rGS2022 infection group, and higher levels of viral load were observed in the rGS2022 infection group (Figure 8C). Only 1/5 of pigs in both infection groups showed PRRSV replication in the submandibular lymph node at 10 dpi (Supplementary Table S3). Taken together, GS2022 and rGS2022 established infection in piglets and exhibited a wide distribution in tissues.

3.7 Humoral immune response to PRRSV infection

Antibody response to PRRSV infection was measured with a commercial ELISA kit that detected N protein-specific antibodies. In the control group, all animals remained seronegative for PRRSV-specific antibodies until the end of the experiment. In the infection groups, 4/5 pigs in the GS2022 infection group and all pigs in the rGS2022 infection group became seroconverted at 7 dpi and all pigs were seropositive at 10 dpi (Figure 8D).

4 Discussion

Since its first isolate reported in China in 1996, PRRSV has changed rapidly in China and led to a huge economic burden on the swine industry. In 2006, the highly pathogenic PRRSV (HP-PRRSV) outbreak in southern China that belongs to lineage 8 rapidly spread to the entire country and became the dominant strain (29). In 2013 and 2017, the NADC30-like and NADC34-like strains were, respectively, imported from the US to China and gradually replaced HP-PRRSV as the new dominant strains in the field (13–15). Since the lineage 1 strains are frequently involved in RNA recombination, a large number of recombinant PRRSV strains derived from NADC30-like and NADC34-like strains have been isolated in the field. Vaccination is one of the key strategies for PRRS control in China. A panel of PRRS vaccines derived from the classical PRRSV and HP-PRRSV strains used in the field could provide good protection against clinical diseases caused by homologous challenges but not heterologous challenges of emerging strains (30, 31). Currently, the diversified PRRSV strains in the field become a great concern to PRRS control in China. In this study, we collected clinical samples from farms experiencing PRRS-like disease outbreaks to monitor PRRSV strains emerging in the field. In the lung of a dead piglet, a PRRSV strain was isolated in PAMs but not in MARC-145 cells, and termed GS2022. Based on the complete genome analysis, GS2022 shares the highest sequence identity with NADC30, although their sequence identity is less than 91%. Phylogenetic analysis based

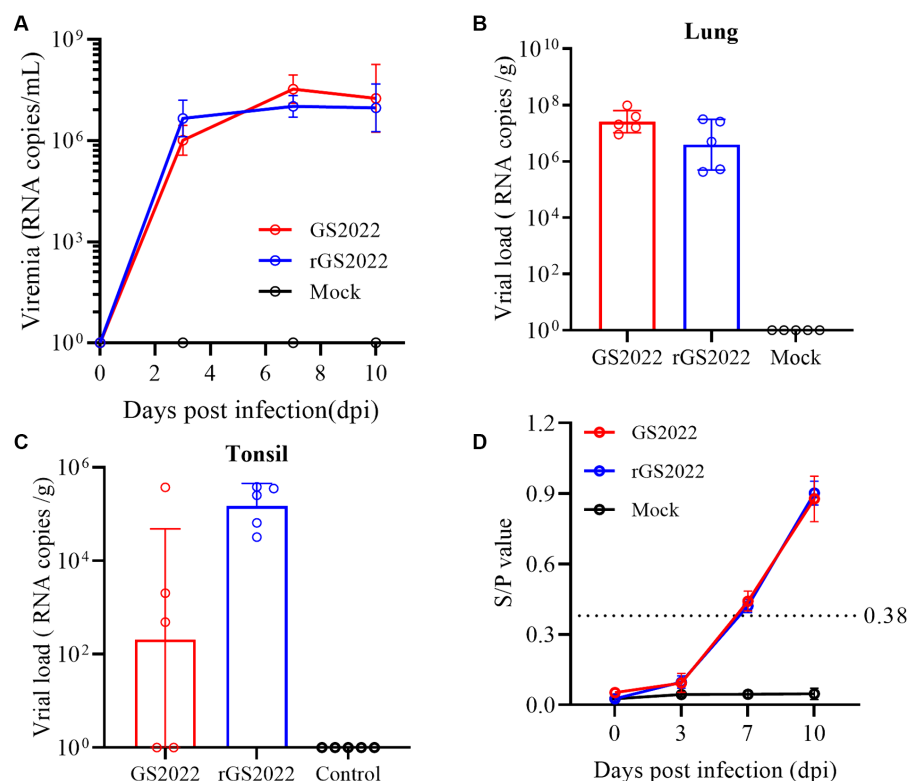


FIGURE 8

The kinetics of viremia, viral loads in tissues, and antibody responses *in vivo*. (A) The kinetics of viremia were evaluated by qRT-PCR. Viral RNA loads in serum samples collected at 0, 3, 7, and 10 dpi were quantified and calculated to viral genomic RNA copies/mL. (B) Viral loads in the lungs were determined to be viral genomic RNA copies/g. (C) Viral loads in the tonsils were determined to be viral genomic RNA copies/g. (D) PRRSV N protein-specific antibodies were measured using a commercial ELISA kit and $S/p > 0.38$ was set as the threshold of seroconversion.

on the complete genome, nsp2-coding region and ORF5 also supported that GS2022 is NADC30-like PRRSV-2 in lineage 1. A full-length cDNA clone of GS2022 was created to rescue the isogenic recombinant virus, rGS2022. The pathogenicity of GS2022 and rGS2022 to piglets was further determined.

Based on the estimated mutation rate of 10^{-3} – 10^{-2} /site/year (21, 32), PRRSV has one of the highest mutation rates in RNA viruses. The accumulated mutations may lead to a shift in the pathogenicity of the mutant. For instance, critical amino acids in nsp9 determine the fatal virulence of the Chinese HP-PRRSV for piglets (33, 34). GS2022 contains a 131-aa (111 + 1 + 19) discontinuous deletion in nsp2 which was treated as a molecular marker of the NADC30-like PRRSV strains. Besides, a novel deletion of the last amino acid of the N protein was found in GS2022. This deletion has not been found in the PRRSV strains archived in the GenBank, although the last four amino acids of the N protein in PRRSV-2 were determined to be non-essential for virus infectivity (35). 3'UTR plays an important role in PRRSV replication and its secondary structure may be critical to its function (36, 37). In the 3'UTR of GS2022, the insertion of two uridines was identified between the 33rd and 34th nucleotides. Based on the prediction of Mfold, this insertion affects the structures of stem-loop 1 and stem 4, but does not change the overall structure. In the future study, we are going to further characterize the role of these mutations (deletion or insertion) in viral replication using the reverse genetics of GS2022 established in this study.

As the primary target of PRRSV, PAMs are usually collected from the lung lavage of piglets for PRRSV infection. PAMs are very costly and difficult to manipulate. Currently, the MARC-145 cell line is the most commonly used in PRRSV research, including virus isolation, vaccine preparation and investigations of PRRSV infection mechanisms. In recent years, many PRRSV-2 strains isolated using PAMs cannot establish infection in MARC-145 cells (20, 38–40). GP2a-GP3 was identified as the major determinant of PRRSV tropism in MARC-145 cells (40). The K160 residue in GP2a is associated with PRRSV infectivity in MARC-145 cells and PAMs (38). Recently, the 98th amino acid of GP2a was found to play a key role in PRRSV adaptation to MARC-145 cells, and PRRSV strains with phenylalanine at this residue fail to infect MARC-145 cells (39). In line with their finding, GS2022 carrying phenylalanine at the 98th residue of GP2a also can infect PAMs but not MARC-145 cells (Figure 1B). We will confirm whether the 98th residue of GP2a is the only determinant of PRRSV tropism in MARC-145 cells by creating mutant viruses. Due to the non-infectivity of GS2022 in MARC-145 cells, it is almost impossible to plaque purify GS2022 for reverse genetics construction. Based on the consensus sequence of GS2022, an infectious cDNA clone was assembled. Four amino acid mutations were identified between the cDNA clone and the consensus sequence of GS2022 as listed in Supplementary Table S2. The cloned virus rGS2022 exhibited very similar growth kinetics *in vitro* and *in vivo* (Figures 5D, 8A,B). In comparison to GS2022, rGS2022 infection led to slower body weight gain and higher viral load in tonsils (Figures 6C, 8C). Since rGS2022 is one of the quasispecies of GS2022, we speculate that rGS2022 and GS2022 may have some difference in pathogenicity. However, due to the limited number of animals included in each group and no significant difference in clinical symptoms of piglets between the two infection groups, it is difficult to demonstrate pathogenicity differences between GS2022 and rGS2022 with our results.

RNA recombination greatly enhanced the adaptation of PRRSV-2 strains in lineage 1 in the field (16). In recent years, many recombinant

viruses have been isolated and characterized in China (19, 31, 41–44). Since the recombination patterns are quite random, the mechanism of PRRSV-2 strains in lineage 1 prone to RNA recombination remains unknown. Based on the low sequence identity (<91%) shared by GS2022 with other known strains, we speculated that GS2022 is a novel recombinant PRRSV. Recombination analysis suggested that GS2022 might be generated through three recombinations, including two inter-lineage recombinations between NADC30 and JXA1, and an intra-lineage recombination between NADC30 and 15HEN1. 15HEN1 is a recombinant PRRSV with NADC30 and JXA1-R (43). In the genome of GS2022, five breakpoints were predicted in nsp1 α , nsp3, nsp7 β , nsp9, and nsp10. NADC30 served as the major parental virus, while JXA1 and 15HEN1 served as the minor parental viruses. The 5' end 465 nucleotides and the genomic region encoding nsp9 C-terminus (511 ~ 685) and nsp10 N-terminus (1 ~ 104 aa) may come from HP-PRRSV JXA1. Nsp9 and nsp10 were demonstrated to be key factors associated with the high pathogenicity of HP-PRRSV and the key residues in nsp9 have been identified (26, 33, 34). Previously, several recombinant viruses derived from NADC30 PRRSV exhibited enhanced pathogenicity in piglets or sows (41, 42, 45). The farm where the GS2022 strain was isolated has experienced a PRRS outbreak, and more than 60 pigs died from respiratory diseases. Therefore, in comparison to NADC30, GS2022 may have increased pathogenicity in piglets. Not as expected, inoculation of GS2022 and rGS2022 caused mild diseases and pathological lesions in piglets, and all animals survived the challenge. However, the limitation of this study is that the animal challenge only lasted for 10 days because of the shortage of animal facilities. Since the clinical scores were still increasing at the end of the animal study (Figure 6C), more serious clinical symptoms and death may observed if the animals have been raised for a longer time. In the future study, a panel of recombinant viruses will be generated with reverse genetics to further characterize the effect of the predicted RNA recombination on the replication and pathogenicity of GS2022.

5 Conclusion

In conclusion, we isolated a novel recombinant NADC30-like PRRSV in a farm experiencing a PRRS outbreak, termed GS2022. Unique deletion and insertion were identified in the GS2022 genome. An infectious cDNA clone of GS2022 was established for future investigations. Both GS2022 and rGS2022 have caused clinical symptoms and pathological lesions in piglets but no death, suggesting that GS2022 has a moderate pathogenicity in piglets.

Data availability statement

The datasets presented in this study can be found in online repositories. The names of the repository/repositories and accession number(s) can be found at: <https://www.ncbi.nlm.nih.gov/genbank/>, PP235415.1.

Ethics statement

The animal study was approved by the Institutional Animal Care and Use Committee of the Jiangsu Key Laboratory for

High-Tech Research and Development of Veterinary Biopharmaceuticals, Jiangsu Agri-animal Husbandry Vocational College. The study was conducted in accordance with the local legislation and institutional requirements.

Author contributions

JG: Formal analysis, Investigation, Methodology, Writing – original draft, Writing – review & editing. CL: Investigation, Validation, Writing – review & editing. HL: Formal analysis, Investigation, Methodology, Writing – review & editing. BW: Formal analysis, Investigation, Writing – review & editing. LZ: Formal analysis, Investigation, Writing – review & editing. JD: Investigation, Validation, Writing – review & editing. XJ: Investigation, Writing – review & editing. QL: Investigation, Writing – review & editing. SZ: Funding acquisition, Resources, Supervision, Writing – review & editing. AW: Project administration, Supervision, Writing – review & editing, Investigation. YL: Conceptualization, Formal analysis, Funding acquisition, Investigation, Methodology, Project administration, Resources, Software, Supervision, Validation, Visualization, Writing – original draft, Writing – review & editing, Data curation.

Funding

The author(s) declare financial support was received for the research, authorship, and/or publication of this article. This research was funded by the National Natural Science Foundation of China, grant number 32072833; the Innovation and Entrepreneurship Team of Jiangsu Province, grant number JSSCTD202224; the 111 Project D18007, and a project funded by

the Priority Academic Program Development of Jiangsu Higher Education Institutions (PAPD).

Acknowledgments

We would like to acknowledge Mr. Qingkang Zhou and Miss Nannan Tang from the Jiangsu Key Laboratory for High-Tech Research and Development of Veterinary Biopharmaceuticals for providing technical support during the animal study.

Conflict of interest

The authors declare that the research was conducted in the absence of any commercial or financial relationships that could be construed as a potential conflict of interest.

Publisher's note

All claims expressed in this article are solely those of the authors and do not necessarily represent those of their affiliated organizations, or those of the publisher, the editors and the reviewers. Any product that may be evaluated in this article, or claim that may be made by its manufacturer, is not guaranteed or endorsed by the publisher.

Supplementary material

The Supplementary material for this article can be found online at: <https://www.frontiersin.org/articles/10.3389/fvets.2024.1434539/full#supplementary-material>

References

- Brinton MA, Gulyaeva AA, Balasuriya UBR, Dunowska M, Faaborg KS, Goldberg T, et al. ICTV virus taxonomy profile: Arteriviridae 2021. *J Gen Virol.* (2021) 102:001632. doi: 10.1099/jgv.0.001632
- Benfield DA, Nelson E, Collins JE, Harris L, Goyal SM, Robison D, et al. Characterization of swine infertility and respiratory syndrome (SIRS) virus (isolate ATCC VR-2332). *J Vet Diagn Invest.* (1992) 4:127–33. doi: 10.1177/104063879200400202
- Wensvoort G, Terpstra C, Pol JM, ter Laak EA, Bloemraad M, de Kluyver EP, et al. Mystery swine disease in the Netherlands: the isolation of Lelystad virus. *Vet Q.* (1991) 13:121–30. doi: 10.1080/01652176.1991.9694296
- Li YH, Tas A, Sun Z, Snijder EJ, Fang Y. Proteolytic processing of the porcine reproductive and respiratory syndrome virus replicase. *Virus Res.* (2015) 202:48–59. doi: 10.1016/j.virusres.2014.12.027
- Fang Y, Treffers EE, Li YH, Tas A, Sun Z, van der Meer Y, et al. Efficient-2 frameshifting by mammalian ribosomes to synthesize an additional arterivirus protein. *Proc Natl Acad Sci USA.* (2012) 109:E2920–8. doi: 10.1073/pnas.1211145109
- Li YH, Treffers EE, Napthine S, Tas A, Zhu LC, Sun Z, et al. Transactivation of programmed ribosomal frameshifting by a viral protein. *Proc Natl Acad Sci USA.* (2014) 111:E2172–81. doi: 10.1073/pnas.1321930111
- Fang Y, Snijder EJ. The PRRSV replicase: exploring the multifunctionality of an intriguing set of nonstructural proteins. *Virus Res.* (2010) 154:61–76. doi: 10.1016/j.virusres.2010.07.030
- Lunney JK, Fang Y, Ladinig A, Chen NH, Li YH, Rowland B, et al. Porcine reproductive and respiratory syndrome virus (PRRSV): pathogenesis and interaction with the immune system. *Annu Rev Anim Biosci.* (2016) 4:129–54. doi: 10.1146/annurev-animal-022114-111025
- Johnson CR, Griggs TF, Gnanandarajah J, Murtaugh MP. Novel structural protein in porcine reproductive and respiratory syndrome virus encoded by an alternative ORF5 present in all arteriviruses. *J Gen Virol.* (2011) 92:1107–16. doi: 10.1099/vir.0.030213-0
- Yu F, Yan Y, Shi M, Liu HZ, Zhang HL, Yang YB, et al. Phylogenetics, genomic recombination, and NSP2 polymorphic patterns of porcine reproductive and respiratory syndrome virus in China and the United States in 2014–2018. *J Virol.* (2020) 94:e01813–19. doi: 10.1128/JVI.01813-19
- Shi M, Lam TT, Hon CC, Murtaugh MP, Davies PR, Hui RK, et al. Phylogeny-based evolutionary, demographical, and geographical dissection of north American type 2 porcine reproductive and respiratory syndrome viruses. *J Virol.* (2010) 84:8700–11. doi: 10.1128/JVI.02551-09
- Li C, Zhuang J, Wang J, Han L, Sun Z, Xiao Y, et al. Outbreak investigation of NADC30-like PRRSV in south-East China. *Transbound Emerg Dis.* (2016) 63:474–9. doi: 10.1111/tbed.12530
- Zhao K, Ye C, Chang XB, Jiang CG, Wang SJ, Cai XH, et al. Importation and recombination are responsible for the latest emergence of highly pathogenic porcine reproductive and respiratory syndrome virus in China. *J Virol.* (2015) 89:10712–6. doi: 10.1128/JVI.01446-15
- Zhou L, Wang Z, Ding Y, Ge X, Guo X, Yang H. NADC30-like strain of porcine reproductive and respiratory syndrome virus, China. *Emerg Infect Dis.* (2015) 21:2256–7. doi: 10.3201/eid2112.150360
- Zhang HL, Zhang WL, Xiang LR, Leng CL, Tian ZJ, Tang YD, et al. Emergence of novel porcine reproductive and respiratory syndrome viruses (ORF5 RFLP 1-7-4 viruses) in China. *Vet Microbiol.* (2018) 222:105–8. doi: 10.1016/j.vetmic.2018.06.017
- Wu Z, Chang T, Wang D, Zhang H, Liu H, Huang X, et al. Genomic surveillance and evolutionary dynamics of type 2 porcine reproductive and respiratory syndrome virus in China spanning the African swine fever outbreak. *Virus Evol.* (2024) 10:veae016. doi: 10.1093/ve/veae016

17. Chen P, Tan X, Lao M, Wu X, Zhao X, Zhou S, et al. The novel PRRSV strain HBap4-2018 with a unique recombinant pattern is highly pathogenic to piglets. *Viral Sin.* (2021) 36:1611–25. doi: 10.1007/s12250-021-00453-0
18. Song S, Xu H, Zhao J, Leng C, Xiang L, Li C, et al. Pathogenicity of NADC34-like PRRSV HLJDZD32-1901 isolated in China. *Vet Microbiol.* (2020) 246:108727. doi: 10.1016/j.vetmic.2020.108727
19. Sun YF, Liu Y, Yang J, Li WZ, Yu XX, Wang SY, et al. Recombination between NADC34-like and QYYZ-like strain of porcine reproductive and respiratory syndrome virus with high pathogenicity for piglets in China. *Transbound Emerg Dis.* (2022) 69:e3202–7. doi: 10.1111/tbed.14471
20. Yuan L, Zhu Z, Fan J, Liu P, Li Y, Li Q, et al. High pathogenicity of a Chinese NADC34-like PRRSV on pigs. *Microbiol Spectr.* (2022) 10:e0154122. doi: 10.1128/spectrum.01541-22
21. Hanada K, Suzuki Y, Nakane T, Hirose O, Gojobori T. The origin and evolution of porcine reproductive and respiratory syndrome viruses. *Mol Biol Evol.* (2005) 22:1024–31. doi: 10.1093/molbev/msi089
22. Li Y, Ren C, Li C, Xiao Y, Zhou Y. A recombinant porcine reproductive and respiratory syndrome virus stably expressing a Gaussia luciferase for antiviral drug screening assay and luciferase-based neutralization assay. *Front Microbiol.* (2022) 13:907281. doi: 10.3389/fmicb.2022.907281
23. Hu J, Li C, Zhou Y, Ding J, Li X, Li Y. Allicin inhibits porcine reproductive and respiratory syndrome virus infection in vitro and alleviates inflammatory responses. *Viruses.* (2023) 15:1050. doi: 10.3390/v15051050
24. Kumar S, Stecher G, Li M, Knyaz C, Tamura K. MEGA X: molecular evolutionary genetics analysis across computing platforms. *Mol Biol Evol.* (2018) 35:1547–9. doi: 10.1093/molbev/msy096
25. Martin DP, Murrell B, Golden M, Khoosal A, Muhire B. RDP4: detection and analysis of recombination patterns in virus genomes. *Virus Evol.* (2015) 1:vev003. doi: 10.1093/ve/vev003
26. Li Y, Zhou L, Zhang J, Ge X, Zhou R, Zheng H, et al. Nsp9 and Nsp10 contribute to the fatal virulence of highly pathogenic porcine reproductive and respiratory syndrome virus emerging in China. *PLoS Pathog.* (2014) 10:e1004216. doi: 10.1371/journal.ppat.1004216
27. Zuker M. Mfold web server for nucleic acid folding and hybridization prediction. *Nucleic Acids Res.* (2003) 31:3406–15. doi: 10.1093/nar/gkg595
28. De Rijk P, Wuyts J, De Wachter R. RnaViz 2: an improved representation of RNA secondary structure. *Bioinformatics.* (2003) 19:299–300. doi: 10.1093/bioinformatics/19.2.299
29. Tian K, Yu X, Zhao T, Feng Y, Cao Z, Wang C, et al. Emergence of fatal PRRSV variants: unparalleled outbreaks of atypical PRRS in China and molecular dissection of the unique hallmark. *PLoS One.* (2007) 2:e526. doi: 10.1371/journal.pone.0000526
30. Chai W, Liu Z, Sun Z, Su L, Zhang C, Huang L. Efficacy of two porcine reproductive and respiratory syndrome (PRRS) modified-live virus (MLV) vaccines against heterologous NADC30-like PRRS virus challenge. *Vet Microbiol.* (2020) 248:108805. doi: 10.1016/j.vetmic.2020.108805
31. Chen XX, Zhou X, Guo T, Qiao S, Guo Z, Li R, et al. Efficacy of a live attenuated highly pathogenic PRRSV vaccine against a NADC30-like strain challenge: implications for ADE of PRRSV. *BMC Vet Res.* (2021) 17:260. doi: 10.1186/s12917-021-02957-z
32. Guo J, Liu Z, Tong X, Wang Z, Xu S, Chen Q, et al. Evolutionary dynamics of type 2 porcine reproductive and respiratory syndrome virus by whole-genome analysis. *Viruses.* (2021) 13:2469. doi: 10.3390/v13122469
33. Xu L, Zhou L, Sun W, Zhang P, Ge X, Guo X, et al. Nonstructural protein 9 residues 586 and 592 are critical sites in determining the replication efficiency and fatal virulence of the Chinese highly pathogenic porcine reproductive and respiratory syndrome virus. *Virology.* (2018) 517:135–47. doi: 10.1016/j.virol.2018.01.018
34. Zhao K, Gao JC, Xiong JY, Guo JC, Yang YB, Jiang CG, et al. Two residues in NSP9 contribute to the enhanced replication and pathogenicity of highly pathogenic porcine reproductive and respiratory syndrome virus. *J Virol.* (2018) 92:e02209-17. doi: 10.1128/JVI.02209-17
35. Tan F, Wei Z, Li Y, Zhang R, Zhuang J, Sun Z, et al. Identification of non-essential regions in nucleocapsid protein of porcine reproductive and respiratory syndrome virus for replication in cell culture. *Virus Res.* (2011) 158:62–71. doi: 10.1016/j.virusres.2011.03.011
36. Sun Z, Liu C, Tan F, Gao F, Liu P, Qin A, et al. Identification of dispensable nucleotide sequence in 3' untranslated region of porcine reproductive and respiratory syndrome virus. *Virus Res.* (2010) 154:38–47. doi: 10.1016/j.virusres.2010.08.027
37. Xiong J, Cui X, Zhao K, Wang Q, Huang X, Li D, et al. A novel motif in the 3'-UTR of PRRSV-2 is critical for viral multiplication and contributes to enhanced replication ability of highly pathogenic or LI PRRSV. *Viruses.* (2022) 14:166. doi: 10.3390/v14020166
38. Chaudhari J, Leme RA, Durazo-Martinez K, Sillman S, Workman AM, Vu HLX. A single amino acid substitution in porcine reproductive and respiratory syndrome virus glycoprotein 2 significantly impairs its infectivity in macrophages. *Viruses.* (2022) 14:2822. doi: 10.3390/v14122822
39. Chen Y, Huo Z, Jiang Q, Qiu Z, Shao Z, Ma C, et al. The significance of the 98th amino acid in GP2a for porcine reproductive and respiratory syndrome virus adaptation in Marc-145 cells. *Viruses.* (2024) 16:711. doi: 10.3390/v16050711
40. Zhang HL, Tang YD, Liu CX, Xiang LR, Zhang WL, Leng CL, et al. Adaptions of field PRRSVs in Marc-145 cells were determined by variations in the minor envelope proteins GP2a-GP3. *Vet Microbiol.* (2018) 222:46–54. doi: 10.1016/j.vetmic.2018.06.021
41. Chang H, Zheng J, Qiu Y, Chen C, Li Q, Wu Q, et al. Isolation, identification, and pathogenicity of a NADC30-like porcine reproductive and respiratory disorder syndrome virus strain affecting sow production. *Front Vet Sci.* (2023) 10:1207189. doi: 10.3389/fvets.2023.1207189
42. Chen N, Ye M, Li S, Huang Y, Zhou R, Yu X, et al. Emergence of a novel highly pathogenic recombinant virus from three lineages of porcine reproductive and respiratory syndrome virus 2 in China 2017. *Transbound Emerg Dis.* (2018) 65:1775–85. doi: 10.1111/tbed.12952
43. Zhao H, Han Q, Zhang L, Zhang Z, Wu Y, Shen H, et al. Emergence of mosaic recombinant strains potentially associated with vaccine JXA1-R and predominant circulating strains of porcine reproductive and respiratory syndrome virus in different provinces of China. *Virol J.* (2017) 14:67. doi: 10.1186/s12985-017-0735-3
44. Zhou L, Yu J, Zhou J, Long Y, Xiao L, Fan Y, et al. A novel NADC34-like porcine reproductive and respiratory syndrome virus 2 with complex genome recombination is highly pathogenic to piglets. *Infect Genet Evol.* (2023) 112:105436. doi: 10.1016/j.meegid.2023.105436
45. Liu JK, Zhou X, Zhai JQ, Li B, Wei CH, Dai AL, et al. Emergence of a novel highly pathogenic porcine reproductive and respiratory syndrome virus in China. *Transbound Emerg Dis.* (2017) 64:2059–74. doi: 10.1111/tbed.12617



OPEN ACCESS

EDITED BY

Lingxue Yu,
Chinese Academy of Agricultural
Sciences, China

REVIEWED BY

Zhang Teng,
Nanyang Normal University, China
Peter Oba,
International Livestock Research
Institute, Uganda

*CORRESPONDENCE

Tanja Opriessnig
✉ tanjaopr@iastate.edu;
✉ tanja.opriessnig@moredun.ac.uk

RECEIVED 23 April 2024

ACCEPTED 17 June 2024

PUBLISHED 19 July 2024


CITATION

Opriessnig T, Halbur P, Bayne J, Rawal G,
Tong H, Mou K, Li G, Zhang D, Zhang J and
Muwonge A (2024) Exploratory application of
a cannulation model in recently weaned pigs to
monitor longitudinal changes in the enteric
microbiome across varied porcine
reproductive and respiratory syndrome virus
(PRRSV) infection statuses.
Front. Vet. Sci. 11:1422012.
doi: 10.3389/fvets.2024.1422012

COPYRIGHT

© 2024 Opriessnig, Halbur, Bayne, Rawal,
Tong, Mou, Li, Zhang, Zhang and Muwonge.
This is an open-access article distributed
under the terms of the [Creative Commons
Attribution License \(CC BY\)](#). The use,
distribution or reproduction in other forums is
permitted, provided the original author(s) and
the copyright owner(s) are credited and that
the original publication in this journal is cited,
in accordance with accepted academic
practice. No use, distribution or reproduction
is permitted which does not comply with
these terms.

Exploratory application of a cannulation model in recently weaned pigs to monitor longitudinal changes in the enteric microbiome across varied porcine reproductive and respiratory syndrome virus (PRRSV) infection statuses

Tanja Opriessnig^{1,2*}, Patrick Halbur², Jenna Bayne³,
Gaurav Rawal², Hao Tong², Kathy Mou², Ganwu Li²,
Danyang Zhang², Jianqiang Zhang² and Adrian Muwonge ⁴

¹Department of Vaccines and Diagnostics, Moredun Research Institute, Pentlands, United Kingdom,

²Department of Veterinary Diagnostic and Production Animal Medicine, College of Veterinary
Medicine, Iowa State University, Ames, IA, United States, ³Department of Clinical Sciences, College of
Veterinary Medicine, Auburn University, Auburn, AL, United States, ⁴The Digital One Health Laboratory,
Roslin Institute and The Royal (Dick) School of Veterinary Studies, University of Edinburgh, Midlothian,
United Kingdom

Introduction: The enteric microbiome and its possible modulation to improve feed conversion or vaccine efficacy is gaining more attention in pigs. Weaning pigs from their dam, along with many routine procedures, is stressful. A better understanding of the impact of this process on the microbiome may be important for improving pig production. The objective of this study was to develop a weaner pig cannulation model, thus allowing ileum content collection from the same pig over time for 16S rRNA sequencing under different porcine reproductive and respiratory syndrome virus (PRRSV) infection statuses.

Methods: A total of 15 3-week-old pigs underwent abdominal surgery and were fitted with an ileum cannula, with ileum contents collected over time. In this pilot study, treatment groups included a NEG-CONTROL group (no vaccination, no PRRSV challenge), a POS-CONTROL group (no vaccination, challenged with PRRSV), a VAC-PRRSV group (vaccinated, challenged with PRRSV), a VAC-PRO-PRRSV group (vaccinated, supplemented with a probiotic, challenged with PRRSV), and a VAC-ANTI-PRRSV group (vaccinated, administered an antibiotic, challenged with PRRSV). We assessed the microbiome over time and measured anti-PRRSV serum antibodies, PRRSV load in serum and nasal samples, and the severity of lung lesions.

Results: Vaccination was protective against PRRSV challenge, irrespective of other treatments. All vaccinated pigs mounted an immune response to PRRSV within 1 week after vaccination. A discernible impact of treatment on the diversity, structure, and taxonomic abundance of the enteric microbiome among the groups was not observed. Instead, significant influences on the ileum microbiome were observed in relation to time and treatment.

Discussion: The cannulation model described in this pilot study has the potential to be useful in studying the impact of weaning, vaccination, disease challenge,

and antimicrobial administration on the enteric microbiome and its impact on pig health and production. Remarkably, despite the cannulation procedures, all vaccinated pigs exhibited robust immune responses and remained protected against PRRSV challenge, as evidenced by the development of anti-PRRSV serum antibodies and viral shedding data.

KEYWORDS

pigs, porcine reproductive and respiratory syndrome virus, antibiotics, probiotics, vaccination, ileum microbiome

1 Introduction

In recent years, substantial advances in understanding the gut microbiome have been facilitated by highly efficient sequencing tools (1–3). The link between the gut microbiome and health or disease is evident (4, 5). Often, parenterally administered attenuated porcine reproductive and respiratory syndrome virus (PRRSV) vaccines have less than desired efficacy under field conditions. Research in human vaccinology indicated that probiotic bacteria modulate both innate and adaptive immunity in the host (6, 7). Gut microbes have been suggested to support immune responses against viral infections by facilitating the processing and secretion of proinflammatory cytokines. In humans, probiotics are believed to have a potential influence on the response to influenza vaccination, leading to recommendations for dietary changes before the scheduled vaccinations (8, 9). Commonly, in pig production, pigs are weaned from their dam at 3–4 weeks of age and co-mingled with other litters and administered vaccines (10).

The potential benefits of gut bacteria may also be affected by the prophylactic administration of antimicrobials to pigs at the time of weaning. In addition, weaning is known to induce “dysbiosis” of the gut microbiota (11).

Currently, microbiome studies in pigs are often limited to the analysis of rectal swabs from pigs in the field with unknown disease or immune status. Previously, we studied the microbiome of pigs experimentally infected with *Lawsonia intracellularis* and treated with different types of probiotics (12). For the 16S rRNA sequencing, we used ileum samples, which required us to euthanize the pigs. The obtained results indicated significant differences in microbiome diversity across different treatment groups (12). However, the terminal study offered only a single time point glance at possible differences among treatment groups, which was associated with clinical differences among treatment groups. Identifying a way to investigate the enteric microbiome in pigs over time to assess the impact of vaccination or other treatments would be valuable.

The objectives of this pilot study were to develop a model (1) to investigate the effect of the administration of probiotics at the time of parenteral PRRSV vaccination on PRRSV vaccine efficacy (viremia, antibody response, clinical outcomes) and (2) to investigate the gut microbiome in these pigs over time using a cannulation approach followed by characterization of the bacterial population using 16S rRNA sequencing.

2 Materials and methods

2.1 Animal approval

Institutional Review Board Statement: The study was conducted according to the guidelines of the Declaration of Helsinki and approved by the Iowa State University Institutional Animal Care and Use Committee (Approval number IACUC-21-031; Date of approval: 05-April-2021) and by the Iowa State University IBC Committee (Approval number IBC 21-019; Date of approval: 6-April-2021). Environmental enrichment was provided, and independent veterinarians, not part of the research team, assessed the pigs and made decisions on welfare and euthanasia.

2.2 Pigs and housing

At 3 weeks of age, 15 conventional pigs were purchased from a specific pathogen-free herd, free of PRRSV, influenza A virus, and *Mycoplasma hyopneumoniae* based on monthly testing using serology and pooled PCR tests. The pigs were housed in the Livestock Infectious Disease Isolation Facility (LIDIF) at Iowa State University. Initially, all pigs were kept in one large room with five pens. The pens were placed directly on a concrete floor, with each pen enclosed by galvanized steel gates (~2 × 3 m). Each pen had a nipple drinker and a self-feeder. The pigs were offered an age-appropriate pelleted diet free of Antibiotics (Heartland Co-Op, Prairie City, IA, USA). Shortly before the pigs were vaccinated with a commercially modified live PRRSV vaccine strain, the two non-vaccinated groups (NEG-CONTROL and POS-CONTROL pigs) were moved to another room that contained two pens as described above. Before being challenged with the PRRSV strain, the POS-CONTROL pigs were moved to a separate room.

2.3 Experimental design

Upon arrival at the research facility, the pigs were randomly allocated to five different treatment groups (Table 1), including a NEG-CONTROL group (no vaccination, no PRRSV challenge), a POS-CONTROL group (no vaccination, challenged with PRRSV), a VAC-PRRSV group (vaccinated and challenged with PRRSV), a VAC-PRO-PRRSV group (vaccinated, supplemented with an oral probiotic every day from 19 days before vaccination

TABLE 1 Experimental design.

Group	Pig #	Treatment	Vaccination	Challenge
NEG-CONTROL	3	-	-	-
POS-CONTROL	3	-	-	PRRSV
VAC-ANTI-PRRSV	3	Antibiotic	Yes	PRRSV
VAC-PRO-PRRSV	3	Probiotic	Yes	PRRSV
VAC-PRRSV	3	-	Yes	PRRSV

until study termination, and challenged with PRRSV), and a VAC-ANTI-PRRSV group (vaccinated, administered a systemic antibiotic 3 days before vaccination, and challenged with PRRSV).

After an acclimation period, all pigs underwent surgery at 4 weeks of age (Figure 1) to place a stainless steel cannula into the terminal ileum, with a port on the outside of the abdominal wall to access the ileum contents. At 6 weeks of age, pigs in the VAC-PRRSV, VAC-ANTI-PRRSV, and VAC-PRO-PRRSV groups were vaccinated against PRRSV using a parenteral commercial modified live virus vaccine (Ingelvac® PRRS MLV, Boehringer Ingelheim, St. Joseph MO, USA). At 10 weeks of age, with the exception of pigs in the NEG-CONTROL group, pigs in all other groups were challenged with a wild-type PRRSV strain that was administered intranasally. All pigs were euthanized and necropsied 10 days later (Figure 1).

2.4 Study treatments

2.4.1 Probiotic treatment

Each pig in the VAC-PRO-PRRSV group received probiotics (1 g/pig/day) orally, starting 2 days after arrival (Supplementary Figure S1). The probiotic contained 25% *Bacillus subtilis*, 25% *Bacillus amyloliquefaciens*, and 50% *Enterococcus faecium* (CH3, batch 21CC0601, lot 707756, Chr. Hansen, A/S, Hørsholm, Denmark). To be consistent with the feeding routine, the pigs were fed every day between 12:00 and 15:00, except for the day of surgery when they were fed after recovery. Initially, the probiotic was mixed with Pedialyte (Abbott, Abbott Park, IL, USA) via oral lavage. In brief, each pig was picked up and placed in an upright sitting position, with extra care handling them post-operatively, and fed the solution. The probiotic carrier used was CaCO₃, which will not dissolve even if shaken and typically remains at the bottom of the liquid. This is not considered a problem as the spores are in the liquid phase. Pigs tolerated feeding in this position moderately well with minimal waste. However, catching the pigs for this procedure became stressful as they got older. From 3 days prior to vaccination onwards, the pigs were given cereal (Captain Crunch®) mixed with the probiotic and the Pedialyte, which was then placed on top of their normal feed. This method was less stressful on the pigs and led to less waste, as the pigs would eat the entirety of the cereal, and any waste liquid would be consumed via their regular feed. All

other groups of pigs were also given the cereal/Pedialyte mixture without probiotics.

2.4.2 Antimicrobial treatment

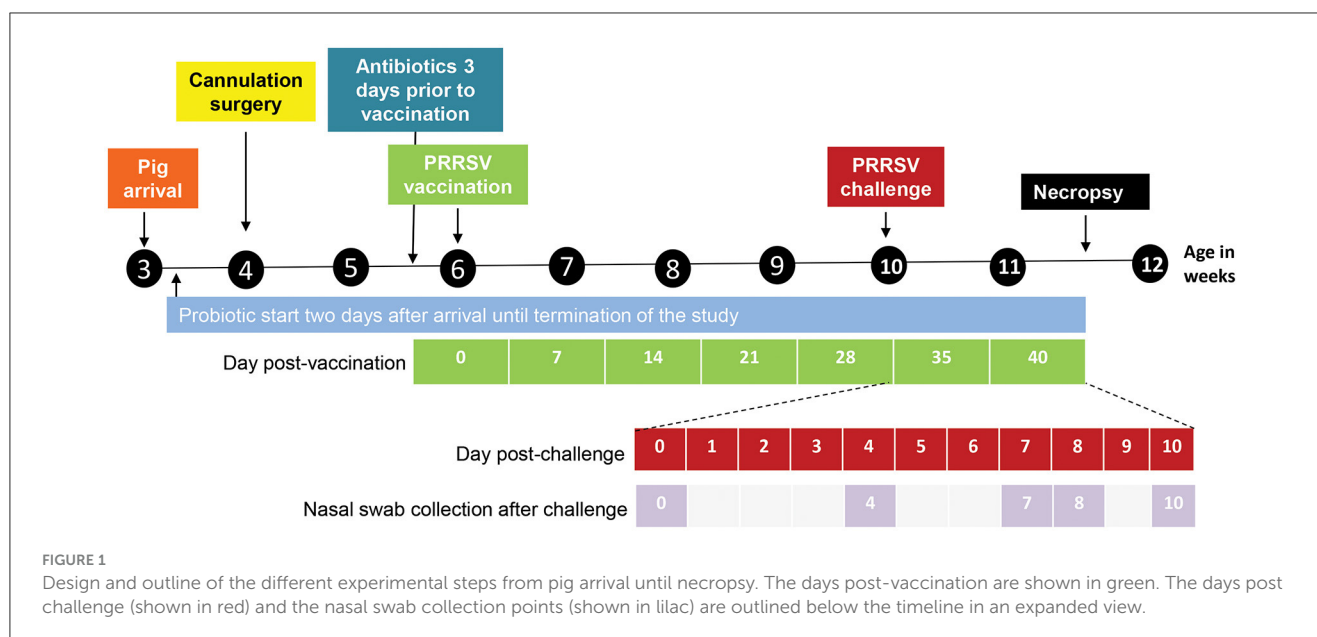
Each VAC-ANTI-PRRSV pig received Excede® for swine (Zoetis, expiration date: 12-2021; Lot ID: 408011) intramuscularly once at 3 days before vaccination according to the manufacturer's instructions (a single dose in the neck at a dosage of 2.27 mg ceftiofur equivalents/lb body weight). This ready-to-use formulation contains the crystalline-free acid of ceftiofur, which is a broad-spectrum cephalosporin antibiotic that is active against gram-positive and gram-negative bacteria including β -lactamase-producing strains, and is effective for 7 days.

2.4.3 Vaccination

When the pigs were 6 weeks old, groups VAC-PRRSV, VAC-PRO-PRRSV, and VAC-ANTI-PRRSV were vaccinated with a commercial PRRSV vaccine (Ingelvac PRRS® MLV, Boehringer Ingelheim, serial number: 2451391A, expiration date: 17-Aug-2022) according to the manufacturer's instructions. In brief, the vaccine was reconstituted immediately before the planned vaccination, and each pig received 2 ml of the vaccine via intramuscular injection into the neck area using a hypodermic needle (23 gauge \times 1/3 in.).

2.5 Clinical monitoring

Pigs were weighed on arrival at 3 weeks of age, at PRRSV vaccination at 6 weeks of age, and at necropsy at 12 weeks of age. Average daily weight gain (ADG) was calculated. After surgery, all pigs were monitored for signs of clinical disease daily. Specifically, pigs were observed for the following: fecal consistency (0 = solid; 1 = semisolid; 2 = pasty; 3 = unformed; and 4 = profuse liquid) (13); respiratory score (0 = normal; 1 = mild dyspnea and/or tachypnea when stressed; 2 = mild dyspnea and/or tachypnea when at rest; 3 = moderate dyspnea and/or tachypnea when stressed; 4 = moderate dyspnea and/or tachypnea at rest; 5 = severe dyspnea and/or tachypnea when stressed; and 6 = severe dyspnea and/or tachypnea when at rest) (14); behavior (0 = normal; 1 = depressed or listless but still standing; 3 = depressed and recumbent); and body condition score (0 = normal; 1 = mild-to-moderate gaunt; 3 = severely gaunt).



In addition, rectal temperatures were recorded on pigs if there were concerns from animal caretakers or staff. Surgical wound healing was checked daily, monitoring for heat, swelling, pain on palpation, discharge, or dehiscence as well as position and patency of cannula. Defecation, abdominal distention, vomiting, diarrhea, or other signs of abdominal distress were monitored and recorded. Cannulas initially were opened daily to confirm that digesta was flowing correctly, cannulas and wounds were periodically cleaned as needed, and wounds were treated with 1% silver sulfadiazine (SSD, Flammazine) cream (Dr. Reddy's Laboratories, LA, USA) to support healing.

2.6 Cannulation surgery of the pigs

In previous publications, duodenal cannulation surgery has been described in detail (15–17). We obtained T-shaped cannulas (Supplementary Figure S2) from a supplier (Kremer Precision, LLC, Phoenix, AZ, USA). Specifically, the cannula barrel length was 4 cm with the distal 2.5 cm threaded on the outside. The cannula barrel's inner diameter was 1.3 cm. Details of the surgical procedure are provided in Supplementary Information S3.

2.7 Surgery practice on a dead pig

Before live pig cannulation, the surgical team practiced the procedure on a dead pig to comply with the Replacement, Reduction, and Refinement (3R) principle and to avoid unnecessary suffering of pigs. Once the surgical team (under the leadership of JB, an experienced surgeon) was satisfied with the surgical procedure, they proceeded to perform surgery on live pigs. More details on the surgery methods have been previously published (15, 16, 18, 19). Images from the cannulation surgery in this study are shown in Figure 2.

2.8 Transport to the surgery facility and pre-operative procedures

On the day of surgery, the pigs were allowed to fast overnight but were provided water. The surgeries were conducted in the surgical suite of the Food Animal and Camelid Hospital of the Iowa State University College of Veterinary Medicine. The pigs were transported in dog carriers in an enclosed van from the LIDIF to the surgery suite with a travel time of ~5 min. Upon arrival, the pigs were placed under general anesthesia and positioned in left lateral recumbency. Preoperative medications included Naxcel® (ceftiofur sodium, Zoetis, Kalamazoo, MI, USA), 2.2 mg/kg, IM) and Banamine®-S (flunixin meglumine, Merck Animal Health, Madison, NJ, USA, 2.2 mg/kg, IM). The right flank, from the level of the stifle to the last intercostal space cranially and from the ventral to the transverse processes dorsally, was clipped and aseptically prepared with chlorhexidine and 70% isopropyl alcohol. The surgical site was draped in a routine aseptic manner. The surgeon surgically scrubbed their hands and arms using 4% chlorhexidine scrub, followed by Avagard™ (Chlorhexidine Gluconate 1% Solution and Ethyl Alcohol 61% w/w (3M Health Care, St. Paul, MN, USA), and then were aseptically gowned. Between surgeries, following the doffing of the surgical gown and gloves, Avagard™ alone was utilized before donning a new sterile surgical gown and gloves. New sterile packs and surgical instruments were utilized for each pig.

2.9 Challenge

For the PRRSV challenge, PRRSV strain VR2332 (NCBI: txid300559) was propagated on MARC-145 cells for three passages to a titer of $10^{5.25}$ 50% tissue culture infectious dose (TCID₅₀) per ml. Each pig was infected using 5 ml of the PRRSV stock administered intranasally by slowly dripping 2.5 ml of the virus stock into each nostril. The PRRSV challenge was done 4 weeks after vaccination.

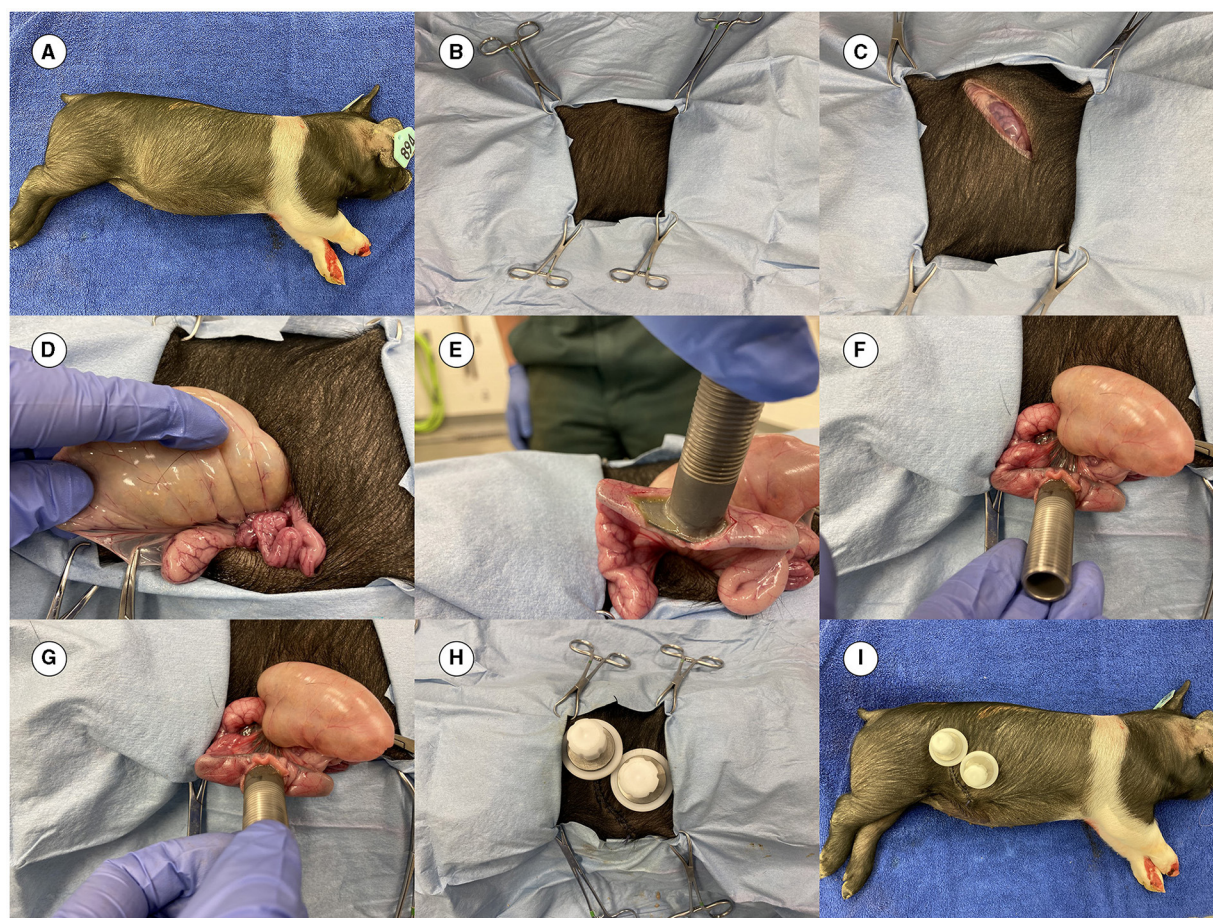


FIGURE 2

Images from the surgery. (A) Dead 4-week-old pig prepared for practicing the cannulation surgery. (B) Pig covered with surgical drapes having an opening for the incision. (C) Initial incision completed. (D) Ileum out of the abdominal cavity to locate the site for placing the cannula. (E) Cannula inserted before placement of the purse string suture. (F) Canula at the site of surgery. (G) Cannula is fixed in the ileum. (H) Final view of the placed cannula (both an ileal and a cecal cannula were inserted in the pig in this practice session). (I) The final complete look of the cannulas.

2.10 Sample collection

Blood samples were collected every week in vacutainer tubes before the challenge and at 3 and 6 days after the challenge (dpc), spun down, and serum was aliquoted into 2-ml tubes. In addition, nasal swabs were collected. In brief, sterile polyester-tipped swabs (Puritan®, Catalog No. 10805-165, Puritan Medical Products Co., Guilford, ME, USA) were inserted into each nostril, rotated 3–4 times, and placed in a 5-ml falcon tube containing 1 ml saline. The serum and the nasal swabs were stored at -70°C for further testing. Ileum content was collected once a week by restraining the pigs, unscrewing the cannula cap, and allowing the intestinal content to flow out of the cannula briefly before collecting fresh contents in a 50 ml tube, which was later allocated to small snap-top tubes and frozen at -70°C .

2.11 Serum and nasal swab analysis

Serum samples were tested by a commercial indirect PRRSV enzyme-linked immunosorbent assay (IDEXX PRRS X3 Ab Test;

IDEXX Inc). A sample was considered positive when the sample-to-positive (S/P) value was equal to or >0.4 . Serum (PRRSV viremia) and nasal swabs (PRRSV shedding) were tested using a commercial real-time PCR for the presence and quantity of PRRSV RNA. Nucleic acids were extracted from serum samples and nasal swabs using the MagMAX™ Pathogen RNA/DNA kit (Thermo Fisher Scientific) and a Kingfisher Flex instrument (Thermo Fisher Scientific) following the manufacturer's instructions. For each sample, 100 μl of the nucleic acids were eluted into 90 μl of elution buffer as described (20). A quantitative reverse transcription (RT) PCR was performed using the Commercial PRRSV screening RT-PCR, VetMAX™ PRRSV NA&EU Reagent (Thermo Fisher Scientific). A total of 8 μl nucleic acid extract was included in the final 20 μl PCR reaction. Amplification reactions were performed on an ABI 7500 Fast instrument (Thermo Fisher Scientific) using the standard mode with the following conditions: one cycle of 50°C for 5 min, one cycle of 95°C for 20 s, and 40 cycles of 95°C for 3 s and 60°C for 30 s. The analysis was done using an automatic baseline. A cycle threshold (Ct) of < 37 was considered positive, and a $\text{Ct} \geq 37$ was considered negative for PRRSV. A NEG-CONTROL group was used for monitoring after cross-contamination. A POS-CONTROL group was included concerning

accounting for any problem with the virus strain used for the challenge. The NEG-CONTROL pigs were expected to remain negative for the entire study duration and served as a control for possible unintended cross-contaminations between the pig rooms. The POS-CONTROL pigs were expected to show higher viremia and nasal shedding as compared to vaccinated pigs.

2.12 Necropsy

All pigs were humanely euthanized at 10 dpc by pentobarbital overdose and necropsied. The severity of macroscopic lung lesions was scored as a percentage of the lung surface affected by lesions by a pathologist (PGH) blinded to the treatment status of the pigs. Tissues (lungs and tracheobronchial lymph nodes) were collected in 10% neutral buffered formalin for histopathology, and lungs were scored for the severity of interstitial pneumonia ranging from 0 (normal) to 6 (diffuse, severe), as described by Halbur et al. (21). The PRRSV antigen load in lung tissues was assessed using immunohistochemistry (IHC) (22), with scores ranging from 0 (no PRRSV present) to 3 (large levels of antigen diffusely distributed) by a pathologist (PGH) blinded to the treatment status of the pigs.

2.13 Statistical analysis

Means and SEM were calculated using R v 4.3.3. A $p < 0.05$ was considered significant. A type 1 one-way analysis of variance (ANOVA) was used for pairwise comparison of the average daily weight gain. The analysis for serology over time and PRRSV RNA in serum or nasal swabs was conducted using linear mixed-effects models with “Treatment”, “Day”, and “Treatment*Day” as fixed effects and “Pig ID” as the random effect. The model was fitted using the “lme4” package v.1.1-35.1 in R v.4.3.3. Thereafter, *post-hoc* pairwise comparisons (with the Tukey’s method for adjustment) among treatment groups on each day were conducted using estimated marginal means via the ‘emmeans’ package v.1.10.0 to determine whether the groups significantly differed from each other in terms of their effects on the serology. Gross lesions, interstitial pneumonia, and PRRSV IHC scores were analyzed using a non-parametric ANOVA (the Kruskal–Wallis rank sum test).

2.14 Microbiome analysis

Ileum content sample collections at 6 (vaccination), 9 (dpv 21), 10 (challenge), and 12 (necropsy) weeks of age were used for the analysis of the microbiome based on 16S rRNA gene V4 region amplicon diversity analysis using the Illumina MiSeq platform and mothur MiSeq Standard operating protocol. A phyloseq object (<https://joey711.github.io/phyloseq/>) generated from the mothur <https://mothur.org/> was used in the Microbiome package in R (<https://microbiome.github.io/tutorials/>) to analyze changes to the beta, alpha diversity, taxonomic composition including the core microbiome trajectories of the ileum. We then used the permutational multivariate analysis of variance (PERMANOVA) to attribute any structural variations in the ileum microbiome

to our experiments. To quantify multivariate community-level differences among groups, we used the statistical analyses in the Microbiome package in R (<https://microbiome.github.io/tutorials/>), including PERMANOVA (23). Canonical analysis of principal coordinates or “CAP” was used for analysis of principle components (<https://esajournals.onlinelibrary.wiley.com/doi/full/10.1890/0012-9658%282003%29084%5B0511%3ACAOPCA%5D2.0.CO%3B2>).

3 Results

3.1 Recovery of the pigs and transport back to the pig facilities

Once the surgery was completed for a given pig, it was transported back to the research facility and placed on a rubber mat under a heat lamp. The recovery process was closely monitored by Laboratory Animal Resources (LAR) technicians. Overall, the surgeries went well, with the first group of pigs back in their pens and awake and active within 2–3 h. Images of the pigs right after being returned to their pens are provided in [Supplementary Figure S4](#).

3.2 Clinical signs and post-surgery observations

Within 3–4 h after surgery, most pigs were active and alert and eating feed. Pigs that developed complications and were treated and/or euthanized are summarized in [Supplementary Table S5](#). During the days after cannulation surgery, 4 out of 15 pigs developed clinical signs and had to be euthanized (a POS-CONTROL pig, a VAC-ANTI-PRRSV pig, a VAC-PRRSV pig, and a VAC-PRO-PRRSV pig), reducing treatment group size from 3 to 2 pigs. Necropsy of the four pigs euthanized due to complications from surgery revealed peritonitis. This peritonitis was associated with the end of the cannula eroding or tearing through the intestine rather than leakage at the purse-string at the enterotomy site. This erosion or tearing may have been due to the flange of the cannula being too large for the diameter of the intestines and/or too much movement of cannulas associated with threads not keeping the cannula flush with the abdominal wall. Thus, a grommet and spacer were added to the canulas of several pigs post-operatively ([Supplementary Figure S6](#)).

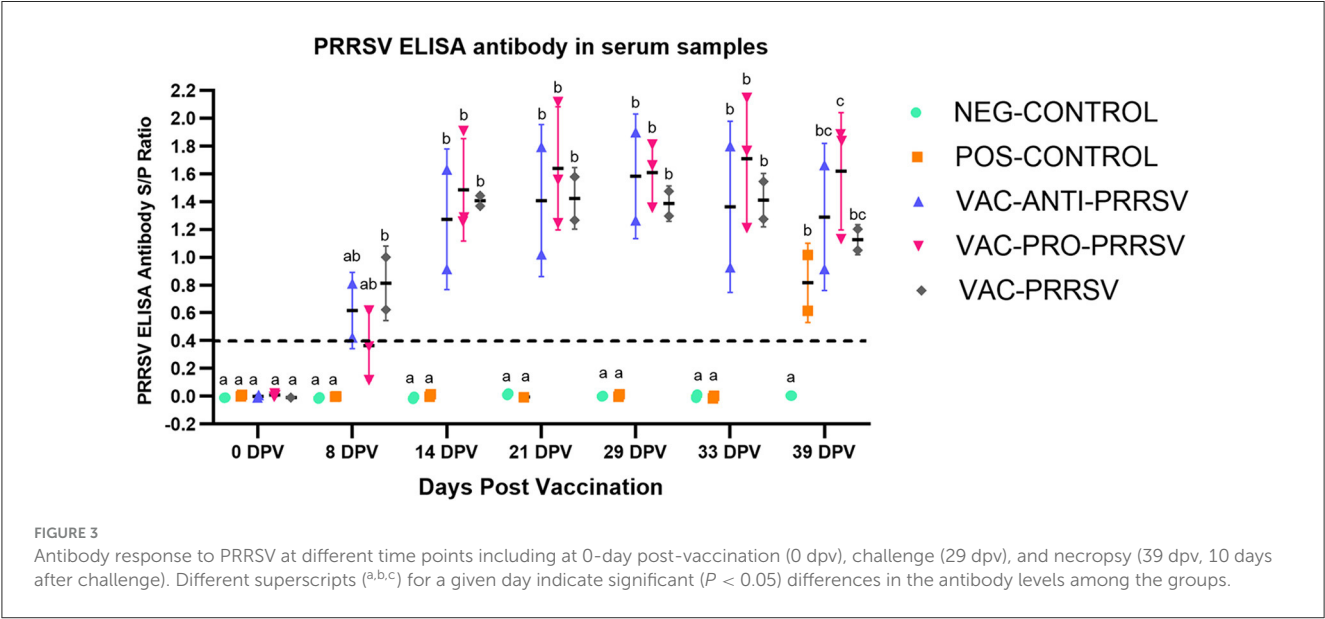
3.3 Average daily gain

The average daily gain is summarized in [Table 2](#). There were no significant differences among groups. Upon arrival, the pigs’ weights ranged from 5.0 to 6.6 kg. At necropsy, the lightest pig weighed 34.9 kg, whereas the heaviest pig weighed 43.4 kg.

TABLE 2 Average daily weight gain of the pigs during different phases in kg ± SEM (2 pigs per group).

Group	Number of pigs	Arrival to vaccination	Arrival to necropsy	Vaccination to necropsy
NEG-CONTROL	2	0.320 ± 0.03	1.195 ± 0.02	1.453 ± 0.01
POS-CONTROL	2	0.319 ± 0.03	1.186 ± 0.12	1.44 ± 0.05
VAC-ANTI-PRRSV	2	0.313 ± 0.01	1.235 ± 0.09	1.521 ± 1.04
VAC-PRO-PRRSV	2	0.273 ± 0.06	1.105 ± 0.04	1.369 ± 0.01
VAC-PRRSV	2	0.306 ± 0.03	1.265 ± 0.06	1.575 ± 0.06

There were no significant differences among computed group weight gain ($P < 0.05$) between arrival and vaccination (21 days), arrival and necropsy (61 days), and vaccination and necropsy (40 days).



3.4 Serology response to vaccination and challenge

All pigs tested negative for anti-PRRSV antibodies at arrival and on the vaccination day (0 dpv). NEG-CONTROL pigs remained antibody-negative throughout the study, while all vaccinated pigs seroconverted to PRRSV ~1 week after vaccination (Figure 3). While the VAC-PRO-PRRSV group had numerically the highest level of seroconversion, this was not significantly different from the VAC-ANTI-PRRSV and the VAC-PRRSV groups. The non-vaccinated POS-CONTROL pigs only seroconverted at the time of necropsy, 10 days after the challenge.

3.5 PRRSV viremia and nasal shedding after challenge

The NEG-CONTROL pigs remained negative for PRRSV RNA in both serum and nasal swab samples throughout the study (Figures 4, 5). The vaccinated pigs (VAC-ANTI-PRRSV, VAC-PRO-PRRSV, and VAC-PRRSV groups) became viremic, starting with 1 week after vaccination. In these groups, the highest viremia level was detected at 8 dpv, and PRRSV genomic copies in serum started to decline afterward. There were no

significant differences regarding the viremia levels between the three vaccinated groups at each time point during 8–29 dpv. After the challenge, the POS-CONTROL pigs had the highest viremia level among all groups at 33 dpv (4 dpc) and 39 dpv (10 dpc), while the viremia levels among the vaccinated groups were overall not significantly different (Figure 4). In nasal swabs, RNA-positive samples were only detected in the POS-CONTROL pigs post-challenge (Figure 5). Nasal shedding is important in the transmission of PRRSV, and it appears that the shedding was blocked by vaccination, regardless of treatment at vaccination.

3.6 Macroscopic and microscopic lesions and PRRSV IHC results in lung tissues

At necropsy, macroscopic lung lesions were characterized by multifocal consolidation and a dark red color (Table 3). Microscopic lesions were characterized by mild-to-moderate type 2 pneumocyte hypertrophy and hyperplasia and mild lymphocytic septal infiltration. PRRSV antigen was demonstrated by IHC associated with lung lesions in the POS-CONTROL pigs (score of 2) and in one VAC-ANTI-PRRSV pig. No PRRSV antigen was detected in the lungs of the other pigs. No significant differences

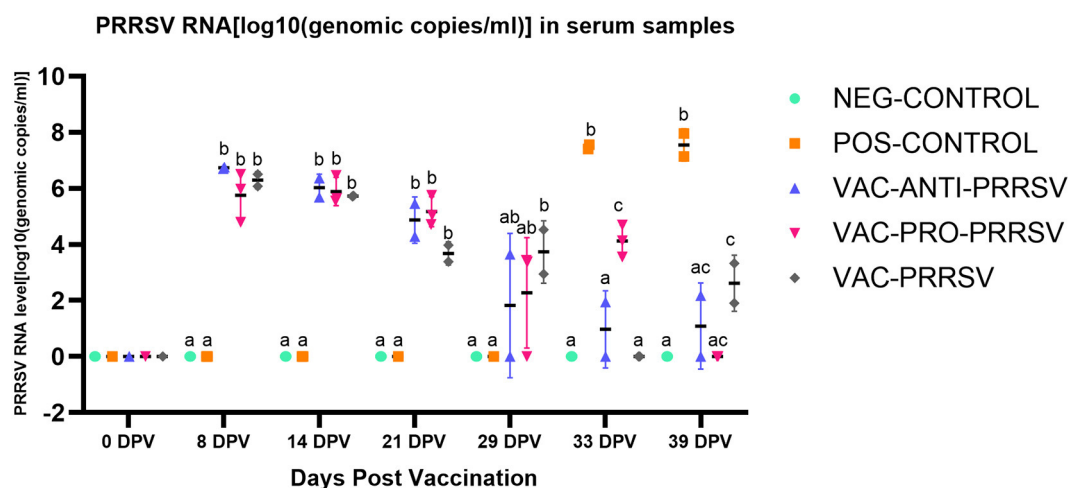


FIGURE 4

PRRSV viremia (serum) at different days post-vaccination (dpv) including initial vaccination at 0 dpv, challenge (29 dpv, 0 day post-challenge), and necropsy (39 dpv, 10 days post-challenge). Different superscripts for a given day (^{a,b,c}) indicate significant ($P < 0.05$) differences among groups.

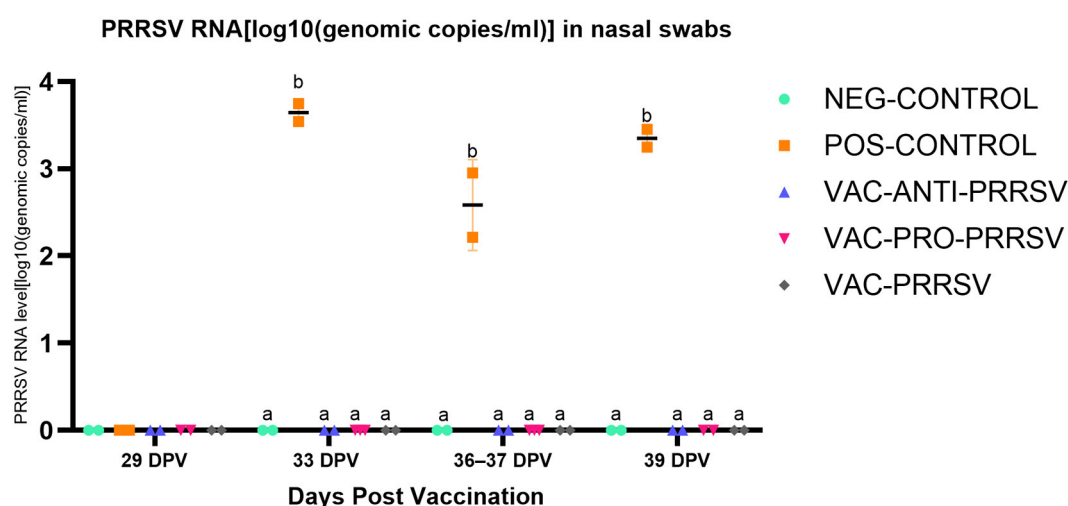


FIGURE 5

PRRSV shedding (nasal swabs) at different days post-vaccination (dpv). Samples tested included challenge at 29 dpv (corresponding to 0 day post-challenge [0 dpc]), and 33 dpv (4 dpc), 36–37 dpv (7–8 dpc), and 39 dpv (= necropsy day; 10 dpc). Different superscripts for a given day (^{a,b}) indicate significant ($P < 0.05$) differences among groups.

were observed among the groups for gross lung lesion scores, the severity of interstitial pneumonia, or PRRSV IHC scores.

3.7 Ileum microbiome over time

A comparison of alpha diversity indices, i.e., Shannon and Inverse Simpson indices, between vaccinated and non-vaccinated animals is shown in Figure 6A. Although the vaccinated pigs had a slightly lower variation yet higher means of the alpha diversity index when compared to the non-vaccinated pigs, this difference was not statistically significant. However, when both the treatment and time were considered as shown (Figures 6B, C), clear trends became evident in both indices, including the richness, rare taxa

(Shannon), evenness, and dominant taxa (Simpson). The major trends observed included a gradual decline in the NEG-CONTROL group, a rapid decline in the POS-CONTROL group, an initial increase followed by a decline toward the end in the VAC-ANTI-PRRSV group, a gradual decline with high variations in the VAC-PRO-PRRSV group, and a rapid increase followed by a decline toward the end in the VAC-PRRSV group.

The taxonomic composition showed a temporal change at the phylum level with a notable surge in Proteobacteria midway through the experimental period (Figure 7A). At the genus level, these shifts are predominantly driven by the ileal-adapted *Romboustia*, *Streptococcus*, and *Clostridium* (Figure 7B). Investigating this trajectory of the core genera at Amplicon Sequence Variants (ASV) revealed that two variants of *Romboustia*

TABLE 3 Group means (2 pigs per group) for macroscopic lung lesions, interstitial pneumonia, and PRRSV antigen in lung tissues, as determined by IHC.

Group	Pig#	Gross lung lesions (Score: 0–100%)	Interstitial pneumonia (Score: 0–6%)	PRRSV IHC (Score: 0–3)
NEG-CONTROL	2	0/2 (0) ^a	1/2 (0.5 ± 0.5) ^a	0/2 (0) ^a
POS-CONTROL	2	2/2 (17.5 ± 12.5) ^a	2/2 (2 ± 1.0) ^a	2/2 (2 ± 0) ^a
VAC-ANTI-PRRSV	2	0/2 (0) ^a	1/2 (0.5 ± 0.5) ^a	1/2 (0.5 ± 0.5) ^a
VAC-PRO-PRRSV	2	0/2 (0) ^a	2/2 (1 ± 0) ^a	0/2 (0) ^a
VAC-PRRSV	2	0/2 (0) ^a	2/2 (1 ± 0) ^a	0/2 (0) ^a

Different superscripts ^{a,b} within a given column indicate significant (P < 0.05) differences among the groups.

TABLE 4 PERMANOVA output.

Variable	Degrees of freedom	R2	P-value
Treatment	4	0.07	0.0001
Time	3	0.36	0.0002
Residual	36	0.56	-
Total	43	1	

and *Clostridium* exhibit distinct abundance in the treatment groups of vaccinated pigs, as shown in Figure 7C. This observation was validated by analysis of composition of microbiomes (ANCOM) at the genus (L6) level, which shows three genera that were differentially abundant among the treatment groups over time: *Streptococcus*, *Turicibacter*, and *Clostridium_sensu_stricto_6*. This is evidence that they may act as beneficial bacteria in the gut flora (24–26). Both the NEG-CONTROL group and the VAC-PRO-PRRSV group had relatively higher abundance levels of *Streptococcus* over time compared to the NEG-CONTROL group and the VAC-ANTI-PRRSV group. All four groups showed the highest abundance levels of *Streptococcus* at the time of necropsy 10 days after the PRRSV challenge.

For *Turicibacter*, the NEG-CONTROL group showed a considerable increase in *Turicibacter* abundance from dpv 21 to dpc 10, relative to the other four groups. In addition, pigs in the VAC-ANTI-PRRSV and VAC-PRO-PRRSV groups shared a similar trend of having a low abundance of this genus relative to the other groups across the entire study. Finally, for *Clostridium_sensu_stricto_6*, all groups except the NEG-CONTROL group shared a similar trend in the abundance of this genus throughout the entire period of the study, including the highest abundance levels of this genus 4 weeks after vaccination (dpv 28) relative to the other time points.

Similar to the alpha indices, there were no discernible differences in the abundance at any of the taxonomic levels between the vaccinated and the non-vaccinated groups based on the ANCOM using QIIME composition.

The results in Figure 8 demonstrated a distinctive clustering of samples by time, indicating that time explained approximately 32.9% of the microbiome structural variation. When using PERMANOVA, considering the individual animal variation, it is evident that approximately 43% of the structural variation in the ileum was explained by time (36%) and treatment (7%). We used the constrained principal coordinate analysis (PCoA) here. When

we constrained the PCoA by time, 32.9% of the structural variation in the microbiome was explained based on CAP1 (18.6) plus CAP2 (14.3). This was validated by the PERMANOVA (Table 4), which indicated that time explained 36.4% of the microbiome structural variation.

4 Discussion

The novelty of this pilot study is the description and utilization of a cannulation method in young pigs to collect small intestine contents for dynamic evaluation of the microbiota. Cannulated pigs are commonly used in nutrition studies (27–29) but are rarely utilized in infectious disease research. Currently, the pig microbiome is often investigated by sequencing rectal swabs (30, 31). However, the porcine gut microflora changes dramatically across the different gut sections; thus, the microbiome from rectal swabs is likely not representative of much of the gut microbiome, particularly the small intestines. In this study, we developed and described a cannulation method to collect small intestine contents from pigs to investigate dynamic changes in the microbiomes. Previous studies have shown that the microbiota of the small intestine is phylogenetically much less diverse than that of the colon but more dynamic (32). Future applications of this cannulation model could advance our understanding of the colonialization sites of microbes (pathogenic and nonpathogenic), the impact of feed additives, including probiotics, and the vaccines utilized to mitigate enteric and systemic diseases.

Several research groups have found a consistent difference between microbial communities of the upper and lower gastrointestinal tracts. In humans, it has been shown that one community colonizes the duodenum down to the proximal ileum dominated by *Pseudomonadota*, *Streptococcaceae*, and *Veillonellaceae* among others, while other bacteria colonize the distal ileum down to the rectum (generally dominated by *Bacteroidaceae*, *Lachnospiraceae*, and *Ruminococcaceae*) (33). In our study, there were no major differences over time among bacterial genera (Figure 7). However, in Figure 7B, there is evidence of a higher abundance of *Romboutsia* in the VAC-ANTI-PRRSV group compared to the VAC-PRO-PRRSV group. In contrast, *Streptococcus* appeared more abundant in the VAC-PRO-PRRSV than in the ANTI-PRRSV group. Possible explanations for these findings include a direct impact of the treatments (probiotics and antibiotics) or intrinsic regulation of the intestinal flora balance due to other reasons. Much work remains to be done to

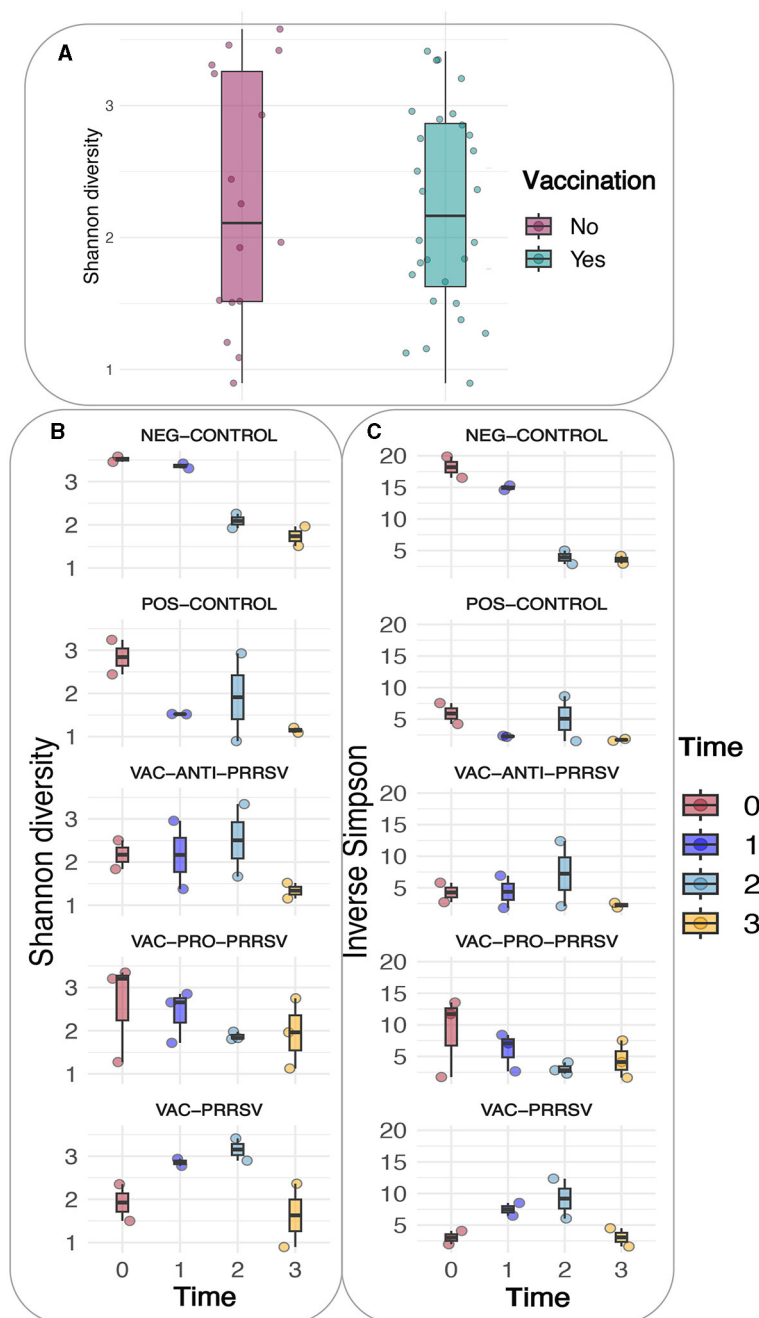


FIGURE 6

(A) Shannon diversity based on vaccination status. (B) Shannon diversity of the different groups. (C) Inverse Simpson of the different groups.

identify essential microbes that may trigger enhanced immune responses, and such discoveries would be a major breakthrough in vaccinology and preventative medicine in animals and humans.

The impact of the gut microbiota on vaccine efficacy is still poorly understood. Under normal circumstances, vaccines for pigs are readily available and commonly effective, as evidenced by the reduction in disease spread and the reduced impact of clinical signs on both the individual pig and the herd levels. In human studies, there is an indication that the composition and function of the gut microbiota are important to overall health, as they are the key factors in modulating the immune responses to vaccination

(34). The intrinsic gut microbiota is a complex accumulation of bacteria, viruses, archaea, and fungi, which likely affect humans and animals, similarly, by maintaining gastrointestinal homeostasis, regulating immune system development, metabolizing nutrients, and preventing pathogen colonization (35). In addition, microbiota could also act as a natural adjuvant, regulate host immune responses, and carry epitopes that are similar to vaccine antigens to induce cross-reaction and other ways to affect vaccine efficacy (36). Nevertheless, despite the optimistic prospects of improving gut health to enhance vaccinations, gut microbiota could also adversely affect vaccine efficacy by biasing antibody responses

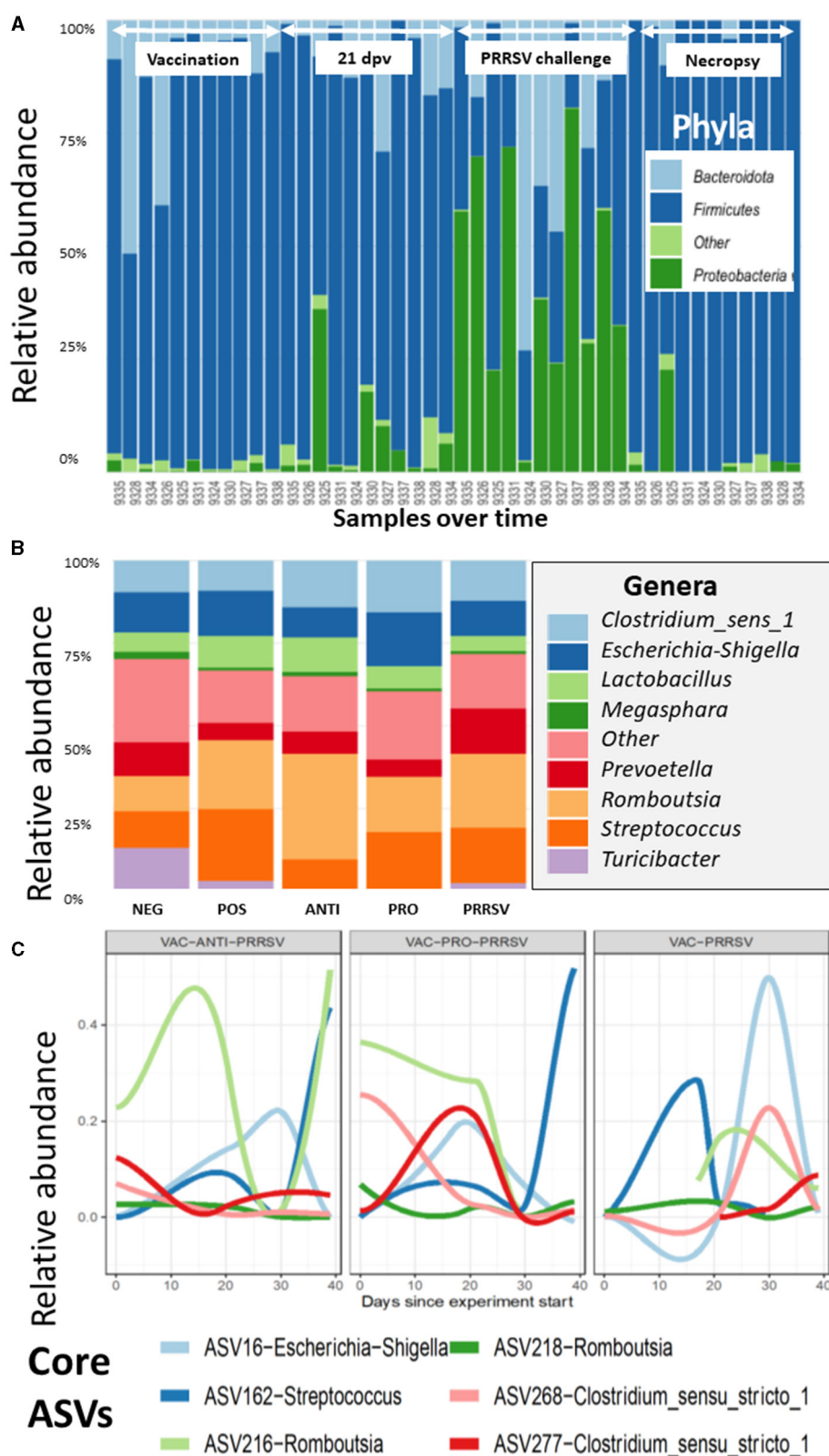


FIGURE 7

(A) The variation of the taxa of all the samples arranged by time at the phylum level, as demonstrated for the Proteobacteria, which have a distinctive shift over time. Time points and arrows on top indicate the different sample collections. Day post vaccination is indicated by dpv. (B) The contribution of major bacterial genera is compared in the different treatment groups. (C) The composition of the core microbiome is tracked over time, and it appears that the vaccinated groups show clear differences in the core trajectory over time.

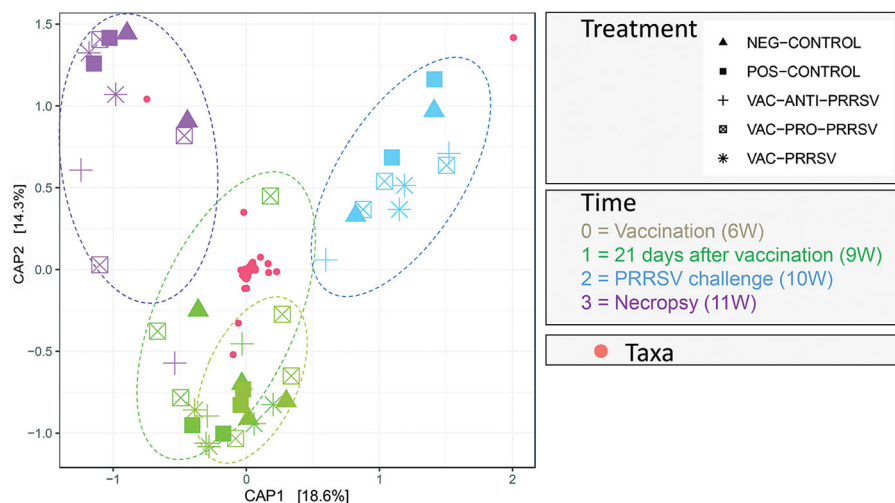


FIGURE 8

Principal Coordinate of Analysis plot showing the clustering of each pig treatment groups' microbiome by age in weeks (W).

toward non-protective vaccine antigens similar to commensal bacterial antigens (37). At this point, larger studies on the impact of certain microbiota in pigs are lacking. We anticipate that the development and description of our model will allow researchers to identify new pathways to further improve vaccine efficacy and better understand the use of probiotic supplementation.

After cannulation surgery on 4-week-old pigs, four pigs were euthanized due to complications from surgery. However, in the future, this can likely be prevented by the use of a smaller cannula that would be less likely to result in damage to the intestinal wall and associated peritonitis. The use of older pigs may also result in fewer complications related to cannula size but may not be appropriate to investigate the microbiome in newly weaned pigs.

In this study, the limited sample size of only 2–3 pigs per group at the time of vaccination and PRRSV challenge did not provide sufficient statistical power for robust analysis and conclusions. Nevertheless, it is noteworthy that, despite having a cannulation surgery and receiving various treatments, the pigs displayed a good antibody response after vaccination. The antibody responses together with the PCR results in serum and nasal swab samples suggest that the pigs were able to mount humoral immunity successfully, thereby preventing PRRSV infection and shedding in vaccinated and challenged pigs. These findings suggest that cannulation surgery may not significantly impact the pig's reaction to infectious agents, including induction of antibody response. This evidence is promising as it supports the viability of this model for use in a large cohort of pigs, potentially enabling the detection of treatment differences.

The benefits of a healthy gut microbiome in controlling enteric infections are already widely appreciated (38–40). One of the main outcomes of this research is the development of a model that can better assess the utility of probiotics for the improvement of the efficacy of vaccines through modulation of the gut microbiome. In this context, we evaluated the effect of a probiotic on PRRSV vaccine efficacy; however, the study outcome could be applied to other viral or bacterial vaccines for pigs.

In conclusion, while microbiome studies over time have been previously performed using rectal swabs, to our knowledge, this study provides novel information on the dynamics of ileum microbiota in recently weaned pigs. The microbiome in fecal samples vs. intestinal content can vary quite dramatically, and hence, rectal swabs may not provide an accurate reflection of the microbiome in the ileum or other small intestinal sections. Although this small-scale pilot study did not allow us to conclude the impact of microbiota on PRRSV vaccination, we believe it is important to disseminate the findings from the current study using the cannulation model for the scientific community. In the future, the procedure could be further refined to result in a reliable model for longitudinal microbiome studies in recently weaned pigs.

Data availability statement

Raw sequencing files are available from the European Nucleotide Archive BioProject number (<https://www.ebi.ac.uk/ena/browser/view/PRJEB72452>).

Ethics statement

The animal study was approved by the study was conducted according to the guidelines of the Declaration of Helsinki and approved by the by the Iowa State University Institutional Animal Care and Use Committee (Approval number IACUC-21-031; Date of approval: 05-April-2021) and by the Iowa State University IBC Committee (Approval number IBC 21-019; Date of approval: 6-April-2021). Environmental enrichment was provided and independent veterinarians, not part of the research team, assessed the pigs and made decisions on welfare and euthanasia. The study was conducted in accordance with the local legislation and institutional requirements.

Author contributions

TO: Writing – review & editing, Writing – original draft, Supervision, Funding acquisition, Project administration, Methodology, Conceptualization. PH: Investigation, Writing – review & editing, Writing – original draft, Supervision. JB: Methodology, Conceptualization, Writing – review & editing, Writing – original draft, Supervision. GR: Supervision, Writing – review & editing, Writing – original draft. HT: Methodology, Writing – review & editing, Writing – original draft. KM: Writing – review & editing, Writing – original draft, Data curation. GL: Data curation, Writing – review & editing, Writing – original draft. DZ: Writing – review & editing, Writing – original draft, Formal analysis. JZ: Formal analysis, Writing – review & editing, Writing – original draft. AM: Data curation, Visualization, Methodology, Writing – review & editing, Writing – original draft.

Funding

The author(s) declare financial support was received for the research, authorship, and/or publication of this article. The study was funded by Boehringer Ingelheim, USA. Boehringer Ingelheim, USA was not involved in the study design, collection, analysis, interpretation of data, the writing of this article, or the decision to submit it for publication. AM was supported by the Biotechnology and Biological Sciences Research Council (BBSRC) core funding Institute Strategic Programme Grant awarded to the Roslin Institute (BBS/E/D/20002173) and the Institutional Strategic Support Fund (ISSF3) award (S3-R1.09 19/20).

References

1. Lee J, Htoo JK, Klunemann M, González-Vega JC, Nyachoti CM. Effects of dietary protein content and crystalline amino acid supplementation patterns in low protein diets on intestinal bacteria and their metabolites in weaned pigs raised under Different sanitary conditions. *J Anim Sci.* (2023) 101:skad252. doi: 10.1093/jas/skad252
2. Pandey S, Kim ES, Cho JH, Song M, Doo H, Kim S, et al. Swine gut microbiome associated with non-digestible carbohydrate utilization. *Front Vet Sci.* (2023) 10:1231072. doi: 10.3389/fvets.2023.1231072
3. Trudeau MP, Mosher W, Tran H, de Rodas B, Karnezos TP, Urriola PE, et al. Experimental facility had a greater effect on growth performance, gut microbiome, and metabolome in weaned pigs than feeding diets containing subtherapeutic levels of antibiotics: a case study. *PLoS ONE.* (2023) 3:e0285266. doi: 10.1371/journal.pone.0285266
4. Melendez Hebib V, Taft DH, Stoll B, Liu J, Call L, Guthrie G, et al. Probiotics and human milk differentially influence the gut microbiome and nec incidence in preterm pigs. *Nutrients.* 15:2585. doi: 10.3390/nu15112585
5. Rutjens S, Verecke N, Sauer J, Croubels S, Devreese M. Cefquinome shows a higher impact on the pig gut microbiome and resistome compared to ceftiofur. *Vet Res.* (2023) 54:45. doi: 10.1186/s13567-023-01176-8
6. Fox BE, Vilander AC, Gilfillan D, Dean GA, Abdo Z. Oral vaccination using a probiotic vaccine platform combined with prebiotics impacts immune response and the microbiome. *Vaccines.* (2022) 10:1465. doi: 10.3390/vaccines10091465
7. Lenoir-Wijnkoop I, Merenstein D, Korchagina D, Broholm C, Sanders ME, Tancredi D. Probiotics reduce health care cost and societal impact of flu-like respiratory tract infections in the USA: an economic modeling study. *Front Pharmacol.* (2019) 10:1182. doi: 10.3389/fphar.2019.00980
8. Boge T, Rémy M, Vaudaine S, Tanguy J, Bourdet-Sicard R, van der Werf S. A probiotic fermented dairy drink improves antibody response to influenza

Acknowledgments

We thank veterinary students Alex Bishop and Jared McGinley for assistance with bleeding and probiotic administration. We also thank the Laboratory Animal Research (LAR) including Michelle Thacker for the excellent care of the pigs and Li Wang for assistance with figure outlines.

Conflict of interest

The authors declare that the research was conducted in the absence of any commercial or financial relationships that could be construed as a potential conflict of interest.

Publisher's note

All claims expressed in this article are solely those of the authors and do not necessarily represent those of their affiliated organizations, or those of the publisher, the editors and the reviewers. Any product that may be evaluated in this article, or claim that may be made by its manufacturer, is not guaranteed or endorsed by the publisher.

Supplementary material

The Supplementary Material for this article can be found online at: <https://www.frontiersin.org/articles/10.3389/fvets.2024.1422012/full#supplementary-material>

vaccination in the elderly in two randomised controlled trials. *Vaccine.* (2009) 27:5677–84. doi: 10.1016/j.vaccine.2009.06.094

9. Zimmermann P, Curtis N. The influence of probiotics on vaccine responses - a systematic review. *Vaccine.* (2018) 36:207–13. doi: 10.1016/j.vaccine.2017.08.069

10. González-Solé F, Camp Montoro J, Solà-Oriol D, Pérez JF, Lawlor PG, Boyle LA, et al. Effect of mixing at weaning and nutrient density of the weaner diet on growth performance and welfare of pigs to slaughter. *Porcine Health Manag.* (2023) 9:38. doi: 10.1186/s40813-023-00334-w

11. Luo Y, Ren W, Smidt H, Wright AG, Yu B, Schyns G, et al. Dynamic distribution of gut microbiota in pigs at different growth stages: composition and contribution. *Microbiol Spectr.* (2022) 10:e0068821. doi: 10.1128/spectrum.00688-21

12. Muwonge A, Karuppannan AK, Opriessnig T. Probiotics mediated gut microbiota diversity shifts are associated with reduction in histopathology and shedding of *Lawsonia intracellularis*. *Anim Microbiome.* (2021) 3:22. doi: 10.1186/s42523-021-00084-6

13. Opriessnig T, Gerber PE, Shen H, de Castro AMMG, Zhang J, Chen Q, et al. Evaluation of the efficacy of a commercial inactivated genogroup 2b-based porcine epidemic diarrhea virus (PEDV) vaccine and experimental live genogroup 1b exposure against 2b challenge. *Vet Res.* (2017) 48:69. doi: 10.1186/s13567-017-0472-z

14. Halbur PG, Paul PS, Meng XJ, Lum MA, Andrews JJ, Rathje JA. Comparative pathogenicity of nine US porcine reproductive and respiratory syndrome virus (PRRSV) isolates in a five-week-old cesarean-derived, colostrum-deprived pig model. *J Vet Diagn Invest.* (1996) 8:11–20. doi: 10.1177/104063879600800103

15. Metzler-Zebeli BU, Rosenfelder-Kuon P, Brehm H, Eklund M, Mosenthin R. Improved simple T-cannula technique to facilitate surgery and daily skin care of growing pigs. *J Anim Sci.* (2020) 98:skaa091. doi: 10.1093/jas/skaa091

16. Stein HH, Shipley CF, Easter RA. Technical note: a technique for inserting a T-cannula into the distal ileum of pregnant sows. *J Anim Sci.* (1998) 76:1433–6. doi: 10.2527/1998.7651433x
17. Wubben JE, Smiricky MR, Albin DM, Gabert VM. Improved procedure and cannula design for simple-T cannulation at the distal ileum in growing pigs. *Contemp Top Lab Anim Sci.* (2001) 40:27–31.
18. Radcliffe JS, Rice JP, Pleasant RS, Apgar GA. Technical Note: Improved technique for fitting pigs with steered ileocecal valve cannulas. *J Anim Sci.* (2005) 83:1563–7. doi: 10.2527/2005.8371563x
19. Dorado-Montenegro S, Lammers-Jannink K, Gerrits W, de Vries S. (2023). Insoluble fibers affect digesta transit behavior in the upper gastrointestinal tract of growing pigs, regardless of particle size. *J Anim Sci.* 101:skad299. doi: 10.1093/jas/skad299
20. Opriessnig T, Rawal G, McKeen L, Filippesen Favaro P, Halbur PG, Gauger PC. Evaluation of the intranasal route for porcine reproductive and respiratory disease modified-live virus vaccination. *Vaccine.* (2021) 39:6852–9. doi: 10.1016/j.vaccine.2021.10.033
21. Halbur PG, Paul PS, Frey ML, Landgraf J, Eernisse K, Meng X, et al. Comparison of the pathogenicity of two US porcine reproductive and respiratory syndrome virus isolates with that of the Lelystad virus. *Vet Pathol.* (1995) 32:648–60. doi: 10.1177/030098589503200606
22. Halbur PG, Andrews JJ, Huffman EL, Paul PS, Meng XJ, Niyo Y. Development of a streptavidin-biotin immunoperoxidase procedure for the detection of porcine reproductive and respiratory syndrome virus antigen in porcine lung. *J Vet Diagn Invest.* (1994) 6:254–7. doi: 10.1177/104063879400600219
23. Anderson MJ. Permutational multivariate analysis of variance (PERMANOVA). In: Balakrishnan N, Everitt TC, Piegorisch W, Ruggeri F, Teugels JL, editor. *Wiley Stats Ref: Statistics Reference Online.* (2017). p. 1–15. Available online at: <https://onlinelibrary.wiley.com/action/showCitFormats?doi=10.1002%2F9781118445112.stat07841>
24. Guo P, Zhang K, Ma X, He P. Clostridium species as probiotics: potentials and challenges. *J Anim Sci Biotechnol.* (2020) 11:24. doi: 10.1186/s40104-019-0402-1
25. Lynch JB, Gonzalez EL, Choy K, Faull KF, Jewell T, Arellano A, et al. Gut microbiota Turicibacter strains differentially modify bile acids and host lipids. *Nat Commun.* (2023) 14:3669. doi: 10.1038/s41467-023-39403-7
26. Wylensek D, Hitch TCA, Riedel T, Afrizal A, Kumar N, Wortmann E, et al. A collection of bacterial isolates from the pig intestine reveals functional and taxonomic diversity. *Nat Commun.* (2020) 11:6389. doi: 10.1038/s41467-020-19929-w
27. Heyer CME, Wang LF, Beltranena E, Rodehutsord M, Zijlstra RT. Effect of increasing dietary fermentable fiber on diet nutrient digestibility and estimation of endogenous phosphorus losses in growing pigs. *J Anim Sci.* (2023) 101:skad204. doi: 10.1093/jas/skad204
28. Lammers-Jannink KCM, Pellikaan WF, de Vries S, Stigter ECA, Gerrits WJJ. Standardisation of the C:N ratio in ileal digesta changes relationships among fermentation end-products during in vitro hindgut fermentation in pigs. *Animal.* (2023) 17:101026. doi: 10.1016/j.animal.2023.101026
29. Zhao S, Lv L, Wu T, Feng Z, Li Q, Lei L, et al. A combined pig model to determine the net absorption of volatile fatty acids in the large intestine under different levels of crude fiber. *Animal Model Exp Med.* (2023) 6:375–80. doi: 10.1002/ame2.12329
30. Choudhury R, Kleerebezem M. Assessing the impact of diet on the mucosa-adhered microbiome in piglets using comparative analysis of rectal swabs and colon content. *Front Microbiol.* (2022) 13:804986. doi: 10.3389/fmicb.2022.804986
31. He Y, Tiezzi F, Howard J, Huang Y, Gray K, Maltecca C. Exploring the role of gut microbiota in host feeding behavior among breeds in swine. *BMC Microbiol.* (2022) 22:1. doi: 10.1186/s12866-021-02409-6
32. Choudhury R, Middelkoop A, Bolhuis JE, Kleerebezem M. Legitimate reliable determination of the age-related intestinal microbiome in young piglets; rectal swabs and fecal samples provide comparable insights. *Front Microbiol.* (2019) 10:1886. doi: 10.3389/fmicb.2019.01886
33. Jensen BAH, Heyndrickx M, Jonkers D, Mackie A, Millet S, Naghibi M, et al. Small intestine vs. colon ecology and physiology: why it matters in probiotic administration. *Cell Rep Med.* (2023) 4:101190. doi: 10.1016/j.xcrm.2023.101190
34. Huang B, Wang J, Li L. Recent five-year progress in the impact of gut microbiota on vaccination and possible mechanisms. *Gut Pathog.* (2023) 15:27. doi: 10.1186/s13099-023-00547-y
35. Jordan A, Carding SR, Hall LJ. The early-life gut microbiome and vaccine efficacy. *Lancet Microbe.* (2022) 3:e787–94. doi: 10.1016/S2666-5247(22)00185-9
36. Lynn DJ, Benson SC, Lynn MA, Pulendran B. Modulation of immune responses to vaccination by the microbiota: implications and potential mechanisms. *Nat Rev Immunol.* (2022) 22:33–46. doi: 10.1038/s41577-021-00554-7
37. Williams WB, Liao HX, Moody MA, Kepler TB, Alam SM, et al. HIV-1 VACCINES. Diversion of HIV-1 vaccine-induced immunity by gp41-microbiota cross-reactive antibodies. *Science.* (2015) 349:aab1253. doi: 10.1126/science.aab1253
38. Liao SF, Nyachoti M. Using probiotics to improve swine gut health and nutrient utilization. *Anim Nutr.* (2017) 3:331–43. doi: 10.1016/j.aninu.2017.06.007
39. Pereira WA, Franco SM, Reis IL, Mendonça CMN, Piazzentin ACM, Azevedo POS, et al. Beneficial effects of probiotics on the pig production cycle: an overview of clinical impacts and performance. *Vet Microbiol.* (2022) 269:109431. doi: 10.1016/j.vetmic.2022.109431
40. Vasquez R, Oh JK, Song JH, Kang DK. Gut microbiome-produced metabolites in pigs: a review on their biological functions and the influence of probiotics. *J Anim Sci Technol.* (2022) 64:671–95. doi: 10.5187/jast.2022.e58



OPEN ACCESS

EDITED BY

Mengmeng Zhao,
Foshan University, China

REVIEWED BY

Heng Wang,
South China Agricultural University, China
Zhendong Zhang,
Yangzhou University, China

*CORRESPONDENCE

Xiaowen Li
✉ lxw8272@163.com

RECEIVED 16 June 2024

ACCEPTED 05 August 2024

PUBLISHED 14 August 2024

CITATION

Ren J, Li F, Yu X, Li Y, Li M, Sha Y and
Li X (2024) Development of a TaqMan-based
multiplex real-time PCR for simultaneous
detection of porcine epidemic diarrhea virus,
Brachyspira hyodysenteriae, and *Lawsonia
intracellularis*.
Front. Vet. Sci. 11:1450066.
doi: 10.3389/fvets.2024.1450066

COPYRIGHT

© 2024 Ren, Li, Yu, Li, Sha and Li. This is an
open-access article distributed under the
terms of the [Creative Commons Attribution
License \(CC BY\)](#). The use, distribution or
reproduction in other forums is permitted,
provided the original author(s) and the
copyright owner(s) are credited and that the
original publication in this journal is cited, in
accordance with accepted academic
practice. No use, distribution or reproduction
is permitted which does not comply with
these terms.

Development of a TaqMan-based multiplex real-time PCR for simultaneous detection of porcine epidemic diarrhea virus, *Brachyspira hyodysenteriae*, and *Lawsonia intracellularis*

Jing Ren^{1,2}, Fujun Li³, Xue Yu^{1,2}, Yang Li³, Meng Li^{1,2}, Yujie Sha^{1,2}
and Xiaowen Li^{1,3*}

¹Shandong Engineering Research Center of Swine Health Data and Intelligent Monitoring, Dezhou University, Dezhou, China, ²Shandong Provincial Key Laboratory of Biophysics, Institute of Biophysics, Dezhou University, Dezhou, China, ³Shandong Engineering Research Center of Pig and Poultry Health Breeding and Important Disease Purification, Shandong New Hope Liuhe Co., Ltd., Qingdao, China

Introduction: PEDV, *Brachyspira hyodysenteriae*, and *Lawsonia intracellularis*, are highly contagious diarrheal pathogens that have caused significant harm to the global swine industry. Co-infections with multiple pathogens are common, making it challenging to identify the actual causative agents depending only on clinical information. It is crucial to develop a reliable method to simultaneously detect and differentiate these pathogens.

Methods: Based on the conserved regions of the M gene of PEDV, NADH oxidase gene of *B. hyodysenteriae*, and the 16S rDNA gene of *L. intracellularis*, specific probes and primers for the multiplex real-time PCR assay were designed. The concentrations of primers and probes were optimized using a matrix method.

Results: The approach demonstrated high specificity and no cross-reactivity with major pathogens related to diarrheal diseases. It showed high sensitivity with a detection limit of 10 copies/μL for *B. hyodysenteriae* and *L. intracellularis*, and 100 copies/μL for PEDV, respectively. It also demonstrated high reproducibility and stability with low coefficients of variation. Results from the multiplex real-time PCR method were in complete agreement with the commercial singleplex real-time PCR kit for detecting PEDV, *B. hyodysenteriae* and *L. intracellularis*. Clinical data revealed single infection rates of 31.46% for PEDV, 58.43% for *B. hyodysenteriae*, and 98.6% for *L. intracellularis*. The co-infection rates were 16.85% for PEDV + *B. hyodysenteriae*, 31.46% for PEDV + *L. intracellularis*, 57.86% for *B. hyodysenteriae* + *L. intracellularis*, and 16.85% for PEDV + *B. hyodysenteriae* + *L. intracellularis*, respectively.

Discussion: The new multiplex real-time PCR method can simultaneously differentiate PEDV, *B. hyodysenteriae* and *L. intracellularis*, making it a valuable diagnostic tool for preventing and controlling infectious diseases, as well as aiding in epidemiological investigations.

KEYWORDS

multiplex real-time PCR, PEDV, *Brachyspira hyodysenteriae*, *Lawsonia intracellularis*, porcine diarrheal diseases

1 Introduction

Diarrheal disease is a major threat to the global swine industry, causing significant losses in pig production (1, 2). It is caused by various infectious organisms, such as viral and bacterial pathogens. Numerous causative pathogens have been identified in swine, including porcine epidemic diarrhea virus (PEDV), porcine delta coronavirus (PDCoV), transmissible gastroenteritis virus (TGEV), porcine enteric alpha coronavirus (PEAV), porcine rotavirus (PoRV), *Salmonella*, *Escherichia coli*, *Brachyspira hyodysenteriae*, *Lawsonia intracellularis*, and so on (3). Among these pathogens, PEDV, *B. hyodysenteriae*, and *L. intracellularis* are the most destructive pathogens causing anorexia, diarrhea, dehydration, and vomiting (4–7). With the rapid development of intensive aquaculture, co-infection or secondary infection with these pathogens is prevalent, leading to more severe consequences than single-pathogen infection (4, 8).

Porcine epidemic diarrhea (PED) is a highly contagious diarrheal disease in pigs caused by an enveloped, single-stranded RNA virus belonging to the *Alphacoronavirus* genus in the *Coronaviridae* family (9). It is particularly severe in piglets, often leading to 100% mortality (4, 9). PED was first reported in England in 1971, followed by an outbreak in Belgium in 1977, and subsequently identified in China during the 1980s (1, 10, 11). A highly virulent strain emerged in China in December 2010, resulting in over 1 million piglet deaths (11). These strains have since spread worldwide in the swine industry (1, 11).

B. hyodysenteriae, a gram-negative anaerobic bacterium, is the classical agent of swine dysentery, a severe mucohaemorrhagic diarrheal disease affecting weanling to finishing pigs (12). This widespread disease can lead to significant mortality rates and decreased feed conversion efficiency, resulting in substantial economic losses for intensive pig production systems globally (12, 13). *L. intracellularis*, a gram-negative obligate intracellular bacterium, is the causative agent of porcine proliferative enteropathy (PPE) (14). PPE is a commonly observed bacterial disease with a high prevalence ranging from 48 to 100% at swine production facilities worldwide (6). Due to the fastidious characteristics of *L. intracellularis*, the obligate anaerobic bacteria are extremely difficult to culture *in vitro* (13, 14).

Rapid and accurate diagnostic methods are essential for effective treatment and prevention programs. However, pigs infected with PEDV, *B. hyodysenteriae*, and *L. intracellularis* show similar symptoms and pathology, making it hard to differentiate them. The high incidence of co-infection with these pathogens further exacerbates the complexities in clinical diagnosis (13). Hence, developing a highly sensitive diagnostic system is necessary to quickly detect and differentiate these causative pathogens to minimize economic losses from diarrheal disease.

Current diagnostic tests for pathogens, such as immunochromatography, antigen detective enzyme-linked immunosorbent assay, conventional PCR, and singleplex real-time PCR, can only detect one pathogen at a time and cannot confirm co-infections (15, 16). Simultaneous detection of multiple pathogens in clinical diagnostics requires multiple reactions, leading to wasted reagents and increased costs. Conversely, multiplex real-time PCR enables the simultaneous detection of multiple pathogens in a single reaction system, making it a widely utilized method in clinical diagnostics (16–18). While numerous multiplex real-time PCR assays have been employed in clinical detection of viral infectious diseases, the simultaneous detection of viral and bacterial pathogens is rarely reported. In this study, we developed a

multiple real-time PCR assay using TaqMan probe to simultaneously and accurately detect PEDV, *B. hyodysenteriae*, and *L. intracellularis*. This assay demonstrated high sensitivity and specificity for the target genes, making it a useful tool for rapid pathogen identification.

2 Materials and methods

2.1 Viruses, bacteria, and clinical samples

Positive samples for various swine pathogens, including PEDV, porcine reproductive and respiratory syndrome virus (PRRSV), porcine circovirus (PCV2, PCV3), African swine fever virus (ASFV), PoRV, PDCoV, *B. hyodysenteriae*, *L. intracellularis*, *Haemophilus parasuis* (HP), *Streptococcus suis* (SS), and *Salmonella enteritidis* (SE), confirmed by PCR and DNA sequencing, were stored in our laboratory. A total of 356 clinical samples were collected from pig farms in Shandong and Hebei provinces, including 217 fecal samples and 139 rectal swabs.

2.2 Nucleic acid extraction from pathogens

Nucleic acids were extracted from viral and bacterial pathogens, as well as clinical samples, using the NPA-96E Automatic Nucleic Acid Extractors from Bioer Technology Co., Ltd. (Hangzhou, China). The viral nucleic acids were extracted using the VAMNE Virus DNA/RNA Extraction Kit (Nanjing Vazyme Biotech Co., Ltd.), and bacterial nucleic acids were extracted using the TaKaRa MiniBEST Universal Genomic DNA Extraction Kit (Takara Biomedical Technology (Beijing) Co., Ltd.), following the manufacturer's guidelines. For RNA viruses, cDNA was synthesized using the TransScript Probe One-Step qRT-PCR SuperMix (Beijing Transgen Biotech Co., Ltd.). The extracted DNA and synthetic cDNA were stored at -80°C until used.

2.3 Design of the primers and probes

Primers and probe for PEDV used in the study were previously designed by Ren et al. (4), while those for *B. hyodysenteriae* and *L. intracellularis* were based on at least 30 genome sequences downloaded from NCBI. The primers were designed to target the NADH oxidase gene of *B. hyodysenteriae* and the 16S rDNA gene of *L. intracellularis*. Utilizing Primer Premier 5 software (Premier, Canada), primers and probes were designed based on the most conserved regions. TaqMan probes for PEDV, *B. hyodysenteriae*, and *L. intracellularis* were fluorescently labeled with FAM, VIC, and Cy5 at the 5' end, respectively, with all quenchers at the 3' end being BHQ. Sequences of the primers and probes can be found in Table 1 and were synthesized by Sangon Biotech (Shanghai) Co., Ltd.

2.4 Construction of standard plasmids

The target fragments of PEDV, *B. hyodysenteriae*, and *L. intracellularis* were amplified individually by PCR. The PCR fragments were purified and cloned into the pMD18-T vector (Takara Biomedical Technology (Beijing) Co., Ltd.). The transformed clones were then introduced into the *Escherichia coli* DH5 α strain. Positive

TABLE 1 Primers and probes designed for the multiplex real-time PCR.

Virus	Primer/probe	Sequence(5'-3')	Size (bp)	Target gene
PEDV	Forward	CATCTGATTCTGGACAGTTG	226	M
	Reverse	CTATACACCAACACAGGCTC		
	Probe	(FAM)TTTCAGAGCAGGCTGCATAT(BHQ1)		
<i>L. intracellularis</i>	Forward	CACCTGGACGATAACTGACACT	110	16 s DNA
	Reverse	TAACTCCCCAGCACCTAGCAC		
	Probe	(CY5) GAGGTGCGAAAGCGTGGGG (BHQ3)		
<i>B. hyodysenteriae</i>	Forward	GTAGGAAGAAGAAATCTGACAATGCA	142	NADH oxidase gene
	Reverse	TATGAAGAAGGCAGCAGACGTTTAT		
	Probe	(VIC) GCTTCAGCATGATTGTGT (BHQ1)		

clones were cultured, and plasmid extraction was done with the TaKaRa MiniBEST Universal Genomic DNA Extraction Kit. The plasmid was confirmed by DNA sequencing and used as the standard positive control. Quantification was done with a UV-visible spectrophotometer, and copy numbers were determined using the following formula (17):

$$\text{Plasmid copies}/\mu\text{L} = \frac{(6.02 \times 10^{23}) \times (X \text{ ng}/\mu\text{L} \times 10^{-9})}{\text{plasmid length}(bp) \times 660}$$

A tenfold serial dilution was performed on each plasmid, with concentrations ranging from 1.0×10^8 copies/ μL to 1.0×10^1 copies/ μL . For the multiplex standard curves, each plasmid was individually diluted to 3.0×10^9 copies/ μL and pooled in equal volumes to achieve a final concentration of 1.0×10^9 copies/ μL for each plasmid. The combined plasmid solution was then subjected to a tenfold serial dilution, resulting in concentrations ranging from 1.0×10^8 copies/ μL to 1.0×10^1 copies/ μL , for the establishment of multiplex standard curves.

2.5 Optimization of multiplex real-time PCR assay

The concentrations of primers and probes were optimized using a matrix method. Different concentrations of primers (10 μM) ranging from 0.2 to 0.8 μL each, as well as probes (10 μM) ranging from 0.1 to 0.4 μL each, were tested at varying annealing temperatures between 48°C and 57°C to optimize the reaction. Given that PEDV is an enveloped RNA virus, the amplification process was conducted using a one-step reaction, where the entire reaction from cDNA synthesis to real-time PCR amplification was performed in a single well. The main objective was to minimize the C_q value and maximize the fluorescence intensity (RFU). Amplification was carried out on a Bio-Rad CFX96™ Real-time System (Bio-Rad, Hercules, CA, United States), with fluorescence signal being automatically recorded at the end of each cycle. All real-time PCR results were analyzed using CFX Manager™ software.

2.6 Sensitivity, specificity, and repeatability test of the multiplex real-time PCR assay

To determine the limit of detection (LOD) for the multiplex real-time PCR method, the aforementioned pooled standard plasmids were diluted in a tenfold serial manner, ranging from 1.0×10^8 copies/

μL to 1.0×10^{-1} copies/ μL in nuclease-free water. These diluted standard plasmids served as templates for the amplification via multiplex real-time PCR, with the reliable LOD being the lowest concentration that achieved a 95% positive detection rate.

To avoid false positives resulting from the presence of other viruses or bacteria in the samples, a specificity test of a multiplex real-time PCR assay was conducted using three RNA viruses (PRRSV, PoRV, and PDCoV), three DNA viruses (PCV2, PCV3, and ASFV), and three bacteria (*H. parasuis*, *S. suis*, and *S. enteritidis*). Standard plasmids of PEDV, *B. hyodysenteriae*, and *L. intracellularis* were used as positive controls, with nuclease-free water as the negative control. Three clinical samples from healthy pigs were also tested to confirm specificity.

To test repeatability of the multiplex real-time PCR, pooled standard plasmids with concentrations ranging from 1.0×10^6 copies/ μL to 1.0×10^4 copies/ μL were used as templates. Each reaction was done in triplicate under identical conditions to assess intra-assay repeatability. Inter-assay repeatability was determined by conducting the assays three times at different time points. The coefficient of variation (CV) of the C_q values was calculated to estimate repeatability, and data analysis was done using Microsoft Excel.

2.7 Clinical sample testing

The standard plasmids and ddH₂O were utilized as positive and negative controls, respectively, in conjunction with optimized reaction conditions for multiplex real-time PCR analysis aimed at detecting the presence of each pathogen. Infection rates were determined by analyzing results from clinical samples.

3 Results

3.1 Optimization of the reaction conditions for the multiplex real-time PCR

After multiple tests, the optimal reaction conditions for multiplex real-time PCR were determined as follows: 10 μL of 2 \times AceQ qPCR Probe Master Mix (Vazyme, Nanjing, China), 1 μL One Step Q Probe Enzyme Mix (Vazyme, Nanjing, China), 0.4 μL each of forward/reverse primers (10 μM), 0.2 μL each of probes (10 μM), 4 μL of template, and ddH₂O added to a final volume of 20 μL . The reaction program was as follows: 50°C for 5 min, 95°C for 5 min, 40 cycles of 95°C for 10 s, and 52°C for 30 s.

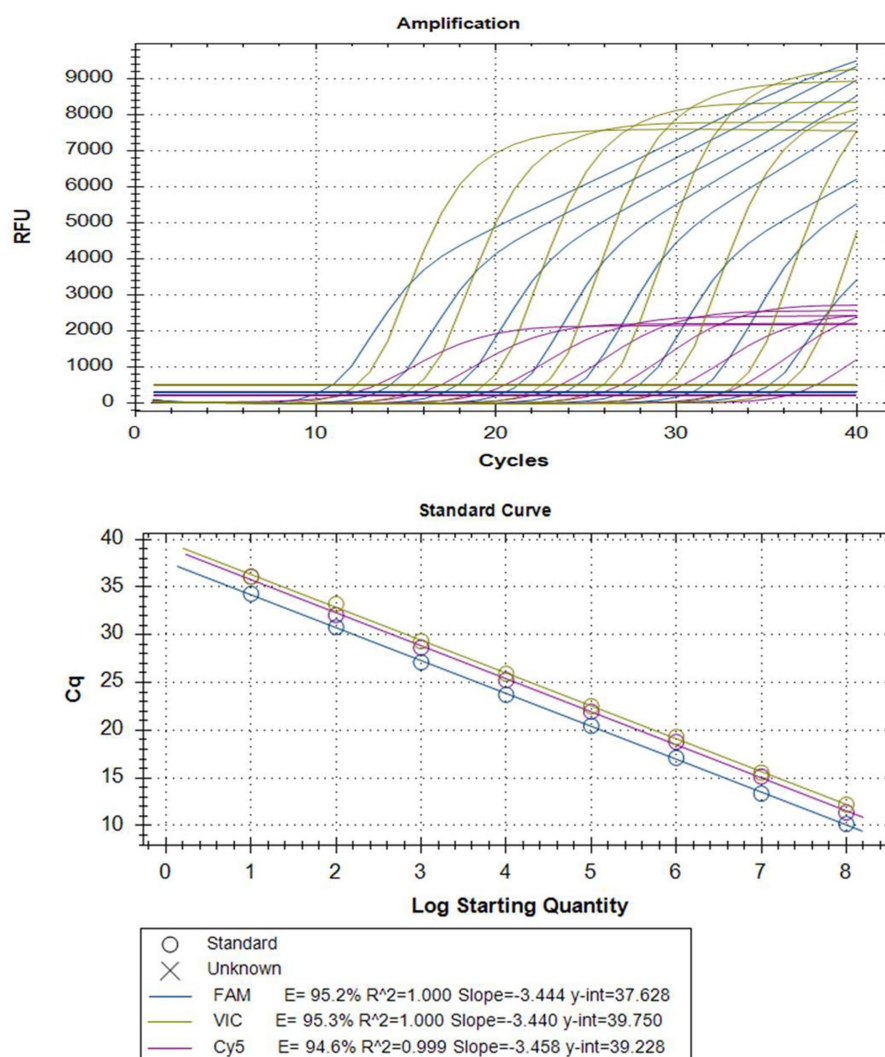


FIGURE 1

Amplification curves (top) and standard curves (bottom) of optimized multiplex real-time PCR for simultaneous detection of PEDV, *L. intracellularis*, and *B. hyodysenteriae*. The concentrations of each plasmid standard are from 1×10^8 copies/ μ L to 1×10^1 copies/ μ L. TaqMan probes for PEDV, *B. hyodysenteriae*, and *L. intracellularis* were fluorescently labeled with FAM, VIC, and Cy5, respectively.

3.2 Standard curves of the multiplex real-time PCR

Serial dilutions of mixed plasmid standards were utilized as templates for multiplex real-time PCR amplification with optimized reaction conditions. Standard curves were automatically generated by the fluorescence quantitative PCR instrument, showing high correlation coefficients and amplification efficiency for each pathogen, for details, PEDV ($R^2 = 1.000$; $E = 95.2\%$), *B. hyodysenteriae* ($R^2 = 1.000$; $E = 95.3\%$), and *L. intracellularis* ($R^2 = 0.999$; $E = 94.6\%$) (Figure 1). This result confirms the validity and reliability of the multiplex real-time PCR assay.

3.3 The specificity of the multiplex real-time PCR assay

The optimized reaction protocol was utilized for the detection of nucleic acids from a range of porcine pathogens, such as PRRSV, PoRV,

PDCoV, PCV2, PCV3, ASFV, *H. parasuis*, *S. suis*, and *S. enteritidis*. As shown in Figure 2, successful detection of all target pathogens was achieved, with no positive signal detected from the aforementioned nine pathogens, the negative control, and three clinical samples from healthy pigs. This finding indicated that the multiplex real-time PCR assay was highly specific, without any cross-reactivity with common pathogens.

3.4 The sensitivity of the multiplex real-time PCR assay

The sensitivity of the multiplex real-time PCR assay was tested using different concentrations of pooled standard plasmids, ranging from 1.0×10^8 copies/ μ L to 1.0×10^{-1} copies/ μ L. Figure 3 shows that the lowest detection limits for PEDV (Figure 3A) and *B. hyodysenteriae* (Figure 3B) were 1.0×10^1 copies/ μ L, and for *L. intracellularis* was 1.0×10^0 copies/ μ L (Figure 3C). However, further experiments revealed that the detection rate for *L. intracellularis* and PEDV at those levels

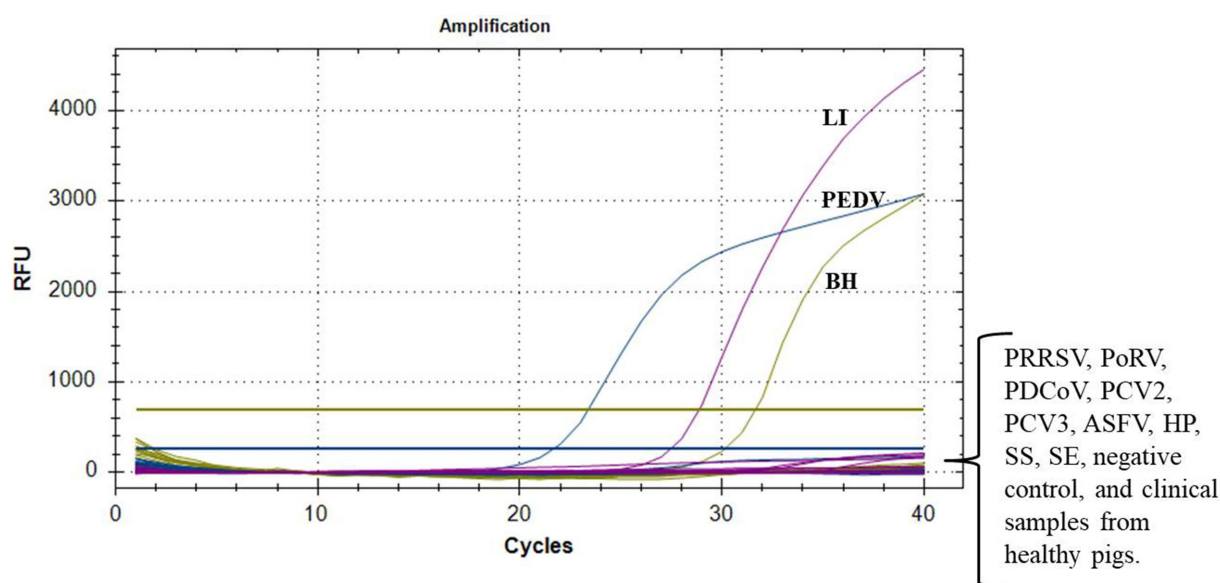


FIGURE 2

Specificity tests of multiplex real-time PCR. Only PEDV, *L. intracellularis* (LI), and *B. hyodysenteriae* (BH) showed positive fluorescence signals, while other swine pathogens and clinical samples from healthy pigs exhibited no fluorescence signals.

was less than 95% of replicates (Supplementary Table S1). Therefore, the reliable detection limit for *B. hyodysenteriae* and *L. intracellularis* is 1.0×10^1 copies/ μ L, while it is 1.0×10^2 copies/ μ L for PEDV.

3.5 Repeatability of the multiplex real-time PCR assay

The data in Table 2 shows that the variation coefficients of Cq values range from 0.15 to 0.74% in intra-group tests and from 0.12 to 3.5% in inter-group tests. These results suggest the high reproducibility of the multiplex real-time PCR assay developed in this study.

3.6 Verification of the multiplex real-time PCR assay by commercial singleplex real-time PCR kit

Thirty clinical samples were utilized to conduct a comparative analysis between multiplex real-time PCR and a commercial singleplex real-time PCR kit. Results were consistent between the two methods, indicating that the multiplex real-time PCR assay can replace the commercial singleplex real-time PCR kit for detecting PEDV, *B. hyodysenteriae*, and *L. intracellularis* simultaneously (Supplementary Table S2).

3.7 Clinical application of the multiplex real-time PCR

A total of 356 clinical samples were tested using the multiplex real-time PCR assay established in this study. As shown in Table 3, the single infection rates for PEDV, *B. hyodysenteriae*, and *L. intracellularis*

were 31.46% (112/356), 58.43% (208/356), and 98.60% (351/356), respectively. Co-infection rates for PEDV + *B. hyodysenteriae*, PEDV + *L. intracellularis*, and *B. hyodysenteriae* + *L. intracellularis* were 16.85% (60/356), 31.46% (112/356), and 57.86% (206/356), respectively. The mixed infection rate for PEDV + *B. hyodysenteriae* + *L. intracellularis* was 16.85% (60/356).

4 Discussion

PEDV, *B. hyodysenteriae*, and *L. intracellularis* are highly contagious diarrheal pathogens that have caused significant harm to the global swine industry (4–7). Previously, antibiotics were extensively utilized in animal husbandry to prevent and treat bacterial infections, as well as to promote growth and enhance feed efficiency, resulting in a reduced incidence of bacterial diarrhea. However, the Chinese government implemented a ban on the inclusion of antibiotics in animal feed in 2020. Since the enactment of this regulation, the prevalence of *B. hyodysenteriae* and *L. intracellularis* has been increasing annually. Especially, co-infections with viruses and bacteria are common in some pig herds due to intensive swine production. Distinguishing the specific causative agent based on clinical information alone is difficult due to similarities in symptoms and pathology. Thus, it is essential to develop a reliable method for the differential detection of PEDV, *B. hyodysenteriae*, and *L. intracellularis* in the laboratory and diagnose them accurately in clinical settings.

In this study, three pairs of specific primers and corresponding probes were designed for the conserved regions of the PEDV M gene, *B. hyodysenteriae* NADH oxidase gene, and *L. intracellularis* 16S rDNA gene. Following multiple optimization iterations, a multiplex TaqMan probe-based real-time PCR assay was successfully established for the simultaneous detection of three predominant diarrheal pathogens, namely PEDV, *B. hyodysenteriae*, and *L. intracellularis*, in a single amplification reaction. The method developed in this study is

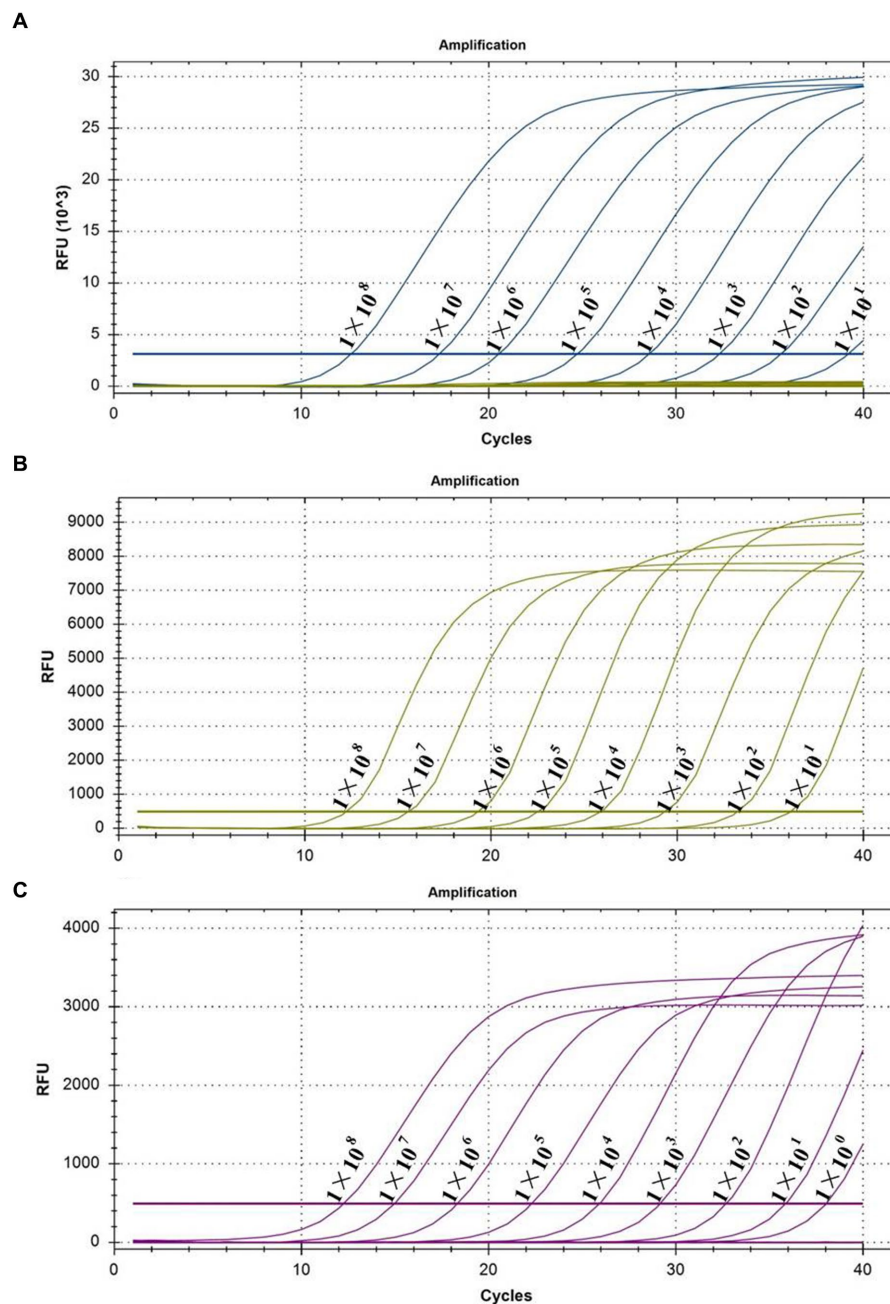


FIGURE 3

Sensitivity tests of multiplex real-time PCR. (A) The test for the sensitivity of PEDV; (B) the test for the sensitivity of *B. hyodysenteriae*; and (C) the test for the sensitivity of *L. intracellularis*.

highly sensitive, with a detection limit of 10 copies/ μ L for *B. hyodysenteriae* and *L. intracellularis*, and 100 copies/ μ L for PEDV. The multiplex real-time PCR assay also demonstrated good repeatability with coefficients of variation ranging from 0.15 to 0.74% for intra-assays and 0.12–3.5% for inter-assays, which proves the stability and reliability of the results. A comparison was made between a commercial singleplex real-time PCR kit and the multiplex real-time PCR method developed in this study for detecting PEDV, *B. hyodysenteriae*, and *L. intracellularis*, in thirty clinical samples. Results showed complete agreement between the two methods,

indicating that the multiplex assay is a viable alternative for simultaneous differentiation of the pathogens.

The multiplex real-time PCR assay developed in this study has been widely applied for the early detection of pathogens in clinical samples due to its rapid, highly sensitive, and specific characteristic. A total of 356 clinical samples from Shandong and Hebei provinces in China were tested using multiplex real-time PCR assay to investigate the prevalence of PEDV, *B. hyodysenteriae*, and *L. intracellularis*. Results showed that *L. intracellularis* and *B. hyodysenteriae* are the main pathogens in diarrheal pigs in both

TABLE 2 The repeatability tests of multiplex real-time PCR.

Templates	Concentrations (copies/ μ L)	Inter-assay		Intra-assay	
		Cq values (mean \pm SD)	CV%	Cq values (mean \pm SD)	CV%
PEDV	10 ⁴	29.63 \pm 0.47	1.57	30.42 \pm 0.18	0.58
	10 ⁵	25.20 \pm 0.18	0.71	25.37 \pm 0.07	0.29
	10 ⁶	19.79 \pm 0.69	3.50	20.24 \pm 0.03	0.15
<i>B. hyodysenteriae</i>	10 ⁴	31.95 \pm 0.21	0.67	32.24 \pm 0.13	0.42
	10 ⁵	27.33 \pm 0.06	0.20	27.20 \pm 0.09	0.32
	10 ⁶	22.08 \pm 0.31	1.40	22.30 \pm 0.04	0.17
<i>L. intracellularis</i>	10 ⁴	30.39 \pm 0.19	0.62	30.66 \pm 0.11	0.36
	10 ⁵	25.44 \pm 0.08	0.33	25.50 \pm 0.19	0.74
	10 ⁶	20.71 \pm 0.03	0.12	20.81 \pm 0.09	0.45

TABLE 3 The detection results of 356 clinical diarrhea samples.

Pathogens	Number of positive samples	Infection rate (%)
PEDV	112	31.46
<i>B. hyodysenteriae</i>	208	58.43
<i>L. intracellularis</i>	351	98.60
PEDV + <i>B. hyodysenteriae</i>	60	16.85
PEDV + <i>L. intracellularis</i>	112	31.46
<i>B. hyodysenteriae</i> + <i>L. intracellularis</i>	206	57.86
PEDV + <i>B. hyodysenteriae</i> + <i>L. intracellularis</i>	60	16.85

provinces. *L. intracellularis* had the highest infection rate at 98.6%, followed by *B. hyodysenteriae* at 58.43% and PEDV at 31.46%. The prevalence of *B. hyodysenteriae* and *L. intracellularis* infections in Chinese pig herds appears to be higher than previously believed (5, 13). A previous study conducted on 891 fecal samples from 47 farms revealed that 37.3% of the fecal samples and 93.6% of the farms tested positive for *L. intracellularis* (13). Swine dysentery, mainly caused by *B. hyodysenteriae*, was a prevalent disease in China in the 1990s. But with the expansion of large-scale aquaculture in China and the use of antibiotic additives in feed, the incidence of these bacterial diseases has gradually decreased since 2010. Consequently, there is a paucity of research on the current prevalence of these infections. The rise in infection rates of *L. intracellularis* and *B. hyodysenteriae* may be linked to the comprehensive implementation of the ban on the addition of antibiotics in feed in China since 2020.

Co-infections of bacterial and viral pathogens are common in clinical settings and can impact the severity of each other's infections (19, 20). Our study found that co-infections account for 72.5% (258/356) of samples, suggesting an increasing prevalence of multiple pathogen co-infections associated with expanding large-scale and intensive swine production. Notably, co-infections involving *L. intracellularis* and *B. hyodysenteriae* were found to be prevalent, accounting for 57.86% of cases. Previous study indicated that *L. intracellularis* infection may facilitate the colonization and establishment of *B. hyodysenteriae* in the large intestine, potentially by inducing early changes or impairing the host intestinal immune response (8). This suggests that co-infections of *L. intracellularis* and

B. hyodysenteriae are common in Chinese pig farms, and need to be addressed for prevention and control.

In conclusion, we have successfully developed a reliable multiplex real-time PCR assay to differentiate PEDV, *L. intracellularis*, and *B. hyodysenteriae*. This assay is highly specific, sensitive, and repeatable, and has shown efficacy in the detection of clinical samples, making it a valuable tool for rapid pathogen identification. Rapid and accurate diagnostics, along with immediate quarantine and treatment, can help prevent and control the spread of infectious diseases.

Data availability statement

The original contributions presented in the study are included in the article/[Supplementary material](#), further inquiries can be directed to the corresponding author.

Author contributions

JR: Data curation, Formal analysis, Funding acquisition, Project administration, Supervision, Validation, Visualization, Writing – original draft, Writing – review & editing. FL: Data curation, Investigation, Resources, Writing – review & editing. XY: Data curation, Formal analysis, Investigation, Writing – review & editing. YL: Investigation, Methodology, Writing – review & editing. ML: Formal analysis, Investigation, Writing – review & editing. YS: Formal analysis, Investigation, Software,

Writing – review & editing. XL: Conceptualization, Funding acquisition, Methodology, Project administration, Supervision, Writing – review & editing.

Funding

The author(s) declare financial support was received for the research, authorship, and/or publication of this article. This study was funded by the Natural Science Foundation of Shandong Province (Grant No. ZR2022MC158), Central-guided Funding for Local Technological Development (Grant No. YDZX2023069), and Taishan Industry Leadership Talent Project of Shandong Province in China (Grant No. tscx202306093).

Conflict of interest

FL, YL, and XL were employed by the Shandong New Hope Liuhe Co., Ltd.

References

- Wu X, Liu Y, Gao L, Yan Z, Zhao Q, Chen F, et al. Development and application of a reverse-transcription recombinase-aided amplification assay for porcine epidemic diarrhea virus. *Viruses*. (2022) 14:59. doi: 10.3390/v14030591
- Hou W, Fan M, Zhu Z, Li X. Establishment and application of a triplex real-time RT-PCR assay for differentiation of PEDV, PoRV, and PDCoV. *Viruses*. (2023) 15:1238. doi: 10.3390/v15061238
- Huang X, Chen J, Yao G, Guo Q, Wang J, Liu G. A TaqMan-probe-based multiplex real-time RT-qPCR for simultaneous detection of porcine enteric coronaviruses. *Appl Microbiol Biot*. (2019) 103:4943–52. doi: 10.1007/s00253-019-09835-7
- Ren J, Zu C, Li Y, Li M, Gu J, Chen F, et al. Establishment and application of a TaqMan-based multiplex real-time PCR for simultaneous detection of three porcine diarrhea viruses. *Front Microbiol*. (2024) 15:1380849. doi: 10.3389/fmicb.2024.1380849
- Wang L, Wu W, Zhao L, Zhu Z, Yao X, Fan J, et al. Fecal PCR survey and genome analysis of *Lawsonia intracellularis* in China. *Front Vet Sci*. (2024) 11:1324768. doi: 10.3389/fvets.2024.1324768
- Arnold M, Crien A, Swam H, von Berg S, Jolie R, Nathues H. Prevalence of *Lawsonia intracellularis* in pig herds in different European countries. *Porc Health Manag*. (2019) 5:31. doi: 10.1186/s40813-019-0137-6
- Calderaro A, Bommezzadri S, Piccolo G, Zuelli C, Dettori G, Chezzi C. Rapid isolation of *Brachyspira hyodysenteriae* and *Brachyspira pilosicoli* from pigs. *Vet Microbiol*. (2005) 105:229–34. doi: 10.1016/j.vetmic.2004.10.021
- Daniel AGS, Pereira CER, Dorella F, Pereira FL, Laub RP, Andrade MR, et al. Synergic effect of *Brachyspira hyodysenteriae* and *Lawsonia intracellularis* coinfection: anatomopathological and microbiome evaluation. *Animals*. (2023) 13:2611. doi: 10.3390/ani13162611
- Hu Y, Xie X, Yang L, Wang A. A comprehensive view on the host factors and viral proteins associated with porcine epidemic diarrhea virus infection. *Front Microbiol*. (2021) 12:762358. doi: 10.3389/fmicb.2021.762358
- Si F, Hu X, Wang C, Chen B, Wang R, Dong S, et al. Porcine epidemic diarrhea virus (PEDV) ORF3 enhances viral proliferation by inhibiting apoptosis of infected cells. *Viruses*. (2020) 12:214. doi: 10.3390/v12020214
- Wang D, Fang LR, Xiao SB. Porcine epidemic diarrhea in China. *Virus Res*. (2016) 226:7–13. doi: 10.1016/j.virusres.2016.05.026
- Borgström A, Scherrer S, Kirchgässner C, Schmitt S, Frei D, Wittenbrink MM. A novel multiplex qPCR targeting 23S rDNA for diagnosis of swine dysentery and porcine intestinal spirochaetosis. *BMC Vet Res*. (2017) 13:42. doi: 10.1186/s12917-016-0939-6
- Nathues H, Oliveira CJ, Wurm M, Grosse Beilage E, Givisiez PE. Simultaneous detection of *Brachyspira hyodysenteriae*, *Brachyspira pilosicoli* and *Lawsonia intracellularis* in porcine faeces and tissue samples by multiplex-PCR. *J Vet Med A Physiol Pathol Clin Med*. (2007) 54:532–8. doi: 10.1111/j.1439-0442.2007.00995.x
- Smith SH, McOrist S. Development of persistent intestinal infection and excretion of *Lawsonia intracellularis* by piglets. *Res Vet Sci*. (1997) 62:6–10. doi: 10.1016/s0034-5288(97)90171-5
- Boonham N, Kreuze J, Winter S, van der Vlugt R, Bergervoet J, Tomlinson J, et al. Methods in virus diagnostics: from ELISA to next generation sequencing. *Virus Res*. (2014) 186:20–31. doi: 10.1016/j.virusres.2013.12.007
- Liu G, Jiang Y, Opriessnig T, Gu K, Zhang H, Yang Z. Detection and differentiation of five diarrhea related pig viruses utilizing a multiplex PCR assay. *J Virol Methods*. (2019) 263:32–7. doi: 10.1016/j.jviromet.2018.10.009
- Li X, Hu Y, Liu P, Zhu Z, Liu P, Chen C, et al. Development and application of a duplex real-time PCR assay for differentiation of genotypes I and II African swine fever viruses. *Transbound Emerg Dis*. (2022) 69:2971–9. doi: 10.1111/tbed.14459
- Pan Z, Lu J, Wang N, He WT, Zhang L, Zhao W, et al. Development of a TaqMan-probe-based multiplex real-time PCR for the simultaneous detection of emerging and reemerging swine coronaviruses. *Virulence*. (2020) 11:707–18. doi: 10.1080/21505594.2020.1771980
- Vlasova AN, Amimo JO, Saif LJ. Porcine rotaviruses: epidemiology, immune responses and control strategies. *Viruses*. (2017) 9:48. doi: 10.3390/v9030048
- Saeng-Chuto K, Madapong A, Kaeoket K, Piñeyro PE, Tantituvanont A, Nilubol D. Coinfection of porcine deltacoronavirus and porcine epidemic diarrhea virus increases disease severity, cell tropism and earlier upregulation of IFN- α and IL12. *Sci Rep*. (2021) 11:3040. doi: 10.1038/s41598-021-82738-8

Publisher's note

All claims expressed in this article are solely those of the authors and do not necessarily represent those of their affiliated organizations, or those of the publisher, the editors and the reviewers. Any product that may be evaluated in this article, or claim that may be made by its manufacturer, is not guaranteed or endorsed by the publisher.

Supplementary material

The Supplementary material for this article can be found online at: <https://www.frontiersin.org/articles/10.3389/fvets.2024.1450066/full#supplementary-material>

Frontiers in Veterinary Science

Transforms how we investigate and improve
animal health

The third most-cited veterinary science journal,
bridging animal and human health with a
comparative approach to medical challenges. It
explores innovative biotechnology and therapy for
improved health outcomes.

Discover the latest Research Topics

[See more →](#)

Frontiers

Avenue du Tribunal-Fédéral 34
1005 Lausanne, Switzerland
frontiersin.org

Contact us

+41 (0)21 510 17 00
frontiersin.org/about/contact

